

An activating role for neutrophil serine proteases in rapidly progressive glomerulonephritis

Anne Bevins

A PhD thesis submitted to The University of Birmingham
2011

Supervisors:
Professor C O Savage
Dr G E Rainger

UNIVERSITY OF
BIRMINGHAM

University of Birmingham Research Archive

e-theses repository

This unpublished thesis/dissertation is copyright of the author and/or third parties. The intellectual property rights of the author or third parties in respect of this work are as defined by The Copyright Designs and Patents Act 1988 or as modified by any successor legislation.

Any use made of information contained in this thesis/dissertation must be in accordance with that legislation and must be properly acknowledged. Further distribution or reproduction in any format is prohibited without the permission of the copyright holder.

Acknowledgements

I'd like to thank all of the members of the Renal Immunobiology group for their help and support in carrying out this research, in particular Dr Samantha Tull, Dr Neil Holden and Dr Matthew Morgan for their invaluable advice. Particular thanks also goes to my supervisor, Professor Caroline Savage, for all of her support and guidance. I'd additionally like to thank Hannah Morris and Julie Williams for their help with western blots.

I would like to thank my family for supporting me throughout my PhD, particularly to Mathias for all the time you have given helping me to finish this thesis.

Work Arising from this Thesis

Data from this thesis has been presented at the following conferences

- “Treatment of Endothelial Cells with Serine Proteases induces Exocytosis of Weibel-Palade Bodies” Anne Bevins, Sahithi Panchagnula, Samantha Tull, Matthew Morgan, Simon C. Satchell, Lorraine Harper, G. Ed Rainger, Caroline Savage - Presented at the Renal Association Conference, Manchester, May 2010

- “Phenotypic Changes of Endothelial Cells Resulting in Increased Neutrophil Adhesion in ANCA-Associated Vasculitis” Anne Bevins, Sahithi Panchagnula, Simon C. Satchell, Lorraine Harper, G. Ed Rainger, Caroline Savage, Samantha Tull - Presented at the ANCA Workshop, Lund Sweden, June 2009

- “Effect of serine proteases, Elastase and Proteinase 3, on glomerular endothelial cell-neutrophil interactions” Samantha Tull, Sahithi J Panchagnula, Anne Bevins, Simon C. Satchell, Lorraine Harper, G. Ed Rainger, Caroline Savage - Presented at the Renal Association Conference, Glasgow, May 2008

List of Abbreviations

α 1-AT	α 1-Antitrypsin
ACD	Acid Citrate Dextrose
ACE	Angiotensin-Converting Enzyme
ADAMTS-13	A Disintegrin and Metalloprotease with a Thrombospondin type 1 Motif, Member 13
ADP	Adenosine-Diphosphate
ANCA	Anti-Neutrophil Cytoplasm Antibodies
Ang-1	Angiopoietin-1
Ang-2	Angiopoietin-2
Anti-GBM	Anti-Glomerular Basement Membrane
AP3	Adaptor Protein Complex-3
ASV	ANCA Systemic Vasculitides
ATN	Acute Tubular Necrosis
ATP	Adenosine-5'-Triphosphate
BSA	Bovine Serum Albumin
BVAS	Birmingham Vasculitis Activity Score
C2GNT	Core 2 -1,6- <i>N</i> -acetylglucosaminyltransferase
CaM	Calmodulin
cAMP	Cyclic Adenosine Monophosphate
CDKs	Cyclin-Cyclin Dependant Kinases
CXCL1	CXC chemokine ligand 1
CXCL8	CXC chemokine ligand 8
CXCR1	CXC Chemokine Receptor-1
CXCR2	CXC Chemokine Receptor-2
CTLA-4	Cytotoxic T-Lymphocyte Antigen-4
DMSO	Dimethyl Sulfoxide
EDTA	Ethylenediaminetetraacetic acid
EGM-2-MV	Endothelial Growth Medium-2-Microvascular
ELISA	Enzyme Linked Immunosorbent Assay
ELR motif	Glu ⁴ -Leu ⁵ -Arg ⁶ motif
EnC	Endothelial Cell
FACS	Fluorescence-Activated Cell Sorting
FCS	Fetal Calf Serum
fMLP	Formyl-Methionyl-Leucyl-Phenylalanine
GAG	Glycoaminoglycans
GE _n C	Glomerular Endothelial Cell
GP1b α	Glycoprotein-1b α
H ₂ O ₂	Hydrogen Peroxide
HBH	Hanks Buffered Saline Solution plus Hepes
HCl	Hydrochloric Acid
HK	High Molecular Weight Kininogen
HLE	Human Leukocyte Elastase
HRP	Horseradish Peroxidase
HUVEC	Human Umbilical Vein Endothelial Cells
IFN γ	Interferon- γ
IL-1 β	Interleukin-1 β
IL-6	Interleukin-6
IL-17	Interleukin-17
IL-18	Interleukin-18

ICAM-1	Intercellular Adhesion Molecule-1
JNK	Jun N-Terminal Kinase
KC	Keratinocyte Derived Chemokine
LF	Lipofectamine
LFA-1	Lymphocyte Function-associated Antigen-1 (CD11a/CD18)
LPS	Lipopolysaccharide
M199	Medium199
Mac-1	Macrophage Antigen-1 (CD11b/CD18)
MCP-1	Monocyte Chemoattractant Protein-1
MMPs	Matrix Metalloproteinases
MPO	Myeloperoxidase
MTT	1-(4,5-Dimethylthiazol-2-yl)-3,5-diphenylformazan
NAP-1	Neutrophil Activating Protein
NF κ B	Nuclear Factor- κ B
NMR	Nucleotide Monitoring Reagent
NO	Nitric Oxide
NOD	Non-obese Diabetic
NP40	(Octylphenoxy)phenoxypolyethoxyethanol
NRR	Nucleotide Releasing Reagent
OPD	o-Phenylenediamine Dihydrochloride
PAP	Peroxidase Anti-Peroxidase
PAR	Protease Activated Receptor
PAR-AP	Protease Activated Receptor Agonist Peptide
SDS-PAGE	Sodium Dodecyl Sulfate Polyacrylamide Gel Electrophoresis
Serpin	Serine Protease Inhibitor
PBMC	Peripheral Blood Mononuclear Cells
PBS	Phosphate Buffered Saline
PFA	Paraformaldehyde
PI3K	Phosphatidylinositol 3-Kinase
PKA	Protein Kinase A
PKC	Protein Kinase C
PSGL-1	P-Selectin Glycoprotein Ligand-1
PAF	Platelet Activating Factor
PMN	Polymorphonuclear Cells
PR3	Proteinase 3
ROS	Reactive Oxygen Species
SDS	Sodium Dodecyl Sulfate
SCID	Severe Combined Immunodeficiency
siRNA	Small Interference RNA
SOD	Superoxide Dismutase
TBS	Tris Buffered Saline
TF	Tissue Factor
Tie-1	Tyrosine Kinase with Immunoglobulin and EGF homology domains-1
Tie-2	Tyrosine Kinase with Immunoglobulin and EGF homology domains-2
TLR	Toll-Like Receptor
TMB	3,3',5,5'-Tetramethylbenzidine
TNF α	Tumour Necrosis Factor- α
Treg	Regulatory T-Lymphocytes
VCAM-1	Vascular Cell Adhesion Molecule-1
VEGF	Vascular Endothelial Growth Factor
VDI	Vasculitis Damage Index
vWf	von Willebrand Factor

WG
WPB

Wegener's Granulomatosis
Weibel-Palade Bodies

Abstract

ANCA-systemic vasculitic glomerulonephritides (ASV) are a collection of diseases associated with the presence of autoimmune antibodies directed at the components of neutrophil cytoplasmic granules, known as ANCA. ANCA is proposed to bind to its antigen on the neutrophil surface, from where it can stimulate neutrophil activation and consequently, increased adhesion to the vascular endothelium, as well as production of reactive oxygen species and release of granular contents. It is believed that the components of the alpha neutrophil granules, namely the neutrophil serine proteases, may be involved in the induction of inflammation and endothelial cell injury observed in ANCA systemic vasculitis. This project has focused on the effects of Proteinase 3 (PR3), a neutrophil serine protease, on the glomerular endothelium.

To undertake this research we used two endothelial cell types, primary endothelial cells from human umbilical cords (HUVEC) and a conditionally immortalised glomerular endothelial cell line (GENC). The data in this thesis proposes that the neutrophil serine proteases, PR3 and human leukocyte elastase (HLE), have an early activatory role on the vascular endothelium, with later long-term injurious effects. Short treatments of endothelial cells with PR3 and HLE had no significant effects on mitochondrial activity, endothelial detachment or intracellular ADP/ATP levels, whilst 24 hour treatments resulted in endothelial cell apoptosis. This was further demonstrated by release of von Willebrand Factor (vWf), which was maximal at 24h treatment. Short serine protease treatments resulted in dose-dependant release of vWf from endothelial cells, which along with increased release of chemokine ligand 8 (CXCL8) and expression of P-Selectin, implicates increased exocytosis of the endothelial Weibel-Palade bodies (WPB).

Using a static model of neutrophil adhesion, we demonstrated that PR3 and HLE had the potential to increase neutrophil adhesion to the endothelium. This adhesion occurs through interactions between P-Selectin and its ligand, P-Selectin glycoprotein ligand-1 (PSGL-1), on neutrophils, as endothelial treatment with PR3 and HLE resulted in increased membrane expression of P-Selectin, whilst blocking antibodies directed at PSGL-1 significantly inhibited neutrophil adhesion to protease treated endothelial cells. Further, PR3 and HLE have the ability to cleave CXCL8 for support of inflammation, perhaps inducing activation of leukocyte integrins to increase adhesion. Moreover, inhibition of CXCL8 receptors, CXCR1 and CXCR2, on neutrophils decreased the level of neutrophil adhesion.

The effects of PR3 or HLE on endothelial cell activation do not appear to be occurring through the 'classical' signalling pathways or through protease activated receptor interactions. Interestingly, PR3 treatment does change the pattern of tyrosine and serine/threonine phosphorylation, and further investigation into this may identify a unique signalling pathway, and thereby, possible therapeutic targets.

Table of Contents

ACKNOWLEDGEMENTS	I
WORK ARISING FROM THIS THESIS	II
LIST OF ABBREVIATIONS	III
ABSTRACT	VI
1. AN INTRODUCTION TO ANCA-ASSOCIATED VASCULITIS	1
1.1 VASCULITIC GLOMERULONEPHRITIS	1
1.2 ANTI-NEUTROPHIL CYTOPLASMIC ANTIBODIES AND THEIR ANTIGENS	3
1.3 AETIOPATHOGENESIS OF VASCULITIS	5
1.4 THE NEUTROPHIL	11
1.5 THE NEUTROPHIL SERINE PROTEASES	13
1.6 PR3 AND ENDOTHELIAL APOPTOSIS	16
1.7 ALPHA-1 ANTITRYPSIN: A SERINE PROTEASE INHIBITOR	17
1.8 NEUTROPHILS IN INFLAMMATION: THE PROCESS OF TRANSMIGRATION	18
1.9 CHEMOKINE LIGAND-8 INDUCED NEUTROPHIL ADHESION	22
1.10 NEUTROPHIL PRIMING BY TUMOUR NECROSIS FACTOR- α	23
1.11 OTHER CELL TYPES IMPLICATED IN ASV	25
1.11.1 Macrophages	25
1.11.2 T-cells	27
1.11.3 B-Cells	28
1.12 ENDOTHELIAL CELLS IN INFLAMMATION	30
1.13 GLOMERULAR ENDOTHELIUM: A TARGET IN ANCA-ASSOCIATED VASCULITIS	33
1.14 WEIBEL-PALADE BODIES	35
1.15 VON WILLEBRAND FACTOR (vWf) AND THE COAGULATION CASCADE	37
1.16 vWf IN ANCA-ASSOCIATED VASCULITIS	39
1.17 OTHER CONSTITUENTS OF WPB	39
1.17.1 Angiopoietin-2	39
1.17.2 P-Selectin	41
1.17.3 CD63 (Platelet Glycoprotein gp40)	42
1.17.4 Chemokine Ligand-8	42
1.18 EVIDENCE FOR PROTEASE-ACTIVATED RECEPTORS IN vWf RELEASE	44
1.19 SIGNALLING IN vWf RELEASE FROM WEIBEL-PALADE BODIES	46
1.20 AIMS AND HYPOTHESIS	47
2. MATERIALS AND METHODS	49
2.1. CONDITIONALLY IMMORTALISED GLOMERULAR ENDOTHELIAL CELLS	49
2.2 ISOLATION OF HUVEC FROM UMBILICAL VEINS	51
2.3 MATERIALS	52
2.4 NEUTROPHIL ISOLATION	53
2.5 TREATMENT OF ENDOTHELIAL CELLS WITH TUMOUR NECROSIS FACTOR- α	54
2.6 P-SELECTIN, E-SELECTIN, ICAM-1 AND VCAM-1 CELL SURFACE EXPRESSION ELISA	56
2.7 QUANTIFICATION OF CXCL8 IN CELL SUPERNATANT	57
2.8 PROTEASE DIGESTION OF CXCL8 IN CELL CULTURE SUPERNATANTS	58
2.9 INHIBITION OF NEUTROPHIL ADHESION BY BLOCKING PSGL-1	58
2.10 INHIBITION OF NEUTROPHIL ADHESION BY BLOCKING CXCR1 AND CXCR2	59
2.11 VON WILLEBRAND FACTOR ELISA OF SUPERNATANTS	59
2.12 QUANTIFYING vWf mRNA BY PCR	60
2.13 CELL SURFACE EXPRESSION OF vWf FOLLOWING PROTEASE TREATMENT	62
2.14 vWf EXPRESSION BY FLOW CYTOMETRY	63
2.15 vWf, CD63 AND F-ACTIN STAINING BY CONFOCAL MICROSCOPY	63
2.16 vWf IMMUNOHISTOCHEMISTRY OF KIDNEY BIOPSIES	64
2.17 ANGIOPOIETIN-2 ELISA OF SUPERNATANTS	66
2.18 RELEASE OF vWf BY PAR AGONISTS	67
2.19 KNOCKDOWN OF PAR1 AND PAR2 BY siRNA	67
2.20 RNA ISOLATION AND REAL-TIME PCR OF PAR-1 AND PAR-2	68
2.21 FLOW CYTOMETRY DETERMINATION PAR-1 AND PAR-2 PROTEIN EXPRESSION FOLLOWING siRNA	69
2.22 INHIBITION OF MAJOR PATHWAYS OF vWf RELEASE	70

2.23 PKC INHIBITION OF NEUTROPHIL SUPEROXIDE RELEASE.....	71
2.24 NEUTROPHIL DEGRANULATION ASSAY	72
2.25 INHIBITION OF vWf RELEASE BY F-ACTIN INHIBITOR, CYTOCHALASIN B.....	72
2.26 STIMULATION OF ENDOTHELIAL vWf RELEASE BY OKADAIC ACID.....	73
2.27 TYROSINE AND SERINE/THREONINE PHOSPHORYLATION BY WESTERN BLOTTING.....	73
2.28 NECROSIS VERSUS APOPTOSIS WITH APOGLOW®	75
2.29 CRYSTAL VIOLET STAINING OF ADHERENT CELLS.....	76
2.30 MTT ASSESSMENT OF MITOCHONDRIAL ACTIVITY.....	77
2.31 STATISTICAL ANALYSES	77
3. RESULTS.....	79
3.1 VISUALISATION OF ENDOTHELIAL CELLS AT DIFFERENT TIME POINTS IN CULTURE	79
3.2 CRYSTAL VIOLET STAINING FOR CELL ADHERENCE	81
3.3 MEASURE OF MITOCHONDRIAL ACTIVITY IN SERINE PROTEASE TREATED ENDOTHELIAL CELLS	83
3.4 MEASURE OF APOPTOSIS BY CONVERSION OF ATP INTO ADP.....	85
3.5 VON WILLEBRAND FACTOR RELEASE FROM SERINE PROTEASE TREATED ENDOTHELIAL CELLS.....	91
3.6 INCREASED LEVEL OF INTRACELLULAR vWf PROTEIN AND mRNA FOLLOWING TREATMENT	96
3.7 INHIBITION OF vWf RELEASE BY α 1-ANTITRYPSIN	102
3.8 CHANGES IN vWf SURFACE EXPRESSION FOLLOWING SERINE PROTEASE TREATMENT.....	106
3.9 vWf RELEASE: INTERNAL STORES VERSUS MEMBRANE CLEAVAGE	109
3.10 CONFOCAL STAINING FOR vWf AND THE PLASMA MEMBRANE.....	111
3.11 vWf STAINING IN RENAL BIOPSIES	115
3.11 CHEMOKINE LIGAND-8 RELEASE FOLLOWING SERINE PROTEASE TREATMENT.....	118
3.12 ANGIOPOIETIN-2 RELEASE FROM SERINE PROTEASE TREATED ENDOTHELIAL CELLS.....	123
3.13 CD63 EXPRESSION BY SERINE PROTEASE TREATED GENC	126
3.14 UPREGULATION OF ENDOTHELIAL MEMBRANE P-SELECTIN EXPRESSION BY PR3 AND HLE	128
3.15 vWf RELEASE BY PAR AGONIST PEPTIDES	131
3.16 siRNA KNOCKDOWN OF PAR-1 AND PAR-2 DOES NOT REDUCE vWf RELEASE	135
3.17 SIGNALING PATHWAYS INVOLVED IN vWf RELEASE.....	137
3.18 INHIBITION OF vWf RELEASE BY INHIBITION OF ACTIN POLYMERISATION	148
3.19 INHIBITION OF vWf RELEASE BY INHIBITION OF PHOSPHATASE ACTIVITY	150
3.20 CHANGES IN PHOSHOPEPTIDES FOLLOWING SERINE PROTEASE TREATMENT	154
3.21 NEUTROPHIL ADHESION TO TNF α TREATED ENDOTHELIAL CELLS	158
3.22 NEUTROPHIL ADHESION TO PR3 AND HLE TREATED ENDOTHELIAL CELLS.....	160
3.23 MEMBRANE EXPRESSION OF E-SELECTIN FOLLOWING SERINE PROTEASE EXPRESSION	163
3.24 EXPRESSION OF SURFACE ICAM-1 FOLLOWING SERINE PROTEASE TREATMENT	167
3.25 EXPRESSION OF VCAM-1 ON SERINE PROTEASE TREATED ENDOTHELIAL CELLS	170
3.26 BLOCKING PSGL-1 ON NEUTROPHILS INHIBITS ADHESION.....	173
3.27 INHIBITION OF CXCR1 AND CXCR2 ON NEUTROPHILS INHIBITS ADHESION	175
4. DISCUSSION.....	177
4.1 NEUTROPHIL SERINE PROTEASES DO NOT INDUCE ENDOTHELIAL CELL INJURY FOLLOWING SHORT INCUBATIONS	177
4.2 RELEASE OF vWf OCCURS DUE TO ACTIVATION NOT INJURY.....	179
4.3 CONFOCAL STAINING OF vWf AND THE ENDOTHELIAL MEMBRANE PRODUCES INCONCLUSIVE RESULTS	182
4.4 PR3 AND HLE CAUSE EXOCYTOSIS OF WEIBEL-PALADE BODY CONSTITUENTS.....	183
4.5 vWf IS CLEAVED AND RELEASED	186
4.6 vWf PROTEIN AND mRNA IS INCREASED BY SERINE PROTEASES	188
4.7 vWf EXPRESSION IN RENAL BIOPSIES	190
4.8 PR3 AND HLE SIGNAL THROUGH A UNIQUE PATHWAY TO INDUCE vWf RELEASE	191
4.9 THE SERINE PROTEASES INCREASE NEUTROPHIL ADHESION THROUGH INTERACTIONS BETWEEN P- SELECTIN AND PSGL-1	197
4.10 A ROLE FOR CXCL8 IN NEUTROPHIL ADHESION.....	201
4.11 α 1-ANTITRYPSIN – A POTENTIAL THERAPY IN ANCA VASCULITIS?.....	204
4.12 DIFFERENTIAL ROLES FOR PR3 AND HLE?	206
4.13 CAN A GENC LINE ACCURATELY REPRESENT A PRIMARY GLOMERULAR ENDOTHELIAL CELL?	208
5. CONCLUDING REMARKS.....	210
6. FUTURE WORK	213
7. APPENDICES	216

1. PCR MASTERMIXES	216
2. REAL-TIME PCR MIX.....	217
3. WESTERN BLOT RECIPES.....	217
4. APOGLOW® ASSAY GUIDELINE CRITERIA	220
8. REFERENCES	221

Table of Figures

FIGURE 1 - HYPOTHESISED MECHANISM OF ANCA VASCULITIS	6
FIGURE 2 - THE THEORY OF ANTIGEN COMPLEMENTARITY	8
FIGURE 3 - ANCA-MEDIATED NEUTROPHIL ACTIVATION	9
FIGURE 4 - THE PROCESS OF LEUKOCYTE MIGRATION	20
FIGURE 5 - PROPOSED SIGNALLING PATHWAYS INVOLVED IN vWf RELEASE	47
FIGURE 6 - ACTIVITY TEST FOR ENZYMES AND INHIBITORS	53
FIGURE 7 - VISUALISATION OF ENDOTHELIAL CELLS AT DIFFERENT TIME-POINT	80
FIGURE 8 – TIMECOURSE OF CRYSTAL VIOLET STAINING FOR ENDOTHELIAL DETACHMENT	82
FIGURE 9 - CRYSTAL VIOLET STAINING FOR ENDOTHELIAL DETACHMENT FOLLOWING TREATMENT WITH INCREASING CONCENTRATIONS OF SERINE PROTEASE	82
FIGURE 10 - MITOCHONDRIAL ACTIVITY FOLLOWING A TIMECOURSE OF PROTEASE TREATMENT	84
FIGURE 11 - MITOCHONDRIAL ACTIVITY FOLLOWING TREATMENT WITH INCREASING CONCENTRATIONS OF SERINE PROTEASE	84
FIGURE 12 - CHANGES IN INTRACELLULAR ATP LEVELS AT 2 HOURS	88
FIGURE 13 - CHANGES IN THE ADP:ATP RATIO AT 2 HOURS	88
FIGURE 14 - CHANGES IN INTRACELLULAR ATP LEVELS AT 24 HOURS	89
FIGURE 15 - CHANGES IN THE ADP:ATP RATIO AT 24 HOURS	89
FIGURE 16 - VISUALISATION OF GENC AFTER SERINE PROTEASE TREATMENT	90
FIGURE 17 - vWf RELEASE FROM PR3 AND HLE TREATED ENDOTHELIAL CELLS AT 2 HOURS	93
FIGURE 18 - vWf RELEASE FROM PR3 AND HLE TREATED ENDOTHELIAL CELLS AT 24 HOURS	93
FIGURE 19 - TIMECOURSE OF vWf RELEASE FROM PR3 TREATED ENDOTHELIAL CELLS	94
FIGURE 20 - TIMECOURSE OF vWf RELEASE FROM HLE TREATED ENDOTHELIAL CELLS	94
FIGURE 21 - vWf RELEASE FROM HUVEC AS A PERCENTAGE OF TOTAL vWf	95
FIGURE 22 - vWf RELEASE FROM GENC AS A PERCENTAGE OF TOTAL vWf	95
FIGURE 23 - LEVEL OF INTRACELLULAR vWf REMAINING IN HUVEC AFTER SERINE PROTEASE TREATMENT ..	98
FIGURE 24 - LEVEL OF INTRACELLULAR vWf REMAINING IN GENC AFTER SERINE PROTEASE TREATMENT ..	98
FIGURE 25 - TOTAL vWf AFTER TREATMENT OF HUVEC WITH SERINE PROTEASES	99
FIGURE 26 - TOTAL vWf AFTER TREATMENT OF GENC WITH SERINE PROTEASES	99
FIGURE 27 - CLEAVAGE OF vWf BY PR3 AND HLE	100
FIGURE 28 - vWf mRNA LEVELS FOLLOWING SERINE PROTEASE TREATMENT	101
FIGURE 29 - INHIBITION OF vWf RELEASE BY α 1AT AT 2 HOURS	103
FIGURE 30 - INHIBITION OF vWf RELEASE BY α 1AT AT 24 HOURS	103
FIGURE 31 - α 1AT INHIBITION OF vWf RELEASE FROM HUVEC AT HIGHER CONCENTRATIONS OF SERINE PROTEASE	104
FIGURE 32 - α 1AT INHIBITION OF vWf RELEASE FROM GENC AT HIGHER CONCENTRATIONS OF SERINE PROTEASE	104
FIGURE 33 - HUVEC DETACHMENT FOLLOWING TREATMENT WITH HIGHER DOSES OF PR3 AND HLE	105
FIGURE 34 - GENC DETACHMENT FOLLOWING TREATMENT WITH HIGHER DOSES OF PR3 AND HLE	105
FIGURE 35 - SURFACE EXPRESSION OF vWf ON HUVEC FOLLOWING SERINE PROTEASE TREATMENT	107
FIGURE 36 - SURFACE EXPRESSION OF vWf ON GENC FOLLOWING SERINE PROTEASE TREATMENT	107
FIGURE 37 - SURFACE EXPRESSION OF vWf ON HUVEC CAN BE RESTORED BY α 1AT	108
FIGURE 38 - SURFACE EXPRESSION OF vWf ON GENC CAN BE RESTORED BY α 1AT	108
FIGURE 39 - FACS ANALYSIS OF vWf RELEASE FROM SURFACE AND INTERNAL STORES	110
FIGURE 40 - LOCALISATION OF vWf WITH THE PLASMA MEMBRANE	113
FIGURE 41 - Z-STACK IMAGING OF vWf STAINING	114
FIGURE 42 - vWf STAINING IN RENAL BIOPSIES	117
FIGURE 43 - CHEMOKINE LIGAND-8 RELEASE FROM SERINE PROTEASE TREATED HUVEC	120
FIGURE 44 – CHEMOKINE LIGAND-8 RELEASE FROM SERINE PROTEASE TREATED GENC	120
FIGURE 45 - CLEAVAGE OF CHEMOKINE LIGAND-8 BY PR3 AND HLE	121
FIGURE 46 – CHEMOKINE LIGAND-8 CLEAVAGE BY HLE CAN BE INHIBITED BY α 1AT	121
FIGURE 47 – CHEMOKINE LIGAND-8 RELEASE FOLLOWING REMOVAL OF SERINE PROTEASES 1 HOUR INCUBATION	122
FIGURE 48 – CHEMOKINE LIGAND-8 RELEASE FOLLOWING REMOVAL OF SERINE PROTEASES 1 AND 2 HOUR INCUBATIONS	122
FIGURE 49 - ANGIOPOIETIN-2 RELEASE FROM HUVEC FOLLOWING SERINE PROTEASE TREATMENT	124
FIGURE 50 - ANGIOPOIETIN-2 RELEASE FROM GENC FOLLOWING SERINE PROTEASE TREATMENT	124
FIGURE 51 - PR3 AND HLE CLEAVE ANGIOPOIETIN-2	125
FIGURE 52 - ANGIOPOIETIN-2 RELEASE AFTER REMOVAL OF PR3 AND HLE	125
FIGURE 53 - CD63 STAINING FOLLOWING PROTEASE TREATMENT	127
FIGURE 54 - P-SELECTIN SURFACE EXPRESSION FOLLOWING PR3 AND HLE TREATMENT	130

FIGURE 55 - INHIBITION OF P-SELECTIN EXPRESSION BY α 1AT	130
FIGURE 56 - OPTIMISATION OF PAR AGONIST PEPTIDE INDUCED vWf RELEASE	132
FIGURE 57 - EFFECT OF PAR AGONISTS ON vWf RELEASE	133
FIGURE 58 - EFFECT OF PAR AGONISTS ON ENDOTHELIAL CELL DETACHMENT	133
FIGURE 59 - CONFIRMATION OF KNOCKDOWN OF PAR-1 AND PAR-2 BY mRNA LEVELS	134
FIGURE 60 - CONFIRMATION OF PAR-1 KNOCKDOWN BY FLOW CYTOMETRY	134
FIGURE 61 - KNOCKDOWN OF PAR-1 AND PAR-2 DOES NOT REDUCE vWf RELEASE	136
FIGURE 62 - PR3 MEDIATED vWf RELEASE FOLLOWING INHIBITION OF PKC	139
FIGURE 63 - HLE MEDIATED vWf RELEASE FOLLOWING INHIBITION OF PKC	139
FIGURE 64 - EFFECT OF PKC INHIBITOR ON MITOCHONDRIAL ACTIVITY	140
FIGURE 65 - CONFIRMATION OF THE PKC INHIBITOR BY MEASURING SUPEROXIDE PRODUCTION	140
FIGURE 66 - PR3 MEDIATED vWf RELEASE FOLLOWING INHIBITION OF PKA	141
FIGURE 67 - HLE MEDIATED vWf RELEASE FOLLOWING INHIBITION OF PKA	141
FIGURE 68 - EFFECT OF PKA INHIBITOR ON MITOCHONDRIAL ACTIVITY	142
FIGURE 69 - PR3 MEDIATED vWf RELEASE FOLLOWING INHIBITION OF CALMODULIN	143
FIGURE 70 - HLE MEDIATED vWf RELEASE FOLLOWING INHIBITION OF CALMODULIN	143
FIGURE 71 - EFFECT OF CALMODULIN INHIBITOR ON MITOCHONDRIAL ACTIVITY	144
FIGURE 72 - PR3 MEDIATED vWf RELEASE FOLLOWING INHIBITION OF PI3K	145
FIGURE 73 - HLE MEDIATED vWf RELEASE FOLLOWING INHIBITION OF PI3K	145
FIGURE 74 - EFFECT OF PI3K INHIBITOR ON MITOCHONDRIAL ACTIVITY	146
FIGURE 75 - CONFIRMATION OF THE PI3K INHIBITOR BY MEASURING NEUTROPHIL DEGRANULATION	146
FIGURE 76 - INHIBITION OF ACTIN POLYMERISATION BY CYTOCHALASIN B	147
FIGURE 77 - CONFOCAL STAINING FOR vWf AND F-ACTIN	149
FIGURE 78 - vWf RELEASE BY OKADAIC ACID	152
FIGURE 79 - CRYSTAL VIOLET OF OKADAIC ACID DOSE CURVE	152
FIGURE 80 - EFFECTS OF OKADAIC ACID ON PR3 AND HLE MEDIATED vWf RELEASE	153
FIGURE 81 - MITOCHONDRIAL ACTIVITY AFTER OKADAIC ACID TREATMENT	153
FIGURE 82 - WESTERN BLOT FOR TYROSINE PHOSPHORYLATION	156
FIGURE 83 - WESTERN BLOT FOR SERINE/THREONINE PHOSPHORYLATION	157
FIGURE 84 - NEUTROPHIL ADHESION TO TNF α TREATED ENDOTHELIAL CELLS	159
FIGURE 85 - NEUTROPHIL ADHESION TO PR3/HLE TREATED HUVEC	161
FIGURE 86 - NEUTROPHIL ADHESION TO PR3/HLE TREATED GENC	161
FIGURE 87 - INHIBITION OF NEUTROPHIL ADHESION TO HUVEC BY α 1AT	162
FIGURE 88 - INHIBITION OF NEUTROPHIL ADHESION OF GENC BY α 1AT	162
FIGURE 89 - OPTIMISATION OF E-SELECTIN ELISA	165
FIGURE 90 - E-SELECTIN EXPRESSION ON HUVEC FOLLOWING SERINE PROTEASE TREATMENT	166
FIGURE 91 - E-SELECTIN EXPRESSION ON GENC FOLLOWING SERINE PROTEASE TREATMENT	166
FIGURE 92 - OPTIMISATION OF ICAM-1 ELISA	168
FIGURE 93 - ICAM-1 EXPRESSION ON HUVEC FOLLOWING SERINE PROTEASE TREATMENT	169
FIGURE 94 - ICAM-1 EXPRESSION ON GENC FOLLOWING SERINE PROTEASE TREATMENT	169
FIGURE 95 - OPTIMISATION OF VCAM-1 ELISA	171
FIGURE 96 - VCAM-1 EXPRESSION ON HUVEC FOLLOWING SERINE PROTEASE TREATMENT	172
FIGURE 97 - VCAM-1 EXPRESSION ON GENC FOLLOWING SERINE PROTEASE TREATMENT	172
FIGURE 98 - BLOCKING PSGL-1 ON NEUTROPHILS INHIBITS ADHESION TO HUVEC	174
FIGURE 99 - BLOCKING PSGL-1 ON NEUTROPHILS INHIBITS ADHESION TO GENC	174
FIGURE 100 - BLOCKING CXCR1 AND CXCR2 ON NEUTROPHILS INHIBITS ADHESION TO HUVEC	176
FIGURE 101 - BLOCKING CXCR1 AND CXCR2 ON NEUTROPHILS INHIBITS ADHESION TO GENC	176
FIGURE 102 - SERINE PROTEASES CAUSE DISEASE PROPAGATION BY SUPPORTING INFLAMMATORY PROCESSES	203

Table of Tables

TABLE 1 - SUMMARY OF ANCA-ASSOCIATED SMALL VESSEL VASCULITIDES.....	2
TABLE 2 - OVERVIEW OF NEUTROPHIL GRANULAR CONTENTS.....	12
TABLE 3 - SUMMARY OF FUNCTIONS OF PR3 AND HLE.....	16
TABLE 4 - DIFFERENT SUBSETS OF MACROPHAGES.....	26
TABLE 5 - CONSTITUENTS OF ENDOTHELIAL GROWTH MEDIUM-2-MICROVASCULAR (EGM-2-MV).....	50
TABLE 6 - CONSTITUENTS OF COMPLETE MEDIUM199.....	50
TABLE 7 - TNF- α DILUTIONS.....	55
TABLE 8 - PRIMARY ANTIBODIES FOR ELISA.....	56
TABLE 9 - CONSTITUENTS OF CARBONATE BUFFER.....	60
TABLE 10 - PCR PROGRAMME FOR REVERSE TRANSCRIPTION.....	61
TABLE 11 - PCR PROGRAMME FOR vWf AMPLIFICATION.....	62
TABLE 12 - PRIMARY ANTIBODIES FOR IMMUNOCYTOCHEMISTRY.....	64
TABLE 13 - CONSTITUENTS OF TBS pH 7.6.....	66
TABLE 14 - ANTIBODIES FOR PAR FLOW CYTOMETRY.....	70
TABLE 15 - INHIBITORS USED FOR vWf RELEASE.....	71
TABLE 16 - CONSTITUENTS OF NP40 LYSIS BUFFER.....	74
TABLE 17 - ANTIBODIES USED FOR WESTERN BLOTTING.....	75
TABLE 18 - NUMERICAL DATA FOR APOGLOW® ASSAY AT 2 HOURS.....	87
TABLE 19 - NUMERICAL DATA FOR APOGLOW® ASSAY AT 24 HOURS.....	87
TABLE 20 – TAQMAN® REVERSE TRANSCRIPTION MASTERMIX.....	216
TABLE 21 - PCR MASTERMIX.....	216
TABLE 22 - REAL-TIME PCR MASTERMIX.....	217
TABLE 23 - GEL RECIPES.....	217
TABLE 24 - CONSTITUENTS OF WESTERN BLOT RUNNING BUFFER.....	218
TABLE 25 - CONSTITUENTS OF WESTERN BLOT TBS-T.....	218
TABLE 26 - CONSTITUENTS OF WESTERN BLOT TRANSFER BUFFER.....	218
TABLE 27 - CONSTITUENTS OF SDS-PAGE LOADING BUFFER.....	219
TABLE 28 - CONSTITUENTS OF COOMASSIE STAIN/DESTAIN.....	219

1. An Introduction to ANCA-Associated Vasculitis

1.1 Vasculitic Glomerulonephritis

Vasculitis is defined as the inflammation and consequent necrosis of blood vessel walls. It consists of a group of diseases that can be localised or systemic, although currently there is no robust way of classification. In one system, vasculitides are classified by the size of the vessel predominantly affected [1, 2], however this system disregards the overlap that may occur between the groups (reviewed in [3]).

The small vessel vasculitides are of particular interest, and include Wegener's granulomatosis, microscopic polyangiitis and Churg-Strauss syndrome. These disorders are commonly associated with the presence of anti-neutrophil cytoplasm antibodies (ANCA) directed at antigens within the cytoplasmic granules of neutrophils and monocytes. ANCA-associated systemic vasculitides (ASV) usually affect small vessels of the vasculature, including the arterioles, venules and capillaries; however, they can sometimes affect larger arteries. Although multiple organs can be affected, the pulmonary and renal circulations are preferentially targeted. ASV share common pathological features, including the development of focal necrotizing lesions within the glomerulus of the kidney, which may progress to cause acute renal failure (reviewed in [4]). In Wegener's granulomatosis (WG) approximately 80% of patients present renal involvement at some point during their illness, with over 90% of patients also displaying some form of upper respiratory tract disease, which can progress to pulmonary haemorrhage. Although, other systems may also be involved [5] (see table 1 for more detail). Taken together, ASV have a combined incidence

of 20 per million individuals per year in the UK, with a mean age of 59 (interquartile range 47 - 70 years) [6-9]. The presence of autoantibodies in ASV allows us to describe the associated conditions as autoimmune diseases which is more rigorously backed up by observation that ANCA are directly pathogenic to the neonate after transfer across the placenta [10] and by the observation that vasculitis can be induced in naïve animals following transfer of ANCA IgG [11, 12].

Table 1 - Summary of ANCA-Associated Small Vessel Vasculitides

	Wegener's Granulomatosis	Microscopic Polyangiitis	Churg-Strauss Syndrome
ANCA	Present in 80-90% cases 90% PR3-ANCA 10% MPO-ANCA	Present in 50-70% cases 10% PR3-ANCA 80% MPO-ANCA	Present in 35-45% cases 10% PR3-ANCA 75% MPO-ANCA
Vessels Affected	Small-medium vessels	Small-medium vessels	Small vessels
Histology	Necrotising vasculitis Granulomatous Inflammation	Necrotising vasculitis No Granulomas	Necrotising vasculitis Eosinophilic Infiltrate Extravascular Granulomas
Primary Organ Involvement	Otolaryngeal (ENT) 80-90% Pulmonary 50-80% Renal 50-80% Articular 50-80%	Renal 90-100% Articular 30-70% Skin 40-70%	Pulmonary 96-100% Otolaryngeal 50-80% Skin 50-80% Axonal Peripheral Neuropathy 70%
Average Age	47 years	49 years	47 years
Sex	54% Male	59% Male	51% Male

Adapted from Puechal 2007 [13]

Clinically, disease activity is assessed by two main systems, the Birmingham vasculitis activity score (BVAS) and the vasculitis damage index (VDI). ANCA-associated vasculitis is currently being treated by a cocktail of drugs, including steroids and immunosuppressive agents, which, although having successfully increased the survival rate from 20% survival at 2 years to 80% survival at 5 years, have transformed ASV into a relapsing remitting disease. Additionally, this treatment has been associated with high morbidity and mortality rates due to infection, neoplasm and other complications, with 25% of patients displaying treatment-

associated adverse effects [14]. It is therefore important that research into the underlying issues of ASV and the development of new effective treatments with improved safety profiles be undertaken.

1.2 Anti-Neutrophil Cytoplasmic Antibodies and their Antigens

ANCA were first described in eight patients diagnosed with glomerulonephritis by Davies *et al.*, 1982, who identified IgG antibodies in serum that stained the cytoplasm of neutrophils [15]. This discovery has prompted much interest into the involvement of ANCA in small vessel vasculitides. ANCA are autoantibodies directed predominantly at the components of the primary granules in neutrophils, and lysosomes in monocytes (reviewed in [3]). They are present in 90% of patients with pauci-immune vasculitis where there is little deposition of immune proteins within lesions. It has been suggested that ANCA play an important role in the pathogenesis of ASV by inducing the activation of ANCA-antigen expressing cytokine-primed neutrophils and monocytes [16, 17], although it remains unclear why ANCA production is initially induced. It has previously been demonstrated that ANCA levels can correlate with vasculitic disease activity and severity, and that changes in ANCA titres may reflect changes in disease activity [18, 19]. The two classes of ANCA, cytoplasmic and perinuclear, were first recognised by the differences in their immunofluorescence staining pattern. Falk *et al.*, 1988 demonstrated that c-ANCA produced a granular cytoplasmic staining pattern on ethanol fixed granulocytes, whilst p-ANCA produced a perinuclear staining pattern [20]. It has been demonstrated that both p- and c-ANCA will activate neutrophils *in vitro*, resulting in degranulation and the production of reactive oxygen species (ROS) [16].

There are two clinically relevant ANCA-antigens; these are Proteinase 3 (PR3) and Myeloperoxidase (MPO) (reviewed in [13]). More recently, lysosomal membrane protein-2 (LAMP-2) has been speculated as another target of ANCA, although this is awaiting independent clinical validation. LAMP-2 was first identified as a target for ANCA in 1995 by Kain *et al.*, who immunoblotted neutrophil proteins with patient ANCA [21]. These autoantibodies are suggested to co-exist with PR3- and MPO-ANCA in almost all patients (>90%) with ANCA mediated glomerulonephritis, and have been shown to activate neutrophils *in vitro* and induce endothelial cell injury [22]. The upregulation of LAMP-2 to the neutrophil surface is suggested to mediate adhesion to endothelial E-Selectin [23, 24]. Interestingly, in neutrophils LAMP-2 is expressed in the membrane of the PR3 and MPO containing alpha granules [22].

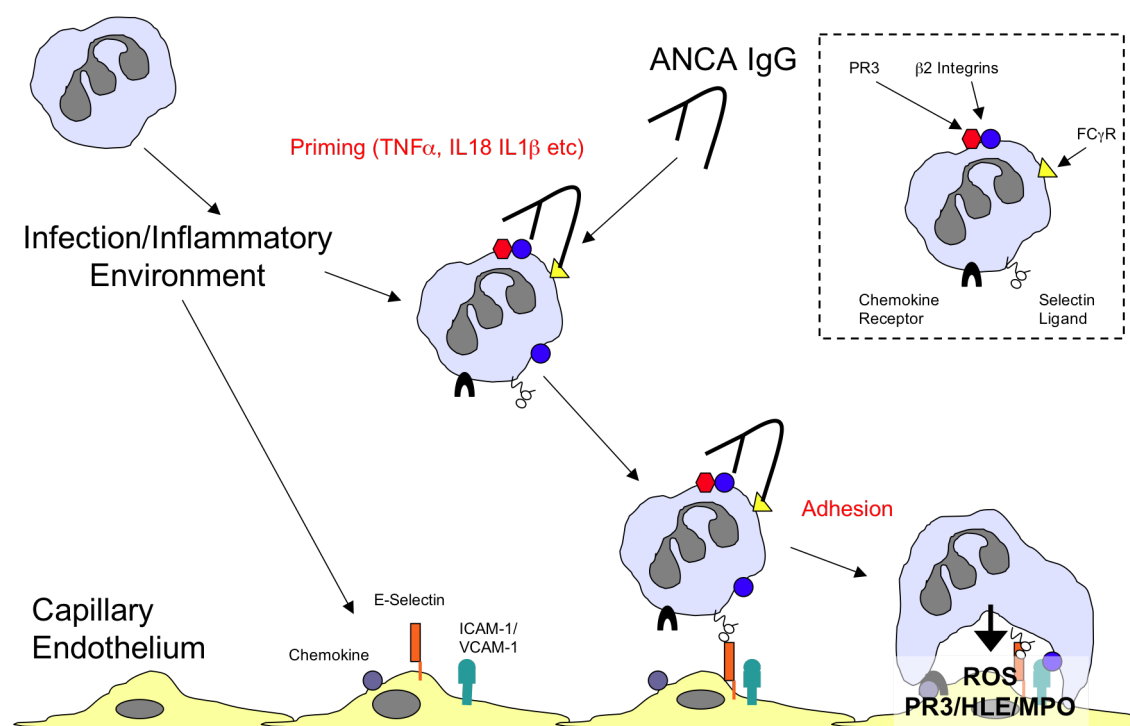
PR3 is the major target of c-ANCA. The development of autoantibodies directed at PR3 is usually associated with Wegener's granulomatosis [25, 26], whereas p-ANCA antibodies directed against MPO are more commonly associated with microscopic polyangiitis and Churg-Strauss syndrome [20, 27-29]. A possible explanation for the development of ANCA is that in "normal" circumstances, PR3 and MPO are quickly scavenged upon release from the cell, however, following neutrophil priming with inflammatory cytokine Tumour Necrosis Factor- α (TNF α) their expression is increased on the cell surface [30, 31], thereby allowing them to be targeted by the non-tolerized immune system and potentially resulting in the production of autoimmune antibodies. However, this may be an over simplistic view. Certainly, ANCA binding to the surface of neutrophils induces excessive respiratory burst and the subsequent release of granule enzymes and cytokines from the cell [16], resulting in an inflammatory response and endothelial cell damage.

1.3 Aetiopathogenesis of Vasculitis

Although the exact underlying mechanism of vasculitis remains unknown, it is hypothesised that infection and an enhanced inflammatory environment leads to an upregulation of ANCA-antigen, PR3, on the surface of the neutrophil [16] (see figure 1). This phenomenon has previously been demonstrated *in vitro*, in which, neutrophil priming with TNF α resulted in the increased expression of surface bound PR3 [30, 31]. This membrane expressed PR3 has been demonstrated to co-localise with the expression of β_2 integrin CD11b/CD18 [32], and the ligation of CD11b/CD18 is essential for activation of the neutrophil by ANCA [33]. ANCA can bind to the membrane expressed PR3/ β_2 integrin on the surface of neutrophils [34] by its Fab₂ domain, whilst the ANCA Fc portion cross-links the Fc γ receptor on the surface of neutrophils [35-37] inducing reactive oxygen species production and degranulation [16]. Together these result in the induction an inflammatory response and endothelial cell damage [38-40]. The activation of the neutrophil by ANCA requires binding of both its Fab₂ and Fc domains [41-43].

It is hypothesised that ASV patients may display an increased expression of membrane PR3, which may allow for recognition by ANCA [44, 45]. A second explanation may be due to a loss of epigenetic silencing of MPO/PR3 genes and consequent abnormal gene transcription and expression [46]. The mRNA level of MPO/PR3 correlates with disease activity in patients displaying unregulated expression during active disease [47].

Figure 1 - Hypothesised Mechanism of ANCA Vasculitis



Increased neutrophil priming and activation of the endothelial monolayer are required for the development of ANCA associated vasculitis. Neutrophil priming and the consequent surface expression of PR3/MPO allow for activation by ANCA. This unnecessary neutrophil activation results in the direct injury to the vascular endothelium associated with vasculitis.

It is proposed that activation of the alternative complement pathway may be involved in disease propagation. Xiao *et al.*, 2007 demonstrated that the binding of ANCA to neutrophils resulted in the release of mediators that resulted in activation of the complement pathway and hence amplification of the inflammatory response. Incubation of normal human serum with ANCA-IgG alone did not result in complement activation. They further identified a requirement for complement in the induction of MPO-ANCA induced glomerulonephritis (GN) by the absence of GN development in complement deficient mice [48]. Mellbye *et al.*, also demonstrated an ability of c-ANCA treated neutrophils to induce complement activation, and identified complement C5b-C9 complex, termed the membrane attack complex (MAC), depositions in 50% of the sera [49]. Activation of the alternative complement pathway causes the activation and cleavage of C3. Whilst C3a is involved in

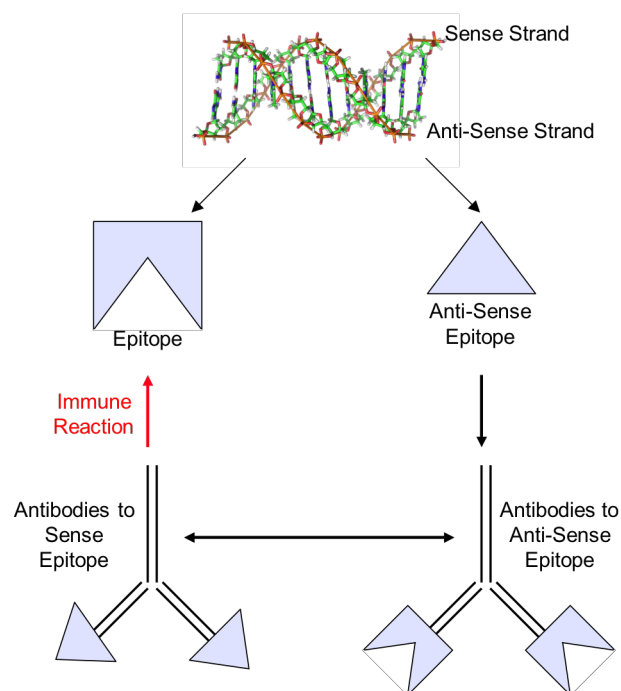
chemotaxis and mast cell degranulation, C3b acts to further enhance the immune response by cleavage of C5 into C5a, a potent neutrophil chemoattractant. The effects of the complement pathway in ASV can be inhibited by blocking antibodies directed towards C5 receptors [50]. Interestingly, mice deficient for C5 are resistant to the development of non-crescentic glomerulonephritis by MPO-ANCA [48]. Furthermore, deposition of the C5b-C9 complex has been identified in fibrous glomerular crescents, whilst tubular interstitial C5b-C9 expression was correlated with plasma creatinine levels and was predictive of renal outcome [51].

Another important field of research has been the investigation into the development of ANCA. Currently there is still much debate over the differing theories. The auto-antigen complementarity theory proposes that complementary proteins may initiate an immune response, from which the anti-idiotypic counter response cross-reacts with PR3/MPO to produce ANCA [52] (see figure 2). The source of this complementary protein is much debated, with some suggesting complementary or mimicking peptides produced and expressed by invading pathogens, whilst the aberrant anti-sense (non-coding) transcription of human PR3/MPO is another possibility.

A second theory suggests that neutrophil extracellular traps (NETs) act as a platform for PR3 to initiate an autoimmune reaction. NETs are made up of fibrous chromatin, DNA and protein deposits, which can trap and bind bacteria. Furthermore, NETs have been shown to degrade virulent peptides and actively kill bacteria [53]. ANCA has been demonstrated to induce the release of NETs containing PR3 and MPO, which can be deposited in the kidney [54]. The release of NETs is dependant upon the neutrophil generation of reactive oxygen species, as the catalytic conversion of hydrogen peroxide into water and dioxygen

completely inhibits the release of NETs [55]. The release of NETs containing the ANCA-antigens is well suited for identification by autoreactive B-Cells [56].

Figure 2 - The Theory of Antigen Complementarity

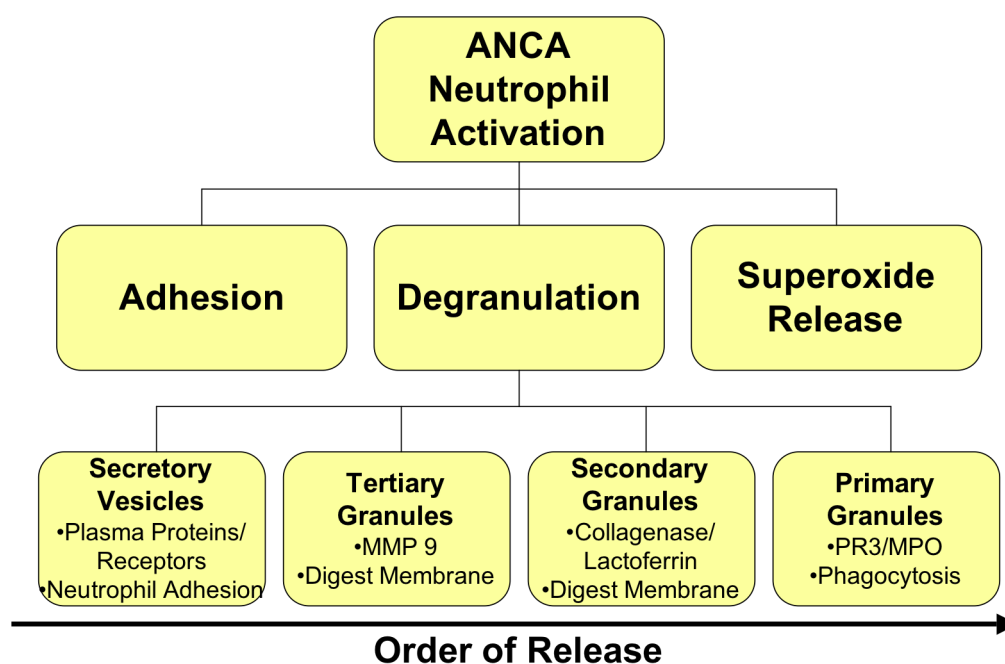


The theory of antigen complementarity requires an initial immune reaction directed against the complementary peptide, in which anti-idiotypic antibodies are produced. Antibodies directed at these anti-idiotypic antibodies can also recognise and interact with the peptide, for example PR3, and induce an immune reaction.

There have been a host of environmental triggers linked to the development of ANCA. Firstly, it was noted that there was an increased incidence of nasal carriage of *Staphylococcus Aureus* in patients with Wegener's granulomatosis compared to healthy controls [57, 58]. Moreover, antibiotic treatment with a combination of trimethoprim and sulfamethoxazole proved beneficial in reducing the rate of relapse in WG patients [59]. Secondly, a link between anti-thyroid treatment and the development of ANCA-vasculitis has been identified. The presence of ANCA in patients receiving long-term propylthiouracil

(PTU) treatment was first demonstrated by Stankus and Johnson in 1992, who described a 72-year old woman with respiratory failure and haemoptysis [60].

Figure 3 - ANCA-Mediated Neutrophil Activation



Activation of neutrophils by ANCA binding results in aberrant neutrophil degranulation as well as increased adhesion to the vascular endothelium and generation of reactive oxygen species. ANCA-mediated neutrophil degranulation results in the release of primary (or azurophilic) granular contents that are normally involved in digestion of phagocytosed pathogens.

Of the patients receiving anti-thyroid treatment, for illnesses such as Graves disease, 88% of those who developed ANCA associated vasculitis were taking PTU as a long-term therapy (>18 months), although ANCA was also present with treatment with other medication, including Carbimazole [61]. Interestingly, 7 of the 8 patients included in the Gunton *et al.*, study, developed ANCA directed at neutrophil MPO. This appears to be a common feature with multiple independent researchers reporting the presence of p-ANCA [62-64]. The development of ANCA against MPO following PTU treatment may be the result of its ability

to enter neutrophils and alter the configuration of MPO [65]. More recently a link between silica dust exposure and the development of ANCA vasculitis has been identified (odds ratio 4.43), whilst pesticide exposure also had an increased odds ratio (2.32) [66]. This association with silica dust was first identified by Gregorini *et al.*, in 1993 using a cohort of 16 ANCA-positive patients and 32 controls [67], with this observation being repeatedly reported from different groups [66, 68, 69].

A genetic risk factor for the development of Wegeners' granulomatosis has been identified in first-degree relatives, although occurrence is low (relative risk 1.56). The relative risk of WG in the children of WG patients is 2.56 [70]. Moreover, the PRTN3 gene, which encodes neutrophil PR3, may be involved in the increased expression of membrane bound PR3 observed in ASV patients [71]. It has been demonstrated that there are populations of neutrophils expressing either low or high membrane PR3. The presence of this high membrane PR3 expressing neutrophil population is significantly increased in patients with ASV (85%) compared to healthy controls (55%) [72]. Witko-Sarsat *et al.*, also demonstrated a genetic disposition to the inheritance of either low or high membrane PR3 over three generations of 2 families. This observation of increased membrane PR3 has been reported by other groups [45, 73], who also further confirmed a genetic factor by demonstrating that high membrane PR3 was strongly correlated in monozygotic twins ($r=0.99$) but not in dizygotic twins ($r=0.06$) [45]. Furthermore, the increased membrane expression of PR3 on neutrophils significantly correlates with an increase rate of relapse [73].

1.4 The Neutrophil

The polymorphonuclear leukocyte (PMN) was first described by Paul Ehrlich in 1900. Neutrophils are the predominant cell of the innate immune system, accounting for approximately 60% of the total leukocyte pool in humans, with on average 3 to 6 million cells per millilitre of blood in healthy individuals. They are short-lived cells, circulating in the blood for around 12 hours prior to migration into tissues, following stimulation, where they can survive for up to a further 5 days. Neutrophils play an important role in the rapid development of defence mechanisms against invading microbial pathogens, particularly during a bacterial infection. These antimicrobial actions of neutrophils involve the phagocytosis of the invading pathogen, and/or the degranulation and release of microbicidal molecules from intracellular granules. The granules present within the neutrophil were originally classified on the presence of MPO (reviewed in [74]), thus producing two groups that became known as the primary granules, described as spherical, and the secretory specific granules, which appear more irregular in shape [75]. It has been suggested that the specific granules are involved in the mediation of an inflammatory response [76], whereas the primary granules are more associated with the antimicrobial actions following phagocytosis [77, 78]. The neutrophil primary granules are formed from the golgi apparatus during the maturation of the cell from a myeloblast into a promyeloblast, whilst the specific granules are formed later in development during the myelocyte stage [75, 79]. As research has progressed it has been established that the granules can be sub-classified on the presence of intragranule proteins (reviewed in [74]). The primary granules, which are positive for MPO, can be either positive or negative for defensin, whilst the specific granules have been further classified as secondary, lactoferrin positive, or tertiary, gelatinase positive, granules; with another group known as the secretory vesicles added to the classifications [80-82].

Exocytosis of the granular content following elevation of intracellular Ca^{2+} [83, 84], involves the fusion of the vesicle membrane with, and incorporation into, the plasma membrane. Therefore, proteins present on the inner membrane of the vesicle will become expressed on the surface of the cell [85-87]. It has been shown that the mobilisation of the neutrophil secretory vesicles is mediated by signalling through selectin molecules [88, 89] or in response to inflammatory mediators such as Histamine or Loxosceles venom [90, 91].

Table 2 - Overview of Neutrophil Granular Contents

	Secretory Granules	Teritary Graules	Secondary Granules	Primary Granules
Other Names	Secretory vesicles	Gelatinase graules	Specific granules	Alpha granules Azurophilic granules
Main Constituents	CR1 Mac-1 (CD11b/CD18) FPR CD14 CD16 Proteinase 3 Cytochrome b588 Plasma proteins	Gelatinase (MMP9) Lysozyme Leukolysin NRAMP1 Cytochrome b588	Lactoferrin Cathelicidin Lysozyme Collagenase Leukolysin Cytochrome b588 NGAL	Myeloperoxidase Elastase Cathepsin G Proteinase 3 Azurocidin Bacterial Permeability-increasing protein Defensins
Primary Function	Neutrophil adhesion	Breaks down collagen & basement membrane	Breaks down collagen & basement membrane	Digests engulfed pathogens/debris Bacteriocidal

The antimicrobial actions of the neutrophil involves two separate mechanisms. Firstly there is the generation and release of reactive oxygen species (ROS), which results in direct injury to pathogens, and secondly the neutrophil can release enzymatic or antimicrobial proteins from the intracellular granules. Both the peroxidase positive and negative granules have been shown to be required for the release of reactive oxygen species from neutrophils. The primary granules contain MPO, which converts hydrogen peroxide (H_2O_2), a product of NADPH oxidase, into hypochlorous acid [92], whilst the peroxidase negative granules

contain flavocytochrome b₅₅₈, a component of the NADPH oxidase molecule [93]. ROS have also been implicated, along with human leukocyte elastase (HLE), to be involved in the conversion of gelatinase and collagenases from their pro-form into active proteases, which can inflict damage onto the invading pathogen [94-96].

1.5 The Neutrophil Serine Proteases

There are four families of proteinases; serine, cysteine, aspartic and metallo, defined by the most prominent functional group in the enzymes active site. The serine proteases cleave peptides by the formation of a covalent tetrahedral state to form two smaller peptides [97]. HLE and PR3 are chymotrypsin-like serine proteases found in the neutrophil primary granules, which are released following neutrophil degranulation. These proteases have the ability to degrade components that make up the extracellular matrix. PR3, a 29kDa glycoprotein, was first described in 1978 by Baggiolini *et al.* [98], and has since been identified as a key target in ASV [26, 99]. It has been demonstrated to degrade elastin *in vitro*, resulting in tissue damage to the lungs when administered to hamsters via inhalation [100], and is suggested to have serine protease, antibiotic and myeloblastic activity [25, 101, 102]. PR3 exhibits high sequence homology with HLE, demonstrated by Rao *et al.*, 1991 [103] by analysis of the first 40 residues having approximately 60% homology, whilst the first four N-terminal residues are identical to HLE. They also reinforced the idea that PR3 was the antigenic target for c-ANCA by confirming that the first 20 residues of PR3 were identical to that of the proposed target antigen. The high sequence homology between PR3 and HLE posed the question as to whether HLE also plays a role in ASV. Tervaert *et al.*, 1993 tested for the presence of HLE autoantibodies in patient serum samples by enzyme

linked immunosorbent assay (ELISA), and identified patients that were positive for HLE with a p-ANCA staining pattern. PR3, however, did not test positive in these patients and there were no positive HLE serum with a c-ANCA pattern [104]. This proposes that PR3 and HLE are not targeted by the same antibodies. More recently HLE was again identified as a target for p-ANCA by the presence of HLE-ANCA following the injection of rats with syngenic apoptotic neutrophils [105]. Although they may be targeted by separate antibodies, both PR3 and HLE are released from neutrophil primary granules simultaneously, and have been shown to induce apoptosis of endothelial cells via chromatin condensation and DNA fragmentation [106], hence, PR3, in particular, may be both a target for autoantibodies and an important mediator of endothelial injury. A key area of interest is the effect of the neutrophil granule contents, including the serine proteases, on the vascular endothelium following neutrophil degranulation. It is believed that ANCA activated neutrophils become trapped and inappropriately activated in the small vessels, thereby releasing granular contents directly onto the microvasculature.

PR3 is shown to promote endothelial apoptosis, as well as inducing chemokine ligand-8 (CXCL8) production, a chemotactic factor for neutrophils [107], and promoting monocyte chemoattractant protein-1 (MCP-1) expression by endothelial cells, thereby resulting in increased monocyte recruitment [108]. It is suggested that treatment with PR3 can result in the increased expression of intercellular adhesion molecule-1 (ICAM-1) and vascular cell adhesion molecule-1 (VCAM-1) on endothelial cells, resulting in increased static adherence of neutrophils to the vascular walls via an ICAM-1/ β 2 integrin interaction [108, 109], whilst PR3-ANCA is also suggested to increase VCAM-1 expression [110].

Although stored in the primary granules, PR3 is also stored in the secretory granules and so can be easily mobilised to the neutrophil surface following gentle stimulation [111]. These

granules are released from the neutrophil during adhesion to the endothelial membrane. PR3 has been demonstrated to degrade matrix proteins [112], which may aid neutrophil trafficking. Other physiological roles of PR3 include cytokine/chemokine cleavage, for example cleavage of CXCL8 to a more active form to enhance neutrophil recruitment [113]. As well the amplification of CXCL8 activity, PR3 and HLE has a host of effects on chemokine activity during inflammation. Both serine proteases have been implicated in the fragmentation and inactivation of IL-6 at sites of inflammation [114, 115], thereby promoting a negative feedback loop against further inflammation and prevention of the acute phase response [116]. Interestingly, however, IL-6 possesses both pro- and anti-inflammatory properties and is also involved in the induction of immuno-suppressive agents. HLE is also reported to cleave and inactivate IL-2. This cleavage of IL-2 results in the formation of three products, one of which naturally antagonises the proinflammatory adhesive properties of IL-2 [117]. Unlike PR3, HLE can induce the inactivation of TNF α and CXCL8 [118-121], whilst PR3 acts to convert the inactive precursors of TNF α and IL-1 β into functional cytokines [122, 123].

One of the key functions of the neutrophil serine proteases is their ability of intralysosomal degradation of engulfed cell debris and microorganisms. HLE mediates its bactericidal effects by degrading the bacterial cell wall, thereby facilitating the entry of other antimicrobial agents [124]. HLE also potentiates the antibiotic effects of cathepsin G and MPO, as well as the lytic activity of lysozyme [124-126]. PR3 had been demonstrated to have microbicidal effects against both gram-negative and gram-positive bacteria [127].

Table 3 - Summary of Functions of PR3 and HLE

	Proteinase 3	Human Leukocyte Elastase
Abbreviation	PR3	HLE
Protein Size	222 amino acids 29kDa [103]	218 amino acids 30kDa [128]
Concentration	3.24pg/cell (\pm 0.24 SD) [129]	1-3pg/cell [113, 130-132]
Location in Neutrophil	Primary (azurophilic/alpha) granules Secretory vesicles [111]	Primary (azurophilic/alpha) granules [111]
Functions	Intralysosomal proteolysis Degradation of matrix proteins [100] Microbicidal [127] Induction of apoptosis [106] Increased adhesion molecule expression [108]	Intralysosomal proteolysis Degradation of matrix proteins [100, 133] Anti-Microbial [124, 125, 134] Induction of apoptosis [106]
Roles in Apoptosis	Detachment and cytolysis [135] Internalisation [136, 137] DNA fragmentation [106] Nuclear fragmentation [136] Chromatin condensation [106] Stops cell cycle at G ₀ /G ₁ phase [136] Cleavage of p21 ^{Waf1} [138] Proapoptotic signalling through JNK and p38 MAPK [137]	Detachment and cytolysis [135] Internalisation [137] DNA fragmentation [106] Chromatin condensation [106] Proapoptotic signalling through p38 MAPK [137]
Cytokine Interactions	Inactivation of IL-6 and IL-2 [115, 139] Activation of IL-1 β , TNF α and IL-18 [122, 123, 140] Amplification of CXCL8 [113]	Inactivation of TNF α , IL-6, CXCL8 and IL-2 [114, 115, 117-121] Receptor shedding of IL-2R α , TNF- RII and IL-6R [139, 141] Processing of TGF- α [142]

1.6 PR3 and Endothelial Apoptosis

Neutrophil serine proteases, PR3 and HLE, were initially suggested to induce endothelial cell detachment and cytolysis [135], however, further research into this has unveiled a role for these proteases in apoptosis. Endothelial treatment with PR3 and HLE was demonstrated to increase DNA fragmentation at concentrations of 1 μ g/ml, whilst visualisation of these cells confirmed an apoptotic role for PR3 and HLE [106]. PR3 can traverse the endothelial cell membrane and consequently induce cell apoptosis [136]. Both the catalytically active

and inactive forms of PR3 have been shown to induce endothelial cell apoptosis. Inactive PR3 causes apoptosis within 24 hours [136] possibly due to interactions at the C-terminal region of the peptide [138], whilst active PR3 results in cleavage and consequent inactivation of nuclear factor- κ B (NF κ B) and sustained activation of Jun N-terminal kinase (JNK) [137].

More recently PR3 has been demonstrated to enter endothelial cells and cleave p21^{Waf1} [138]. p21^{Waf1} is a major determinant of cell fate, primarily involved in the regulation of the cell cycle [143]. p21^{Waf1} is potent inhibitor of G1 cyclin-cyclin dependant kinase (CDK) activity. The CDKs are required for the transition from the G1 phase, growth and biosynthetic activity of the cell, to the S phase, DNA synthesis in preparation for mitosis, of the cell cycle. In particular p21^{Waf1} inhibits the actions of CDK2 and CDK4. The cleavage of p21^{Waf1} by caspase 3 is required for endothelial cell apoptosis. Cleavage of endothelial p21^{Waf1} by PR3 results in the loss of p21^{Waf1} from the cytoplasm and from CDKs [138]. This cleavage does not occur following HLE treatment in *in vitro* cellular models [144].

1.7 Alpha-1 Antitrypsin: A Serine Protease Inhibitor

Alpha-1 antitrypsin (α 1AT) is a natural inhibitor for the neutrophil serine proteases [145]. α 1AT is a small globular glycoprotein that can readily diffuse throughout interstitial fluids. It is primarily produced by liver hepatocytes [146], although there is evidence that α 1AT can also be produced by macrophages, monocytes, and lung alveolar epithelial cells [147-150]. The production of α 1AT by monocytes and macrophages is only about 0.15% of that produced in the liver [151]. α 1AT is one of the most abundant serine protease inhibitors

(serpin), with an average plasma concentration of 1.3mg/ml in healthy individuals. α 1AT is an acute phase protein, and plasma concentrations can increase 2-4 fold upon inflammation [152, 153]. One of the most potent stimuli for α 1AT production in hepatocytes is interleukin-6 (IL-6), via signalling through nuclear factor interleukin-6 (NF-IL6) or JAK/STAT pathways [149, 154]. As well as stimulation of α 1AT production by IL-6, release from monocytes, macrophages and lung epithelial cells can also be induced by lipopolysaccharide (LPS), IL-1 β and TNF α [150, 155, 156].

Although α 1AT is a general serine protease inhibitor, its prime targets are the neutrophil proteases, in particular HLE. Importantly, α 1AT is involved in the protection of the lower respiratory tract from HLE [157, 158], for instance in the prevention of emphysema. α 1AT prevents the enzymatic actions of HLE by the rapid formation of an irreversible 1:1 complex, which renders the serine protease inactive until it can be removed from the circulation. Further investigation has proposed that this α 1AT:HLE complex may also have a role in neutrophil chemotaxis, itself acting as a chemoattractant molecule [159]. Recently, a defective α 1AT allele (piZ), which results in the loss of functional protein, has been identified at an increased frequency in patients with ANCA-associated vasculitis [160-163].

1.8 Neutrophils in Inflammation: The Process of Transmigration

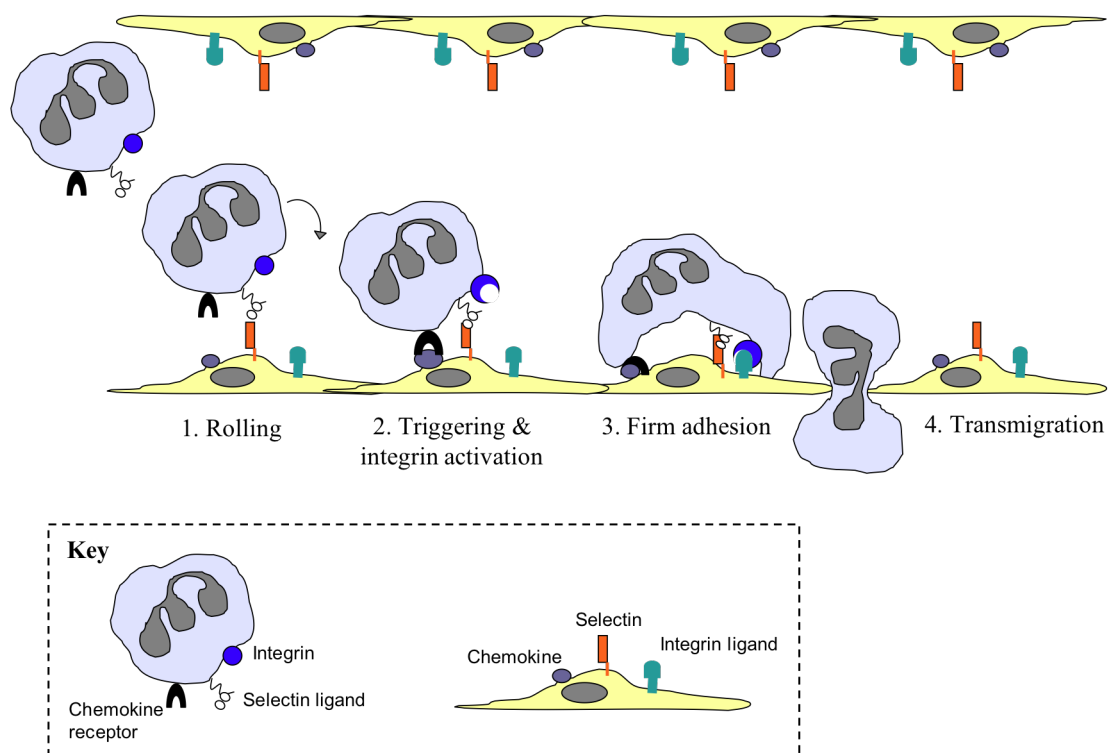
Serine proteases play important roles in a host of physiological processes, of which, we are particularly interested in their roles during leukocyte recruitment from the circulation previously discussed by Henson *et al.*, 1987 [164]. Recently there has been much interest

into the development of an animal model for vasculitis. Two key publications have both reported an increase in leukocyte transmigration *in vivo* in an MPO-model of vasculitis. Nolan *et al.*, 2008 treated mice with anti-MPO IgG directed at murine MPO on chemokine ligand-1 (CXCL1) (also known as keratinocyte derived chemokine (KC) and Gro α) stimulated leukocytes, thereby demonstrating an increased conversion of rolling leukocytes into firmly adherent and transmigrated leukocytes across the vascular endothelium [165]. The other important study reported that intramuscular injection of MPO IgG, thereby inducing production of anti-MPO antibodies directed at rat leukocytes, resulted in increased adhesion and transmigration in response to stimulation with CXCL1 [166]. Both of these animal models support a role for MPO-ANCA in the induction of neutrophil recruitment in the presence of CXCL8. Furthermore, patient ANCA-IgG have been demonstrated to increase neutrophil adhesion and transmigration in *in vitro* flow models of adhesion [167, 168].

Leukocyte trafficking is a well-regulated multi-step process; involving capture from flow, firm adhesion and migration into surrounding tissues (see figure 4). Leukocytes circulate close to the vascular endothelium rather than in the centre of the vessel. This is known as margination, and facilitates the capture of circulating leukocytes by adhesion molecules expressed on the vascular endothelium. A group of adhesion molecules known as the selectins play a crucial role in the capture and rolling of leukocytes along the endothelium [169-172]. The selectins are a family of carbohydrate-recognising transmembrane proteins. There are three known types of selectin, L-Selectin is constitutively expressed on leukocytes, whilst P- and E-Selectin are expressed on the vascular endothelium [173]. The selectins form weak bonds between sialyl-lewis^x surface glycans on the leukocyte and endothelium [174], which are repeatedly broken and reformed giving the appearance of the leukocyte rolling across the endothelial surface.

One of the best-characterised selectin ligands involved in leukocyte rolling is P-Selectin glycoprotein ligand-1 (PSGL-1). Although PSGL-1 is the major ligand for P-Selectin, it has been suggested to weakly interact with E-Selectin and L-Selectin. PSGL-1 is constitutively expressed on the membrane of leukocytes, and contains a sialyl lewis^x domain that is recognised by endothelial Selectins [175]. Expression of sialyl lewis^x and core 2-1,6-*N*-acetylglucosaminyltransferase (C2GnT) domains are both required for binding of PSGL-1 by P-Selectin, as PSGL-1 on CHO cells, which do not express sialyl lewis^x, was unable to bind to P-Selectin [176].

Figure 4 - The Process of Leukocyte Migration



The process of leukocyte recruitment. First, flowing leukocytes are captured by weak transient bonds between endothelial selectins and their ligands (rolling). The leukocyte is activated by chemokine signals causing integrin molecules to undergo a conformational change. Interactions between these activated integrins and their endothelial ligands results in the firm adhesion of the leukocyte to the endothelial surface. From here the leukocyte can traverse the endothelial membrane and migrate to sites of tissue inflammation.

The rolling leukocytes that are in contact with the endothelium are guided by chemoattractant gradients produced by activated endothelial cells, for example the production of CXCL8 and platelet activating factor (PAF). The second stage of leukocyte migration involves the integrin-mediated firm adhesion to the vascular endothelium, thereby enabling migration through endothelial tight junctions. Integrins are a family of $\alpha\beta$ heterodimers, constitutively expressed on leukocytes, that can be increased following stimulation, e.g. with TNF α . All leukocytes express β_2 integrins, whilst eosinophils, monocytes and lymphocytes also express β_1 , β_7 and α_4 integrins. Stimulation by chemokines results in a conformational change brought about by inside-out signalling within the leukocyte, which include the activation of surface integrin molecules to the extended conformation structure required for high affinity adhesion [177], as well as the polymerisation of G-Actin into F-Actin (reviewed in [173]). An increase in this conversion to F-Actin has been noted in neutrophils following treatment with ANCA IgG [178], and it is likely that the consequent increase in cell rigidity may be involved in the increased neutrophil sequestration in capillary beds of vasculitic patients. Integrin interactions are dependent upon this conformational change in order to achieve the firm adhesion of the leukocyte. For neutrophils, firm adhesion is dependent upon the interactions of the integrins, lymphocyte function-associated antigen-1 (LFA-1, CD11a/CD18) and macrophage antigen-1 (Mac-1, CD11b/CD18), with the vascular surface. It has been demonstrated that patients deficient in these β_2 integrins have an inability to recruit neutrophils from the vasculature (reviewed in [179]). Integrins interact with members of the immunoglobulin superfamily on the surface of endothelial cells; in particular, LFA-1 and Mac-1 bind to ICAM-1 [180, 181], whilst LFA-1 also interacts with ICAM-2 [182]. The immunoglobulin superfamily encompasses a wide range of molecules with multiple Ig-like domains. ICAM-1 is constitutively expressed on many cell types, however its expression on endothelial cells can be further regulated and increased upon stimulation. ICAM-2 is also expressed on

endothelial cells, however it is not increased following activation [183]. It has previously been demonstrated that patients suffering with Wegener's Granulomatosis display increased expression of ICAM-1 and VCAM-1 in tissues [184, 185], which may play a role in the increased level of neutrophil adhesion to the vascular endothelium observed in vasculitic patients.

1.9 Chemokine Ligand-8 Induced Neutrophil Adhesion

Chemokine ligand-8 (CXCL8, also known as interleukin-8 and neutrophil activating protein NAP-1) is a pro-inflammatory cytokine, primarily concerned with neutrophil recruitment to sites of inflammation, although, it has previously been suggested to also have a role in the increased adhesion and transmigration of leukocytes across endothelial membranes. Neutrophils stimulated with CXCL8 have been shown to become activated and migrate across the endothelium [186]. This increased neutrophil adhesion occurs both in the presence or absence of the inflammatory stimuli $TNF\alpha$, with the presence of $TNF\alpha$ having an additive effect on the levels of neutrophil adhesion [187]. Other functions of CXCL8 include neutrophil granule exocytosis and respiratory burst [188].

Early reports suggest that CXCL8 can act to increase expression of adhesion molecules, probably by surface remodelling following granule exocytosis, thereby increasing leukocyte transmigration (reviewed in [188], [189]). CXCL8 has been identified on the luminal surface of endothelial cells, from where it can stimulate the conversion of neutrophils from rolling to firmly adhered through interactions between ICAM-1 and the neutrophil β_2 integrins [190]. CXCL8 induces rapid rates of adhesion via LFA-1 dependant and Mac-1 dependant adhesion

to ICAM-1, which can be inhibited by the addition of blocking antibodies directed at the endothelial CXCL8 receptors CXCR1 and CXCR2 [191]. CXCR1 is an CXCL8 specific membrane receptor, however, CXCR2 is known to also interact with other circulating chemokines of the ELR family that are directed towards neutrophils [192, 193]. A key adhesion molecule of interest is the β_2 integrin Mac-1. CXCL8 has been shown to stimulate the binding activity of Mac-1 [189], with transmigration through the vascular endothelium reliant upon CXCL8 induced Mac-1 activation [194]. Arndt *et al.*, 1996, demonstrated that by blocking CXCL8 or CD11b they could reduce the level of leukocyte adhesion to the vascular endothelium in rat venules. They suggested that CXCL8 was acting to promote adhesion by increasing the surface expression or activation of Mac-1 [195]. CXCL8 can also induce the redistribution of the P-Selectin ligand, PSGL-1, in neutrophils to promote rolling [196]. Furthermore, CXCL8 has been shown to increase actin polymerisation in neutrophils [197], thereby inducing cellular shape changes that facilitate adhesion and transmigration.

1.10 Neutrophil Priming by Tumour Necrosis Factor- α

It has previously been demonstrated that TNF α mRNA expression and cytokine release is upregulated during active ASV, particularly in Wegener's granulomatosis and microscopic polyangiitis [198-200]. This may result in the priming of neutrophils for an ANCA-induced respiratory burst [16, 201, 202]. Neutrophil priming by TNF α enhances the ability of the neutrophil to undergo respiratory burst following ANCA stimulation [203]. It has been reported that this priming of neutrophils may also be crucial in the induction of surface expression of ANCA-antigens [16, 204]. TNF α priming of neutrophils can increase the membrane expression of PR3 2-fold, however, the addition of PR3-ANCA amplifies this

system, increasing membrane PR3 expression 24-fold [205]. It has also been shown that TNF α can induce accelerated apoptosis of neutrophils in a caspase-dependant manner, thereby suggesting a dual role for TNF α in both neutrophil activation and death [206]. It has been suggested that the activation of neutrophils by ANCA induces unregulated neutrophil apoptosis, driven by the production of reactive oxygen species. This may result in the formation of an enhanced inflammatory environment, especially as ANCA-activated neutrophils have been shown to have a delay in the expression of surface phosphatidylserines that are necessary for the recognition and clearance of apoptotic cells by macrophages [207]. It is possible that this could drive the progression of cells from apoptosis towards secondary necrosis and the consequent release of pro-inflammatory cell contents, potentially resulting in endothelial cell damage.

In vivo, TNF α is released into the circulation during an inflammatory response and therefore, may play a key role in the priming of neutrophils and consequently the increased ANCA-induced neutrophil activation observed in vasculitis patients [16]. TNF α stimulation of neutrophils has been demonstrated to increase the level of adhesion to the vascular endothelium [208], allowing for the direct release of neutrophil granular contents onto the endothelial surface. The stimulation of endothelial cells with TNF α also results in an increased level of neutrophil adhesion [208]. This is likely to be due to the increased expression of classical endothelial adhesion molecules, P-Selectin, E-Selectin, ICAM-1 and VCAM-1 [209, 210]. Further investigation has identified a role for tyrosine kinase signalling in the upregulation of ICAM-1 by TNF α on endothelial cells [211].

1.11 Other Cell Types Implicated in ASV

1.11.1 Macrophages

The migration of monocytes into tissues allows for their terminal differentiation into macrophages. Macrophages are central to the innate immune response. Activation of these cells in inflamed tissues results in phagocytosis and the production of a host of inflammatory cytokines. Macrophages can be characterised into two distinct subsets depending on their method of activation [212]. M1 macrophages are classically activated by stimuli including IFN γ , lipopolysaccharide (LPS), TNF α and GM-CSF. These classically activated macrophages produce IL-12 and IL-23 to support a Th1/Th17 immune response. The alternatively activated macrophages, known as M2, can be further subdivided by their activatory stimuli (see table below) [213]. The alternative pathway of activation is thought to have immunosuppressive functions [214] and have more of an effect on the resolution of inflammation by endocytic clearance and decreased production of proinflammatory cytokines [215].

These different subsets of macrophage have very distinct functions in renal inflammation. Most glomerular diseases are characterised by an infiltration of macrophages. Here macrophages have dual roles in the modulation of the immune response and repair processes as well as the clearance of debris and apoptotic cells. However, the continuous production of growth factors by macrophages can result in renal fibrosis and ultimately chronic kidney disease [213]. This progression to renal scarring occurs as a result of interplay between T-cells, dendritic cells and macrophage responses [216-218], although ultimately macrophages are the dominant cell type involved in fibrosis. Interestingly, the injection of anti-inflammatory IL-4 expressing M2 macrophages into the renal artery in a rat model of

nephrotoxic nephritis caused reduced proteinuria and albuminuria, and further decreased glomerular macrophage infiltration [219].

Table 4 - Different Subsets of Macrophages

	Activating Stimuli	Functions	Cytokine Profile
M1	IFN γ LPS TNF α GM-CSF	Proinflammatory Th1/Th17 Response	IL-12 ^{Hi} IL-23 ^{Hi} MHC class II ^{Hi} CD80/86
M2a	IL-4 IL-13	Immunoregulation Tissue Remodelling	Mannose Receptor Scavenger Receptor MHC class II ^{Hi} Decoy IL-1R11
M2b	Immune Complexes IL-1 β LPS	Immunoregulation Th2 Activation	CD86 MHC class II ^{Hi} IL-12 ^{Lo} IL-10 ^{Hi}
M2c	IL-10 TGF- β Glucocorticoids	Immunosuppression Tissue Remodelling	SLAM (CD150) Mannose Receptor MHC class II ^{Lo}

Adapted from Ricardo 2008 [213]

In ANCA-associated vasculitis it is believed that inappropriate activation of macrophages results in tissue damage, which is maintained by further recruitment of monocytes [220]. Macrophages were first identified in isolated glomeruli from patients with crescentic glomerulonephritis in 1976 [221]. More recently macrophages were identified in the glomeruli in renal biopsies from ANCA-associated vasculitis patients [184]. Histological analysis of ANCA positive renal biopsies demonstrated that, along with glomerular infiltration of macrophages and monocytes, T cell and neutrophil infiltrates are present within the renal interstitium [222].

The mechanism of recruitment of macrophages to glomerular inflammatory infiltrates remains elusive, however, it is generally believed to be due to a combination of increased adhesion molecule expression, increased circulating chemotactic factors, and changes in haemodynamic conditions [220, 223]. Adhesion molecules ICAM-1 and VCAM-1 have a well-established role in the trafficking of leukocytes and other inflammatory cells into tissues. In ASV, expression of ICAM-1 by glomerular endothelial cells is increased. More interestingly, VCAM-1, which is normally only expressed by epithelial cells of the Bowman's Capsule, has been demonstrated to be expressed in the glomerular crescents with extracapillary damage [223].

1.11.2 T-cells

Patients with Wegener's granulomatosis have been demonstrated to display a shift in their peripheral T-cell populations from CD4⁺ to CD8⁺ T-cells. This is suggested to be due to both a decreased number of circulating naive CD4⁺ T-cells, apparent in both patients with active disease and those in remission who are not receiving immunosuppressive therapy, and increased percentages and absolute numbers of CD8⁺ T-cells [224-227]. Patients with active WG also display an increased number of activated CD4⁺ and CD8⁺ T-cells compared to control [227]. Other features in these patients include the decreased expression of co-stimulatory molecule CD28 and increased CD80/CD86 [225, 226, 228, 229]. Activation of T-cells with CD28 costimulation primarily promotes differentiation into T-helper-2 cells, which supports plasma cell antibody production. The combined effects of the decreased CD28 expression along with increased expression of CD80/CD86 expression promote differentiation of CD4⁺ T-cells into T-helper-1 cells, which go on to activate macrophages.

These T-cells also display increased expression of cytotoxic T-lymphocyte antigen-4 (CTLA-4) [230], which is suggested to induce resistance to apoptosis [231]. It has been reported that polymorphisms in CTLA-4 may be responsible for the on-going activation of T-cells in ASV [232].

More recently an IL-17 producing subset of CD4⁺ T-cells, known as Th17 cells, have been implicated in the pathogenesis of vasculitis. An expansion in Th17 T-cell population has been identified in the blood of patients with WG [233]. The IL-17 produced from these cells induces release of pro-inflammatory cytokines, including IL-1 β and TNF α [234], which themselves may contribute to the neutrophil priming required for ANCA activation. Furthermore, WG patients have been shown to have an expanded population of functionally defective regulatory T-lymphocytes (Treg) [235]. This has been previously identified in other autoimmune diseases, and indicates that a breakdown in Treg self-tolerance may be contributing to pathogenesis of ASV.

1.11.3 B-Cells

It is well known that, in normal physiology, B-cells can act to support an immune response by interactions with antigen presenting cells, as well as acting as antigen presenting cells themselves, supporting T-cell mediated responses and the production of antibodies [236]. Activated CD4⁺ helper T-cells can deliver activating signals to B-cells in a process known as linked recognition, which occurs through common recognition of a pathogen and requires B-cell surface expression of the antigen on its MHC class II. The release of IL-4, along with CD40 stimulation, from Th2 cells induces B-cell proliferation, which can then differentiate

into memory B-cells or antibody producing plasma cells [237]. The isotype of the antibody produced is influenced by the cytokine stimulation received by the plasma cell, in particular IL-5 is required to induce recombination, whilst IL-4 (IgG₁, IgE), TGFβ (IgA) and IFNγ (IgG_{2a} IgG₃) may also be involved [238, 239].

Recently B-cells have been suggested to be involved in the loss of T-cell tolerance and the development of autoreactivity. T-cell function is reliant upon correct B-cell function, and together these cells create a positive feedback process that results in expansion of the immune response [240]. Aberrant T-cell function is a known feature of ANCA vasculitis, and may be a downstream effect of abnormal interactions between B-cells and T-cells. This has previously been described in rheumatoid arthritis, in which B-cell depleted mice could not support T-cell activation, whilst treatment with anti-CD20 mAb, a B-cell targeting therapy, inhibited inflammatory cytokine production [241]. Furthermore, an accumulation of B-cells has been identified in a host of tissues affected by autoimmune diseases, as well as in inflamed renal biopsies from patients with membranous glomerulonephritis [242]. Whilst in vasculitis, abnormal B-cell clusters have been identified in ANCA positive nasal biopsies [243].

Currently a major part of the treatment regime for ANCA-vasculitis involves targeting the immune response through a combination of chemotherapy agents and broad-spectrum immunosuppressive steroids. Due to the side effects associated with this treatment, more recent studies have been directed at anti-B-cell therapies. Two trials in particular have compared treatment with this current regime to an anti-B-cell therapy called Rituximab. Rituximab is an anti-CD20 monoclonal antibody that can bind to CD20 expressed on B-cells, from where it can induce apoptosis. CD20 is expressed on all B-cells excluding the antibody producing plasma cells. Two impartial clinical trials both demonstrate that the

treatment of ANCA-vasculitis by Rituximab results in the same level of induction into remission as treatment with the standard treatment regime [244, 245]. Although, improvements in the long-term side effects of this treatment is awaited from patient follow-up.

1.12 Endothelial Cells in Inflammation

The endothelium is the thin layer of cells that line the blood vessels of the body. The phenotype of the vascular endothelium is dependant on the microenvironment in which it exists, thereby aiding its organ specific functions. The endothelial cells play an important role in the regulation of vessel structure and function, as well as the transit of immune cells from the vasculature into tissues during inflammation. A key characteristic of endothelial cells is their ability to undergo rapid cell division and migration, which is of particular importance following injury to the vessel wall.

The vascular endothelium has a constant need to remodel to accommodate the needs and requirements of the surrounding tissues. The activation of the endothelial cells in response to inflammation results in changes to the ability of the endothelium to recruit inflammatory cells, as well as the initiation of angiogenesis [246]. The increased requirement for trafficking of immune cells is associated with an increased vascular endothelial leakiness. This is achieved by the increased production of vascular endothelial growth factor (VEGF), nitric oxide (NO), and angiopoietin-2 (Ang-2) [247, 248]. The endothelial barrier consists of two types of junctions, namely the tight junctions; consisting of claudins, occludins and junctional adhesion molecules, and the adheren junctions, consisting of catenins and

cadherins [246]. VEGF acts to increase endothelial permeability through adherens junctions, mainly through VE-cadherin [249, 250], whilst Ang-2 acts as a natural inhibitor to angiopoietin-1 (Ang-1), thereby increasing vascular permeability [248, 251, 252]. During inflammation there is also a need for the development of new vessels as the requirement for immune cells increases. This is achieved by endothelial sprouting, which involves the colonisation of non-vascularised areas by migrating/proliferating endothelial cells.

The anti-thrombotic state influenced by the vascular endothelium is important to maintain, as the induction of thrombosis can contribute to the pathophysiology of vasculitis. Glomerular thrombus formation is often present in glomerulonephritic kidneys, and may be involved in the progression to acute renal failure. Using a mouse model of thrombotic glomerulonephritis, the β_2 integrin Mac-1 was highlighted as a key molecular link in the induction of neutrophil recruitment, endothelial injury, and thrombotic glomerular lesions [253]. Furthermore, engagement of Mac-1 on neutrophils can induce release of HLE [254], which can further potentiate glomerular injury. Mac-1 can also interact with platelet GP1b α to promote thrombosis, thereby supplying a link between the induction of inflammation and thrombus formation [253].

The vascular endothelium has the ability to upregulate the expression of adhesion molecules to increase leukocyte migration for immune surveillance and aid the inflammatory response. The expression of endothelial adhesion molecules varies upon site, with high constituent expression at sites of continuous immune cell recruitment [255], such as the lymph nodes, whilst inflamed sites require endothelial activation for the upregulation of adhesion molecules upon requirement. ICAM-1 is an example of an endothelial adhesion molecule that is constitutively expressed on many types of endothelial cell, although expression is further increased upon activation. ICAM-1 binding by its ligands has reported to induce the

production of endothelial chemokines, CXCL8 and RANTES [256]. Activation of ICAM-1 by leukocyte binding is suggested to regulate the endothelial actin cytoskeleton thereby aiding leukocyte migration [257]. VCAM-1 is also reported to induce endothelial shape change by regulation of actin following lymphocyte binding or anti-VCAM-1 antibodies [258, 259]. Binding of lymphocytes to VCAM-1 results in the production of ROS via the activation of NADPH oxidase, as demonstrated in murine endothelial cells [259]. One of these reported reactive oxygen species produced is hydrogen peroxide (H_2O_2). Low concentrations of H_2O_2 are produced by endothelial cells following VCAM-1 activation, which is suggested to induce the delayed activation of matrix metalloproteinases (MMPs) (2-5 hours after lymphocyte binding to VCAM-1) [260]. The MMPs are required for degradation of the endothelial cell matrix and junctional adhesion molecules, for example VE-Cadherin [261], to facilitate migration.

The endothelium also plays a fundamental role in vascular repair following injury and the initiation of the coagulation cascade. The endothelium forms a barrier between tissue factor (TF) expressing fibroblasts and smooth muscle cells, and their ligand, circulating Factor VII/VIIa. A breakage in this endothelial barrier results in the exposure of TF and the rapid activation of the coagulation cascade [262]. Another way by which the endothelium is involved in clotting is by the release and expression of von Willebrand factor (vWf). vWf is constitutively expressed in endothelial cells and released in response to activation or stress signals. vWf induces platelet adhesion to the endothelium at sites of vascular injury by binding to activated factor VIII, platelet glycoproteins, or constituents of connective tissue, thereby activating the coagulation cascade.

1.13 Glomerular Endothelium: A Target in ANCA-Associated Vasculitis

The glomerular endothelium is a prime target in ASV, with glomerulonephritis observed in 50-80% of patients presenting with Wegener's granulomatosis and 90-100% of patients with microscopic polyangiitis [13] (see table 1 for more detail). The glomerulus consists of a specialised collection of capillaries in the kidney, which function as a site for filtration and removal of waste products from the blood. The endothelial monolayer here provides the first stage of a three-layer filter crucial to the charge-dependant and size-dependant filtration. The endothelial monolayer consists of flattened cells with thin cytoplasmic areas, large nuclei and very few mitochondria. Another characteristic of the glomerular endothelium is the presence of many fenestrations without diaphragms [263, 264], also key to the filtration process. The endothelial cell monolayer sits on top of a structure known as the glomerular basement membrane, which itself sits on top of visceral epithelial cells, known as podocytes. The basement membrane is considered to be the principle barrier in the filtration of large molecules, with abnormalities in the structural components of the basement membrane linked to proteinuria. The endothelial glycocalyx forms part of the endothelial surface layer, along with a loosely attached glomerular cell coat. The negatively charged properties of the glycocalyx are suggested to contribute to the charge selective filtration of the glomerular filter, first described by a preference for filtration of neutral dextran over negatively charged dextran sulfate [265]. The glycocalyx is comprised of a host of glycoproteins and lipids, of which the glycoaminoglycans (GAG) are of particular importance in the maintaining the charge-selective filtration. Enzymatic degradation of these GAGs alters this charge-selective filtration and consequently decreases the transendothelial resistance [266], thereby altering the glycocalyx charge density [267], and increasing the flux of albumin across the glomerular filter [266, 268]. This observation has also been reported following the injection of rats with hypertonic sodium chloride solution, which increased albumin flux whilst having

no effect on the filtration of neutral ficoll [267]. The ability of angiotensin-1 to increase the depth of the glycocalyx to decrease water permeability and albumin flux [269], provides a mechanism by which the kidneys can control and alter the charge-selective properties of the glomerular filter.

The glycocalyx forms a mesh-like structure across the surface of all vascular endothelial cells. This barrier, in part, regulates inflammation by masking the adhesion molecules essential for leukocyte transmigration [270]. Furthermore, the perfusion of hydrocortisone or antithrombin has been shown to maintain the glycocalyx structure by decreasing shedding, which consequently reduces aberrant leukocyte adhesion in a model of ischemia-reperfusion injury [271]. Henry *et al.* demonstrated that, upon the induction of inflammation, TNF α can modify the glycocalyx to support inflammatory cell recruitment by reducing the thickness of the glycocalyx, which allowed increased permeation of the glycocalyx by larger macromolecules including dextran, albumin and IgG, as well as increasing leukocyte adherence, presumably by exposing endothelial adhesion molecules [272]. The acute phase protein, C-reactive protein, has also been shown to reduce the thickness of the glycocalyx, resulting in increased ICAM-1 release and monocyte adhesion to arterial endothelial cells [273].

Human glomerular endothelial cells were first isolated in culture by Striker *et al.*, 1984, who used von Willebrand factor (vWf) and angiotensin-converting enzyme (ACE) as markers for characterisation [274]. The disadvantage of primary endothelial cell cultures is their limited life span and their loss of characteristics following passage, thereby indicating a requirement for a conditionally immortalised human glomerular endothelial cell line. The development of this cell line by Satchell *et al.*, in 2006 has allowed for greater progress into the

understanding of the physiological functions of the glomerulus and its relationship with ASV [275].

1.14 Weibel-Palade Bodies

The endothelial monolayer provides an important barrier between the bloodstream and surrounding tissues and therefore must be repaired quickly upon injury, a phenomenon known as coagulation. vWf plays a key role in the initiation of this coagulation cascade and mediation of platelet aggregation following vascular injury, and therefore has been referred to as a marker of endothelial dysfunction [276]. It is exclusively produced by megakaryocytes and endothelial cells and stored in rod-shaped storage vesicles known as Weibel-Palade bodies (WPBs) [277, 278]. Although vWf is the major component of WPBs, these structures have also been suggested as a storage site for other proteins, including P-Selectin, Ang-2, CD63 and CXCL8. The formation of these ‘bodies’ begins with the monomeric form of vWf, derived from the trans-golgi network. Monomeric PrePro-vWf dimerises by the formation of a disulfide bond between its cystine knots as it is translocated to the endoplasmic reticulum. This Pro-vWf is transported to the golgi network where it undergoes cleavage and formation of a second disulfide bond. The acidic environment of the golgi prevents disulfide rearrangement, allowing linkage of subunit inter-chain disulfide bonds, thereby resulting in the formation of vWf multimers [279]. Small amounts of monomeric vWf are constitutively released, although the majority dissociates from the golgi as clathrin coated secretory granules [280], which mature into WPBs [281]. This idea is supported by evidence that dogs with severe von Willebrand disease lack the WBP biogenesis, which can be restored upon expression of vWf [282]. Recent studies have

suggested that, apart from vWf, the components of WPBs can differ, indicating a range of WPB subsets. It is proposed that CXCL8 is only stored in the WPBs of human umbilical vein endothelial cells (HUVEC) after its synthesis has been stimulated by other inflammatory cytokines. The stimulation of HUVEC with IL-1 β does not induce expression of CXCL8 in all WPBs of an endothelial cell, suggesting WPBs not expressing CXCL8 were formed prior to the inflammatory stimulation [283-285]. Alternatively, there is evidence demonstrating CXCL8 co-localisation with vWf with no prior stimulation in other endothelial cell types including the human microvascular endothelial cells [283]. Although both identified in WPBs, angiopoietin-2 expression appears to be completely separate from P-Selectin, and previous studies have demonstrated no co-localisation between the two [286]. Furthermore, it has been demonstrated that components of WPBs can occur independently of one another. Cleator *et al.*, showed that HUVEC stimulated with cyclic adenosine monophosphate (cAMP) or protease activated receptor-2 agonist peptides (PAR2-APs) resulted in release of vWf from WPBs with minimal release of P-Selectin, thereby proposing different mechanisms for release of the different components of the WPBs [287].

Mature WPB are susceptible to stimulation by secretagogues, including thrombin and histamine, which induce WPB exocytosis by raising intracellular calcium levels or stimulating the production of cAMP, a process that can occur very rapidly [288, 289]. Although the mechanism of exocytosis is yet to be clarified, a selection of GTPases have been implicated in WPB release. Overexpression of activated Rab3D inhibits the release of WPB contents, indicating a negative regulatory role [290], whilst overexpression of RalA initiates exocytosis [291, 292]. The incubation of endothelial cells with thrombin results in WPB exocytosis via a calcium dependant pathway, which has been suggested to result in the activation of GTPase RhoA, whilst cAMP mediated release of WPB results in the activation of a different GTPase, Rap1 [293].

1.15 Von Willebrand Factor (vWf) and the Coagulation Cascade

vWf is a multimeric glycoprotein, which, when released from endothelial cells in response to activation and/or stress, acts to support platelet adhesion to the vascular endothelium at sites of injury. Its functions in coagulation are highlighted in patients with von Willebrand Disease, who display mild bleeding symptoms due to a hereditary loss in the expression of a functional vWf protein.

vWf mediates its actions by binding to components of the coagulation cascade, particularly activated factor VIII, as well as platelet glycoproteins and constituents of exposed connective tissue. Following vascular injury, vWf is secreted from endothelial cells as a high molecular weight molecule known as ultra-large vWf (ULVWF). ULVWF is composed of between 50-100 monomers which join to form a large multimer that can reach molecular weights of up to 20MDa [294]. This ULVWF is released from endothelial cells as large strings that can capture multiple platelets along its length. To prevent inappropriate platelet capture, multimeric ULVWF is cleaved into smaller monomers by metalloproteinase ADAMTS-13 (a disintegrin and metalloproteinase with a thrombospondin type 1 motif, member 13) [295]. Failure to cleave the larger multimers of vWf can result in thrombus formation [294].

vWf can bind to a range of collagens that form part of the endothelial connective tissue [296]. In particular collagen type VI has demonstrated a key role in vWf mediated coagulation [297], although other components of the endothelial connective tissue may also be involved, thereby allowing recruitment of platelets from flow and thrombus formation. Although vWf is one of the many molecules involved in platelet capture at low flow rates, it is the main protein involved in capture at high shear flow rates [295]. The interaction between platelets and adhered vWf is reliant upon the glycoprotein Ib-IX-V complex on non-

activated platelets [296], in particular the glycoprotein-1b α (GP1b α) chain of the complex [298]. GP1b α acts to form weak bonds between the endothelial tissue and the platelets. These bonds are easily broken under the high flow rates, however, are key in slowing platelets in flow so that stronger interactions can be formed [299, 300]. Another mechanism by which vWf can induce platelet aggregation is via interactions with integrin $\alpha_{2b}\beta_3$. $\alpha_{2b}\beta_3$ has also been shown to bind fibrinogen and fibronectin [301, 302], further components of the coagulation cascade. vWf interactions with $\alpha_{2b}\beta_3$ result in the firm adhesion of platelets to the site of vascular injury, and the consequent formation of a thrombus [295]. This interaction is mainly responsible for the non-reversible binding of platelets to the subendothelium at high shear flow [303]. The kidneys receive approximately one fifth of the cardiac output, so glomerular capillaries are exposed to high flow rates.

Although vWf is involved in repairing the vasculature following injury, is not a specific marker of endothelial cell damage. It is also released in the absence of vascular injury as an acute plasma reactant, as well as following endothelial cell stimulation. There have been very few *in vivo* models of vWf as a marker of dysfunction, with most experiments having been carried out *in vitro* on endothelial cell lines [304], so whilst it has been shown to be released from the endothelium following vascular injury, it can only be used as a marker for damage if this is verified by use of a second marker. vWf expression has been previously identified on the surface of endothelial cells as WPBs fuse with the cell membrane. This vWf expression occurs in small patches and has a life-time of up to 20 minutes [305]. vWf can also adhere to the endothelial surface by forming a complex with Factor VIII [306]. vWf acts to stabilise Factor VIII, increasing its half-life by up to 20-fold [294].

1.16 vWf in ANCA-Associated Vasculitis

There has been little research into the expression and actions of vWf during active vasculitis, or else the actions of PR3 on vWf release and expression by the endothelium. Previous studies into ASV have demonstrated an increased level of circulating vWf in patients with active Wegener's granulomatosis or microscopic polyangiitis [307, 308]. Also, Lu *et al.*, 2006 identified increased levels of vWf release from endothelial cells following culture with ANCA-activated neutrophils, which could be abolished with the addition of serine protease inhibitors [309]. They also demonstrated an increase in vWf release following the addition of PR3 directly to endothelial cells. This discovery was fundamental in establishing a role for serine proteases in mediating the endothelial cell injury known to be associated with vasculitis. However, the detailed consequences of the direct effects of proteinase 3 on vWf release from endothelial cells has yet to be determined, as is a mechanism by which serine proteases are inducing release of vWf.

1.17 Other Constituents of WPB

1.17.1 Angiopoietin-2

Angiopoietin-2 (Ang-2) belongs to a family of growth factors involved in the formation and regulation of the vasculature. Currently four members of the angiopoietin family have been identified, of which only Ang-2 is present in endothelial WPBs [286]. Whilst Ang-2 is almost exclusively present in endothelial cells, it is most abundantly expressed at sites of vessel remodelling [310]. Ang-2 has been identified as a natural antagonist for its sister

ligand, Angiopoietin-1. Ang-1 mediates its anti-inflammatory actions by “sealing” vessels, preventing plasma leakage and inflammatory cell migration, whilst its anti-apoptotic effects maintain endothelial cell integrity and survival [311-313]. Ang-1 is also instrumental in the maturation of blood vessels. The exact roles of Ang-2 in inflammation remain elusive. To date it has been demonstrated to increase vessel leakage by destabilisation of the endothelial cell-cell junctions and consequently promoting inflammation and endothelial cell detachment [286, 314, 315]. Ang-2 is also associated with the expression of vascular endothelial growth factor (VEGF). Together they act to induce new vessel formation, whilst the addition of Ang-1 can inhibit this VEGF-Ang-2 mediated angiogenesis [316]. The actions of VEGF on increasing vascular permeability are primarily mediated through signalling through VEGF receptor-2 (VEGFR2) [317, 318]. Furthermore, VEGF has been implicated in increasing paracellular permeability by promoting contraction of the actin cytoskeleton and opening of the cell-cell junctions [319-321].

Tie-2 has been identified as the principle receptor for the angiopoietins, although they can also interact with the Tie-1 receptor. Both of these receptors have been shown to be expressed by vascular endothelial cells. The Tie receptors are members of the tyrosine-kinase group of receptors, with an extracellular domain consisting of three Ig-like domains divided by three epidermal growth factor-like cysteine repeats and followed by three fibronectin typeIII domains [251]. Ang-1 and Ang-2 bind to this extracellular binding domain of Tie-2 in an autocrine fashion as homodimers or multimers [322, 323].

Currently there has been little research into a role for Angiopoietin-2 in vasculitis. However, it has recently been demonstrated that patients with active glomerulonephritis have increased serum concentrations of Ang-2 compared to patients in remission, and that these concentrations decreased steadily during treatment [324].

1.17.2 P-Selectin

Whilst being storage vesicles for vWf, the Weibel-Palade bodies also contain P-Selectin (also known as GMP-140 and CD62p) [278, 325], an important adhesion molecule in leukocyte capture from flow and ultimately migration from the vasculature. The selectin family of adhesion molecules are associated with the initial capture stage of leukocyte transmigration. The selectins have the ability to form weak bonds with leukocytes at high shear rates, which cause the leukocyte to slow along the endothelial surface. The repeated formation and breakage of these selectin bonds give the impression that the cell is rolling across the endothelium, and allow for the formation of stronger integrin bonds between the leukocyte and the endothelium, which ultimately results in transmigration. The perfusion of neutrophils over P-Selectin in a flow model of adhesion resulted in neutrophil rolling in more than 97% of these cells. Further, perfusion of ANCA IgG over rolling these neutrophils caused the slow conversion of rolling to firmly adherent cells [309, 326, 327].

Along with CD63, P-Selectin comprises the major membrane protein of WPBs [328]. Fusion of WPBs with the endothelial membrane results in the rapid expression of P-Selectin on the endothelial surface [278, 329]. Following this brief exposure, of approximately 20 minutes, the P-Selectin is recycled back into the endothelial cell, where it can return to the trans golgi network and reform WPBs along with vWf [328, 330]. Although vWf and P-Selectin have demonstrated to be co-expressed in WPBs, their release can occur independently of one another [287].

1.17.3 CD63 (Platelet Glycoprotein gp40)

The tetraspanin glycoprotein, CD63, is universally expressed in a host of cell types, whilst more recently identified as another constituent of the WPB membrane. As with P-Selectin, membrane expressed CD63 can be recycled back into the endothelial cell and into developing WPBs [331]. However, unlike P-Selectin this incorporation into WPBs does not occur at the early trans-golgi network stage of development, but rather CD63 is recruited to later more developed WPB. Furthermore, P-Selectin trafficking occurs via an adaptor protein complex-3 (AP-3) independent mechanism, whilst CD63 is reliant upon AP-3 signalling [332]. CD63 has been implicated in the adhesion and activation of platelets, and has been demonstrated to interact with integrins $\alpha_4\beta_1$, $\alpha_3\beta_1$, $\alpha_6\beta_1$, and members the β_2 family, including LFA-1 [333].

A role for CD63 in vasculitis has been demonstrated in neutrophils and other inflammatory cells, however, a role for endothelial CD63 has yet to be determined. Patients with active disease display increased CD63 on neutrophils than healthy controls. Whilst expression of CD63 correlated with BVAS (Birmingham Vasculitis Activity Score) but not with ANCA titres [17].

1.17.4 Chemokine Ligand-8

CXCL8 is a pro-inflammatory chemokine released from the activated vascular endothelium [334]. CXCL8 has two known receptors, CXCR1 and CXCR2, widely expressed on various cells, which have a high affinity for binding CXCL8 [335]. Whilst CXCR1 is specific for

recognising CXCL8, CXCR2 has also been shown to interact with other chemokines [192, 193]. Both CXCL8 and its receptors have been shown to be expressed by endothelial cells [336-338] and have been suggested to play a role in endothelial cell proliferation [339]. Other cells types have been shown to produce CXCL8, including monocytes, lymphocytes, fibroblasts and epithelial cells [340-343]. Synthesis of IL8 by endothelial cells can be increased by treatment with TNF α , lipopolysaccharide (LPS) and IL-1 β [341, 344-346], whilst TNF α stimulated increase from HUVEC can be inhibited by the presence of interferon- γ (IFN γ) [347]. *In vivo*, CXCL8 is suggested to have many physiological roles in inflammation, including increased leukocyte chemotaxis and transmigration, and endothelial cell angiogenesis [339, 348]. The primary actions of CXCL8 are in the activation of neutrophils [349], including directional migration, increased expression and activation of adhesion molecules, and induction of neutrophil degranulation and reactive oxygen species production (reviewed in [188], [189, 350]). This effect of CXCL8 on increased neutrophil adhesion to the endothelial monolayer remains controversial, with many researchers reporting conflicting statements. Some suggest that CXCL8, once secreted by activated endothelial cells, inhibits the adhesion of neutrophils to the endothelium [351], however, the majority report a pro-inflammatory role for CXCL8 in increasing adhesion and migration of immune cells. CXCL8 produced by endothelial cells has been shown stimulate the binding activity of integrin Mac-1 (CD11b/CD18) on the surface of neutrophils [189].

The presence of increased CXCL8 levels in an inflamed environment has led to speculation of a possible involvement in the progression of ASV. Harper *et al.*, 2001 demonstrated increased production of CXCL8 and IL-1 from macrophages following phagocytosis of ANCA-opsonised apoptotic neutrophils when compared to non-ANCA-opsonised neutrophils [352]. It has also been shown that direct treatment of HUVEC with PR3 and HLE for 24 hours can result in increased secretion of CXCL8, which can be inhibited with

the presence of α 1-antitrypsin [107]. Although the intracellular location for CXCL8 storage is widely speculated, it has been suggested that a proportion of the chemokine may be stored in Weibel-Palade bodies along with vWf and P-Selectin [284]. This colocalisation of CXCL8 and vWf poses a role for protease-activated receptors (PARs) in the release of CXCL8 from endothelial cells upon stimulation. It has previously been reported that co-stimulation of PAR-1 and PAR-2 on epithelial cells results in increased release of CXCL8 [353]. Further evidence supporting a possible role for PARs was produced by Compton *et al.*, 2000, who demonstrated that endothelial cells secrete CXCL8 following 24h stimulation with mast cell tryptase [354], a known stimulant of PAR-2 [355]. CXCL8 is of key importance in ASV, particularly as PR3 has been demonstrated to cleave and process CXCL8 into its more active form [113], potentially aiding neutrophil chemotaxis and transmigration to sites of vascular inflammation. Serine proteases have also been demonstrated to alter the activity of other cytokines including TNF α , IL-6 and IL-18 [139] (see table 3 for more detail).

1.18 Evidence for Protease-Activated Receptors in vWf Release

The protease-activated receptors are a family G-protein coupled receptors, of which four have currently been identified as PAR-1 to PAR-4 [356]. All four PARs have been shown to be expressed on the endothelial surface, although expression of PAR-2 and PAR-4 are increased in inflammatory environments [357]. PAR signalling requires the proteolytic cleavage of the amino terminus, thereby exposing a new ligand and initiating signal transduction [358, 359]. PAR-1, -3 and -4 have been identified as substrates for thrombin, whilst PAR-2 can be activated by tryptase and trypsin [355, 360]. Previous studies have

demonstrated a role for PAR activation in the release of vWf from endothelial cells. Stimulation of PAR-1 on the endothelial surface induces reorganisation of the cytoskeleton and the exocytosis of Weibel-Palade bodies [361], and therefore, the release of vWf, CXCL8 and mobilisation of P-Selectin [284, 325]. PAR-2 has also been shown to be involved in the regulated release of vWf from these storage vesicles [361, 362]. This can be induced by trypsin treatment of endothelial cells [363]. The expression of PAR-2 has been observed in several tissues [364], with high expression on endothelial and epithelial cells [365]. It is suggested to play a role in the inflammatory process, as mice deficient for PAR-2 demonstrate impaired immune responses [366]. Cleator *et al.*, 2006 demonstrated that PAR-2 agonist peptides selectively stimulate the release of vWf, whilst only causing minimal release of P-Selectin [287]. PR3 has been shown to interact with PAR-2 on the surface of oral epithelial cells resulting in cell activation and secretion of cytokines CXCL8 and MCP-1 [367, 368]. An interaction between PR3 and PAR-2 on immature dendritic cells has also been demonstrated, inducing dendritic cell differentiation into mature antigen presenting cells [369], although there remains no direct evidence for an interaction on endothelial cells.

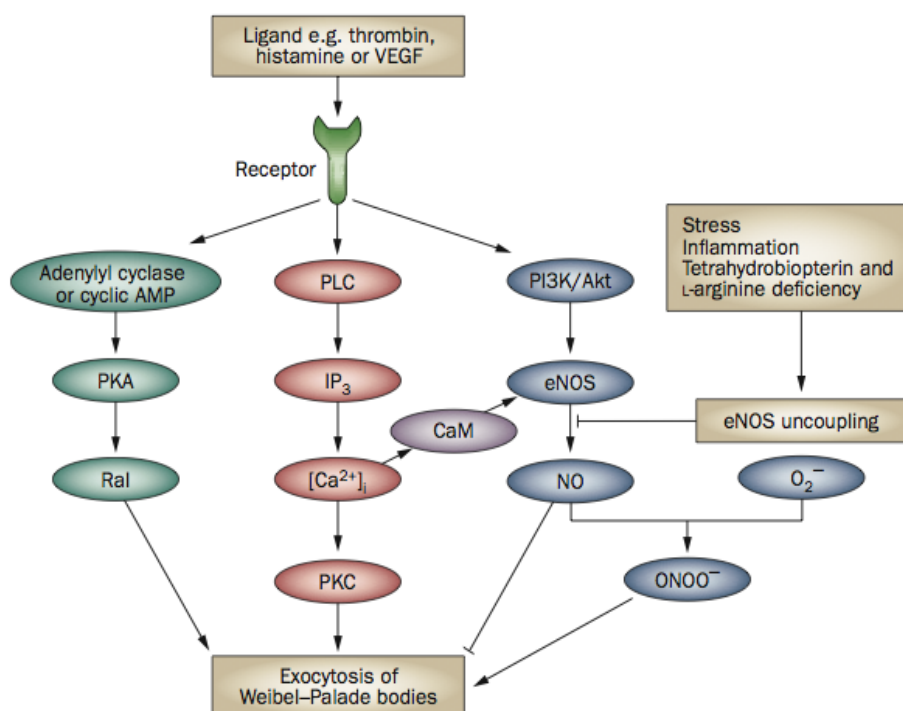
Another receptor of interest is the Toll-Like Receptor (TLR). TLR2 and TLR4 have been implicated in release of vWf from endothelial cells, as mice deficient for these receptors cannot release vWf in response to uric acid [281]. TLR2 has been shown to signal via elevations in the intracellular calcium concentration. More recently it has been demonstrated that the incubation of PR3 with high molecular weight kininogen (HK) results in the formation of bradykinin with 2 additional amino terminals, termed PR3-Kinin, and this has been shown to bind to B₂ receptors on endothelial cells [370]. Bradykinin has been demonstrated to mediate proinflammatory leukocyte recruitment.

1.19 Signalling in vWf release from Weibel-Palade Bodies

The signalling mechanisms involved in the release of vWf from WPBs are yet to be fully defined, with a host of mediators suggested to be involved (see figure 5 below). It is known that vWf release from WPB's can occur through both calcium and cAMP signalling pathways. Thrombin and PAR-1 agonist peptides are known to induce the calcium dependant release of vWf, whilst PAR-2 agonists stimulate release via cAMP. One of the best studied signalling pathways of vWf release is that of VEGF stimulation. Currently two contrasting mechanisms exist. Initially VEGF mediated vWf release from HUVEC was shown be inhibited by the addition of a selection of protein kinase C (PKC) inhibitors, whilst these inhibitors had no effect on histamine mediated release. Small interference RNA (siRNA) allowed further evaluation for a role of PKC δ in this release [371]. More recently, VEGF induced release was shown to be reliant upon signalling through VEGFR2, which signalled through phospholipase C γ 1 (PLC γ 1) and protein kinase A (PKA) to induce full vWf release [372]. Moreover, PKA has been implicated in the mobilisation and clustering of WPBs, as seen during cAMP mediated vWf release [293, 373].

A second well-studied signalling pathway is that of thrombin mediated release. Thrombin mediated vWf release can be inhibited by the addition of calcium chelator MAPTA (bis-(2-amino-5-methylphenoxy)-ethane-N,N,N',N'-tetraacetic acid) in the presence of Ethylenediaminetetraacetic acid (EDTA), whilst the addition of inhibitors directed at PKC had no effect [374].

Figure 5 - Proposed Signalling Pathways Involved in vWf Release



Taken from Goligorsky 2009 [281]. The schematic shown here demonstrates the known signalling pathways through which Weibel-Palade body exocytosis can be initiated. vWf release by VEGF is suggested to involve signalling through both the PKC and PKA pathways, whilst thrombin signalling is proposed to involve increased intracellular calcium but does not appear to progress through PKC signalling.

1.20 Aims and Hypothesis

It is well documented that the neutrophil serine proteases, in particular PR3, have the ability to induce endothelial cell injury, detachment and apoptosis, however, previous data suggests that they may also have an immune response in the removal of invading pathogens as well as leukocyte transmigration. It is also noted that these serine proteases are directly released onto the vascular endothelium following ANCA-mediated neutrophil activation. In this project we aim to investigate a role for the neutrophil serine proteases in the vascular activation and injury during ANCA-associated vasculitis. We hypothesised that the neutrophil serine

proteases may be having an early activatory role on the glomerular endothelium for support of inflammatory processes, as well as inducing endothelial cell injury at later time points. Here we aim to investigate the effects that the direct interactions between PR3 and the glomerular endothelium may be having in the development of inflammation. We aim to further evaluate whether, at short time points, PR3 is inducing endothelial cell injury or if these responses are the result of an activatory process. It is also important to investigate any signalling pathways that are involved in PR3 mediated endothelial responses, as this may result in the identification of possible therapeutic targets.

Specifically, this project sought to

1. Investigate the level of endothelial cell detachment, injury and apoptosis at short and longer incubation periods with physiological concentrations of the neutrophil serine proteases, PR3 and HLE.
2. Confirm that PR3 can induce the release of vWf from HUVEC, and repeat this observation on glomerular endothelial cells, comparing the level of PR3 induced vWf release to that following HLE treatment. Cleavage of vWf from the endothelial membrane was also assessed following serine protease treatment.
3. Explore the signalling molecules and receptors that are involved in the PR3 and HLE stimulated release of vWf from endothelial cells.
4. Determine whether PR3 and HLE also induce release or expression of other Weibel-Palade body constituents.
5. Investigate a role for PR3 and HLE in increased leukocyte transmigration, and any mechanisms by which this may be occurring.
6. Determine whether inhibition of PR3 and HLE by serine protease inhibitor, α 1-antitrypsin, can prevent any PR3 or HLE mediated effects.

2. Materials and Methods

2.1. Conditionally Immortalised Glomerular Endothelial Cells

A conditionally immortalised glomerular endothelial cell line (GEnC) was used in all experiments (gift from Dr S. Satchell, Bristol UK) [275]. The GEnC were allowed to proliferate at 33°C (due to growth arrest at 37°C) until confluent. At which point the cells were either divided into three new T75cm² culture flasks for maintenance or into 96- or 24-well culture plates for experimental use. It is believed that the conditionally immortalised cells should retain the morphological features of primary cells until at earliest passage 41. GEnC are grown in Endothelial Growth Medium-2-Microvascular (EGM-2-MV, Lonza, Wokingham UK, see table 5) with 5% fetal calf serum and supplements as supplied.

GEnC were passaged when confluence was reached at 33°C (typically every 4-5 days). Cells were passaged by washing initially in 2.5ml of 0.02% EDTA (Ehtylenediaminetetraacetic Acid Disodium Salt, Sigma-Aldrich, Poole UK), followed by the addition of 2.5ml of 1x Trypsin/EDTA (T4174 Sigma-Aldrich) for 1-2minutes. Firmly tapping the confluent flask dislodges the cells from the surface. The trypsin was neutralised in 5ml of complete EGM-2-MV and the cells were centrifuged at 1500rpm for 5minutes. After discarding the supernatant the pellet was resuspended in 2ml fresh medium and the cells counted on a haemocytometer. Cells were reseeded in T75cm² culture flasks at a dilution of 1:3, or into plates at 2x10⁴ or 4x10⁴ cells per well. The cells were incubated at 33°C until confluence was achieved, at which point the cells were transferred to 37°C. Cells were kept at 37°C 24 hours before used in experiments.

Table 5 - Constituents of Endothelial Growth Medium-2-Microvascular (EGM-2-MV)

Medium and Additives	Volume	Final Concentration	Source
Endothelial Basal Medium-2 (EBM-2)	500ml	-	Lonza
Foetal Bovine Serum (FBS)	25ml	5%	Lonza
Human Fibroblast Growth Factor-B	2ml	-	Lonza
GA-1000 (Gentamicin Sulfate, Amphotericin-B)	500µl	-	Lonza
Recombinant-longR-Insulin like Growth Factor-1	500µl	-	Lonza
Vascular Endothelial Growth Factor (VEGF)	500µl	-	Lonza
Hydrocortisone	200µl	-	Lonza
Human Epidermal Growth Factor	500µl	-	Lonza

NB Lonza were unwilling to disclose concentrations of reagents provided in the Bullet Kit

Table 6 - Constituents of Complete Medium199

Medium and Additives	Volume	Final Concentration	Source
Medium 199 with Phenol Red	80ml	-	Gibco
Foetal Calf Serum	20ml	20%	Sigma-Aldrich
Penicillin and Streptomycin	1ml	1mM	Sigma-Aldrich
L-Glutamine	1ml	20mM	Sigma-Aldrich
Epidermal Growth Factor	10µl	1ng/ml	Sigma-Aldrich
Hydrocortisone	10µl	1µg/ml	Sigma-Aldrich
Amphotericin B	1ml	2.5µg/ml	Sigma-Aldrich

2.2 Isolation of HUVEC from Umbilical Veins

Human umbilical cords were collected from consenting donors at Birmingham Women's Hospital UK with ethical approval (Ethics Code 5779). Cords were checked for clamp or needle marks, cleaned with ethanol and placed into an ethanol soaked tray for isolation of endothelial cells. The vein is located at one end of the cord. The cannula was inserted into the vein and held in place using an electrician's tie. Using a 20ml syringe, the cannula and vein were flushed with Dulbecco's phosphate buffered saline (PBS, Sigma Aldrich) until it ran clear, followed by flushing through with air to remove any residual PBS from inside the vein. The other end of the vein was then cannulated and tied in place. Collagenase (Sigma-Aldrich) was diluted to 1mg/ml with PBS, and 10ml injected into the vein and cannulae. The cannulae clips were closed and the cord placed into an ethanol filled plastic bag and incubated for 15 minutes at 37°C in 5% CO₂. Each 10-15cm of umbilical cord was isolated into a 25cm² culture flask. Gelatin (Sigma-Aldrich) was diluted to 1% in PBS and 2.5ml added to each 25cm² flask, which was left for 30minutes. Following the 15minute incubation, the cord was removed from the incubator, the ties tightened, and massaged for 1minute to aid release of the endothelial cells. The cord was washed through with PBS and air, and the contents collected and spun at 1400rpm for 5minutes. The supernatant was aspirated off and a small amount (approx 500µl) of complete M199 (see table 6) added to break up any clumps. The pellet was resuspended in 4ml of complete M199, and was added to the culture flasks following aspiration of the gelatin. The culture flasks were incubated at 37°C in 5% CO₂ until use. The medium was changed following 1 day incubation, then again at 3-4 days incubation. HUVEC were not passaged, but instead put into plates for use in experiments. The cells were harvested from the culture flasks by addition of trypsin, in the same way as GEnC. The cells were counted and applied to plates at 2x10⁴ or 4x10⁴ cells per

well. Plates were kept at 37°C in 5% CO₂ until required for use. Isolated HUVEC were confirmed to be endothelial cells by vWf staining performed by Samantha Tull.

2.3 Materials

Endothelial cells cultured in 96-well plates were treated with PR3 (Athens Research and Technology, Georgia USA, Stock 100µg reconstituted in 100µl sterile H₂O) and HLE (Calbiochem, UK, stock 100µg reconstituted in 100µl PBS) at concentrations between 0.5µg/ml and 5µg/ml (1µg/ml = 34nM). The concentrations of serine protease used in our experiments were based on the assumption that, should all of the enzyme come out of solution, there would be approximately 25pg of protease per endothelial cell (for a 1µg/ml treatment), given that a confluent 96-well culture plate would contain around 40,000 cells. Dilutions of PR3 and HLE were performed in Medium199 + 0.05% bovine serum albumin (BSA, Sigma Aldrich). Following addition of the protease to the EnC monolayer, the cells were incubated at 37°C in 5% CO₂. Endothelial cells were treated for durations of up to 24h with PR3 and HLE prior to use in other procedures.

Serine protease inhibitor, α1-AntiTrypsin, was added to endothelial cell cultures at the same time as protease treatment. α1-AntiTrypsin (α1-AT, a gift from Talecris Biotherapeutics, USA) (stock 1000mg reconstituted in 40ml sterile H₂O) was diluted in M199 + 0.1% BSA to give a working concentration of 140nM. Endothelial cells were treated with α1-AT for durations of up to 24h.

Enzymatic activity of PR3 and HLE was checked for each batch upon first reconstitution of the enzyme. This was achieved by the incubation of 5 μ g/ml PR3 or HLE with N-methoxy-succinyl-ala-ala-pro-val-p-nitroanalide (2mM, Sigma-Aldrich) alone, or in the presence of α 1-AT 36 μ g/ml or FCS (6%) (Sigma-Aldrich), in a 96-well plate. The plates were incubated at room temperature protected from light and read at 5minutes and 4 hours at 405nm. The enzyme activities were assessed in triplicate. Figure 6 demonstrates the mean and standard error from a typical result from an activity test.

Figure 6 - Activity Test for Enzymes and Inhibitors

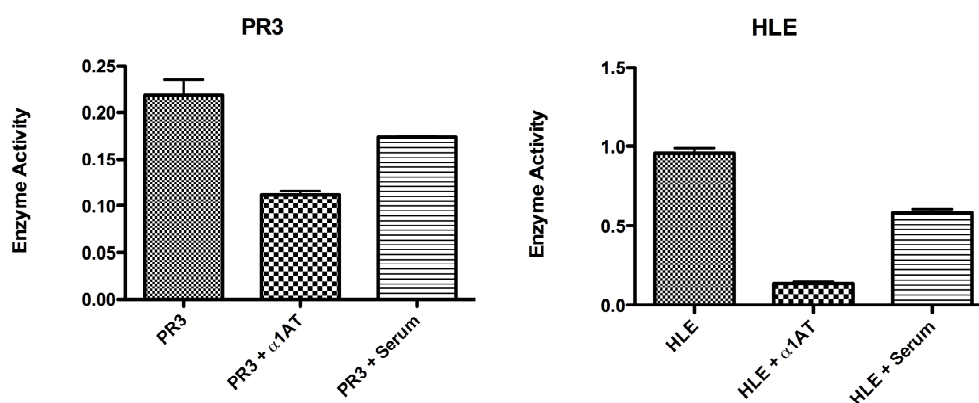


Figure 6 demonstrates a typical enzyme activity test. Enzyme activity tests were routinely performed to check the activity of both the enzymes and inhibitors. 5 μ g/ml PR3 and HLE were incubated for 4 hours with a serine protease substrate (Sigma-Aldrich) in the presence of α 1-Antitrypsin (36 μ g/ml) or fetal calf serum (6%).

2.4 Neutrophil Isolation

Peripheral blood was taken from healthy volunteers, added to 10% acid citrate dextrose (ACD, Sigma Aldrich) and inverted gently to mix. The blood was diluted 1:2 with 2%

dextran (GE Healthcare, UK) and inverted to mix, before spinning at 20g for 20minutes. The supernatants were collected and spun for a further 7minutes at 150g to form a pellet. Percoll gradients (GE Healthcare, Bucks, UK), made up in a 1.5M saline solution (NaCl from Sigma Aldrich), were used to separate the blood into cells types to allow the isolation of neutrophils. The 100% percoll gradient was prepared into 81%, 70% and 55% concentrations by dilution with calcium and magnesium free PBS (Sigma-Aldrich). The gradients were layered, according to density, in a polystyrene conical tube, with 4.5ml of 81% followed by 3ml of 70% and finally 2.5ml of 55% containing the resuspended pellet. The gradients were spun for 30-40minutes at 1500g. Using a sterile pasteur pipette, the top layer from the gradient was removed and discarded. The 55-70% interface contains peripheral blood mononuclear cells (PBMCs) and was also removed and discarded. The neutrophil layer is located at the 70-81% interface and was removed, diluted in PBS and inverted several times to remove the percoll gradient. Following spinning at 400g for 5minutes, the supernatant was removed, and the pellet resuspended and washed in PBS as before. The pellet was finally resuspended in 2ml Hanks buffered saline solution plus hepes (HBH) (Invitrogen) and neutrophils counted on a haemocytometer. The isolated neutrophils had an expected purity of around 95%, whilst Trypan blue (Sigma-Aldrich) staining was used to confirm neutrophil viability (discarded if below 90% viable). Furthermore, neutrophils were size-excluded using a cell counter. Neutrophils were diluted to 5×10^6 cells/ml and used immediately.

2.5 Treatment of Endothelial Cells with Tumour Necrosis Factor- α

Endothelial cells, both GEnC and HUVEC, cultured in a 96-well plate (see sections 2.1 and 2.2 respectively) were grown to confluence at 33°C for three days before transferring to 37°C for 24 hours. The medium was aspirated from the cells and the cells washed twice with PBS (Sigma-Aldrich). TNF- α (NIBSC, stock concentration of 40,000 units/ml) was diluted

accordingly (see table 7) in Medium199 with 0.1% BSA (Sigma-Aldrich) made up to a volume of 1ml.

Table 7 - TNF- α dilutions

TNF-α Units/ml	TNF-α Volume	TNF-α Volume	1:100	Medium199 Volume
0	0	0		1ml
1	0.025 μ l	2.5 μ l		997.5 μ l
5	0.125 μ l	12.5 μ l		987.5 μ l
10	0.25 μ l	25 μ l		975 μ l
25	0.625 μ l	62.5 μ l		937.5 μ l
50	1.25 μ l	125 μ l		875 μ l
100	2.5 μ l	250 μ l		750 μ l

Following removal of PBS from the EnC, 100 μ l of TNF- α was added to the relevant wells and the cells incubated at 37°C for 4 hours. The cells were then washed three times in PBS and 50 μ l of M199 + 0.1% BSA was added to the wells. The neutrophils were added to all wells, excluding the negative control, at a concentration of 2.5x10⁵ cells per well and further incubated at 37°C for an hour. At the same time, the standard curve was prepared. Neutrophils were applied via serial dilution down from a starting concentration of 2.5x10⁵ cells per well. Following the incubation the neutrophils were discarded, and the EnC washed three times with PBS leaving them in 50 μ l PBS. 20 μ l of 1% Triton x100 (Sigma-Aldrich) was added to each well and the cells shaken to lyse. Addition of 100 μ l of o-Phenylenediamine dihydrochloride (OPD) substrate (Sigma-Aldrich) with a 30 minute incubation whilst protected from the light allows for the quantification of neutrophil adherence to the endothelial monolayer when compared to the standard curve. Absorbance was read at 450nm on a Thermo© Multiskan Ascent plate reader.

2.6 P-Selectin, E-Selectin, ICAM-1 and VCAM-1 Cell Surface Expression

ELISA

Endothelial cells were grown to confluence in 96-well culture plates and treated with PR3 and HLE at concentrations of 0.5, 1 and 2 μ g/ml for 2 hours at 37°C with 5% CO₂, with a 4 hour (E-Selectin ELISA) or 8 hour (ICAM-1, VCAM-1 ELISA) treatment with 100units of TNF α , or 15-30min Thrombin (Sigma-Aldrich) (P-Selectin) as a positive control. Following treatment the cells were washed three times in PBS, before being fixed in 2% paraformaldehyde (PFA, Sigma-Aldrich) with 4% sucrose (Sigma-Aldrich) for 20 minutes at 4°C. Following another series of washes the cells were blocked for 30 minutes with StabilCoat® (Direact Ag, Frieberg Germany). The primary antibodies (see table 8) were added in PBS with 4% goat serum (Sigma-Aldrich) and incubated at room temperature on a rotating plate for 1 hour.

Table 8 - Primary Antibodies for ELISA

Antibody	Raised in	Working Dilution	Source
Anti-Human E-Selectin IgG₁	Mouse	1:1000	R&D Systems
Anti-Human P-Selectin IgG₁	Mouse	1:1000	AbCam
Anti-Human ICAM-1 IgG_{2a}	Mouse	1:1000	AbCam
Anti-Human VCAM-1 IgG₁	Mouse	1:1000	R&D Systems
IgG₁ Isotype Control	Mouse	1:1000	Sigma
IgG_{2a} Isotype Control	Mouse	1:2500	R&D Systems

The cells were washed and the secondary antibody, goat anti-mouse IgG HRP-linked (Dako), was applied at a 1:2000 dilution in PBS with 4% goat serum. Following a 45 minute incubation on the rotating plate the cells were washed for a final time and the plate dried by

inverting gently on paper towels. 3,3',5,5'-Tetramethylbenzidine (TMB) solution (Calbiochem) was added to the cells at 50µl per well, and incubated at room temperature protected from light for 15 minutes. The reaction was stopped by the addition of 50µl of 2M hydrochloric acid (HCl, BDH UK) and the plate read at 450nm.

2.7 Quantification of CXCL8 in Cell Supernatant

Endothelial cells were grown to confluence in 96-well culture plates, then treated with graded concentrations of PR3 and HLE in the presence or absence of α 1-AT for a duration of 2 hours at 37°C. CXCL8 was quantified in cell culture supernatants using a capture ELISA kit from BD. A 96-well ELISA plate (NUNC, Thermo Scientific) was coated CXCL8 capture antibody (1:250) overnight at 4°C. The following day the plate was washed in PBS + 0.05% Tween-20 and blocked for 1 hour at room temperature with PBS+10% fetal calf serum (FCS, Sigma-Aldrich). Following a second wash step, the standards and samples were added to the plate in duplicate and incubated at room temperature for 2 hours. Standards were made by serial dilution down from a starting concentration of 400pg/ml. The plate was washed in PBS + 0.05% Tween-20 (Sigma-Aldrich) and the detection antibody plus HRP reagent (1:250) added to the plate for 1 hour. The plate was finally washed and developed with TMB solution (Calbiochem), which was stopped with 2M HCl.

2.8 Protease Digestion of CXCL8 in Cell Culture Supernatants

Endothelial cells were treated for 4 hours with 100 units of TNF α , following which cell culture supernatants were transferred into a second 96 well culture plate. PR3, HLE and α 1-antitrypsin were added to some of the supernatants and incubated for a further 2 hours at 37°C. CXCL8 measurement in the treated supernatants was then performed using the capture ELISA method described in section 2.7.

2.9 Inhibition of Neutrophil Adhesion by Blocking PSGL-1

Neutrophils were isolated, as described in section 2.4, from healthy donors and incubated in the presence of 10 μ g/ml anti-CD162/PSGL-1 (clone PL1) (antibodies-online GmbH, Germany) or the corresponding isotype control for 30minutes. Neutrophils were incubated with protease treated endothelial cells for an hour at 37°C, during which a standard curve was prepared by serial dilution from a starting concentration of 2.5x10⁵ cells per well. Following the incubation, non-adherent neutrophils were removed by washing. The remaining endothelial cell-neutrophil co-culture was left in 50 μ l PBS, then lysed in 1% Triton x100 (Sigma-Aldrich). The neutrophil adherence was quantified by colorimetric assay in which Sigma-Fast OPD substrate (Sigma-Aldrich) is converted to a coloured product by neutrophil MPO. Absorbance was read at 450nm on a BioTek EL808 plate reader using Gen5 software.

2.10 Inhibition of Neutrophil Adhesion by Blocking CXCR1 and CXCR2

Isolated neutrophils were incubated at 37°C on a rocking platform for 30 minutes in the presence or absence of blocking antibodies directed at CXCR1 and CXCR2 (R&D systems, final concentration 4µg/ml). Neutrophils were added to endothelial cells treated for 2 hours with 1µg/ml PR3 or HLE at 2.5×10^5 neutrophils per well and incubated for 1 hour at 37°C. A standard curve was prepared by serial dilution. Following incubation, the supernatants and non-adherent neutrophils were removed. The endothelial cells were washed and left in 50µl PBS. The endothelial cell-neutrophil co-culture was lysed in 1% Triton x100 (Sigma-Aldrich) and 100µl of OPD substrate (Sigma-Aldrich) added, followed by a 30 minute incubation whilst protected from the light. Absorbance was read at 450nm on a BioTek EL808 plate reader.

2.11 Von Willebrand Factor ELISA of Supernatants

Polyclonal rabbit anti-human von Willebrand factor (Dako, UK) diluted 1:500 in carbonate buffer (filter sterilised, see table 9) was added at a volume of 100µl per well into an Immunol2 Dynatech plate (Fisher Scientific) and incubated overnight at 4°C. Excess antibody was removed by washing three times in PBS + 0.05% Tween 20 (Sigma-Aldrich).

Table 9 - Constituents of Carbonate Buffer

Medium Additives	and Volume	Final Concentration	Source
Na₂CO₃	0.40g	19mM	BDH Chemicals LTD, Poole UK
NaHCO₃	0.74g	28mM	Fisons, Ipswich UK
Distilled Water	250ml	-	-

A vWf NIBSC international reference standard (stock 100IU/DL reconstituted in 1ml sterile H₂O) was used to allow quantification of the data. Standards were added to columns 1 and 2 of the 96-well ELISA plate by serial dilution from a starting concentration of 0.625IU/DL. A negative control was also included. All dilutions were performed using PBS + 0.05% Tween 20. Cell culture supernatants were used undiluted and repeated in 100µl triplicates. Following a 1 hour incubation in a wet box, the plate was washed and polyclonal rabbit anti-human vWf-HRP conjugated secondary antibody (Dako) was diluted 1:500 in PBS + 0.05% Tween 20, and added to the wells (100µl per well) for a further hour. Addition of 100µl OPD substrate (Sigma-Aldrich) with 30minutes incubation in the dark allowed for quantification of the vWf present in the supernatants. The plate was read at 450nm.

2.12 Quantifying vWf mRNA by PCR

Endothelial cells treated with PR3 and HLE were removed from culture flasks with trypsin and spun at 1500RPM for 5 minutes to produce a pellet. RNA was isolated using the RNeasy kit (Qiagen) with QIAshredder (Qiagen). Eluted RNA was quantified using the RNA-40 programme on a Nano-Drop. 1.5µg of RNA from each sample was converted to cDNA using

a TaqMan® reverse transcription kit (Applied Biosystems). For TaqMan® reverse transcription mastermix see appendix.

Table 10 - PCR Programme for Reverse Transcription

Temperature	Time	Number of Cycles
25°C	10 min	1
37°C	60 min	1
48°C	30 min	1
95°C	5 min	1
Hold 10°C	-	-

Produced cDNA was quantified using the DNA-50 programme on a Nano-Drop, and purity assessed using the ratio of absorbance at 260 and 280nm (pure cDNA has a ratio approximately 1.8). 1µg of DNA was using added to the PCR mastermix for amplification using vWf primers produced by Alta Bioscience, University of Birmingham (forward primer GCCACCCCACCCCAAACAAGTG, reverse primer TCCCTTTACCGCCCCAGGAGAG, stock 100pm/µl). Primers were used neat, and diluted 1:10 or 1:100 for optimisation. See appendix for constituents of PCR mastermix. TATA-box binding protein (TBP) was used as a house-keeping gene to demonstrate equal loading. TBP primers were produced at Alta Bioscience (forward primer ATGGATCAGAACAACAGCCTG, reverse primer CCCTGTGTTGCCTGCTGGGA, stock 100pm/µl) and used at a 1:32 dilution, the PCR protocol below was used but with a 61°C annealing temperature.

PCR products were diluted in 6x loading buffer (Fermentas) and analysed on a 1% agarose gel (Sigma-Aldrich) in TBE (Gibco) with ethidium bromide (Sigma-Adrich). The gel was visualised and photographed using GeneSnap software.

Table 11 - PCR Programme for vWf Amplification

	Temperature	Time	Number of Cycles
Initial Denaturation	95°C	3min	1
Denaturation	95°C	40sec	40
Annealing	60°C	40sec	40
Extension	72°C	1min	40
Final Extension	72°C	10min	1
Hold	10°C	-	-

2.13 Cell Surface Expression of vWf following Protease Treatment

Endothelial cells were treated with graded concentrations of serine protease (HLE and PR3) in the presence or absence of α 1-AT for 2 hours at 37°C. Following treatment the cells were fixed with 4% sucrose (Sigma-Aldrich) in 2% PFA (Sigma-Aldrich) for 15 minutes, washed with PBS and the endogenous peroxide inhibited with 0.1% hydrogen peroxide (H₂O₂) (Sigma-Aldrich) in methanol for 15 minutes. The endothelial cells were then blocked with 10% marvel in PBS for 1 hour prior to the addition of polyclonal rabbit anti-human vWf-HRP (1:2000) (Dako, Ely UK) for a further hour at room temperature. TMB solution was used to develop the ELISA, and stopped after 10 minutes with 2M HCl (BDH). The plate was read at 450nm.

2.14 vWf Expression by Flow Cytometry

Endothelial cells were grown to confluence in T25 culture flasks and treated for 2h with 1µg/ml PR3 or HLE, or 1Unit Thrombin (Sigma-Aldrich). Cells were washed in blank medium 199 (Gibco) and removed from flasks using cell dissociation buffer (Sigma-Aldrich) and gentle scraping. Cells were washed and split into fluorescence-activated cell sorting (FACS) tubes. Half the cells were fixed in 2% PFA, the other half permeabilised using a Fix&Perm solution (Invitrogen) and stained for vWf using 1:200 sheep anti-human polyclonal vWf (Serotec, Kidlington UK) or the corresponding isotype control (Binding Site). Cells were incubated in the dark at room temperature for 30minutes, resuspended in 2% PFA and analysed immediately on BD FACSCalibur. For each treatment 10000 events were collected and analysed using winMDI.

2.15 vWf, CD63 and F-Actin Staining by Confocal Microscopy

Endothelial cells were grown to confluence on 8-well chamber slides, and treated with 1µg/ml PR3 or HLE. The cells were fixed with ice-cold methanol (Fisher Scientific), for vWf/CD63/Phalloidin staining. Alternatively, a membrane stain, wheat germ agglutinin Alexa fluor®594 (Image-IT™ LIVE, Invitrogen), was incubated with the treated cells for the final 15minutes of treatment, before washing and fixing the cells with 2% PFA. Fixed endothelial cells were prepared using a PAP (Peroxidase Anti-Peroxidase) pen (Dako, UK) and washed in PBS with gentle agitation. Antibodies were prepared in diluent PBS containing 1% BSA and 2% FSC, see table below.

Table 12 - Primary Antibodies for Immunocytochemistry

Antibody	Raised in	Clone	Working Dilution	Source
Polyclonal Anti-Human vWf FITC	Sheep	-	1:100	Serotec
Anti-Human CD63 FITC	Mouse	MEM-259	1:10	Serotec
Phalloidin RPE	Toxin -	-	1:20	Sigma
Image It Live Alexa Fluor 594	-	-	1:200	Invitrogen
Polyclonal Ig FITC	Sheep	-	1:100	Binding Site
IgG₁ Isotype Control FITC	Mouse	F8-11-13	1:10	Serotec

Primary antibody was incubated in the dark for 1 hour at room temperature in a humid chamber. Slides were washed in PBS with gentle agitation and counterstained with a Hoechst (Invitrogen) nuclei stain for 1hour in the dark. Slides were washed in PBS and mounted using slowfade mounting medium (Invitrogen). Slides were viewed immediately by confocal microscope using Zeiss image browser.

2.16 vWf Immunohistochemistry of Kidney Biopsies

Renal biopsy sections were provided by clinical pathology at the Queen Elizabeth Hospital Birmingham under the ethics code 07/Q2602/42. Ethical approval was granted by the North Staffordshire Research and Ethics Committee. Sections were chosen for the number of glomeruli present. Patients included in this research consisted of (i) two female Caucasians, aged 59 and 44 at the time of biopsy, with severe acute-tubular necrosis (both patients have been dialysis dependent at some stage during treatment) (ii) two female Caucasians, aged 59

and 55 at time of biopsy, with severe anti-glomerular basement membrane disease (Goodpastures) and (iii) four patients with ANCA-positive vasculitis. The ASV patients were predominantly female (3 out of 4) with a mean age of 49 (range 33-67). 3 patients were positive for PR3 ANCA and one for MPO (all titres >100EU/ml) with moderate to severe renal failure (mean creatinine 470.5µmol/L, range 240-717).

Removal of paraffin and rehydration of sections was achieved by incubation of slides in Xylene for 10minutes, followed by 100%, 80%, 75% ethanol and running water each for 5minutes respectively. Antigen retrieval was performed by incubation of the sections citrate buffer (S-2369, Dako, UK) for 20 minutes at 95°C in a water bath. Slides were left to cool in the citrate buffer for a further 20 minutes, following which the sections were washed for 10 minutes in cold running water. The slides were blocked for 30 minutes with 0.3% H₂O₂ (Sigma-Aldrich) in methanol. Sections were washed repeatedly with agitation in tris-buffered saline (TBS) (see recipe below) for 5 minutes, before blocking in 20% goat serum (Sigma-Aldrich) for 20 minutes. The primary antibody, rabbit polyclonal vWf (stock 3.1mg/ml, Dako UK) and rabbit IgG isotype control (stock 1mg/ml, R&D systems UK), was diluted 1:400 and 3:400 respectively in TBS and left in a humid chamber overnight at 4°C.

The slides were repeatedly washed in TBS with agitation and developed using a Dako Envision Kit (K5007) following manufacturers guidelines. Sections were counterstained in Harris haematoxylin (Sigma-Aldrich) for 5 min (Tonsil sections) or 10 minutes (Kidney sections). The slides were mounted on ImmunoMount (Thermo Scientific) and visualised using a Nikon Eclipse E400 microscope.

Table 13 - Constituents of TBS pH 7.6

Medium and Additives	Volume	Source
TBS Stock Solution (48.44g in 400ml dH ₂ O)	100ml	Sigma-Aldrich
Distilled Water	1900ml	–
Sodium Chloride	17.6g	Sigma-Aldrich

2.17 Angiopoietin-2 ELISA of Supernatants

Angiopoietin-2 was measured in supernatants from endothelial cells treated with serine proteases for 2 hours using a pre-optimised kit from R&D (DY623). Following manufacturers guidelines, the primary capture antibody was diluted 1:360 (working concentration 1µg/ml) and incubated in NUNC ELISA plates overnight at room temperature. The plate was washed in PBS + 0.05% Tween 20 (Sigma-Aldrich) and blotted dry before blocking with 1% BSA in PBS for 1 hour at room temperature. After further washing, standards were added from a starting concentration of 3500pg/ml (stock 150ng/ml) by serial dilution in 1% BSA in PBS, whilst samples were used neat. The plate was covered and left for 2 hours at room temperature. After washing in PBS + 0.05% Tween 20, the detection antibody was diluted 1:360 (working concentration 2µg/ml) in 1% BSA in PBS and 100µl added to each well. The plate was incubated at room temperature for 2 hours, washed, and incubated for a further 20 minutes in streptavidin-HRP (1:200) avoiding direct light. After a final set of washes the plate developed using TMB solution for 20 minutes in the dark. The reaction was stopped by the addition of 50µl 2M HCl and the plate read at 450nm (subtracting 540nm as background).

2.18 Release of vWf by PAR Agonists

Endothelial cells were grown to confluence in 96-well culture plates at 37°C prior to treatment with graded doses of PR3 and HLE, as well as 100µM of PAR-1 agonist peptide (PAR1-AP) (*H-Thr-Phe-Leu-Leu-Arg-NH₂*, Peptides International), PAR-2 agonist peptide (PAR2-AP) (*H-Ser-Leu-Ile-Gly-Lys-Val-NH₂*, Peptides International) and PAR-2 negative control (*H-Leu-Ser-Ile-Gly-Lys-Val-NH₂*, Peptides International) for 2 hours, (doses and times were determined in preliminary experiments, see figure 56). Following treatment cell culture supernatants were analysed for vWf using the capture ELISA, whilst crystal violet staining was used to determine cell detachment following treatment.

2.19 Knockdown of PAR1 and PAR2 by siRNA

HUVEC were grown to confluence in 24-well culture plates, and incubated for 4 hours with either

- i. Optimem medium alone
- ii. Optimem medium containing 0.2% lipofectamine (LF) RNAiMax
- iii. Optimem medium containing LF RNAiMax, 20nM of Sheath™ RNAi for silencing PAR-1 RNA (FR2 code: HSS103468 – GCUGAUCAUUUCCACGGUCUGUUAU, Applied Biosystems UK)
- iv. Optimem medium containing LF RNAiMax, 20nM of Sheath™ RNAi for silencing PAR-2 RNA (F2RL1 code: HSS103471 – UCAACCACUGUUAAGACCUCC UAUU, Applied Biosystems UK)

- v. Optimem medium containing LF RNAiMax, 20nM of non-silencing Sheath™ RNAi negative control

(all siRNA reagents were supplied by Invitrogen, UK)

After 4hour treatment, HUVEC were incubated with 500µl of complete M199 without antibiotics (penicillin, streptomycin and amphotericin B) for 48-72hours before use in experiments.

2.20 RNA Isolation and Real-Time PCR of PAR-1 and PAR-2

RNA was extracted from siRNA treated HUVEC using the Qiagen RNeasy Mini Kit 50 (Qiagen, UK) following manufacturers guidelines. HUVEC were washed in PBS and lysed with 350µl RTL lysis buffer. 350µl of 70% ethanol was added to the cell lysates and mixed before transferring to columns. Columns were centrifuged for 1 minute at 8000g, the buffer was eluted and 350µl of RW1 added to each column before a further centrifugation at 8000g for 1 minute. 500µl of RPE buffer was added to the columns and centrifuged for 1 minute at 8000g, this was repeated and centrifuged at 8000g for 2 minutes. The columns were placed into new collection tubes and 30µl of RNase free water added. Eluted RNA was quantified for purity and concentration on an Eppendorf Biophotometer.

Real-time PCR was performed using a QuantiTect™ probe RT-PCR kit (Qiagen) following manufacturers guidelines. 10ng of RNA was added to a 96well optimal reaction plate (Applied Biosystems) containing 23µl of mastermix containing QuantiTect™ probe mastermix, RNA water, QuantiTect™ reverse transcriptase mastermix, VIC-labelled β-Actin

primers (Applied Biosystems) and either FAM-labelled PAR-1 primers (Hs00169258_ml, Applied Bioscience) or PAR-2 primers (Hs00608346_ml, Applied Biosystems) see appendix 2. Samples were amplified for 35 cycles and analysed using the 7500 Real-Time PCR machine (Applied Biosystems). The relative expression was determined by comparing the target genes to β -Actin. Changes in mRNA expression were expressed compared to their relative controls (negative siRNA and LF control).

2.21 Flow Cytometry determination PAR-1 and PAR-2 Protein Expression following siRNA

HUVEC treated with siRNA were assessed for changes in protein expression by flow cytometry. Treated HUVEC were grown to confluence in T75 culture flasks. HUVEC were either unstimulated or further treated with 2ng/ml TNF α for 24 hours. HUVEC were washed with 7.5% EDTA (Sigma-Aldrich) before addition of 6.5ml of cell dissociation buffer (Invitrogen). Cells were incubated in dissociation buffer for up to 3 minutes and scraped to remove them from the flask. HUVEC were centrifuged for 5 minutes at 1500rpm, and resuspended in a new tube at a minimum concentration of $5 \times 10^5/100\mu\text{l}$. Primary antibodies (table 14) were added to FACS tubes at 20 μl per tube, followed by 100 μl of the cell suspension.

Table 14 - Antibodies for PAR Flow Cytometry

	Isotype	Clone	Source
PAR-1-PE	IgG1	MOPC-21	BD
Isotype control-PE	IgG1	WEDE15	Fisher Scientific
PAR-1-FITC	IgG1	ATAP2	Santa-Cruz
Isotype control-FITC	IgG1	SC2855	Santa-Cruz
PAR-2-FITC	IgG2a	SAM11	Santa-Cruz
Isotype control-FITC	IgG2a	SC2856	Santa-Cruz

FACS tubes were vortexed and incubated at room temperature for 20 minutes whilst protected from light. Cells were washed by diluting in 1ml FACS buffer (BD) and centrifuged for 5 minutes at 1500rpm. The supernatant was removed, the cells resuspended in FACS buffer and analysed immediately on the BD FACSCalibur flow cytometer.

2.22 Inhibition of Major Pathways of vWf Release

Inhibitors directed at the common signalling pathways associated with vWf release were purchased from Calbiochem. In particular, four signalling molecules were targeted, PKC, PKA, Phosphatidylinositol 3-kinase (PI3K), and Calmodulin (CaM) (see table below). Cells were pre-treated with the inhibitors for 15minutes before the addition HLE or PR3 (2 μ g/ml) into the system. The supernatants were removed and analysed for vWf by ELISA. The cells were analysed by MTT for cell viability.

Table 15 - Inhibitors used for vWf release

Target	Inhibitor	Stock	Source	Working Concentrations
PKC	Gö6983	1000 μ M	Calbiochem	0.01-1 μ M
PKA	Myristoylated PKI (14-22) amide	500 μ M	Calbiochem	0.01-10 μ M
Calmodulin	Calmadizolium	14.5mM	Calbiochem	0.001-1 μ M
PI3K	Wortmannin	58.35mM	Calbiochem	5-20nM

2.23 PKC inhibition of Neutrophil Superoxide Release

Neutrophils were isolated following the method described in section 2.4. HBH and Cytochrome C (final concentration 0.93mg/ml, Sigma-Aldrich) were added to each well. Superoxide Dismutase (SOD, Sigma-Aldrich) was added as a control for inhibited superoxide release (final concentration 1,200U/ml). Neutrophils were primed with 2ng/ml TNF α (NIBSC) and 10 μ M cytochalasin B (Sigma-Aldrich) at 37°C for 15 minutes, and added to each well (100,000/well) in the presence/absence of a stimulus, either ANCA IgG (final concentration 200 μ g/ml) or fMLP (Formyl-Methionyl-Leucyl-Phenylalanine, Sigma-Aldrich) (final concentration 1 μ M), and in the presence/absence of PKC inhibitor (Gö6983) (final concentration 1 μ M). The plate was read at 550nm on a BioTek EL808 plate reader at 5 minute intervals for 120 minutes whilst incubating at 37°C.

2.24 Neutrophil Degranulation Assay

Neutrophils were isolated, as previously described, and diluted to 2.5×10^6 cells/ml in Hanks buffered salt solution with 10mM HEPES (final pH 7.4). Neutrophils were primed for 15 minutes with TNF α (2ng/ml, NIBSC) in the presence of cytochalasin B (10 μ M, Sigma-Aldrich) at 37°C. Primed neutrophils were added to round bottom 96- well culture plates and stimulated with either 200 μ g/ml of ANCA IgG, normal IgG or fMLP (1 μ M, Sigma-Aldrich) as a positive control, for 15 minutes at 37°C. Following stimulation, neutrophils were centrifuged at 400g for 5 minutes and the supernatants collected. The MPO activity within the supernatants was investigated using SigmaFast OPD substrate following manufacture's guidelines. The reaction was stopped with 100% acetic acid (Fisher Scientific) and read at 450nm (Multiskan Thermo-Fisher, MA, USA). This method was provided by Dr Neil Holden.

2.25 Inhibition of vWf release by F-Actin inhibitor, Cytochalasin B

Cytochalasin B is a fungal metabolite that inhibits the polymerisation of the actin cytoskeleton, hence can be used to investigate cellular mobilisation. HUVEC were pre-treated for 5 minutes with a range of dilutions of cytochalasin B (Sigma-Aldrich) in M199+0.5% BSA, before the addition of 2 μ g/ml HLE. The cells were incubated for 2 hours at 37°C, following which, supernatants were removed and analysed for vWf by capture ELISA as described previously. The endothelial cells were then either quantified for changes in mitochondrial activity by MTT or visualised by phase microscopy.

2.26 Stimulation of Endothelial vWf release by Okadaic Acid

Endothelial cells were initially treated with a range of dilutions of Okadaic Acid (sodium salt 459620, Calbiochem, UK) from 500nM to 1nM for 2 hours at 37°C. Cells were also treated with PR3 and HLE for comparative purposes. Following treatment, the supernatants were removed and analysed for vWf release by capture ELISA, the remaining endothelial cells were stained with crystal violet to assess cell detachment (for method see section 2.29). For later experiments Okadaic acid was used at a concentration of 100nM for 2 hours in the presence or absence of serine proteases, this was followed by MTT to assess endothelial cell viability (see section 2.30).

2.27 Tyrosine and Serine/Threonine Phosphorylation by Western Blotting

Endothelial cells were treated with 1µg/ml PR3 and HLE in the presence or absence of α 1AT, or 100nM Okadaic Acid. Following removal of supernatants the cells were scraped into NP40 ((Octylphenoxy)phenoxy polyethoxy ethanol) lysis buffer containing protease inhibitor cocktail III and a phosphatase inhibitor cocktail (Calbiochem, 1:100 dilution), see recipe below.

Table 16 - Constituents of NP40 Lysis Buffer

	Stock Concentration	Volume	Source
NP40		500 μ l	Sigma-Aldrich
Water	N/A	27.8ml	-
EDTA	50mM	2ml	Sigma-Aldrich
Glycerol	99.9%	5ml	Sigma-Aldrich
Tris-HCl	1M	1ml	Calbiochem
Sodium Chloride Solution	0.5M	13.7ml	Calbiochem

Samples were spun at 7000g for 10min at 4°C and the supernatant removed for quantification of protein by Nano-Drop Spectrophotometer ND-1000. 250 μ g of protein was diluted in 6x SDS-PAGE (sodium dodecyl sulfate polyacrylamide gel electrophoresis) loading buffer (see appendix for recipes) and boiled for a further 5min before loading into a 10% SDS-PAGE gel. The gel was run for 1 hour at 120V, and transferred onto a nitrocellulose membrane using a semi dry unit at 34mA for 1 hour. The membrane was blocked for 1 hour in 5% BSA in TBS-0.01% Tween (TBS-T) (powdered BSA, Triza-Base and Tween-20 all from Sigma-Aldrich). Primary antibody was diluted in 5% BSA in TBS-T and incubated overnight at 4°C with agitation. The membrane was washed in TBS-T and incubated with secondary antibody at room temperature for 1 hour with agitation. The blot was incubated with ECL+ (Amersham, GE Healthcare) for 5min, drained and wrapped in saran wrap. The blot was exposed to X-Ray film (Amersham, GE Healthcare) for up to 10min and developed on a Xograph imaging system (compact X4).

Table 17 - Antibodies used for Western Blotting

Antibody	Raised in	Clone	Working Dilution	Source
Anti-Human Phosphotyrosine	Mouse	p-tyr-100	1:1000	New England Biolabs
Polyclonal Anti-Human Phosphoserine/threonine	Rabbit	-	1:750	AbCam
Anti-Mouse HRP	-	-	1:2000	New England Biolabs
Anti-Rabbit HRP	-	-	1:10000	Amersham

2.28 Necrosis versus Apoptosis with ApoGlow®

Apoptosis, necrosis and proliferation was determined by Adenosine-5'-triphosphate (ATP) levels and the Adenosine-diphosphate (ADP):ATP ratio in cultured cells using the ApoGlow® Assay (Lonza, UK). ApoGlow® uses the conversion of ATP into ADP as a marker for apoptosis and necrosis. ATP is measured in endothelial cells as a marker of mitochondrial activity, and is present in all metabolically active cells. As cells undergo apoptosis this level of ATP decreases as it is converted to ADP. ApoGlow® measures ATP in cell lysates by the conversion of ATP and luciferin into oxyluciferin and AMP by the addition of luciferase. The light emitted as a by-product of this reaction is linearly related to the ATP concentration in the cells. ADP is quantified by first converting it into ATP.

Glomerular endothelial cells were treated for durations of 2hours or 24hours with different concentrations of protease (PR3 and HLE) in a 96-well culture plate. The ApoGlow® reagents were made up following the manufacturer's guidelines and allowed to warm to room temperature prior to use. Following treatment, the endothelial cells were removed from

the incubator and allowed to return to room temperature, after which 100µl of nucleotide releasing reagent (NRR) was added to each of the wells and left for a minimum of 5 minutes. Of the cell lysate, 180µl was transferred to a luminescent compatible 96-well plate and 20µl of nucleotide monitoring reagent (NMR) added. The plate was then read on the Mikrowin© program on a Centro LB 960 luminometer (Berthold Technologies, Harpenden, UK). The initial reading (A) gives the level of ATP in the cell lysate, and was followed by a 10minute incubation and a second reading (B). Following the addition of 20µl of ADP-converting reagent and a 5minute incubation protected from the light, a final reading is taken (C) from which the ADP:ATP ratio can be calculated using the following equation:

$$\text{ADP:ATP ratio} = \frac{(C-B)}{A}$$

2.29 Crystal Violet Staining of Adherent Cells

Crystal violet is a cellular dye that can allow for quantification of changes in cell number following treatment. Crystal violet staining was used to assess cell detachment following PR3 and HLE treatment. Endothelial cells were treated with PR3 and HLE for 2 hours in a 96-well culture plate. After which, they were washed with PBS and fixed with 2% formalin (Fisher Scientific) for 15 minutes. 0.1% crystal violet (Sigma-Aldrich) was added to each of the wells for 10 minutes, then washed 5 times with PBS. 1% triton X100 (Sigma-Aldrich) was added 100µl per well for 10 minutes on a shaking plate. The plate was read at 550nm.

2.30 MTT assessment of Mitochondrial Activity

To assess the changes in the mitochondrial activity of the endothelial cells, and hence endothelial injury, following treatment with PR3 and HLE we used an MTT (1-(4,5-Dimethylthiazol-2-yl)-3,5-diphenylformazan, Sigma-Aldrich) assay. The MTT assay works via the conversion of solubilised MTT into formazan crystals by mitochondrial succinate dehydrogenase. These formazan crystals can then be dissolved and quantified as a measure of cellular mitochondrial activity. Endothelial cells were treated in 24-well culture plates. Following treatment cells were washed in PBS, and 5µg/ml MTT in M199 + 0.1% BSA added to each well. Culture plates were incubated at 37°C on a shaking plate for 1 hour. The cells were washed in PBS and the plate dried on a clean tissue via inversion. DMSO (Dimethyl Sulfoxide, Sigma-Aldrich) was added to each of the well and the plate incubated on a shaking plate for a further 30 minutes at 37°C. The samples were transferred in triplicate to a 96-well plate and read at 540nm.

2.31 Statistical Analyses

Experiment data was assessed for significance using GraphPad Prism version 5 (Graphpad Software Inc., USA), and SPSS version 18 (IBM, USA) software. SPSS was used for analyses of experiments in which data sets were missing. Tests for normality were performed using the D'Agostino & Pearson omnibus normality test. Data sets contains greater than 3 variables were assessed for significance using a 1-way ANOVA with pot-hoc test. 2-way ANOVAs were used to compare treatments between cell types. For experiments in which α 1-antitrypsin and inhibitors were used, paired T-tests or wilcoxon signed rank tests

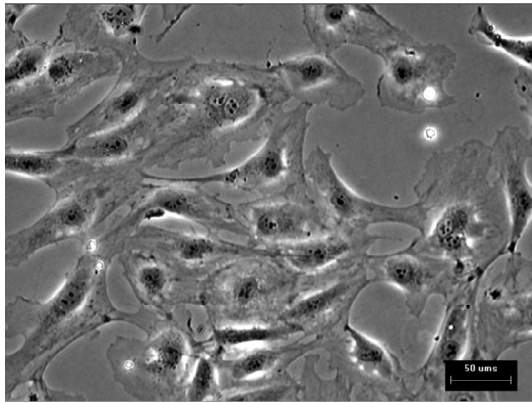
(depending on normality) were used to assess the significance of the inhibition compared to an uninhibited control. Significance was classed as $p < 0.05$ and expressed as $* < 0.05$, $** < 0.01$ and $*** < 0.001$. For experiment with inhibition $^+$ was used to denote significance compared to an uninhibited control.

3. Results

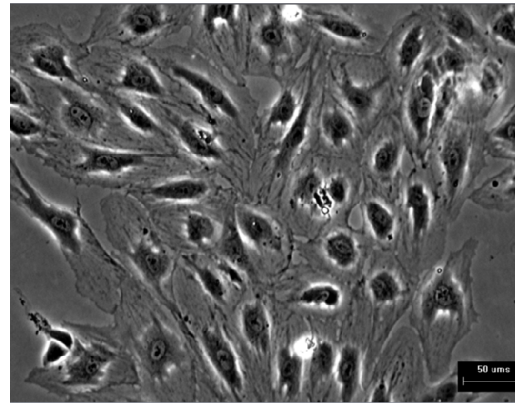
3.1 Visualisation of Endothelial Cells at Different Time Points in Culture

Two types of endothelial cell were used in this thesis, a conditionally immortalised glomerular endothelial cell line (GEnC) (gift from S. Satchell, Bristol UK [275]) and endothelial cells isolated from the human umbilical vein (HUVEC). The conditionally immortalised GEnC have been suggested to retain their morphological features until at least passage 41. GEnC were passaged at day 0 and split into three new culture flasks following the method described in section 2.1, whilst HUVEC were isolated from umbilical cords donated from the Birmingham Woman's Hospital and added to culture flasks (see section 2.2). The cells were visualised at day 3 and day 6 post passage or isolation (figure 7). Visualisation of cells at 3 days clearly demonstrates the endothelial cells in the log phase of development. During this stage of the cell cycle the endothelial cells are undergoing active cell division and proliferation. The cells, themselves, appear stretched and spindle-like as they attempt to form contacts with other endothelial cells. At 6 days, cultured endothelial cells take on the characteristic "cobblestone" appearance previously described by Striker *et al.*, 1984 [274]. The cells are subject to 'contact inhibition' and do not grow on top of each other. The cells become smaller and rounder in shape, forming connections with other cells to form a single endothelial cell monolayer. Endothelial cells were grown to form confluent monolayer before used in experiments.

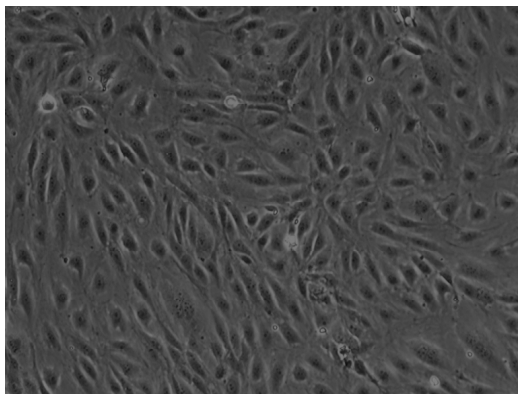
Figure 7 - Visualisation of Endothelial Cells at Different Time-Point



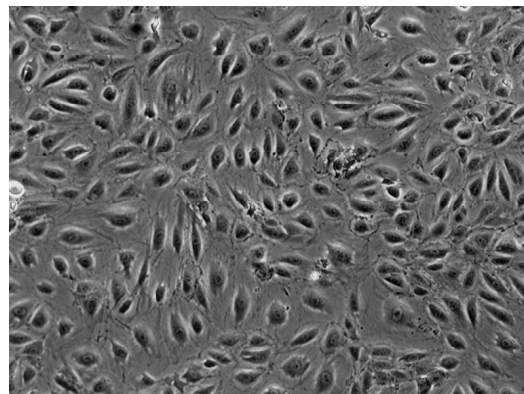
GEnC p28
3 days after passage
(x20)



HUVEC
3 days after isolation
(x20)



GEnC p28
6 days after passage
(x10)



HUVEC
6 days after Isolation
(x10)

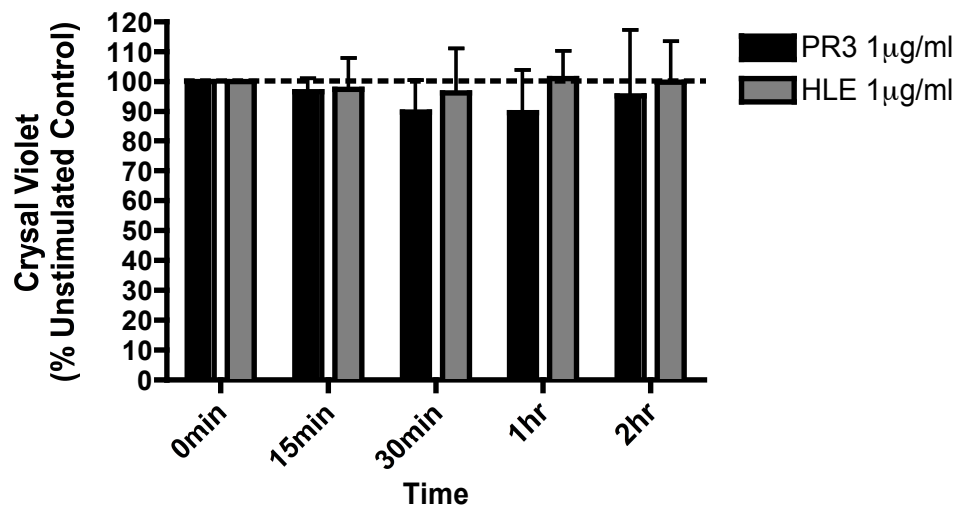
Phase microscopy of glomerular endothelial cells and HUVEC 3 days post passage and isolation respectively. After 6 days of growth, phase microscopy depicts a typical confluent monolayer.

3.2 Crystal Violet Staining for Cell Adherence

To investigate a role for the neutrophil serine proteases in endothelial cell injury, PR3 and HLE were first assessed for their ability to induce endothelial cell detachment after short incubations using a crystal violet cell stain. Changes in endothelial adherence could be assessed by changes in the intensity of crystal violet dye present after lysis of the endothelial cells. An increase in optical density would suggest cellular proliferation, whilst decreases suggest loss of adherent cells. Glomerular endothelial cells were treated with 1 µg/ml of PR3 and HLE for between 15 minutes and 2 hours. Changes in the number of adherent endothelial cells following treatment were represented as percentages of untreated endothelial cells. The glomerular endothelial cells treated with 1 µg/ml PR3 or HLE demonstrated no significant changes in cellular detachment when compared to the untreated control at all time points (figure 8). Further to this, confluent monolayers of glomerular endothelial cells were treated for 2 hours with concentrations of serine protease above and below our 1 µg/ml standard treatment, to assess how a higher dose would affect cellular attachment *in vitro*. Here it was demonstrated that even at higher doses of PR3 and HLE (2 µg/ml) there was no significant increase in endothelial cell detachment following a 2 hour treatment (figure 9).

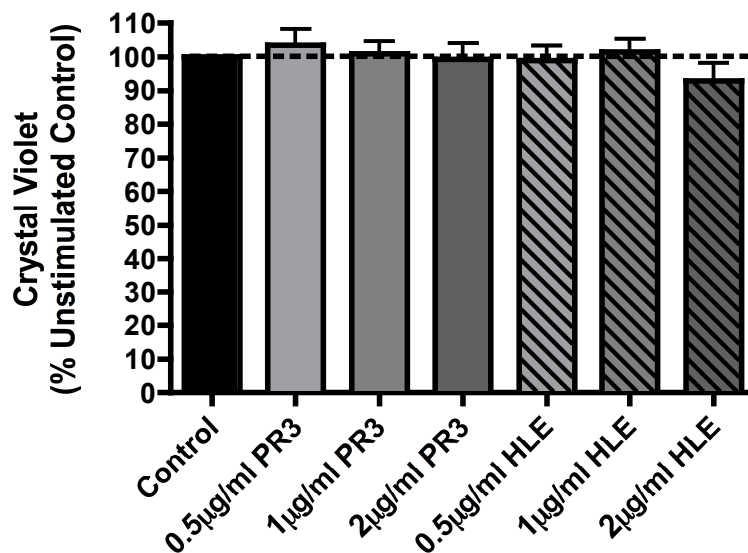
The crystal violet method assumes that the cells contain an equal intensity of dye, so that cell detachment accurately represents the changes in colour intensity. To confirm this we could have seeded known cell numbers and stained with crystal violet to determine if the dye intensity accurately represents the number of adherent cells.

Figure 8 – Timecourse of Crystal Violet Staining for Endothelial Detachment



Glomerular endothelial cells were treated for up to 2 hours with 1µg/ml PR3 or HLE, fixed in 2% PFA and the number of adherent cells quantified by crystal violet staining. The results shown are the mean and standard error of 3 separate experiments displayed as a percentage of the unstimulated control (0min). Statistical significance was calculated using a 2-way ANOVA with Bonferroni post test (treatment $p=0.1408$, time $p=0.9424$).

Figure 9 - Crystal Violet Staining for Endothelial Detachment following treatment with increasing concentrations of Serine Protease

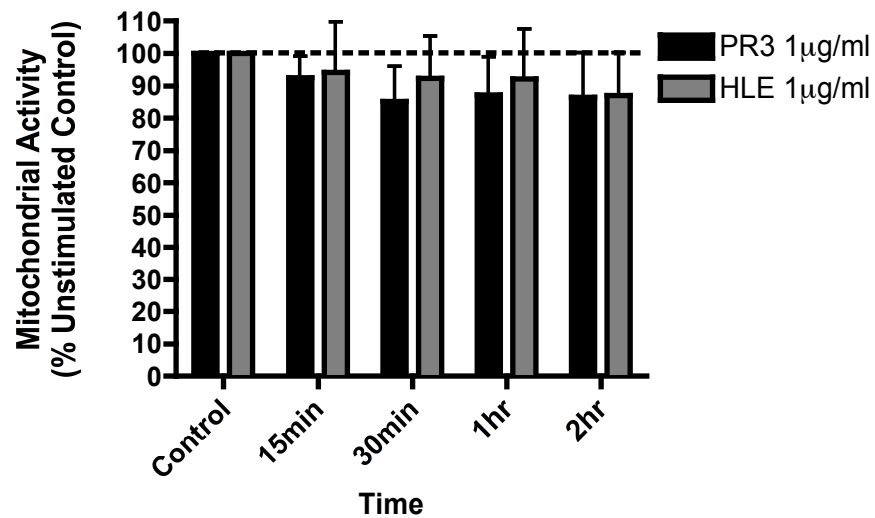


Glomerular endothelial cells were treated with increasing concentrations of PR3 and HLE (0.5µg/ml - 2µg/ml) for 2 hours, fixed in 2% PFA and adherent cells quantified by crystal violet staining. The data shown here are the mean and standard error from 3 separate experiments displayed as a percentage of the unstimulated control. Analysis by 1-way ANOVA with Bonferroni post-test demonstrated no significant difference between control and treated groups (PR3 $p=0.8173$, HLE $p=0.1647$).

3.3 Measure of Mitochondrial Activity in Serine Protease Treated Endothelial Cells

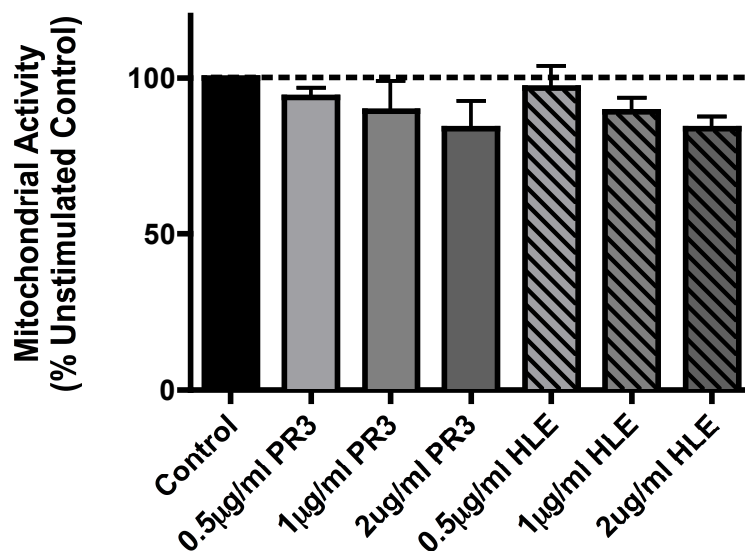
The MTT assay was used in collaboration with the crystal violet to demonstrate changes in the viability of serine protease treated endothelial cells. The MTT assay uses the conversion of the MTT compound by mitochondrial succinate dehydrogenase as a measure of mitochondrial activity. Again, glomerular endothelial cells were treated with 1µg/ml PR3 or HLE for between 15 minutes and 2 hours. Mitochondrial activity of treated glomerular endothelial cells was displayed as a percentage of the unstimulated control. Even at 2 hours treatment there was no significant decrease in mitochondrial activity following treatment with 1µg/ml PR3 or HLE (figure 10). Moreover, GEnC treated with increasing concentrations of PR3 and HLE (0.5µg/ml - 2µg/ml) for 2 hours (figure 11) displayed no significant decrease in the level of mitochondrial activity following treatment of GEnC with higher concentrations of PR3 ($p=0.2114$). The analysis of HLE treatment by 1-way ANOVA demonstrated a significant difference between untreated and HLE treated GEnC ($p=0.0337$), although there was no significant difference between untreated GEnC and individual HLE concentrations (Bonferroni post-test $p>0.05$ for all concentrations).

Figure 10 - Mitochondrial Activity following a Timecourse of Protease Treatment



Glomerular endothelial cells were treated with 1µg/ml of PR3 and HLE for durations of up to 2 hours, after which, they were assessed for changes in mitochondrial activity by MTT assay. The data shown here are the mean and standard error from 3 separate experiments and displayed as a percentage of the unstimulated control. Statistical significance was assessed by 2-way ANOVA with Bonferroni post-test (treatment $p=0.0561$, time $p=0.6347$).

Figure 11 - Mitochondrial Activity following treatment with increasing concentrations of Serine Protease



Glomerular endothelial cells were treated with increasing concentrations of PR3 and HLE (0.5µg/ml - 2µg/ml) for 2 hours, before assessment of mitochondrial activity by MTT assay. The data shown here are the mean and standard error of 3 separate experiments, displayed as a percentage of the unstimulated control. Statistical significance was assessed by 1-way ANOVA with Bonferroni post-test (PR3 $p=0.2114$, HLE $p=0.0337$).

3.4 Measure of Apoptosis by Conversion of ATP into ADP

The Apoglow® assay works on the principle that as cells prepare to undergo apoptosis, intracellular ATP stores are converted to ADP. GEnC treated for 2 hours with 0.5µg/ml - 2µg/ml PR3 or HLE showed no significant decrease in the level of intracellular ATP. Alternatively, GEnC lysed in either water or 1x triton X100, used as positive controls of necrosis, demonstrated greatly reduced levels of ATP compared to untreated GEnC. The serine protease treated endothelial cells also showed no increase in the ADP:ATP ratio at 2 hours, when compared to cells lysed with water or 1x Triton X100 (figures 12 and 13). Alternatively, GEnC treated for 24 hours with PR3 and HLE displayed significantly decreased levels of ATP, which were particularly evident with HLE treatment at concentrations of 1µg/ml and 2µg/ml. These cells also displayed an increased ADP:ATP ratio compared to untreated endothelial cells, however this did not reach significance (figures 14 and 15). In particular, the ADP:ATP ratio from 2µg/ml HLE treated GEnC is more comparable to the levels seen in GEnC lysed in water than the untreated control (see table 20). GEnC treated with 2µg/ml PR3 for 24 hours also demonstrated significantly decreased levels of ATP, as well as a 10-fold increased ADP:ATP ratio, although this also did not reach significance. Furthermore, comparison of endothelial cells at the two time points by 2-way ANOVA indicates a significant difference between the ATP levels in 2 hour and 24 hour treated GEnC ($p=0.002$), whilst untreated endothelial cells incubated for 24 hours only retain approximately 50% of the intracellular ATP present after a 2 hour incubation. Moreover, treatment with 2µg/ml HLE displayed a significantly increased ADP:ATP ratio at 24 hours compared to 2 hours treatment ($p<0.05$, Bonferroni post-test).

It is of note, that whilst the ATP concentrations decreased significantly following a 24 hour incubation with PR3 and HLE, the ADP concentration did not increase by the same magnitude. One would expect that, as the cell converts internal stores of ATP into ADP, we would see an equal decrease and increase, respectively, in concentrations. It is possible that this may be due to technical issues with the ApoGlow® kit, specifically in not accurately converting all internal stores of ADP into ATP for measurement. As cells are not washed following treatment, the loss of ATP or ADP into supernatants would not exclude it from measurement. Because of this, the ADP:ATP ratio data should be regarded with caution, and apoptosis should be confirmed by alternative methods.

Visualisation of the cells after PR3 or HLE treatment at both the 2 hour and 24 hour incubation times was used to help confirm the state of apoptosis and endothelial detachment. Following treatment with serine proteases the endothelial cells were captured using a phase microscope (Olympus). Although there appears to be some level of endothelial cell detachment, the GEnC that received a 2 hour treatment with 1µg/ml PR3 or 1µg/ml HLE still maintain a confluent monolayer. This cannot be seen in those samples that were treated with water. At 24 hours, the serine protease treated endothelial cells no longer uphold this observation, whilst untreated cells still display an intact endothelial monolayer (figure 16).

Table 18 - Numerical Data for ApoGlow® Assay at 2 hours

	Mean ATP (RLU)	Mean ADP:ATP	Outcome
Untreated Control	226731.1667	0.060610713	Healthy
0.5µg/ml PR3	216713.1667	0.27892837	Healthy
1µg/ml PR3	211072.3333	0.317791831	Healthy
2µg/ml PR3	197621.6667	0.342578093	Healthy
0.5µg/ml HLE	232723.3333	0.036910107	Healthy
1µg/ml HLE	227018.5	0.095202433	Healthy
2µg/ml HLE	204005.6667	0.206395723	Healthy
Water	8651.5	1.1125037	Necrosis
1x Triton X100	10012.5	7.707885	Necrosis

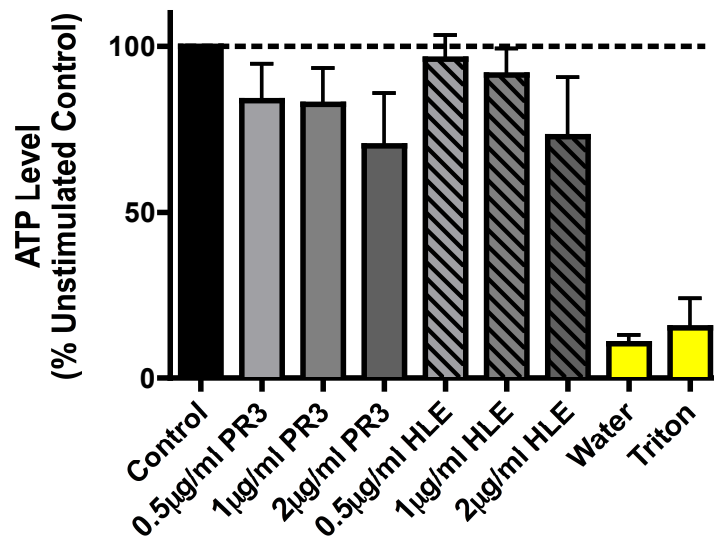
For ApoGlow® assay guideline criteria please see appendix

Table 19 - Numerical Data for ApoGlow® Assay at 24 hours

	Mean ATP (RLU)	Mean ADP:ATP	Outcome
Untreated Control	116003.0167	0.03266337	Healthy
0.5µg/ml PR3	96808.16667	0.082283747	Healthy
1µg/ml PR3	85784.5	0.111148703	Healthy
2µg/ml PR3	64652.5	0.30285567	Early Apoptosis
0.5µg/ml HLE	73216.66667	0.10441851	Arrested Proliferation
1µg/ml HLE	27086.66667	0.3540396	Apoptosis
2µg/ml HLE	11011.33333	0.840836333	Apoptosis
Water	8651.5	1.1125037	Necrosis
1x Triton X100	10012.5	3.2846265	Necrosis

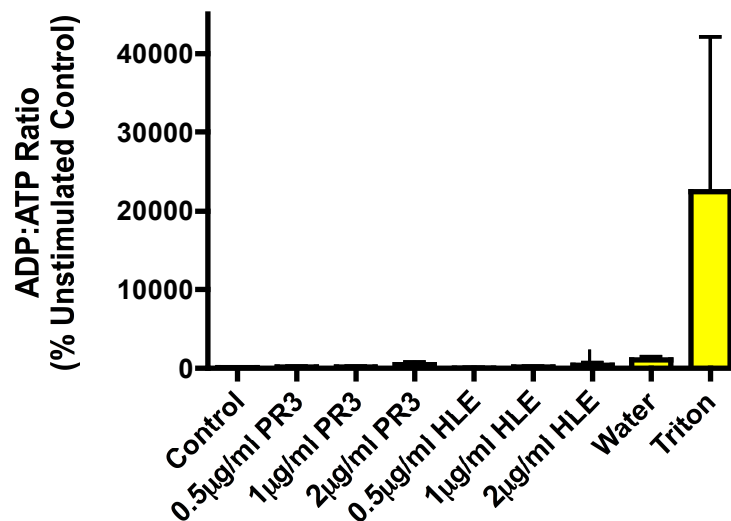
For ApoGlow® assay guideline criteria please see appendix

Figure 12 - Changes in Intracellular ATP levels at 2 hours



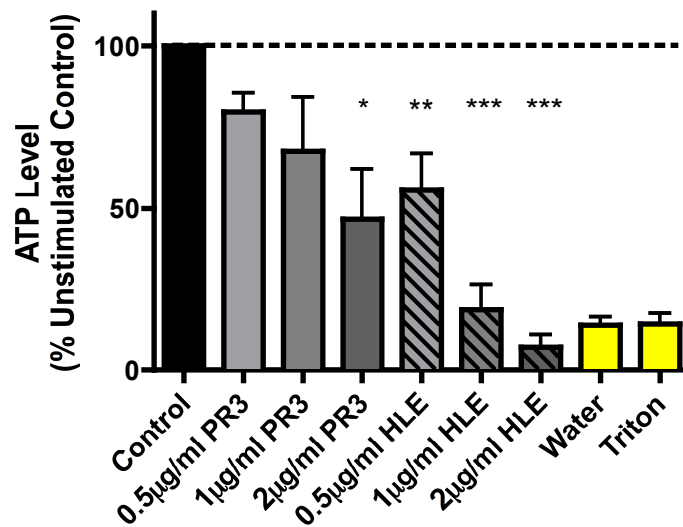
Glomerular endothelial cells were treated with increasing doses of PR3 and HLE (0.5µg/ml - 2µg/ml) for 2 hours and measured for intracellular ATP concentration by the addition of a nuclear monitoring reagent. The level of luminescence produced in this reaction is directly proportional to the level of ATP. The data shown here are the mean and standard error for 3 separate experiments, displayed as a percentage of the unstimulated control. Statistical significance was calculated using a 1-way ANOVA with Bonferroni post-test (PR3 p=0.1185, HLE p=0.1561).

Figure 13 - Changes in the ADP:ATP Ratio at 2 hours



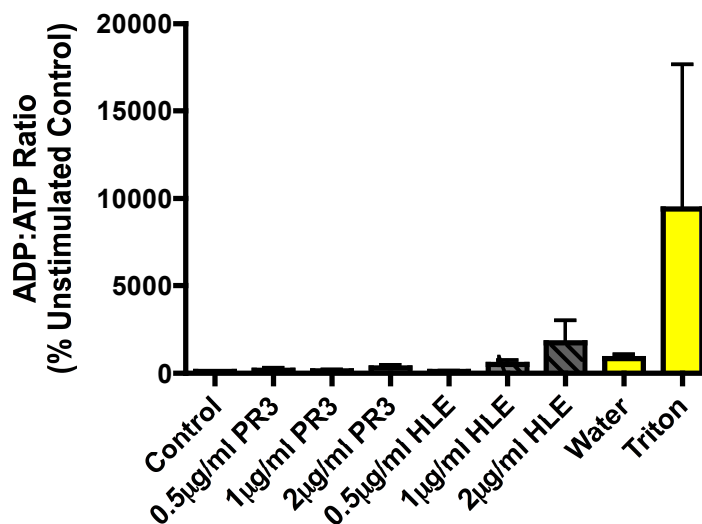
ADP was measured in 2 hour treated glomerular endothelial cells by the conversion into ATP. The luminescence produced was linearly related to the level of ATP. Subtraction of the initial ATP reading from the total ATP reading after ADP conversion was equal to the ADP present within the cell. The data shown here are the mean and standard error from 3 separate experiments, represented as a percentage of the unstimulated control. Statistical significance was assessed by 1-way ANOVA with Bonferroni post-test (PR3 p=0.4585, HLE p=0.3400).

Figure 14 - Changes in Intracellular ATP Levels at 24 hours



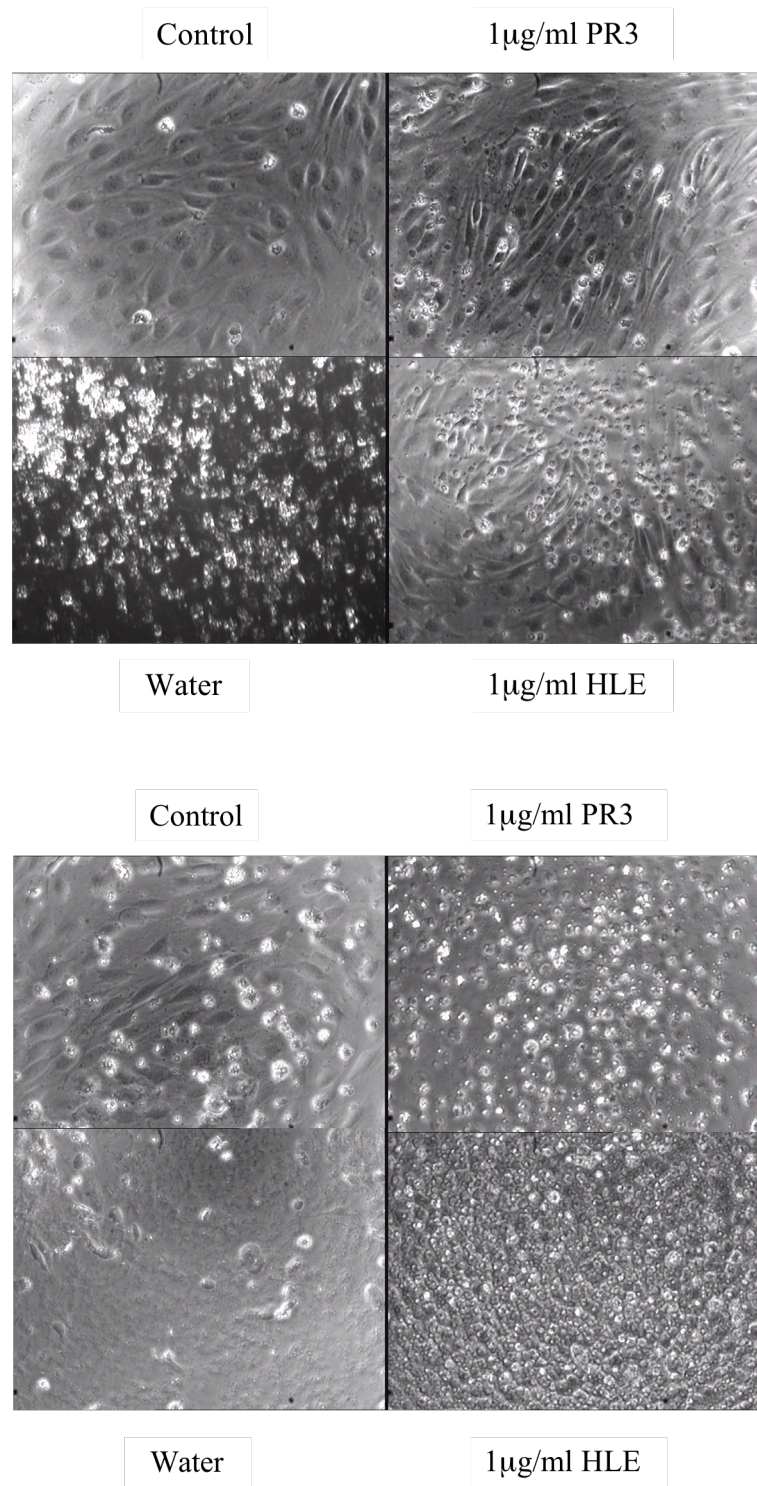
Glomerular endothelial cells were treated with increasing doses of PR3 and HLE (0.5µg/ml - 2µg/ml) for 24 hours and measured for intracellular ATP concentration by the addition of a nuclear monitoring reagent. The level of luminescence produced in this reaction is directly proportional to the level of ATP. The data shown here are the mean and standard error for 3 separate experiments, displayed as a percentage of the unstimulated control. Statistical significance was calculated using a 1-way ANOVA with Bonferroni post-test (PR3 p=0.0198, HLE p<0.0001). *p<0.05, **p<0.01, ***p<0.001

Figure 15 - Changes in the ADP:ATP Ratio at 24 hours



ADP was measured in 24 hour treated glomerular endothelial cells by the conversion into ATP. The luminescence produced was linearly related to the level of ATP. Subtraction of the initial ATP reading from the total ATP reading after ADP conversion was equal to the ADP present within the cell. The data shown here are the mean and standard error from 3 separate experiments, represented as a percentage of the unstimulated control. Statistical significance was assessed by 1-way ANOVA with Bonferroni post-test (PR3 p=0.2513, HLE p=0.2835).

Figure 16 - Visualisation of GEnC after Serine Protease Treatment



The images above are a representative of how unwashed glomerular endothelial cells appear under the microscope following a 2 hour (upper panel) or 24 hour (lower panel) treatment with 1 μ g/ml PR3 and HLE.

3.5 Von Willebrand Factor Release from Serine Protease Treated Endothelial Cells

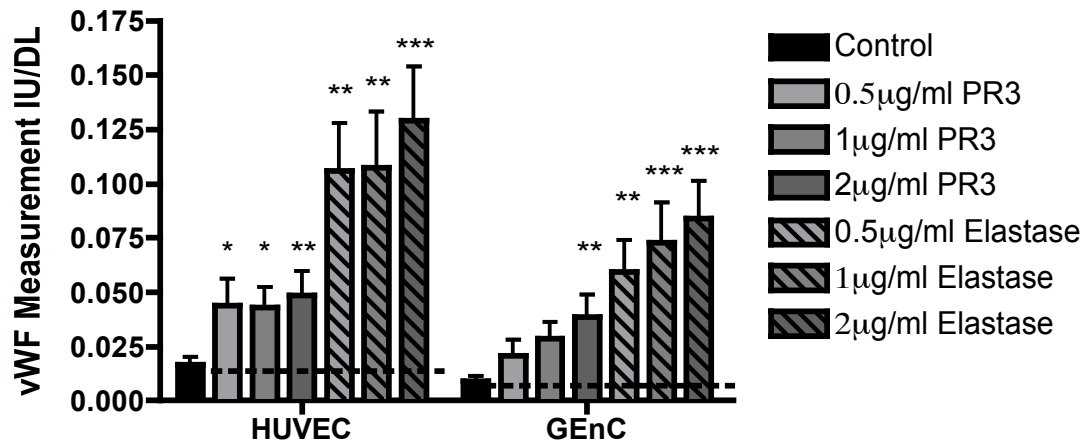
To further assess an injurious role for the neutrophil serine proteases in vasculitis, vWf release was measured from glomerular endothelial cells treated with 0.5 μ g/ml - 2 μ g/ml of PR3 or HLE for 2 hours and 24 hours. The release of vWf from this conditionally immortalized microvascular glomerular endothelial cell line was compared to the level of release from HUVEC, a readily available primary macrovascular endothelial cell. vWf release was significantly increased from GEnC and HUVEC at 2 hours with all concentrations of HLE, with between a 7 and 9 fold increase (HUVEC and GEnC respectively) in vWf release from 2 μ g/ml HLE treated endothelial cells above unstimulated control cells. The increased vWf release from PR3 treated endothelial cells was lower than that from HLE treated cells. Again, treatment of HUVEC with all concentrations of PR3 resulted in significantly increased vWf release above the untreated control (around 2-fold increase), whilst on GEnC, only 2 μ g/ml of PR3 resulted in a significant increase (4-fold), although vWf release does appear to increase at lower PR3 concentrations in a dose dependant fashion (figure 17). Endothelial cells were further treated with a higher concentration of serine protease (5 μ g/ml), however this resulted in endothelial cell detachment (see section 3.7)

Following a 24 hour treatment with PR3 and HLE there was a greatly increased level of release vWf compared to 2 hour treatment, however, this is also true of untreated endothelial cells, and therefore the difference in release between treated and untreated is much less marked. HLE treatment at this timepoint appears to display a dose dependant decrease in vWf release, most evident with HUVEC (figure 18). Earlier timepoints for vWf release (15

minutes - 1 hour) were also investigated but no significant increase in vWf release was observed (figures 19 and 20).

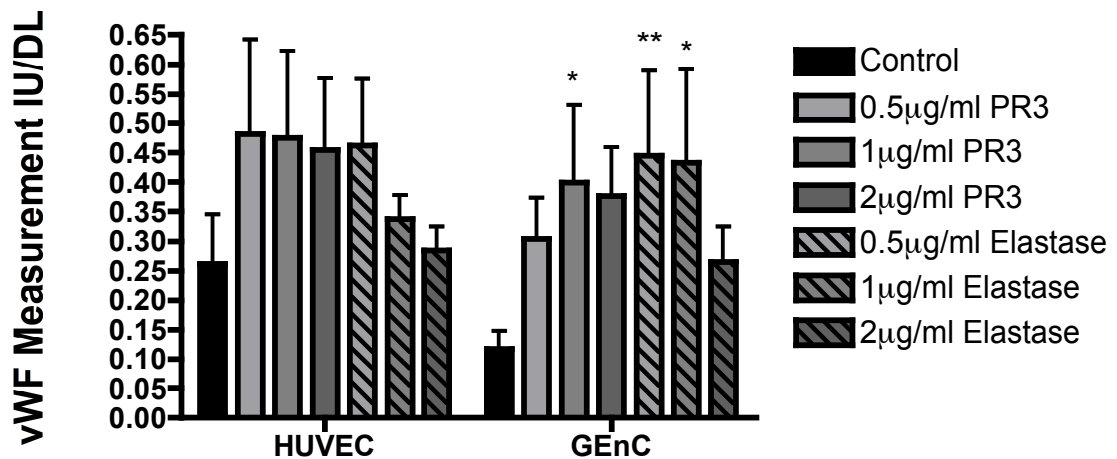
The vWf release from serine protease treated endothelial cells was calculated as a percentage of total endothelial vWf (released plus lysate). Treatment with 2 μ g/ml of HLE stimulated between 40% and 50% of total vWf to be released from HUVEC and GEnC respectively (figures 21 and 22). The percentage release from PR3 treated endothelial cells was not significantly increased and more comparable to the levels seen with untreated endothelial cells, although this is likely to be due to high variation between the individual experiments.

Figure 17 - vWf Release from PR3 and HLE Treated Endothelial Cells at 2 hours



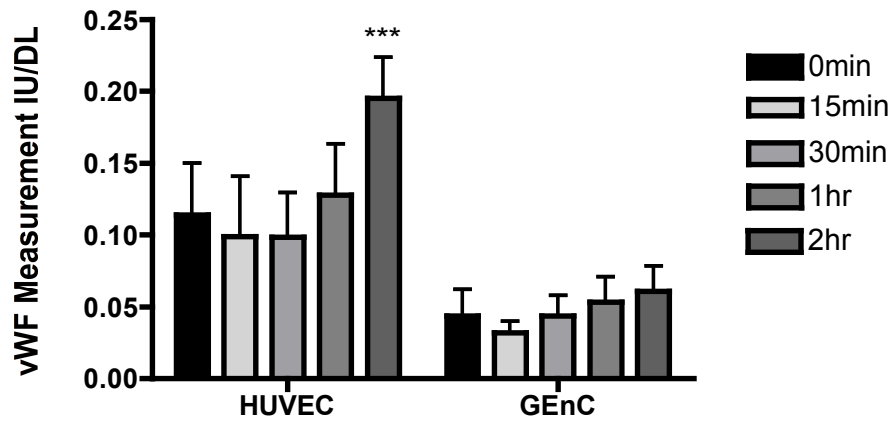
Endothelial cells were treated with increasing concentrations of PR3 and HLE for 2 hours, after which vWf was measured in cell culture supernatants. HUVEC data shown are the mean and standard error of 9 separate experiments. GEnC data shown are the mean and standard error of 10 separate experiments. Statistical significance was calculated by 1-way ANOVA with Bonferroni post-test (HUVEC $p=0.0001$, GEnC $p=0.0003$). A 2-way ANOVA was used to test the significant difference between two cell types ($p=0.0012$). * $p<0.05$, ** $p<0.01$, *** $p<0.001$

Figure 18 - vWf Release from PR3 and HLE Treated Endothelial Cells at 24 hours



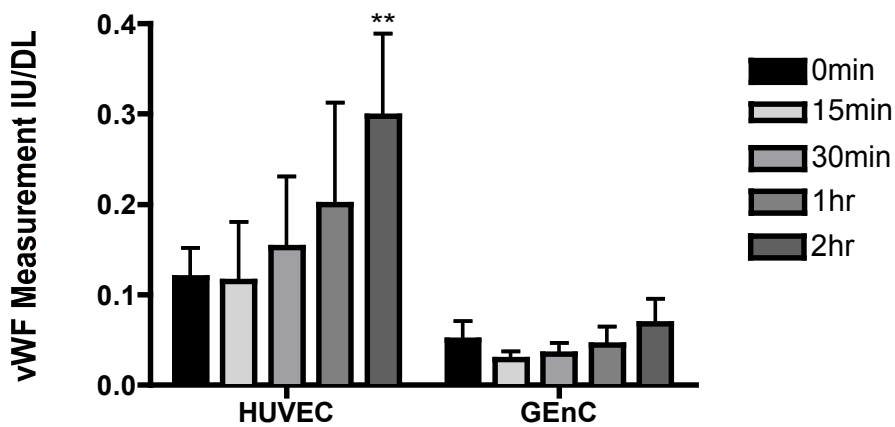
Endothelial cells were treated with increasing concentrations of PR3 and HLE for 24 hours, after which vWf was measured in cell culture supernatants. The data shown here are the mean and standard error of 4 separate experiments. Statistical significance was calculated by 1-way ANOVA with Bonferroni post-test (HUVEC $p=0.0625$, GEnC $p=0.0048$). A 2-way ANOVA was used to test the significant difference between two cell types ($p=0.3097$). * $p<0.05$, ** $p<0.01$

Figure 19 - Timecourse of vWf Release from PR3 Treated Endothelial Cells



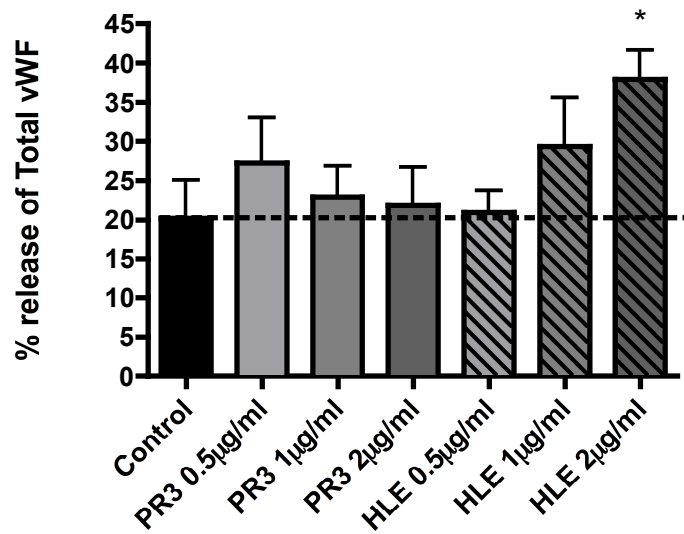
Endothelial cells were treated with 1 μ g/ml PR3 for up to 2 hours to see if vWf release could be detected from the cell at earlier timepoints. vWf was measured in cell culture supernatants by capture ELISA. The data shown here are the mean and standard error of 3 separate experiments. Statistical significance was assessed by 2-way ANOVA with Bonferroni post-test ($P < 0.0001$ time, $P = 0.0930$ cell type). *** $p < 0.001$

Figure 20 - Timecourse of vWf Release from HLE treated Endothelial Cells



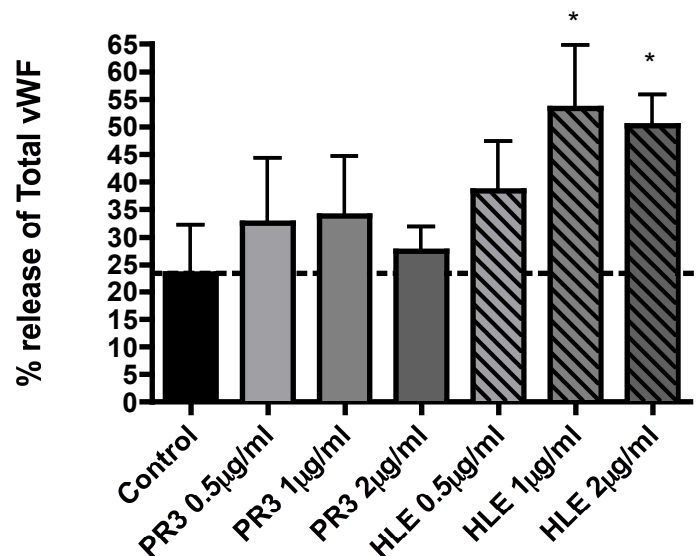
Endothelial cells were treated with 1 μ g/ml HLE for up to 2 hours. vWf was measured in cell culture supernatants by capture ELISA. The data shown here are the mean and standard error of 3 separate experiments. Statistical significance was assessed by 2-way ANOVA with Bonferroni post-test ($P = 0.0384$ time, $P = 0.1357$ cell type). ** $p < 0.01$

Figure 21 - vWf Release from HUVEC as a Percentage of Total vWf



vWf release from 2 hour PR3 and HLE treated HUVEC was calculated as a percentage of total vWf (released vWf + lysed cell vWf). vWf was measured in supernatants of cell lysates by capture ELISA. The data shown are the mean and standard error for 6 separate experiments. Statistical significance was calculated by 1-way ANOVA with Bonferroni post-test (PR3 $p=0.6103$, HLE $p=0.0082$). * $p<0.05$

Figure 22 - vWf Release from GEnC as a percentage of Total vWf



vWf release from 2 hour PR3 and HLE treated GEnC was calculated as a percentage of total vWf (released vWf + lysed cell vWf). vWf was measured in supernatants of cell lysates by capture ELISA. The data shown are the mean and standard error for 4 separate experiments. Statistical significance was calculated by 1-way ANOVA with Bonferroni post-test (PR3 $p=0.6685$, HLE $p=0.0032$). * $p<0.05$

3.6 Increased level of Intracellular vWf Protein and mRNA following Treatment

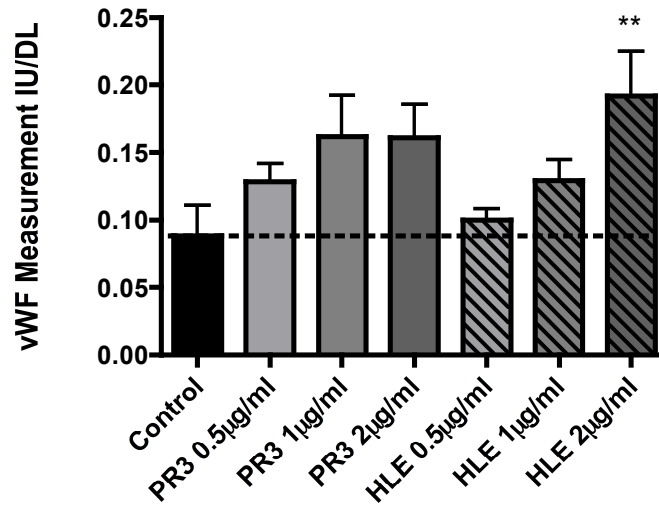
Intracellular vWf was measured in PR3 and HLE treated endothelial cells by lysis in 1x triton X100 and the endothelial cell lysate quantified for remaining vWf. Surprisingly, there was an increased level of vWf protein remaining in the lysates of 2 hour treated endothelial cells following removal of the supernatants. The lysate vWf concentration was increased in both GEnC and HUVEC following PR3 and HLE treatment in a dose dependant manner, although this only reached significance in HUVEC treated with 2 μ g/ml HLE (figure 23 and 24). There was also an unexpected significant increase in the cells' total vWf (lysate + released) following 2 μ g/ml PR3 and HLE treatment on both GEnC and HUVEC (figures 25 and 26).

Further investigation demonstrated that treatment of recombinant vWf protein with 2 μ g/ml HLE in a cell-free system can increase the level of antibody binding by 30.7% on average (mean of the increased percentage from 7 dilutions of recombinant vWf), whilst PR3 does not have an effect on antibody binding (mean increase -1.67%) (figure 27). These results imply that HLE may be involved in processing of the vWf multimer to expose more antibody binding sites, although this only accounts for around 30% of the increased vWf we are detecting. Alternatively, PR3 does not appear to process the recombinant vWf, implying that the serine proteases are somehow acting to induce the production of vWf in endothelial cells.

Interestingly, treatment of glomerular endothelial cells with 1 μ g/ml of PR3 or HLE for 2 hours appeared to increase the vWf mRNA level (figure 28). The addition of serine protease inhibitor α 1-antitrypsin (140nM) at the beginning of the 2 hour incubation did not appear to

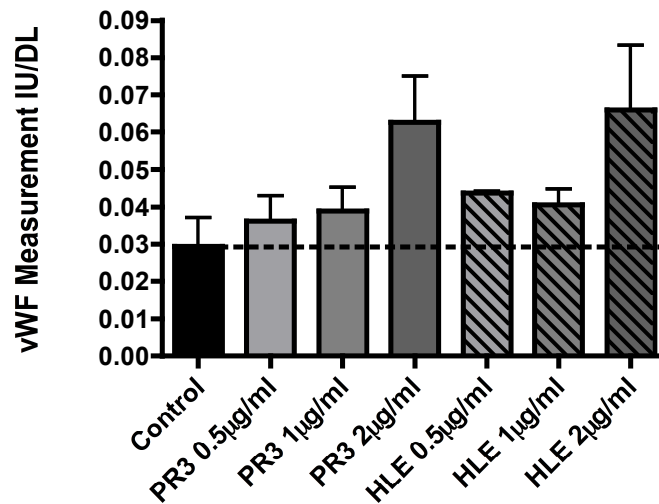
reduce this increase in relative mRNA expression, probably due to early internalization of the protease. There was no difference in the expression of house-keeping gene, TATA-box binding protein, in untreated GEnC and those treated with 1 μ g/ml of PR3 or HLE for 2 hours. The use of the traditional end-point PCR method for assessment of changes in mRNA has limitations in our ability to quantify these changes in vWf mRNA expression. Using this method, vWf mRNA expression could only be estimated by comparing the band intensity. This experiment (n=1) was performed as a preliminary 'look-see' experiment, and now needs to be repeated with more accurate methods. By using a quantitative real-time PCR method, we could use florescent labels to accurately quantify the changes in mRNA expression at each replication cycle. Another advantage of the qPCR method is the absence of a need to run the PCR products on a electrophoresis gel, thereby removing a second potential source of error.

Figure 23 - Level of Intracellular vWf Remaining in HUVEC after Serine Protease Treatment



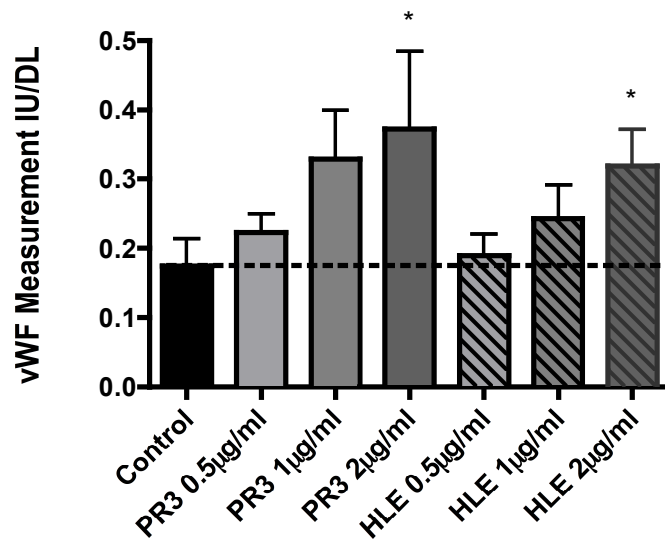
vWf was measured in the lysates of HUVEC that had undergone a 2 hour treatment with increasing concentrations of PR3 and HLE (0.5µg/ml - 2µg/ml) by capture ELISA. The data shown here are the mean and standard error of 6 separate experiments. Statistical significance was calculated by 1-way ANOVA with Bonferroni post-test (PR3 p=0.0504, HLE p=0.0058). **p<0.01

Figure 24 - Level of Intracellular vWf Remaining in GEnC after Serine Protease Treatment



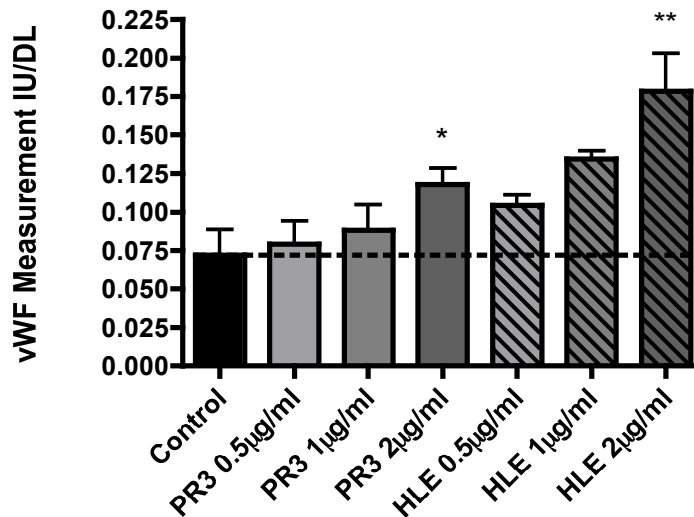
vWf was measured in the lysates of GEnC that had undergone a 2 hour treatment with increasing concentrations of PR3 and HLE (0.5µg/ml - 2µg/ml) by capture ELISA. The data shown here are the mean and standard error of 4 separate experiments. Statistical significance was calculated by 1-way ANOVA with Bonferroni post-test (PR3 p=0.1352, HLE p=0.1798).

Figure 25 - Total vWf after Treatment of HUVEC with Serine Proteases



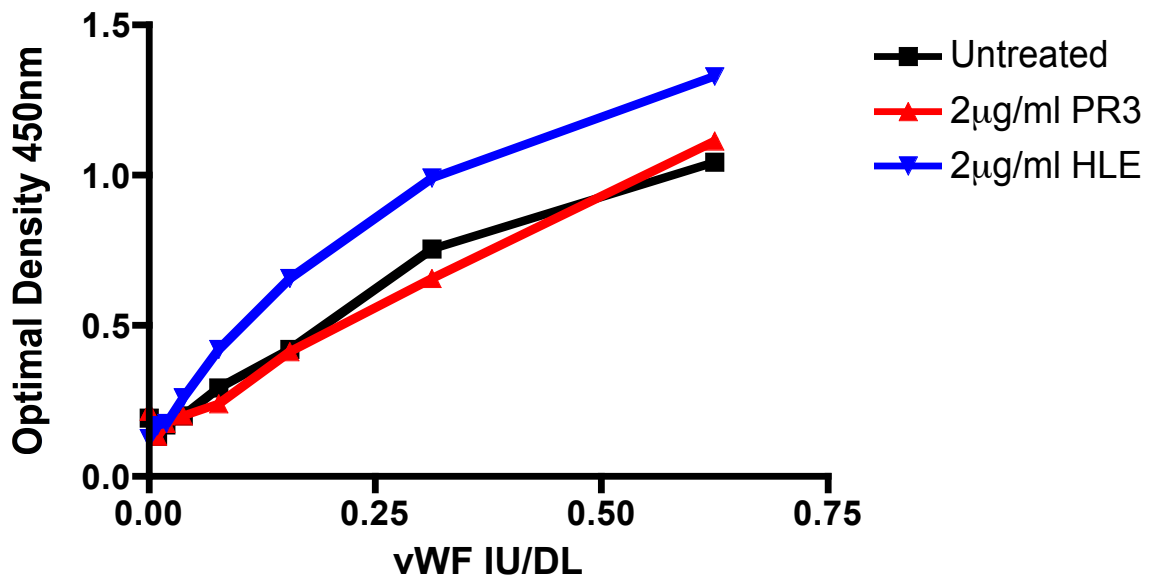
Total vWf was calculated as the sum of vWf release into supernatants plus vWf measured in cell lysates. HUVEC were treated for 2 hours with increasing concentrations of PR3 and HLE. vWf was measured by capture ELISA. The data shown here are the mean and standard error of 6 separate experiments. Statistical significance was assessed by 1-way ANOVA with Bonferroni post-test (PR3 $p=0.0216$, HLE $p=0.0206$). * $p<0.05$

Figure 26 - Total vWf after Treatment of GEnC with Serine Proteases



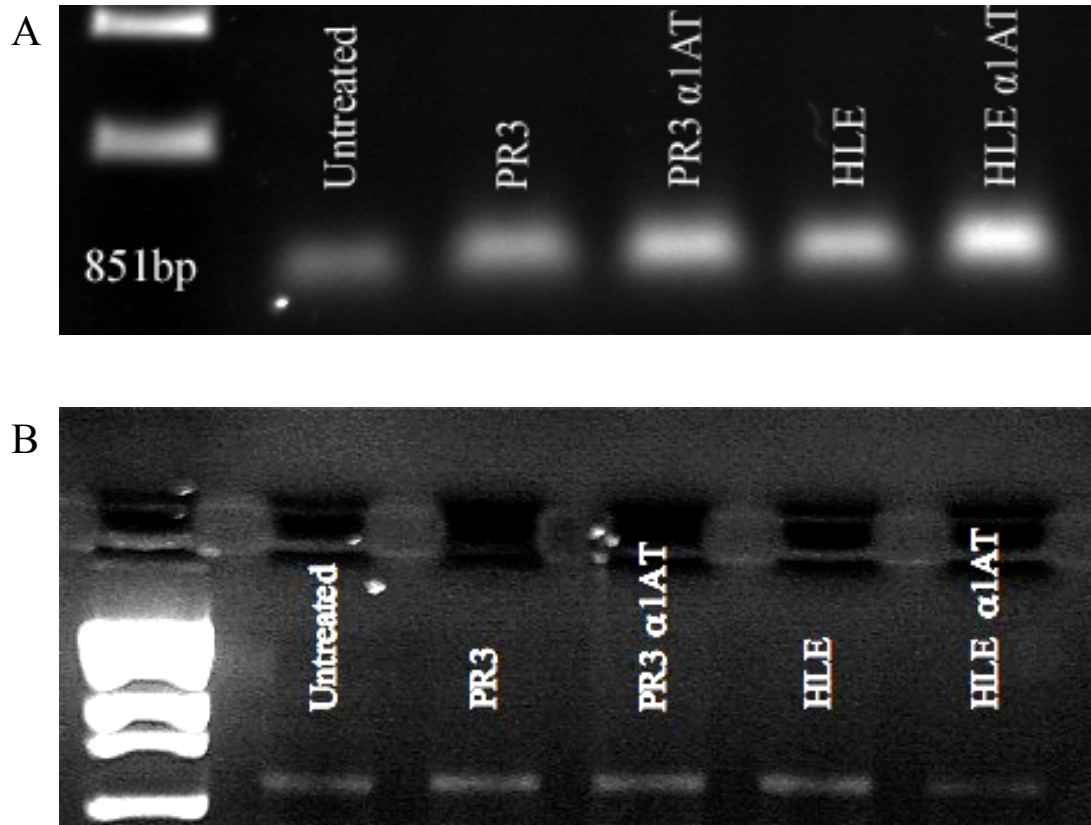
Total vWf was calculated as the sum of vWf release into supernatants plus vWf measured in cell lysates. GEnC were treated for 2 hours with increasing concentrations of PR3 and HLE. vWf was measured by capture ELISA. The data shown here are the mean and standard error of 4 separate experiments. Statistical significance was assessed by 1-way ANOVA with Bonferroni post-test (PR3 $p=0.0281$, HLE $p=0.0086$). * $p<0.05$, ** $p<0.01$

Figure 27 - Cleavage of vWf by PR3 and HLE



A serial dilution of recombinant vWf was incubated with 2µg/ml PR3 or HLE for 2 hours. Detectable vWf was then quantified by capture ELISA. The data shown here is the mean data from 1 experiment.

Figure 28 - vWf mRNA levels following Serine Protease Treatment



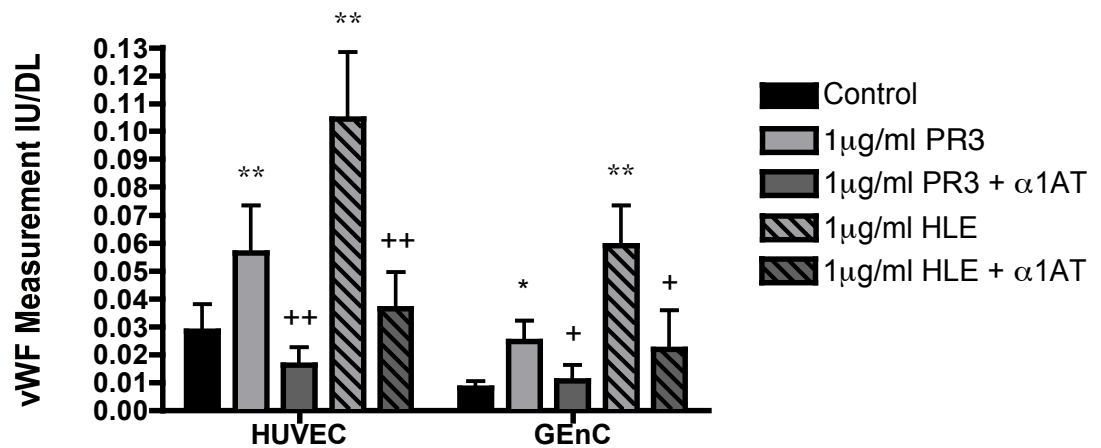
The mRNA level of intracellular vWf (A) and a tubulin binding protein (B) loading control was measured in GEnC following a 2 hour treatment with 1 μ g/ml PR3 and HLE in the presence or absence of α 1AT. mRNA was converted in cDNA via reverse transcription and amplified by PCR. mRNA and cDNA were quantified by Nano-Drop and equally loaded in all samples.

3.7 Inhibition of vWf Release by α 1-Antitrypsin

To confirm that the release of endothelial vWf was due to the enzymatic functions of the serine proteases, the irreversible serine protease inhibitor α 1-antitrypsin was added to endothelial cells during PR3 and HLE treatment. α 1AT was used in a molar excess (four times the concentration of PR3 and HLE) to inhibit the enzymatic functions of PR3 and HLE. vWf release from GEnC and HUVEC treated with 1 μ g/ml PR3 or HLE could be completely abolished by the addition of 140nM α 1AT at both the 2 hour and 24 hour incubation periods (figures 29 and 30). Nevertheless, vWf release remained overall higher following a 24 hour treatment.

vWf release could also be inhibited by α 1AT following treatment with a higher concentration of PR3 and HLE (5 μ g/ml) following a 2 hour treatment. This concentration of PR3 and HLE induced significantly increased release of vWf into supernatants, which was inhibitable to untreated control levels of vWf release by α 1AT (figures 31 and 32). Treatment with 5 μ g/ml HLE also induced significant levels of endothelial cell detachment, most evident with HUVEC, which could also be restored by α 1AT (figures 33 and 34).

Figure 29 - Inhibition of vWf Release by α 1AT at 2 hours

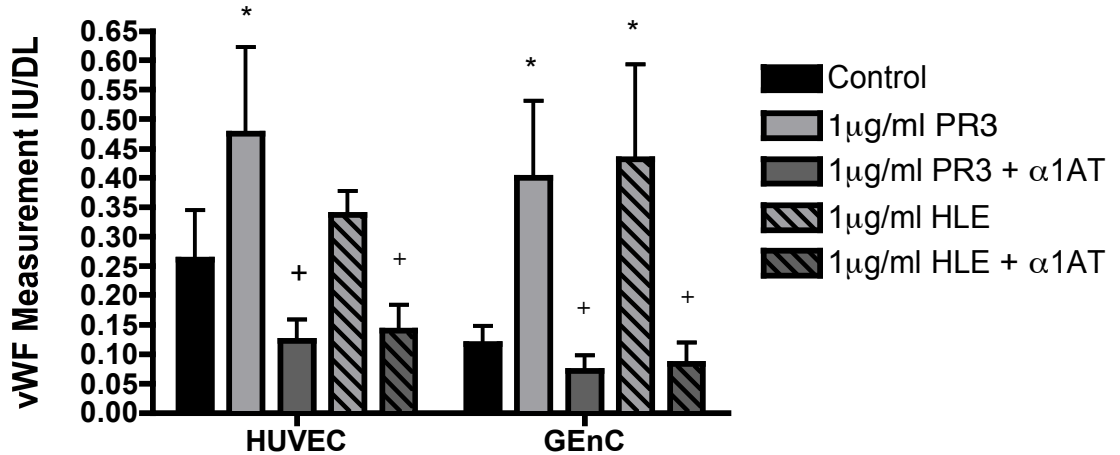


Endothelial cells were treated for 2 hours with 1µg/ml PR3 or HLE in the presence or absence of α 1AT. vWf was measured in cell culture supernatants by capture ELISA. The data shown here are the mean and standard error for 4 separate experiments. Statistical significance was calculated using a Paired T-Test. * and + p<0.05, ** and ++ p<0.01

* compared to untreated cells

+ compared to serine protease treatment

Figure 30 - Inhibition of vWf Release by α 1AT at 24 hours

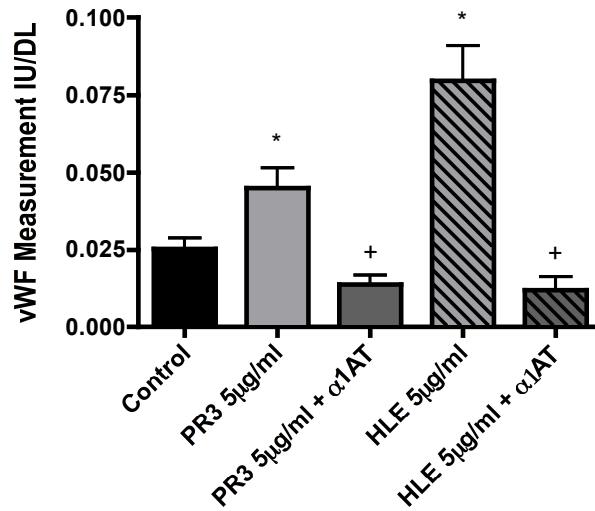


Endothelial cells were treated for 24 hours with 1µg/ml PR3 or HLE in the presence or absence of α 1AT. vWf was measured in cell culture supernatants by capture ELISA. The data shown here are the mean and standard error for 4 separate experiments. Statistical significance was calculated using a Paired T-Test. * and + p<0.05

* compared to untreated cells

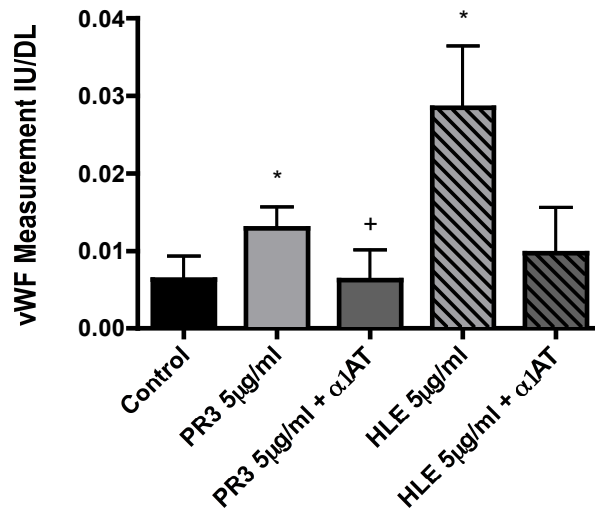
+ compared to serine protease treatment

Figure 31 - α 1AT Inhibition of vWf Release from HUVEC at Higher Concentrations of Serine Protease



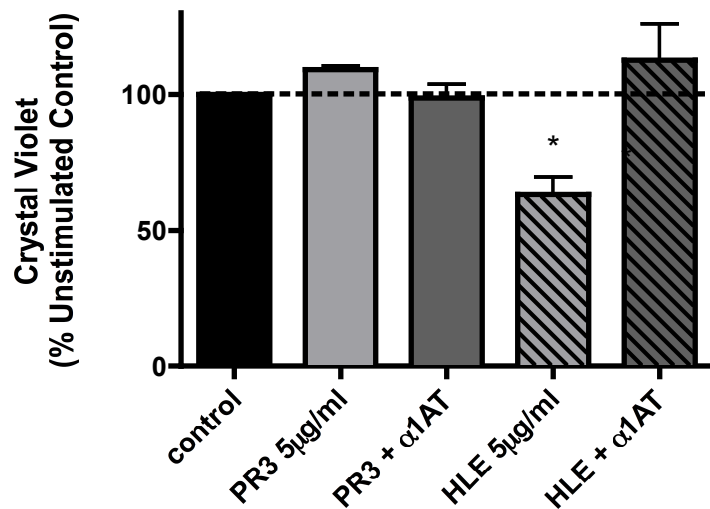
HUVEC were treated for 2 hours with 5µg/ml PR3 or HLE in the presence or absence of α 1AT. vWf was measured in cell culture supernatants by capture ELISA. The data shown here are the mean and standard error for 5 separate experiments. Statistical significance was calculated using a Paired T-Test. * and + p<0.05
 * compared to untreated cells
 + compared to serine protease treatment

Figure 32 - α 1AT Inhibition of vWf Release from GEnC at Higher Concentrations of Serine Protease



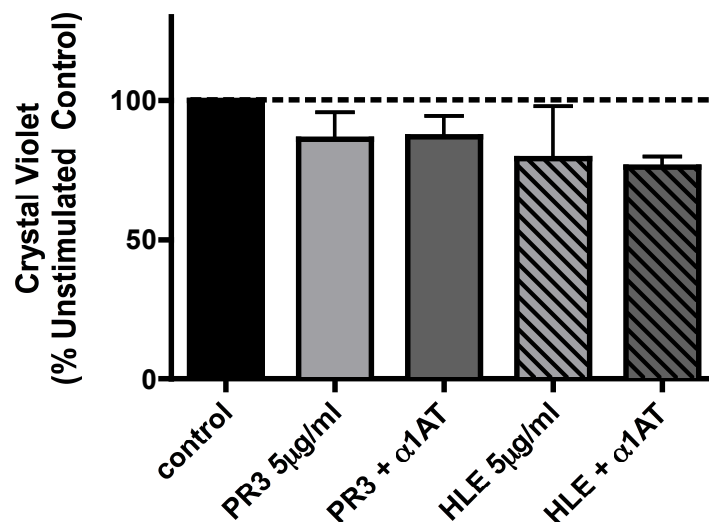
GEnC were treated for 2 hours with 5µg/ml PR3 or HLE in the presence or absence of α 1AT. vWf was measured in cell culture supernatants by capture ELISA. The data shown here are the mean and standard error for 4 separate experiments. Statistical significance was calculated using a Paired T-Test. * and + p<0.05
 * compared to untreated cells
 + compared to serine protease treatment

Figure 33 - HUVEC Detachment Following Treatment with Higher Doses of PR3 and HLE



HUVEC were treated for 2 hours with 5µg/ml PR3 or HLE in the presence or absence of α1AT, fixed in 2% PFA and the level of cell adherence measured using a crystal violet cell stain. The data shown here are the mean and standard error for 3 separate experiments, displayed as a percentage of the unstimulated control. Statistical significance was assessed using a Paired T-Test. * p<0.05
* compared to unstimulated control

Figure 34 - GEnC Detachment Following Treatment with Higher Doses of PR3 and HLE



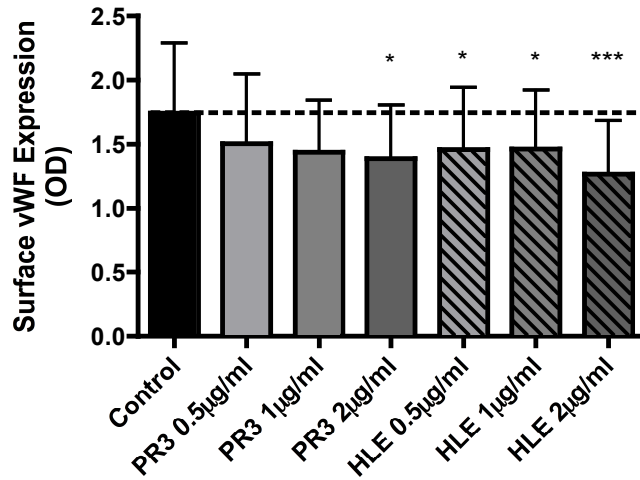
GEnC were treated for 2 hours with 5µg/ml PR3 or HLE in the presence or absence of α1AT, fixed in 2% PFA and the level of cell adherence measured using a crystal violet cell stain. The data shown here are the mean and standard error for 3 separate experiments, displayed as a percentage of the unstimulated control. Statistical significance was assessed using a Paired T-Test.
* compared to unstimulated control

3.8 Changes in vWf Surface Expression Following Serine Protease Treatment

Given the ability of HLE to process the vWf protein, changes in the level of membrane bound vWf were investigated following PR3 and HLE treatment. The treatment of endothelial cells with increasing concentrations of PR3 and HLE (0.5µg/ml - 2µg/ml) significantly decreased the expression of membrane bound vWf (figures 35 and 36). This was most evident with HLE treatment on both GEnC and HUVEC. Interestingly, whilst reducing membrane bound vWf on HUVEC, PR3 treatment did not significantly decrease vWf surface expression on GEnC.

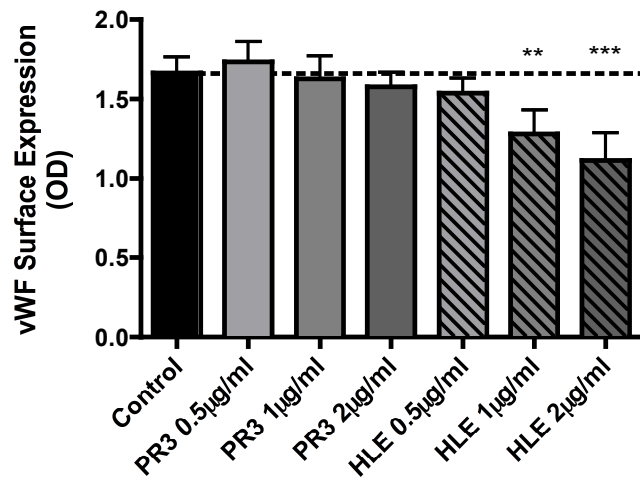
As with vWf release into cell culture supernatants, α 1AT could significantly restore this decreased membrane expression on GEnC (figure 38). α 1AT also restored membrane vWf expression on HUVEC, although this did not reach significance when analysed by 2-tailed paired T-Test (PR3 $p=0.4511$, HLE $p=0.1773$) (figure 37).

Figure 35 - Surface Expression of vWf on HUVEC following Serine Protease Treatment



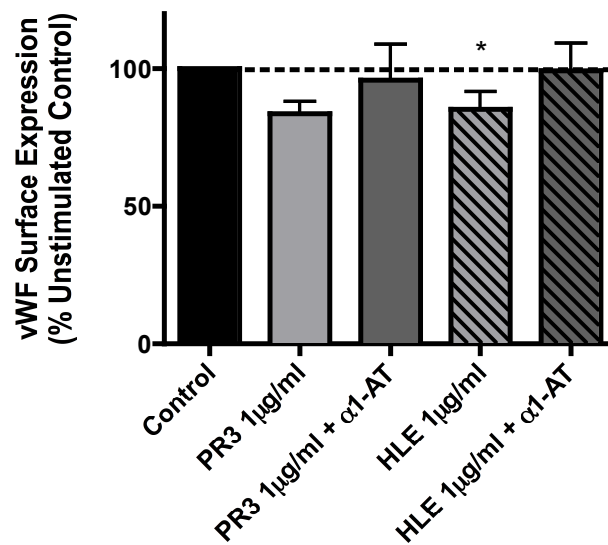
HUVEC were treated for 2 hours with increasing doses of PR3 and HLE, after which they were fixed in 2% PFA and assessed for the level of vWf bound to the cell surface by ELISA. The data shown here are the mean and standard error for 3 separate experiments. Statistical significance was calculated using a 1-way ANOVA with Bonferroni post-test (PR3 $p=0.0206$, HLE $p=0.0008$). * $p<0.05$, *** $p<0.001$

Figure 36 - Surface Expression of vWf on GEnC following Serine Protease Treatment



HUVEC were treated for 2 hours with increasing doses of PR3 and HLE, after which they were fixed in 2% PFA and assessed for the level of vWf bound to the cell surface by ELISA. The data shown here are the mean and standard error for 4 separate experiments. Statistical significance was calculated using a 1-way ANOVA with Bonferroni post-test (PR3 $p=0.2689$, HLE $p<0.0001$). ** $p<0.01$, *** $p<0.001$

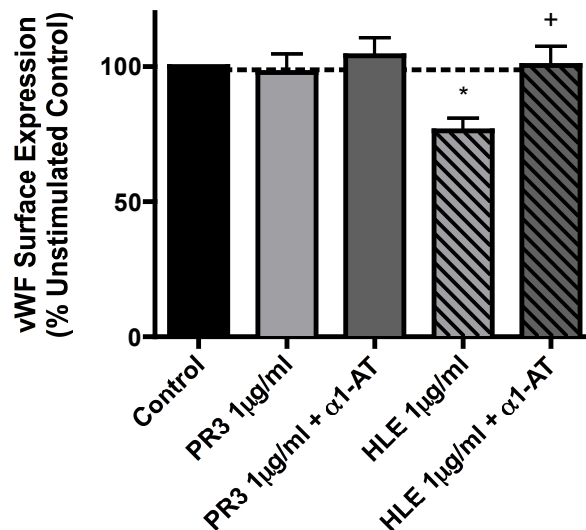
Figure 37 - Surface Expression of vWf on HUVEC can be restored by α 1AT



HUVEC surface expression of vWf was measured after a 2 hour treatment with 1µg/ml PR3 or HLE in the presence or absence of α 1AT by ELISA. The data shown here are the mean and standard error from 3 separate experiments, displayed as a percentage of the unstimulated control. Statistical significance was calculated using a Paired T-Test. * $p < 0.05$

* compared to unstimulated control

Figure 38 - Surface Expression of vWf on GEnC can be restored by α 1AT



GEnC surface expression of vWf was measured after a 2 hour treatment with 1µg/ml PR3 or HLE in the presence or absence of α 1AT by ELISA. The data shown here are the mean and standard error from 3 separate experiments, displayed as a percentage of the unstimulated control. Statistical significance was calculated using a Paired T-Test. * and + $p < 0.05$

* compared to unstimulated control

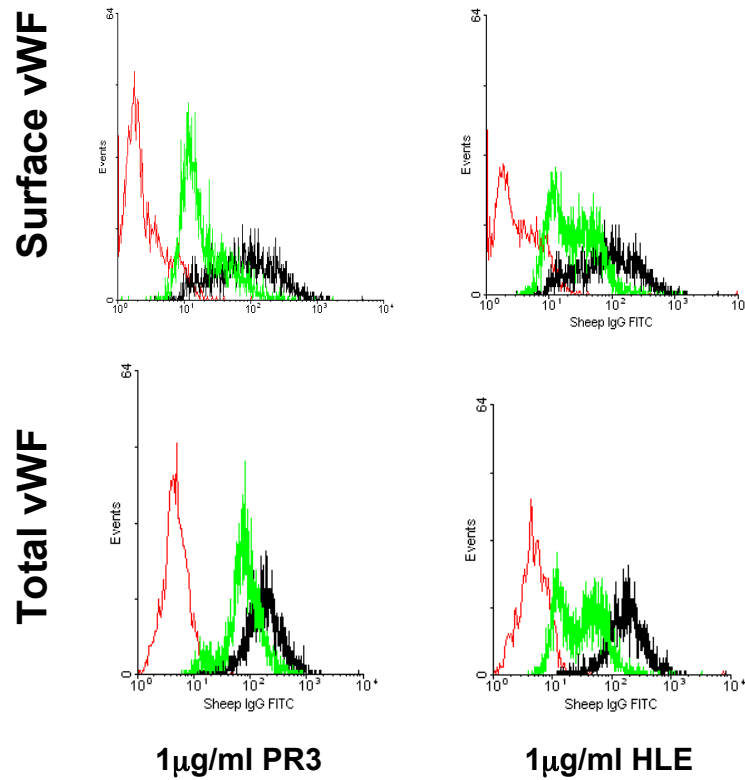
+ compared to serine protease treatment

3.9 vWf Release: Internal Stores versus Membrane Cleavage

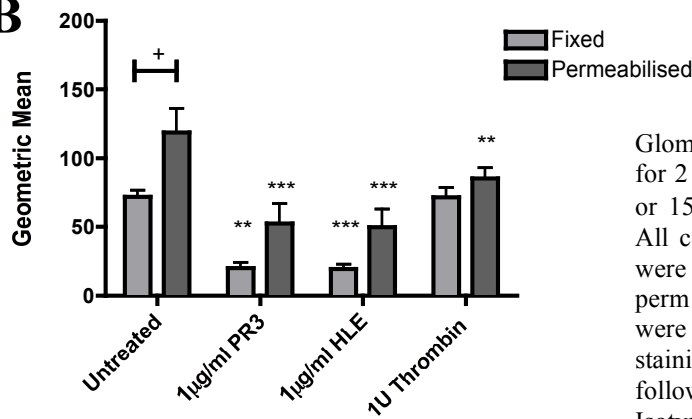
To investigate whether the increased detectable vWf in cell culture supernatants was due to increased release from internal stores or solely due to the increased cleavage of membrane bound vWf, fixed and permeabilised endothelial cells were assessed for changes in vWf levels by flow cytometry in order to allow determination of total levels (internal and surface expression with permeabilised cells), versus surface expression alone (non-permeabilised cells). Figure 39 demonstrates that treatment of GEnC with 1µg/ml of PR3 or HLE significantly reduced both the surface and total levels of vWf when compared to untreated cells. Importantly, there is decreased detectable vWf in the total (fixed and permeabilised cells) compared to the surface expressed vWf following treatment, suggesting that, whilst the majority of vWf detected in supernatants is due to cleavage and release of membrane bound vWf, PR3 and HLE also cause the release of vWf from Weibel-Palade bodies, although this did not reach significance (see figure 39C). Treatment of GEnC for 15 minutes with 1 unit thrombin caused a significant decrease in the level of total vWf, but had no effect on the level of surface bound vWf. This reinforces that thrombin acts a potent secretagogue in inducing Weibel-Palade body exocytosis.

Figure 39 - FACS Analysis of vWf Release from Surface and Internal Stores

A

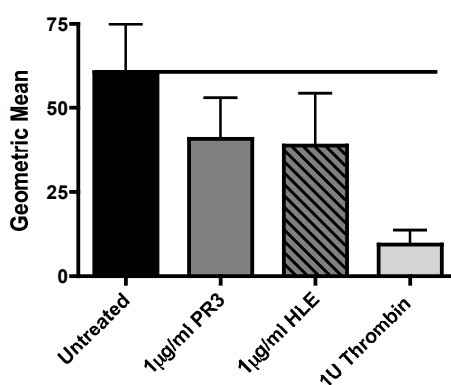


B



Glomerular endothelial cells were treated for 2 hours with 1µg/ml of PR3 or HLE, or 15 minutes with 1Unit of Thrombin. All cells were fixed in 2% PFA, others were also permeabilised using a fix and perm kit, before staining for vWf. Cells were immediately analysed after staining. (A) shows a typical FACS plot following serine protease treatment (■ Isotype Control, ■ Untreated, ■ Enzyme Treated). (B) The data shown here are the mean and standard error of the geometric means from 4 separate experiments, analysed by 2-way ANOVA with Bonferroni post-test (treatment $p < 0.0001$, fix/perm $p = 0.0001$) * compared to untreated endothelial cells, + compared between fixed and permeabilised cells. (C) represents the vWf release from internal stores, as calculated by permeabilised minus fixed geometric means.

C



3.10 Confocal Staining for vWf and the Plasma Membrane

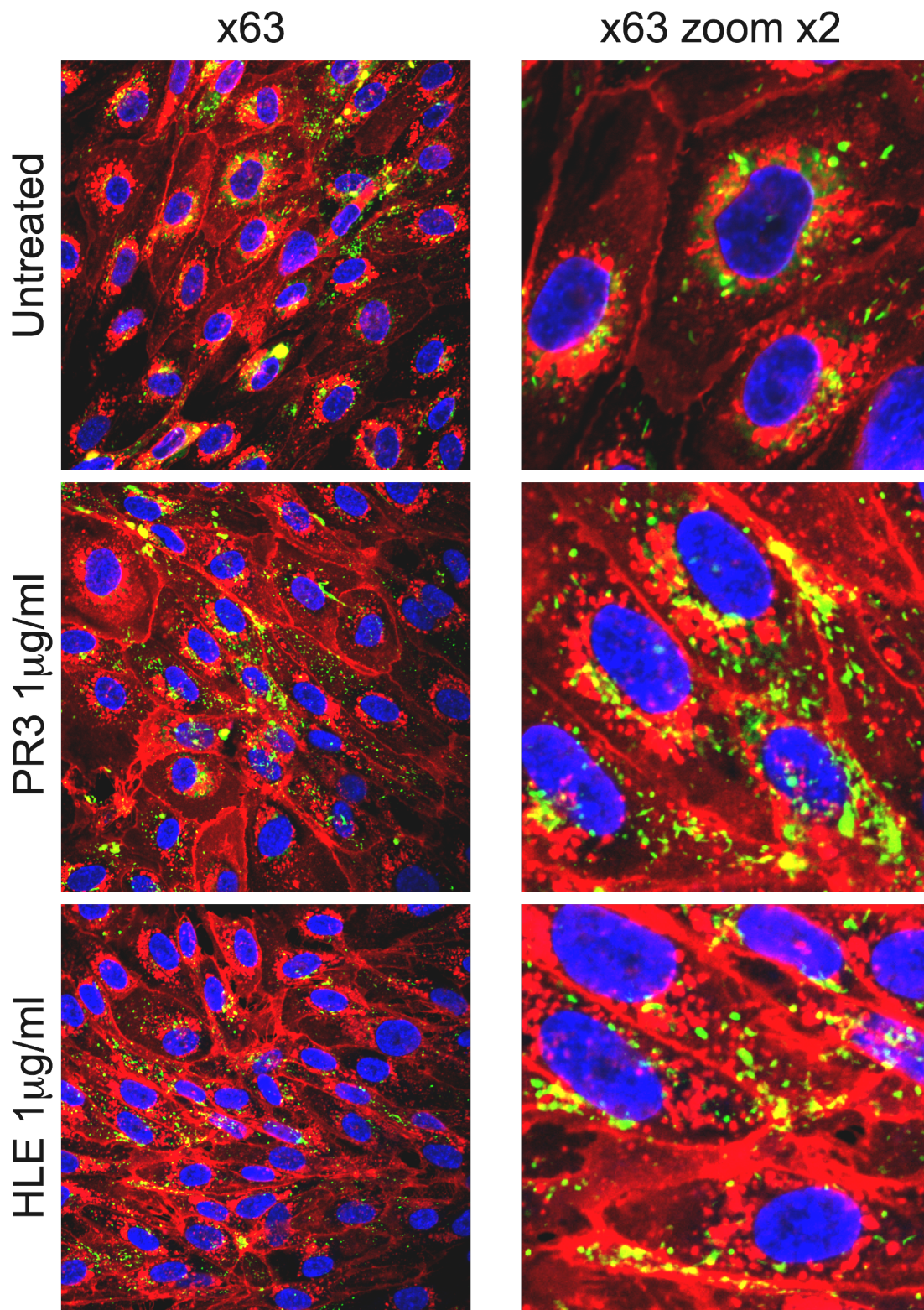
To further investigate the release of vWf from internal stores, glomerular endothelial cells were stained for vWf (FITC) and a membrane stain (Image iT™ Live, Alexa fluor®594) to identify areas of localisation, and thereby exocytosis. Treated glomerular endothelial cells were visualised using confocal microscopy with a 63x magnification and 2x zoom. Figure 40 demonstrates a cross-sectional image across the untreated and 1µg/ml PR3 or HLE treated GEnC. The untreated endothelial cells appear to display less positive staining for vWf compared to PR3 and HLE treated cells. There also appears to be little or no co-localisation between the vWf and the plasma membrane in untreated GEnC. Increased magnification of PR3 and HLE treated GEnC displayed areas of dual staining (yellow) between the vWf and plasma membrane.

To further investigate this observation, GEnC treated with PR3 and HLE were imaged using the Z-stack feature of the Zeiss confocal software. This allowed us to take cross-sectional images at varying depths through the cell to observe the localisation of vWf and direction of release. Images were captured in 1µm sections. Figure 41 shows five of the key sections through the GEnC from bottom to top. This cross-sectional analysis demonstrates the presence of vWf beneath the basal membrane of the monolayer, a well-documented phenomenon in resting endothelial cells [375]. vWf expression appears well distributed throughout both the treated and untreated endothelial cells, although present at a higher concentration close to the basolateral membrane.

The Image-iT™ plasma membrane stain consists of a wheat germ agglutinin, which selectively binds to N-acetylglucosamine and N-acetylneuraminic acid residues. It is suggested to selectively stain the plasma membrane of unpermeabilised cells, although can

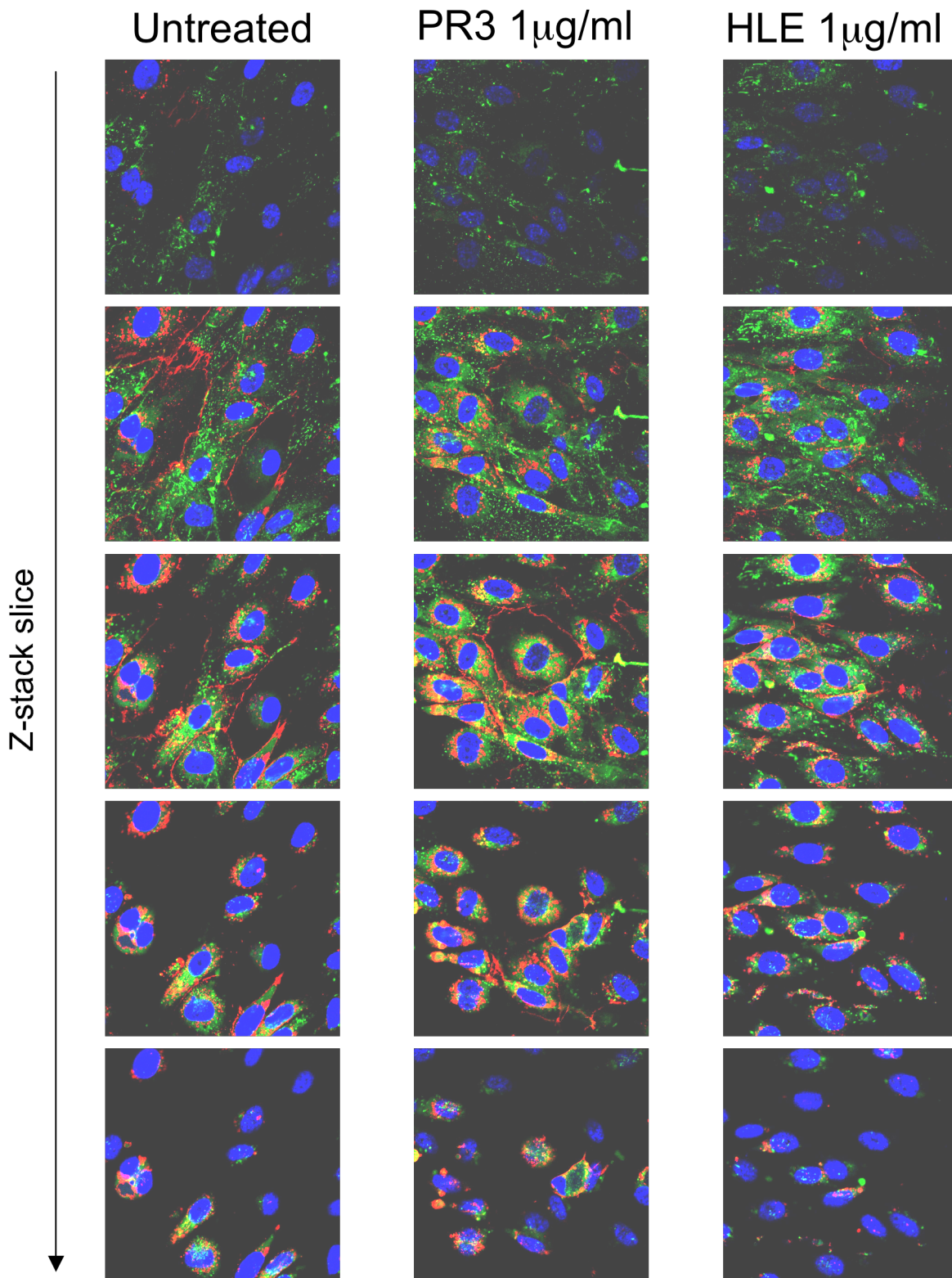
interact with intracellular compartment membranes. Given the high background and pigmentation within the cell, it is likely that some intracellular compartments have been targeted by the wheat germ agglutinin. Other membrane stains exist, including CellMask™ and LavaCell™, but these too can target intracellular components if cells later become permeabilised. For assessment of interactions of WPB with the cell membranes other techniques will need to be investigated.

Figure 40 - Localisation of vWf with the Plasma Membrane



Glomerular endothelial cells treated for 2 hours with 1 µg/ml PR3 or HLE were dual stained for vWf (FITC ■) and membrane stain (Alexa fluor®594 ■), and visualised by confocal microscopy. Nuclei were stained with DAPI (UV ■).

Figure 41 - Z-Stack Imaging of vWf Staining



Glomerular endothelial cells treated for 2 hours with 1µg/ml PR3 or HLE were dual stained for vWf (FITC ■) and a membrane stain (Alexa Fluor 594 ■), and visualised by confocal microscopy. Nuclei were stained with DAPI (UV ■). Cells were imaged using a Z-stack to track changes in vWf localisation following treatment. The images shown above are 5 slices through the cells from bottom to top with a x63 magnification.

3.11 vWf Staining in Renal Biopsies

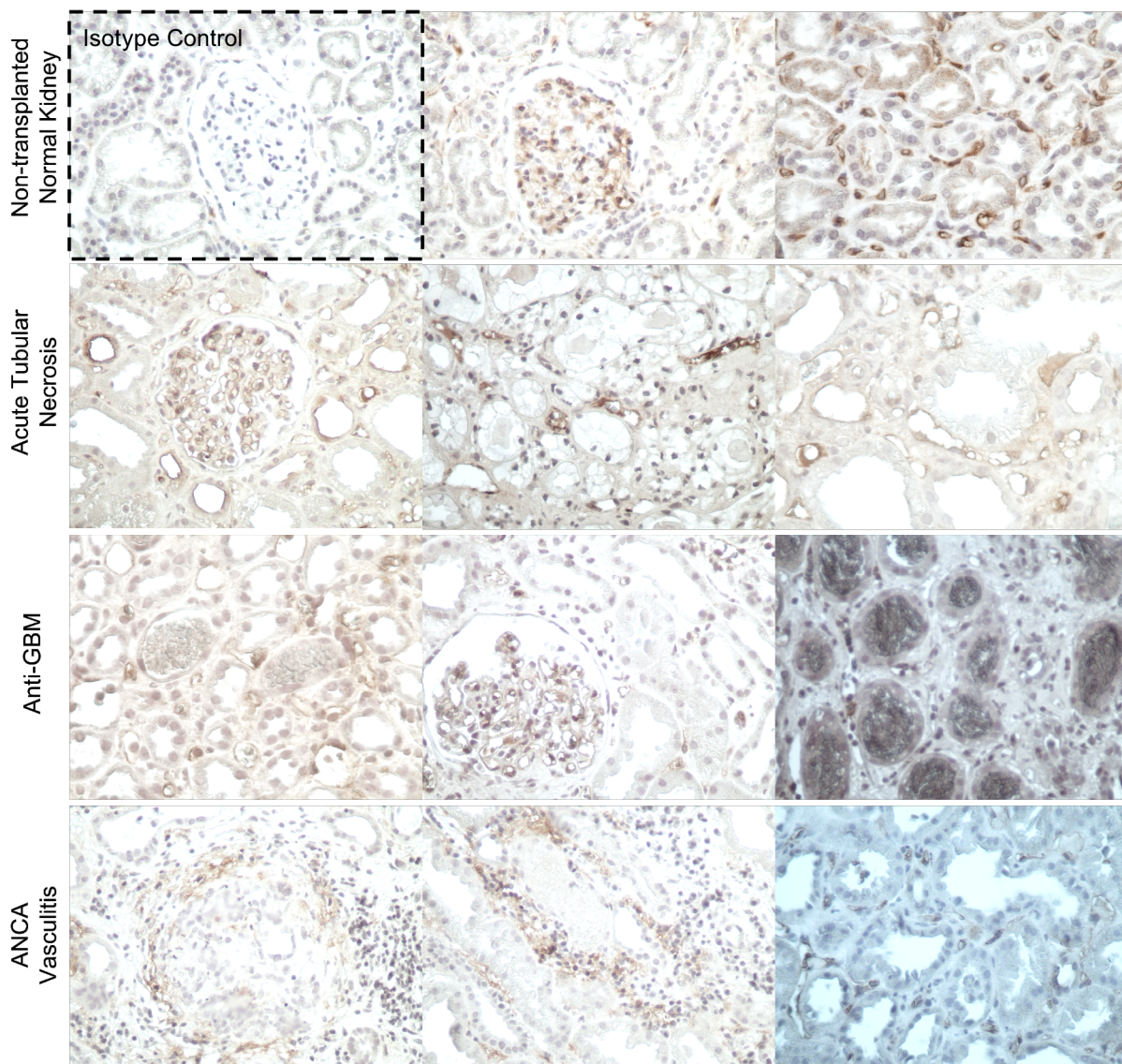
Given the proposed role for the neutrophil serine proteases in inducing vWf release from GEnC following short incubations, we next wanted to investigate how the expression of vWf changes in the glomeruli from kidney biopsies of patients with ANCA associated vasculitis compared to ‘healthy control’ (ethics code 07/Q2602/42). ‘Healthy control’ biopsies were collected from non-transplanted donor kidneys. vWf staining in ASV patients were compared to patients with acute tubular necrosis (ATN), and anti-glomerular membrane antibody disease (anti-GBM).

vWf has been demonstrated to be present in the GEnC and in tubular capillaries (figure 42). This pattern of endothelial vWf staining can be observed in ‘healthy’ non-transplanted kidneys. Biopsies from ASV patients display crescentic glomeruli with inflammatory cell infiltration. Here intraglomerular vWf staining is greatly reduced, with the majority of vWf positive cells present in the surrounding crescent formation. These biopsies still maintain ‘normal’ vWf staining in medullary tubular capillaries. Anti-GBM biopsies have no vWf staining present in affected glomeruli, whilst glomerular vWf staining in ATN appears normal.

This methods has many technical limitations. Firstly, staining of kidney sections with HRP-conjugated antibodies routinely displayed high levels of background staining. Secondly, the precise location of the positive staining within the biopsy is questionable. Here, we are able to see vWf staining within the glomeruli but cannot pinpoint the cell type that may be expressing it, for example the endothelial cells or the platelets captured within the capillaries. To more accurately determine the localisation of the increased vWf expression, this staining should now be repeated using a fluorescent histochemistry technique using confocal

microscopy. By using a fluorescent dual staining approach we can more accurately identify the cells that are expression vWf within the biopsy. This would be achieved by using different fluorescent dyes i.e. PE and FITC, which would appear yellow when both expressed at the same location. Examples of other targets could include CD31 (PECAM-1) for endothelial cells or GP1b for platelets.

Figure 42 - vWf Staining in Renal Biopsies



Paraffin sections from patient biopsies were used to assess changes in vWf distribution within the kidney. Renal biopsy samples collected from patients with ANCA-associated vasculitis, acute tubular necrosis and anti-glomerular basement membrane disease were used. Patient biopsies were compared to vWf staining in a 'healthy' non-transplanted kidney. A total of 2 (ATN and anti-GBM) to 4 (ANCA vasculitis) patients from each group were compared. Insert, top left, shows a representative isotype control staining for the non-transplanted control. The sections were stained for vWf expression (HRP) and counterstained with Harris haematoxylin. Sections were imaged immediately using a x40 magnification, with representative images shown above of cortical glomeruli and medullary tubular staining of vWf.

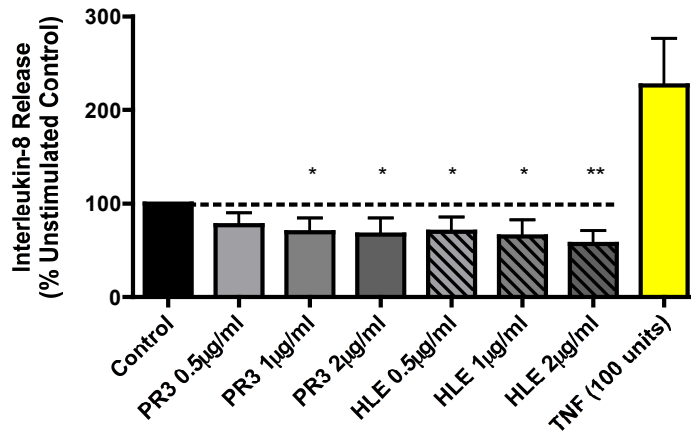
3.11 Chemokine Ligand-8 Release Following Serine Protease Treatment

Further to the identification of increased vWf release into cell culture supernatants, the release of other Weibel-Palade body constituents was investigated, in particular, CXCL8, angiopoietin-2, P-Selectin and CD63. Interleukin-8 release was measured in supernatants by capture ELISA following a 2hour treatment with increasing concentrations of PR3 and HLE (0.5 μ g/ml - 2 μ g/ml). Figures 43 and 44 demonstrate a significantly decreased level of detectable CXCL8 in supernatants following serine protease treatment in both HUVEC and GEnC. This decreased level of CXCL8 occurred in a dose-dependant manner and was most significant with HLE treatment. Further investigation demonstrated that PR3 and HLE could reduce the detectable level of CXCL8 in a cell-free system (figure 45). Again, this decreased level of CXCL8 occurred in a dose-dependant manner, with 2 μ g/ml HLE having the most evident effect. The addition of α 1AT into this system was able to restore the reduced level of CXCL8 with 2 μ g/ml HLE treatment (figure 46). The ability for the serine proteases to decrease CXCL8 detection in a cell-free system suggests that the serine proteases are actively cleaving CXCL8, thereby rendering it undetectable in our assay. This observation has previously been demonstrated by Padrines *et al*, 1994 [113].

To overcome this, GEnC were treated with serine proteases for 2 hours, after which the cells were washed to remove any remaining PR3 or HLE and incubated for a further hour or 2 hours in blank medium. Treatment of GEnC with increasing doses of serine protease following by a 1 hour incubation in blank medium resulted in an increased release of CXCL8 into cell culture supernatants. However this only reached significance following treatment with 2 μ g/ml of HLE (figure 47). Incubation of 2 μ g/ml PR3 or HLE treated GEnC for 2 hours demonstrated significantly increased levels of CXCL8 with both serine proteases (figure 48). This supports the idea that the serine proteases are acting to induce release of

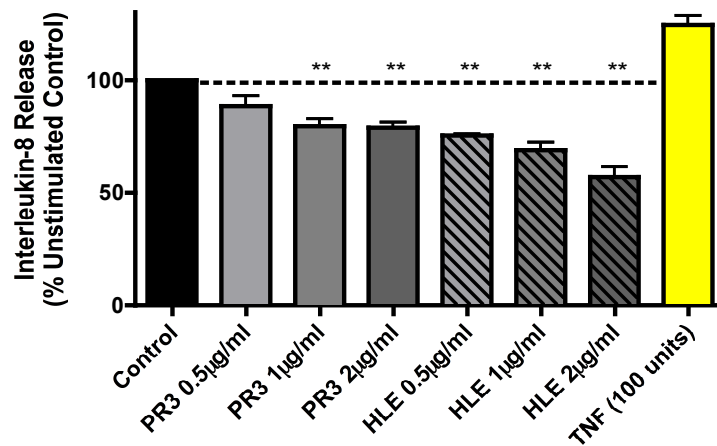
Weibel-Palade body constituents, and implies that this can continue after removal of the enzyme.

Figure 43 - Chemokine Ligand-8 Release from Serine Protease Treated HUVEC



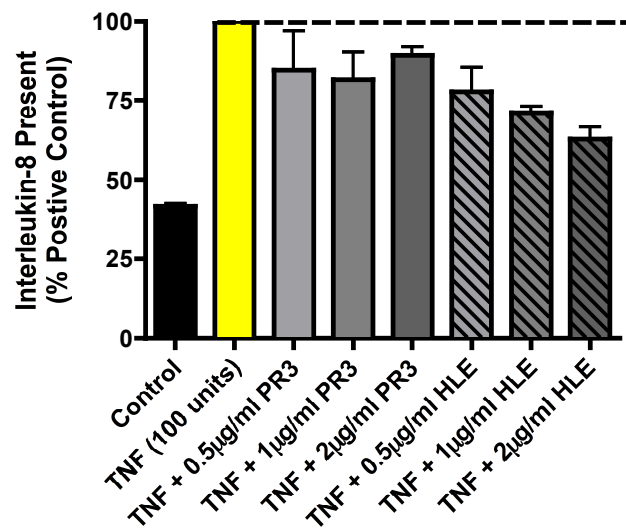
HUVEC were treated with increasing concentrations of PR3 and HLE for 2 hours. CXCL8 was measured in cell culture supernatants by capture ELISA. The data shown here are the mean and standard error from 4 separate experiments, displayed as a percentage of the unstimulated control. Statistical significance was calculated using a 1-way ANOVA with Bonferroni post-test ($p=0.0169$). * $p<0.05$, ** $p<0.01$

Figure 44 – Chemokine Ligand-8 Release from Serine Protease Treated GENC



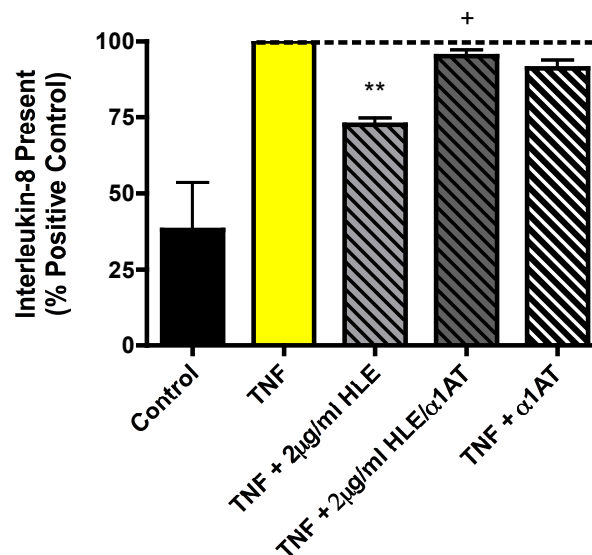
HUVEC were treated with increasing concentrations of PR3 and HLE for 2 hours. CXCL8 was measured in cell culture supernatants by capture ELISA. The data shown here are the mean and standard error from 3 separate experiments, displayed as a percentage of the unstimulated control. Statistical significance was calculated using a 1-way ANOVA with Bonferroni post-test ($p<0.001$). ** $p<0.01$

Figure 45 - Cleavage of Chemokine Ligand-8 by PR3 and HLE



Endothelial cells were treated with 100unit of TNF α for 4 hours, after which the supernatants were transferred to a separate 96-well culture plate and incubated with increasing doses of PR3 and HLE for a further 2 hours. CXCL8 was measured in these supernatants by CXCL8 capture ELISA. The data shown here is the mean and standard error from 1 experiment, displayed as a percentage of TNF α treated endothelial cells with no subsequent serine protease treatment.

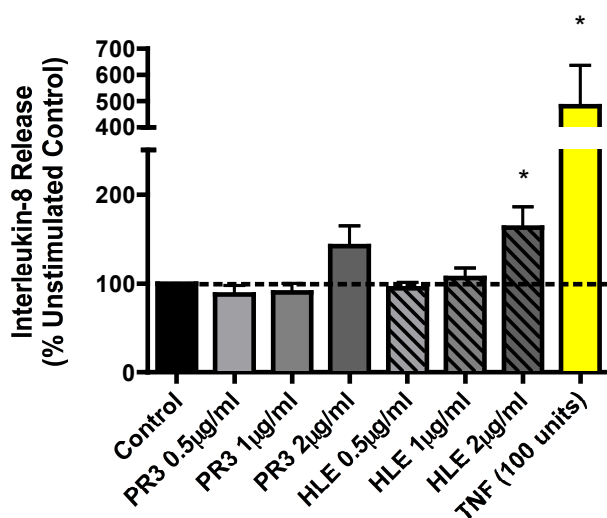
Figure 46 – Chemokine Ligand-8 Cleavage by HLE can be Inhibited by α 1AT



Endothelial cells were treated with TNF α for 4 hours, after which supernatants were transferred to a second 96-well culture plate and incubated with 2µg/ml HLE in the presence or absence of α 1AT, or α 1AT alone, for a further 2 hours. CXCL8 was quantified by capture ELISA. The data shown here are the mean and standard error from 3 separate experiments, displayed as a percentage of TNF α treated cells that received no further treatment. Statistical significance was achieved used a paired T-Test. +p<0.05, **p<0.01

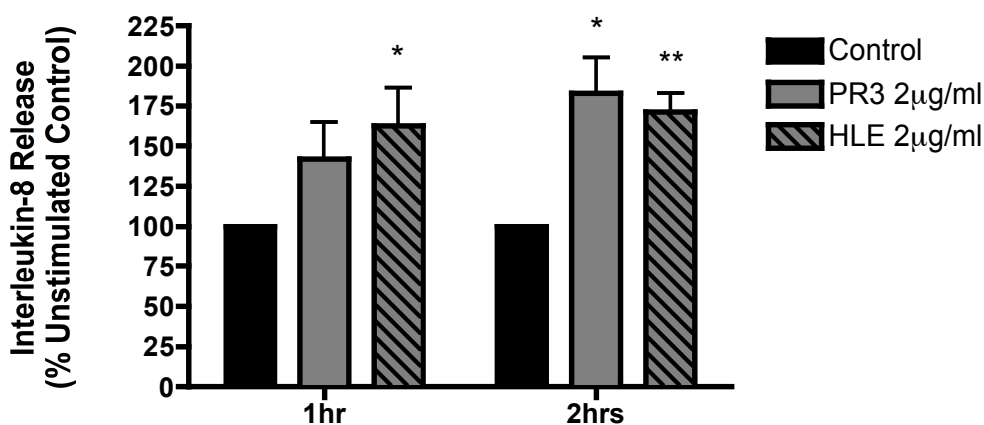
* Compared to positive control
 + Compared to HLE treated EnC

Figure 47 – Chemokine Ligand-8 Release Following Removal of Serine Proteases 1 hour Incubation



GEnC were treated with increasing doses of PR3 and HLE for hours, after which the treated cells were washed to remove and residual enzyme and incubated for a further hour in blank medium 199. CXCL8 was quantified by capture ELISA. The data shown here are the mean and standard error for 3-9 separate experiments, displayed as a percentage of the unstimulated control. Statistical significance was calculated using a 1-way ANOVA with Bonferroni post-test (PR3 $p=0.1268$, HLE $p=0.0303$). * $p<0.05$

Figure 48 – Chemokine Ligand-8 Release following Removal of Serine Proteases 1 and 2 hour Incubations

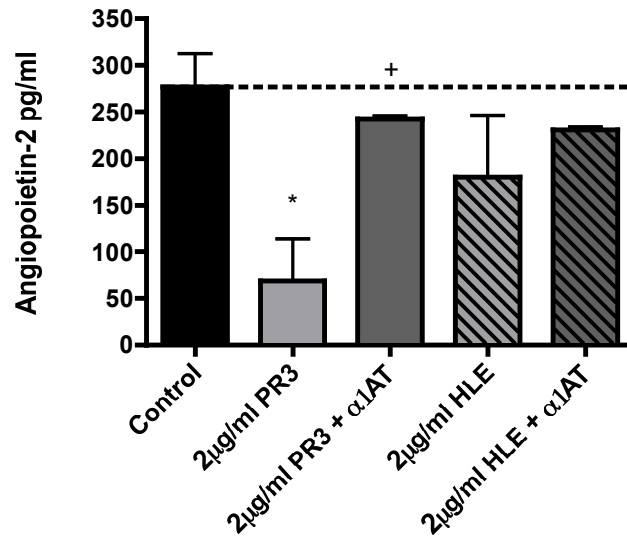


GEnC were treated with 2µg/ml PR3 or HLE for 2 hours, after which the enzyme was removed by washing in PBS and the cells incubated in blank medium for 1 or 2 hours. CXCL8 release from these cells was quantified in supernatants by capture ELISA. The 1 hour data shown here are the mean and standard error from 9 separate experiments, displayed as a percentage of the unstimulated control. The 2 hour data here are the mean and standard error from 5 separate experiments, displayed as a percentage of the unstimulated control. Statistical significance was calculated using a paired T-Test. A 2-way ANOVA was used to determine significance between the two time-points ($p=0.771$). * $p<0.05$, ** $p<0.01$

3.12 Angiotensin-2 Release from Serine Protease Treated Endothelial Cells

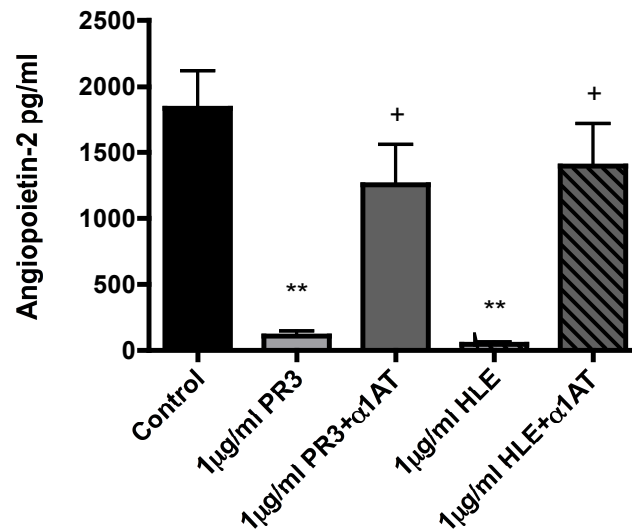
HUVEC and GEnC were treated with 2 μ g/ml of PR3/HLE or 1 μ g/ml PR3/HLE, respectively, for 2 hours, after which, supernatants were assessed for angiotensin-2 release by capture ELISA. Both HUVEC and GEnC demonstrated a significantly decreased level of detectable Ang-2 following PR3 and HLE treatment, although this was most evident on GEnC (figures 49 and 50). HUVEC were originally treated with 1 μ g/ml PR3 or HLE but this did not show as marked a decrease in Ang-2 as with GEnC treatment (data not shown, N=1), so a higher concentration of PR3 and HLE were used in HUVEC treatment. It is also apparent that there are greatly increased levels of Ang-2 released from untreated GEnC compared to HUVEC. The addition of α 1AT into the system significantly inhibited the effects of PR3 and HLE on decreasing detectable Ang-2. The incubation of recombinant Ang-2 with 1 μ g/ml PR3 or HLE for 1 hour reduced the level of detectable Ang-2 in our ELISA, demonstrating that both PR3 and HLE are cleaving Ang-2. Interestingly, PR3 appeared to have a greater effect on the cleavage of Ang-2 (figure 51). This is also demonstrated in the treatment of HUVEC, in which PR3 greatly reduces detectable levels of Ang-2 whilst HLE treatment displays less of an effect (figure 49). The treatment of GEnC for 2 hours and consequent removal of the enzymes, with a further 1 or 2 hours incubation in blank medium, had no effect on increasing Ang-2 release in PR3 or HLE treated cells (figure 52). However, the removal of PR3 and HLE did restore the Ang-2 levels back to those comparable to untreated control levels.

Figure 49 - Angiopoietin-2 Release from HUVEC following Serine Protease Treatment



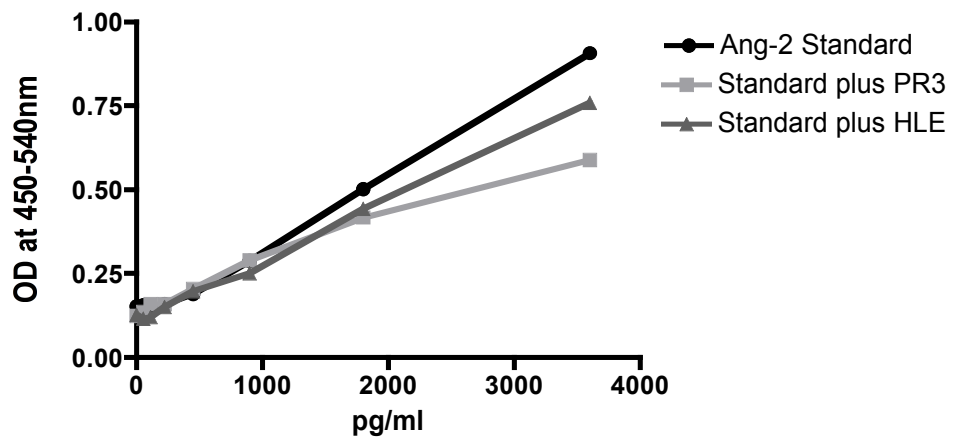
HUVEC were treated with 2µg/ml PR3 or HLE in the presence or absence of α1AT. Angiopoietin-2 was measured in cell culture supernatants by capture ELISA. The data shown here are the mean and standard error for 3 separate experiments. Statistical significance was calculated using a Paired T-Test. * and + p<0.05
 * compared to unstimulated control
 + compared to serine protease treatment

Figure 50 - Angiopoietin-2 Release from GEnC following Serine Protease Treatment



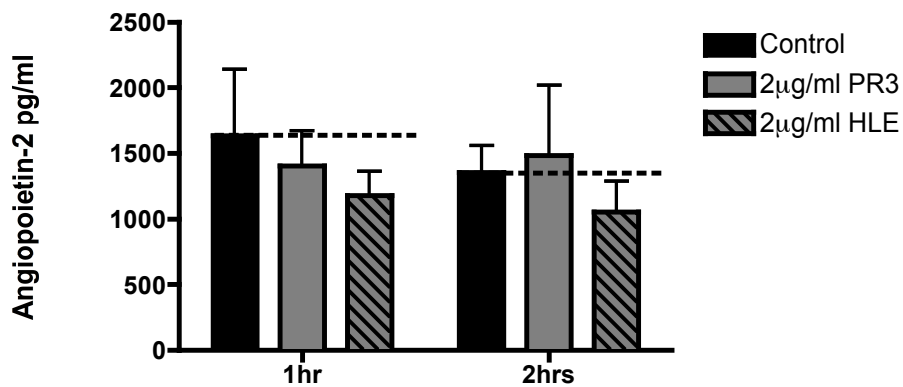
GEnC were treated with 1µg/ml PR3 or HLE in the presence or absence of α1AT. Angiopoietin-2 was measured in cell culture supernatants by capture ELISA. The data shown here are the mean and standard error for 4 separate experiments. Statistical significance was calculated using a Paired T-Test. + p<0.05, **p<0.01
 * compared to unstimulated control
 + compared to serine protease treatment

Figure 51 - PR3 and HLE Cleave Angiopoietin-2



Recombinant Angiopoietin-2 was incubated for 1 hour with 1 μ g/ml PR3 or HLE before analysis of detectable Ang-2 by capture ELISA. The data shown here is the mean from 1 experiment, displayed as Angiopoietin-2 concentration compared to optimal density.

Figure 52 - Angiopoietin-2 Release after Removal of PR3 and HLE

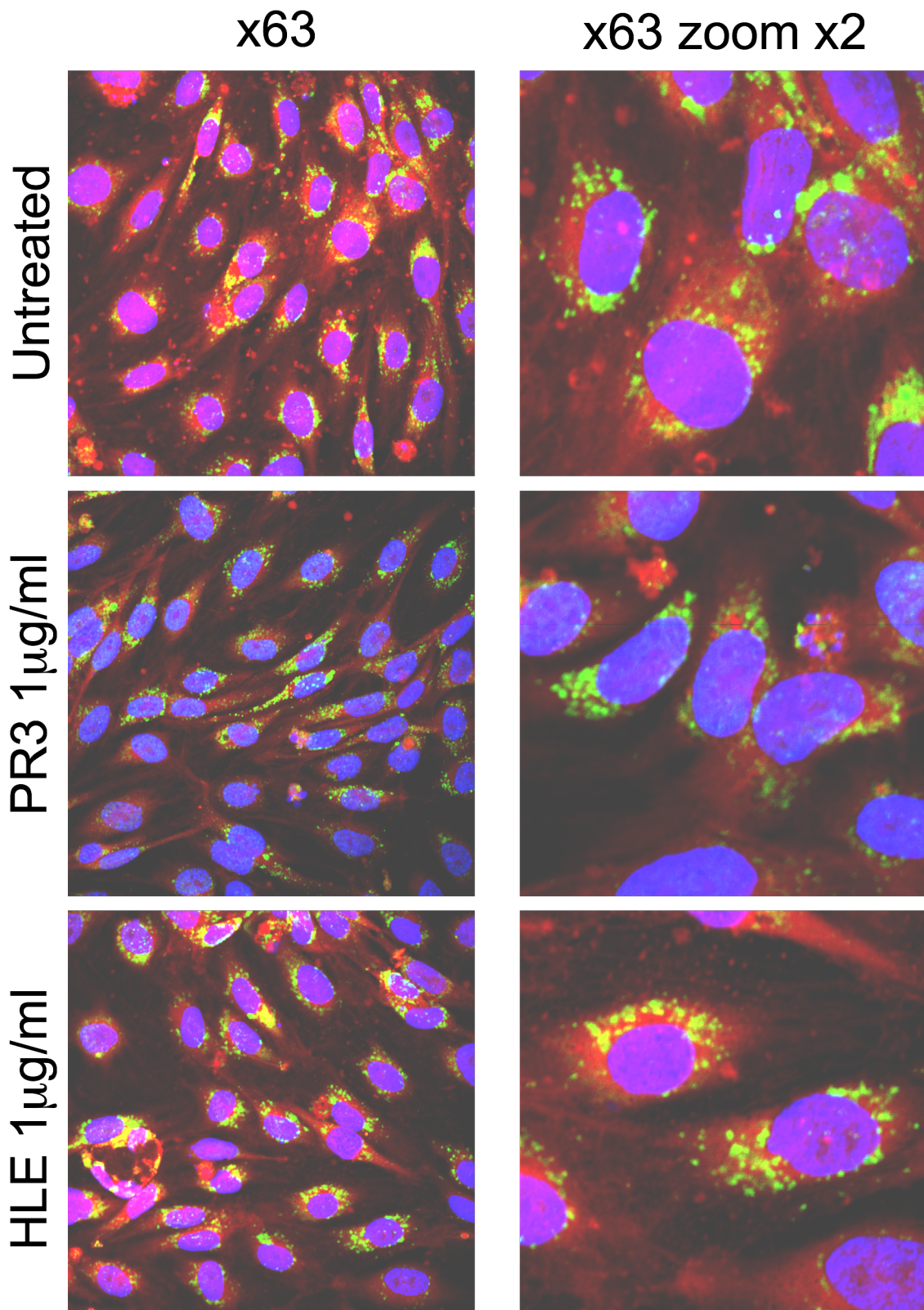


GENC were treated with 2 μ g/ml PR3 or HLE for 2 hours, following which the cells were washed to remove any residual enzyme and incubated for a further 1 or 2hours in blank medium. Supernatants were analysed for Ang-2 by capture ELISA. The data shown here are the mean and standard error from 3 separate experiments. Statistical significance was calculated by 1-way ANOVA with Bonferroni (1h $p=0.669$, 2hr $p=0.697$). A 2-way ANOVA was used to calculate significance between the two time points ($p=0.7092$).

3.13 CD63 Expression by Serine Protease Treated GEnC

CD63 constitutes the second most dominant protein in the membrane structure of Weibel-Palade bodies, although its exact roles in endothelial cells are questionable. The intracellular expression of CD63 (FITC) was assessed in GEnC following treatment with 1µg/ml PR3 or HLE by confocal microscopy. These GEnC were counterstained with Phalloidin Toxin (RPE) and Dapi (UV) to allow for determination of the localisation of CD63 expressing WPBs within the cell. Figure 53 shows a well-distributed localisation of CD63 within cytoplasm of the endothelial cell, with no distinct sites of WPB localisation. This distribution of expression does not appear to change upon treatment with PR3 or HLE for 2 hours, nor does there appear to be any change in the level of expression of CD63 following treatment. It is of note that CD63 does not appear to colocalise with the actin cytoskeleton (phalloidin toxin RPE).

Figure 53 - CD63 Staining following Protease Treatment



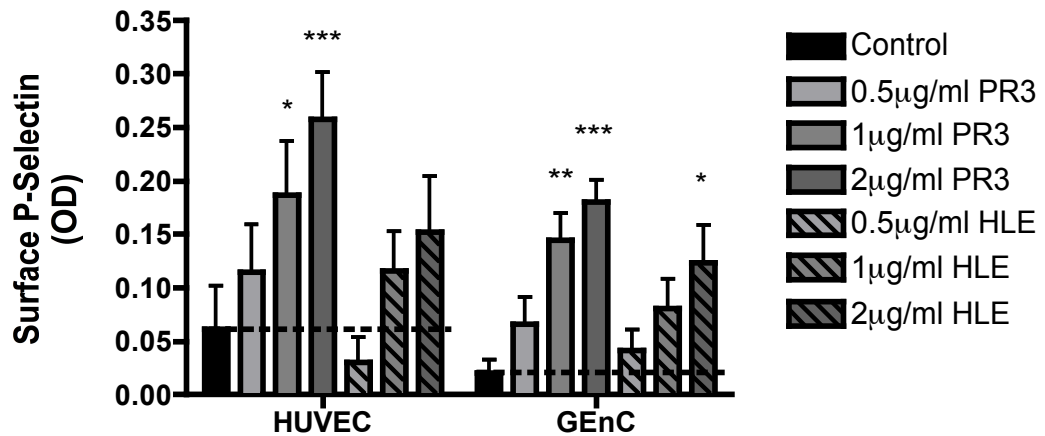
Glomerular endothelial cells treated for 2 hours with 1µg/ml PR3 or HLE were dual stained for CD63 (FITC ■) and phalloidin toxin (RPE ■), which binds to F-Actin, and visualised by confocal microscopy. Nuclei were stained with DAPI (UV ■).

3.14 Upregulation of Endothelial Membrane P-Selectin Expression by PR3 and HLE

Due to the rapid re-internalisation of P-Selectin following membrane expression, endothelial cells were fixed immediately following serine protease treatment. P-Selectin membrane expression was significantly increased on both GEnC and HUVEC following PR3 and HLE treatment when quantified by ELISA. The endothelial membrane expression of P-Selectin appeared to increase in a dose-dependant fashion, and was most markedly increased following PR3 treatment. Alternatively, only treatment with 2 μ g/ml of HLE reached significance (figure 54), although lower concentrations of HLE appear to increase in a dose dependant manner. The PR3 and HLE induced expression of endothelial P-Selectin could be significantly inhibited by the addition of α 1AT into the system (figure 55). In these inhibition experiments, the treatment of GEnC with 1 μ g/ml of HLE also resulted in significantly increased membrane expression of P-Selectin compared to untreated endothelial cells (Paired T-Test $p=0.0370$). Again, treatment of HLE on HUVEC was not quite significant ($p=0.0764$). We believe that with further repeats HLE treatment of HUVEC would have resulted in significantly increased P-Selectin expression, however, due to problems accessing primary HUVEC, these experiments could not be repeated to reach significance. An attempt to reproduce these results using flow cytometry to quantify surface and total P-Selectin in PR3 and HLE treated endothelial cells was unsuccessful, whilst P-Selectin expression could be easily measured on thrombin treated platelets (data not shown). Moreover, P-Selectin staining on GEnC by immunocytochemistry was also unsuccessful. The technical problems encountered when assessing P-Selectin expression by flow cytometry was likely due to the adherent nature of the endothelial cells, which was not an issue when using platelets. Removal of adherent cells from culture flasks after treatment

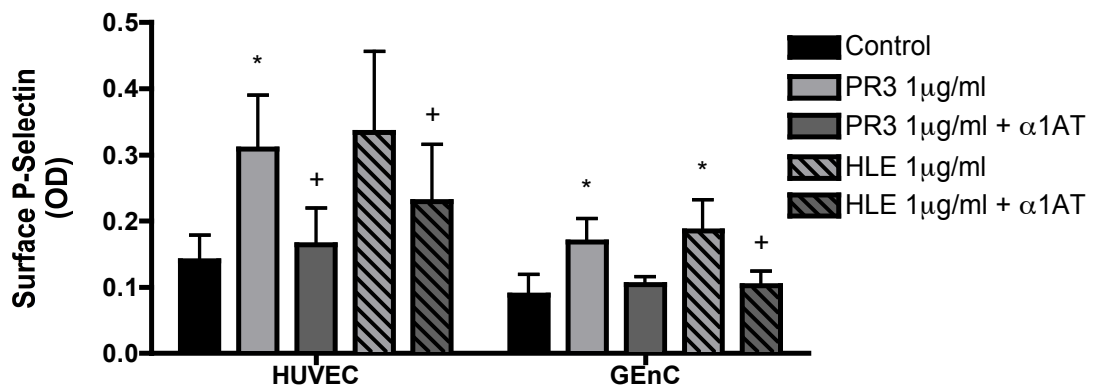
required washing with EDTA followed by scraping. Cells were then centrifuged and stained for P-Selectin. It is possible that the insult to the endothelial during the process of harvesting could have lost any membrane-expressed P-Selectin into supernatants, that could then not be measured by flow cytometry. To overcome this, other methods of cell detachment should be explored that do not require scraping. One such could be longer incubations of endothelial cells with EDTA (15minutes) and tapping the flasks to aid removal. Incubation with citric saline is also reported to aid cell detachment without the need for scraping. Interestingly, measuring P-Selectin expression by confocal was also a problem. P-Selectin was initially performed on HUVEC treated with thrombin and PAR-1 agonists using an anti-human P-Selectin PE (eBioscience, Clone Psel.KO2.3) on fluorescent microscopy, staining was positive but had a high level of background and positive staining within the isotype control. This staining was later repeated on GEnC, due to problems accessing HUVEC, using dual staining with actin on confocal microscopy. For confocal staining P-Selectin antibodies were used at a 1:10 dilution. Once correcting for background no positive P-Selectin staining could not be observed. This may be due to problems with the antibodies suitability for confocal microscopy, or technical handling of the endothelial cells. Experiments should be repeated with a known immunocytochemistry antibody.

Figure 54 - P-Selectin Surface Expression following PR3 and HLE Treatment



Endothelial cells treated with increasing doses of PR3 and HLE were fixed in 2% PFA and surface P-Selectin expression assessed using a cell based ELISA. The HUVEC data shown here are the mean and standard error from 10 separate experiments. The GEnC data shown here are the mean and standard error from 8 separate experiments. Statistical significance was calculated using a 1-way ANOVA with Bonferroni post-test for each cell type. (HUVEC PR3 $p=0.0018$, HLE $p=0.1401$). (GEnC PR3 $p<0.0001$, HLE $p<0.0001$). A 2-way ANOVA was used to measure significance between the cell types ($p=0.0629$) * $p<0.05$, ** $p<0.01$, *** $p<0.001$.

Figure 55 - Inhibition of P-Selectin Expression by α 1AT



Endothelial cells treated with 1µg/ml of PR3 and HLE in the presence or absence of α 1AT were fixed in 2% PFA and surface P-Selectin expression assessed using a cell based ELISA. The data shown here are the mean and standard error from 6 separate experiments. Statistical significance was calculated using a Paired T-Test. A 2-way ANOVA was used to measure significance between the two cell types ($p=0.0095$). * and + $p<0.05$
 * compared to untreated control
 + compared to serine protease treatment

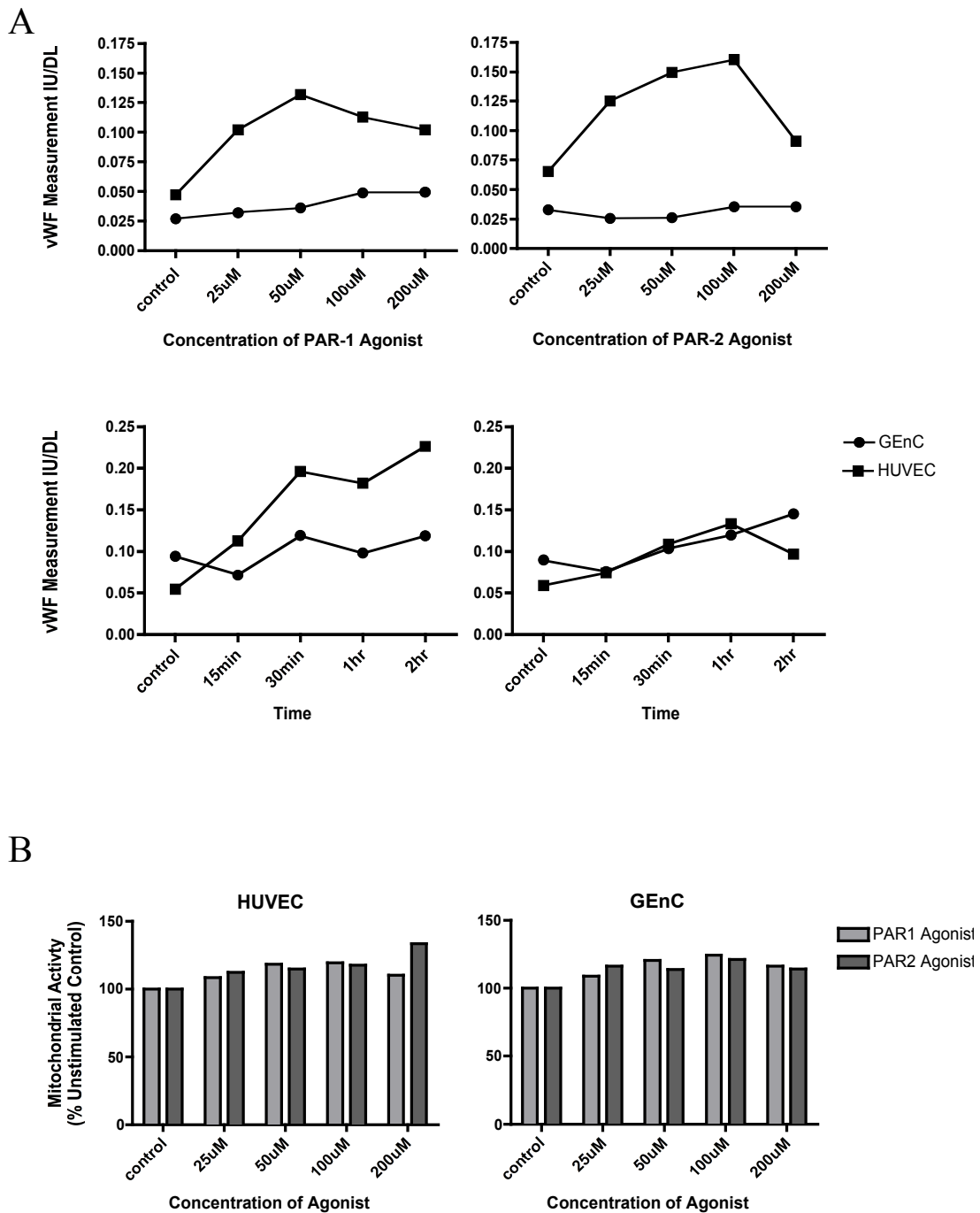
3.15 vWf Release by PAR Agonist Peptides

The release of vWf by PAR agonist peptides was investigated to determine optimal concentrations and times for use in future experiments (figure 56A). Both PAR-1 and PAR-2 agonists had the greatest effects of stimulating vWf release from HUVEC at concentrations of 100 μ M and 2 hour incubations. The release of vWf from GEnC was much lower and didn't appear to peak at any particular concentration or time point. For future experiments the optimal concentrations and times demonstrated on HUVEC were used on both cell types. Figure 56B demonstrates that the addition of increasing concentrations of these peptides had no effect endothelial mitochondrial activity. Furthermore, the treatment of endothelial cells with 100 μ M of PAR agonist for 2 hours also had no significant effect on cellular detachment (figure 58).

The ability of PAR-1 and PAR-2 agonists to stimulate vWf release from HUVEC and GEnC was compared to the levels previously demonstrated following treatment with 1 μ g/ml PR3 or HLE. Figure 57 shows that treatment of endothelial cells with PAR agonist peptides did not result in a significant increase in vWf release, although levels were increased above the unstimulated control. The PAR induced levels of vWf release are more comparable to the levels observed following 1 μ g/ml PR3 treatment.

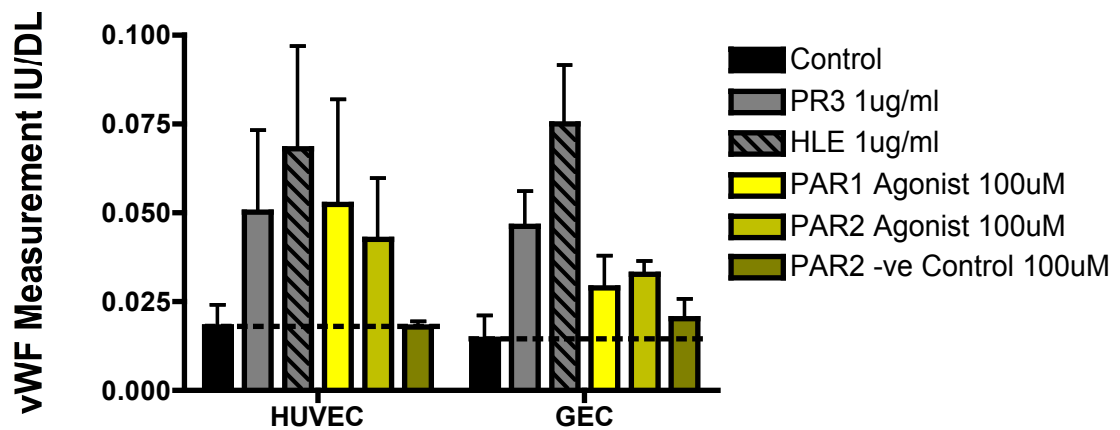
To further assess a role for the PARs in vWf release, original experiments attempted to inhibit vWf release using pharmacological inhibitors directed at PAR-1 and PAR-2. These experiments were discontinued, as the PAR antagonists were unable to inhibit PAR agonist induced vWf release from HUVEC (N=1-3, data not shown).

Figure 56 - Optimisation of PAR Agonist Peptide induced vWf Release



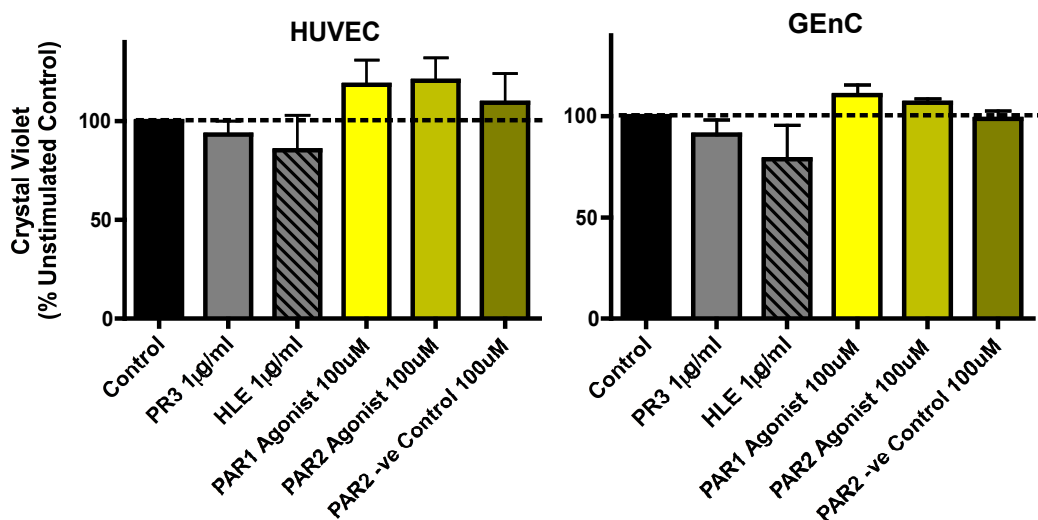
(A) Preliminary experiments were performed to investigate optimal concentrations (at 2 hour incubations) and times (with a 100µM agonist concentration) of PAR agonist peptides (PAR-1 and PAR-2) for release of vWf. vWf was measured in supernatants from treated HUVEC and GEnC by capture ELISA. This data is the mean of 2 replicates from 1 experiment. (B) Mitochondrial activity was measured in HUVEC and GEnC treated with increasing concentrations of PAR agonist peptides by MTT assay. This data is from 1 experiment, displayed as a percentage of untreated control.

Figure 57 - Effect of PAR Agonists on vWf Release



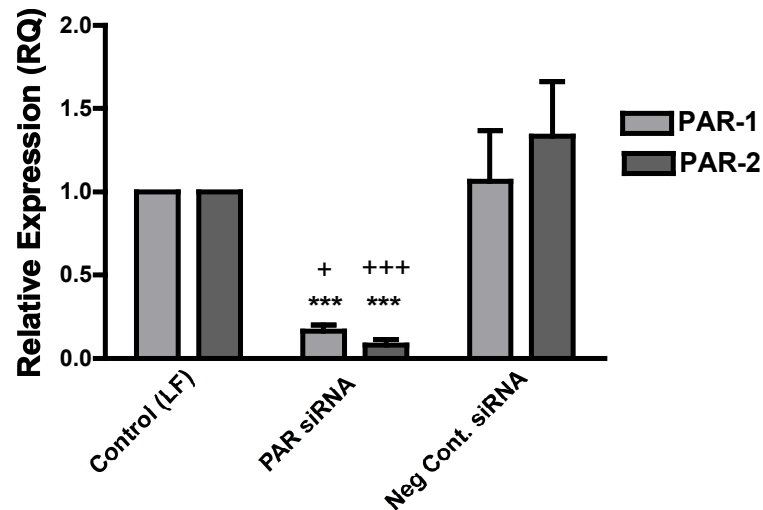
Endothelial cells were treated with 1µg/ml PR3, 1µg/ml HLE, 100µM PAR-1 agonist peptide, 100µM PAR-2 agonist peptide, or a PAR-2 negative control for 2 hours. vWf was measured in cell culture supernatants by capture ELISA. The HUVEC data shown here are the mean and standard error of 3 separate experiments. The GEnC data shown here are the mean and standard error of 5 separate experiments. Statistical significance was calculated using a 1-way ANOVA with Bonferroni post-test (HUVEC p=0.0602, GEnC p=0.0137). A 2-way ANOVA was used to measure significance between the two cell types (p=0.5342).

Figure 58 - Effect of PAR Agonists on Endothelial Cell Detachment



Endothelial cell adherence was measured by crystal violet staining following treatment with PR3, HLE and PAR agonists. The data shown here are the mean and standard error of 3 separate experiments, displayed as a percentage of the unstimulated control. Statistical significance was assessed using a 1-way ANOVA with Bonferroni post-test (HUVEC p=0.0342, GEnC p=0.0671).

Figure 59 - Confirmation of Knockdown of PAR-1 and PAR-2 by mRNA Levels

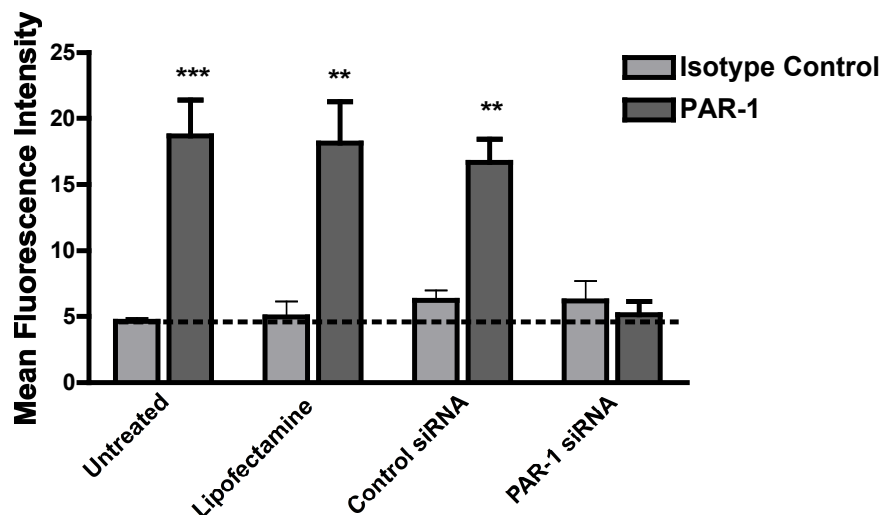


HUVEC were knocked down for the expression of PAR-1 and PAR-2 by small interference RNA (siRNA). Knockdown was confirmed by the reduction of PAR mRNA. PAR-1 and PAR-2 relative mRNA expression was compared to a lipofectamine (LF) and scrambled siRNA control. The PAR-1 siRNA data shown here are the mean and standard error from 5 separate experiments. The PAR-2 siRNA data shown here are the mean and standard error from 4 separate experiments. Statistical significance was calculated using a 1-way ANOVA with Bonferroni post-test (PAR-1 $p=0.0003$, PAR-2 $p<0.0001$). This data was produced by S. Tull. + $p<0.05$, *** and +++ $p<0.001$

* compared to Lipofectamine RNAiMax

+ compared to Control SiRNA

Figure 60 - Confirmation of PAR-1 Knockdown by Flow Cytometry



Successful knockdown of the PAR-1 protein in HUVEC was also confirmed by FACS. The data shown here are the mean and standard error from 3 separate experiments. Statistical significance was calculated using a 1-way ANOVA ($p=0.0004$). A 2-way ANOVA was used to compare any significance between PAR-1 expression and the isotype control (PAR1 versus Isotype $p<0.0001$, treatment $p=0.0090$). This data was produced by S. Tull. ** $p<0.01$, *** $p<0.001$

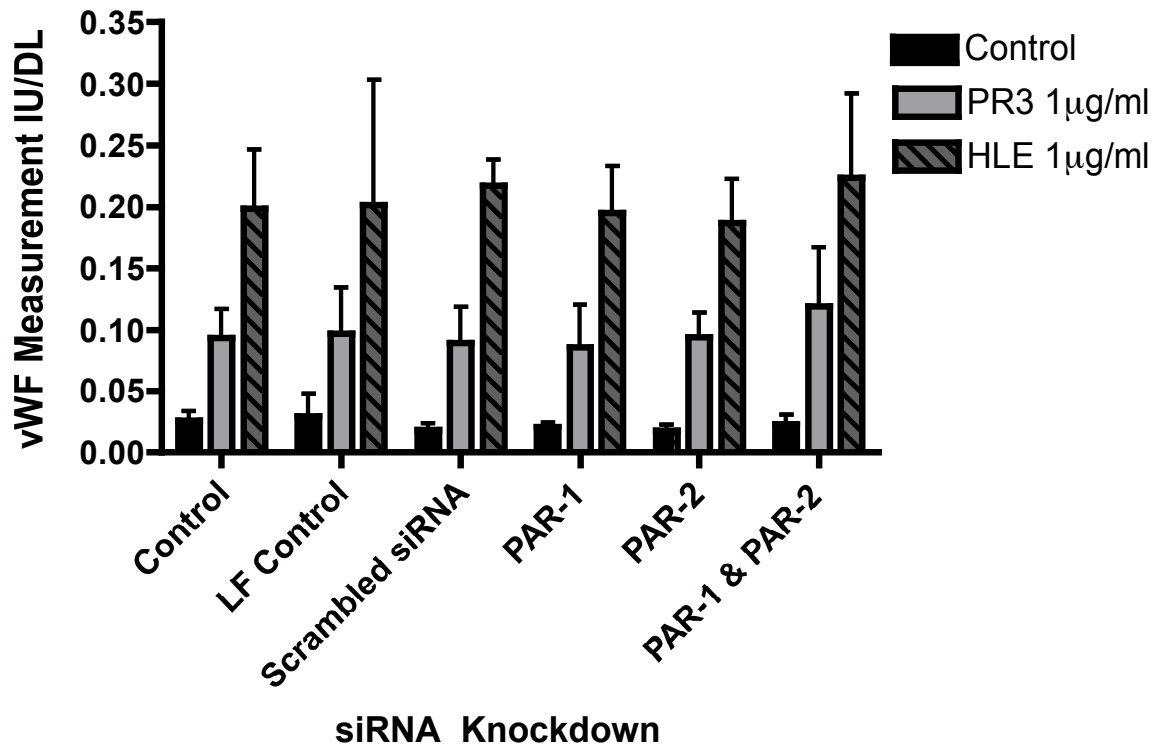
* PAR-1 siRNA compared to all other treatments

3.16 siRNA Knockdown of PAR-1 and PAR-2 does not reduce vWf Release

HUVEC knocked down for the expression of PAR-1 and PAR-2 by small interference RNA (siRNA) were generated in our laboratory by Samantha Tull. Successful knockdown was confirmed by mRNA and protein expression (figure 59 and 60). PAR-1 and PAR-2 mRNA was significantly reduced compared to lipofectamine and control siRNA treated HUVEC. PAR-1 protein expression was not significantly different to the isotype control when assessed by flow cytometry. (All of the data discussed above was produced by Samantha Tull).

We next wanted to investigate a role for the protease-activated receptors in PR3 and HLE mediated vWf release. Using HUVEC knocked down for the expression of PAR-1 and PAR-2 by siRNA, endothelial cells were stimulated with 1 μ g/ml PR3 and HLE to see if the levels of vWf release would be reduced compared to HUVEC that received no siRNA treatment. Figure 61 demonstrates that the knockdown of PAR-1 and PAR-2 in HUVEC has no effect on the release of vWf following treatment with PR3 or HLE. There was no significant difference in vWf release between HUVEC knocked down for the expression of PAR-1, PAR-2 or both, compared to those cells that received no treatment or were knocked down for a scrambled code of siRNA, indicating that PR3 and HLE do not require signalling through the protease activated receptors for Weibel-Palade body exocytosis.

Figure 61 - Knockdown of PAR-1 and PAR-2 does not reduce vWf Release



HUVEC knocked down for the expression of PAR-1 and PAR-2 were compared untreated HUVEC for their ability to release vWf in response to PR3 and HLE stimulation. HUVEC were treated with 1µg/ml PR3 or HLE for 2 hours and vWf measured in cell culture supernatants by capture ELISA. The data shown here are the mean and standard error from 3 separate experiments. Statistical analysis was performed using 2-way ANOVA comparing the siRNA treatment of HUVEC ($p=0.9961$).

3.17 Signalling Pathways involved in vWf Release

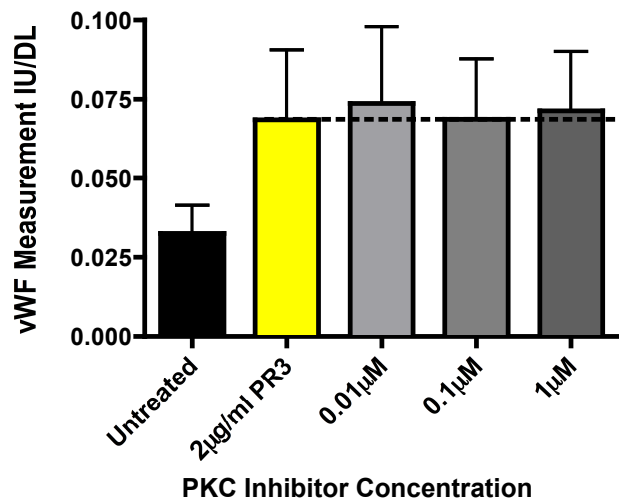
A mechanism by which PR3 and HLE were acting to induce vWf release was investigated using pharmacological inhibitors directed at components of known signalling pathways involved in ligand induced Weibel-Palade body exocytosis. These inhibitors were cultured in increasing concentrations (a log above and below their optimal IC₅₀ concentration) with PR3 or HLE on GEnC for 2 hours.

Incubation with PKC inhibitor, Gö6983, had no effect on reducing the level of PR3 or HLE mediated vWf release into cell culture supernatants (figures 62 and 63). Importantly, this inhibitor did not induce vWf release when cultured in the absence of any serine protease (data not shown), and did not affect mitochondrial activity (figure 64). The activity of Gö6983 was confirmed by its ability to inhibit ANCA and fMLP induced superoxide production from healthy donor neutrophils (figure 65). Interestingly, neither the PKA inhibitor, myristoylated PKI (14-22) amide, nor the calmodulin inhibitor, Calmadizolium, had an inhibitory effect on vWf release when incubated with 2µg/ml PR3 or HLE (figures 66, 67, and 69, 70 respectively). As with Gö6983, these inhibitors were also unable to induce vWf when cultured alone, and had no effect on mitochondrial activity (figures 68 and 71). The PI3-kinase inhibitor, wortmannin, has been routinely used in our lab to inhibit the effects of ANCA on inducing neutrophil degranulation (figure 75, data produced by Neil Holden). However, it had no effect on the inhibition of vWf release from glomerular endothelial cells in our system (figures 72 and 73). Again, wortmannin, itself, was unable to induce vWf release (data not shown) and had no effect on mitochondrial activity (figure 74). Statistical analyses for the inhibition of vWf release by these pharmacological inhibitors were performed by 1-way ANOVA, in which all inhibited cells were compared to an

uninhibited serine protease control. The level of vWf from untreated endothelial cells is also displayed on these data sets as an indication of the level of desired inhibition.

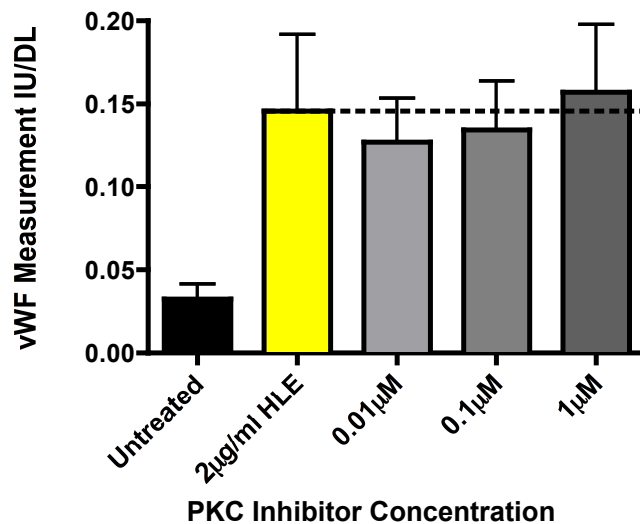
The use of these pharmacological inhibitors was also investigated in vWf release from HUVEC treated with 2 μ g/ml of HLE (N=3, data not shown). As with the GEnC, there was no effect on inhibition of vWf release (PKC p=0.2847, PKA p=0.5449, Calmodulin p=0.6701, PI3K p=0.1588).

Figure 62 – PR3 Mediated vWf Release following Inhibition of PKC



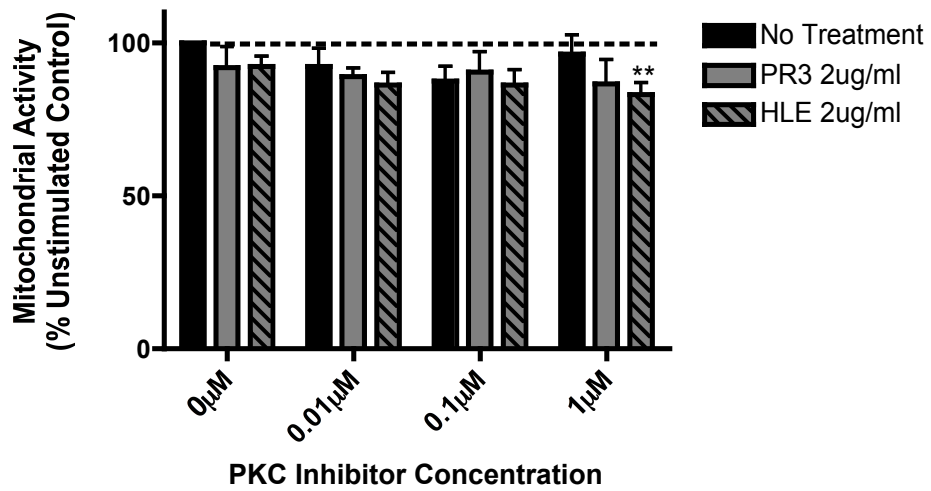
Glomerular endothelial cells were treated with PR3 with increasing doses of PKC inhibitor, Gö6983, for 2 hours. vWf was measured in cell culture supernatants by capture ELISA. The data shown here are the mean and standard error from 4 separate experiments. Statistical significance was assessed by 1-way ANOVA with Bonferroni post-test ($p=0.9529$).

Figure 63 - HLE Mediated vWf Release following Inhibition of PKC



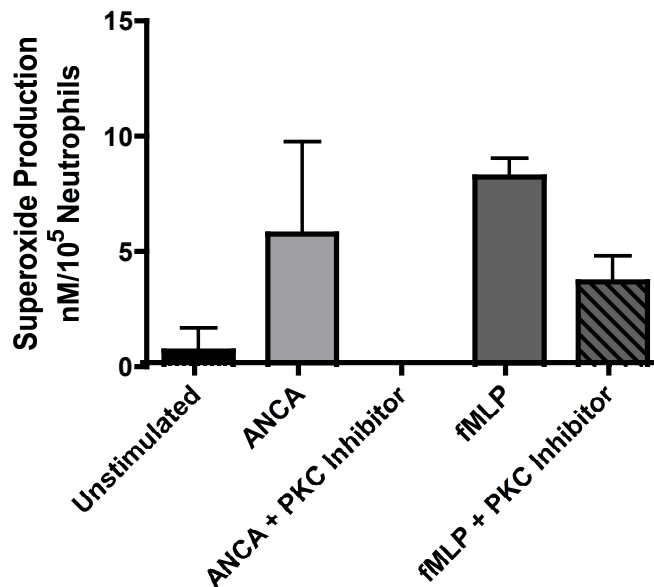
Glomerular endothelial cells were treated with HLE with increasing doses of PKC inhibitor, Gö6983, for 2 hours. vWf was measured in cell culture supernatants by capture ELISA. The data shown here are the mean and standard error from 4 separate experiments. Statistical significance was assessed by 1-way ANOVA with Bonferroni post-test ($p=0.4390$).

Figure 64 - Effect of PKC Inhibitor on Mitochondrial Activity



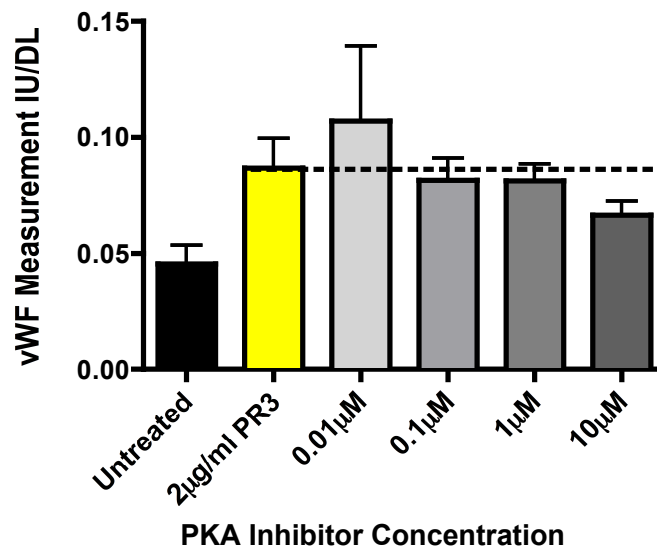
Glomerular endothelial cells were treated with 2µg/ml PR3 or HLE with increasing doses of PKC inhibitor, Gö6983, for 2 hours, fixed in 2% PFA and mitochondrial activity measured by MTT assay. The data shown here are the mean and standard error from 3 separate experiments. Statistical significance was assessed by 2-way ANOVA with Bonferroni post-test (inhibitor concentration $p=0.1764$). ** $p<0.01$

Figure 65 - Confirmation of the PKC Inhibitor by measuring Superoxide Production



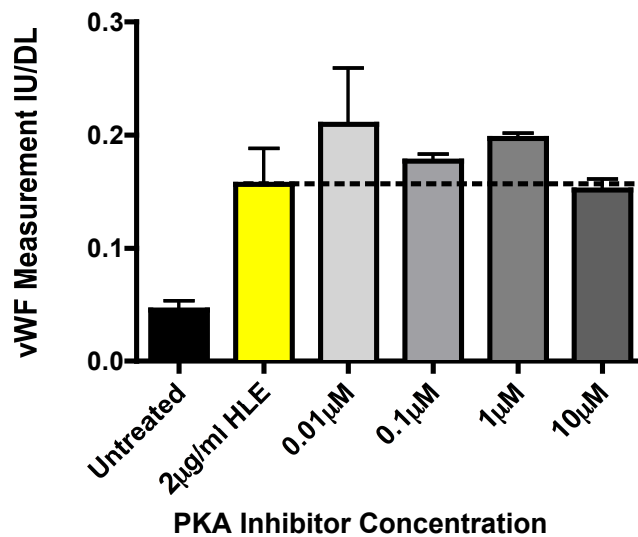
The activity of Gö6983 (1µM) was assessed by its ability to inhibit the production of superoxide from ANCA IgG (200µg/ml) stimulated neutrophils. The data shown here is the mean and standard error from 1 experiment.

Figure 66 - PR3 Mediated vWf Release following Inhibition of PKA



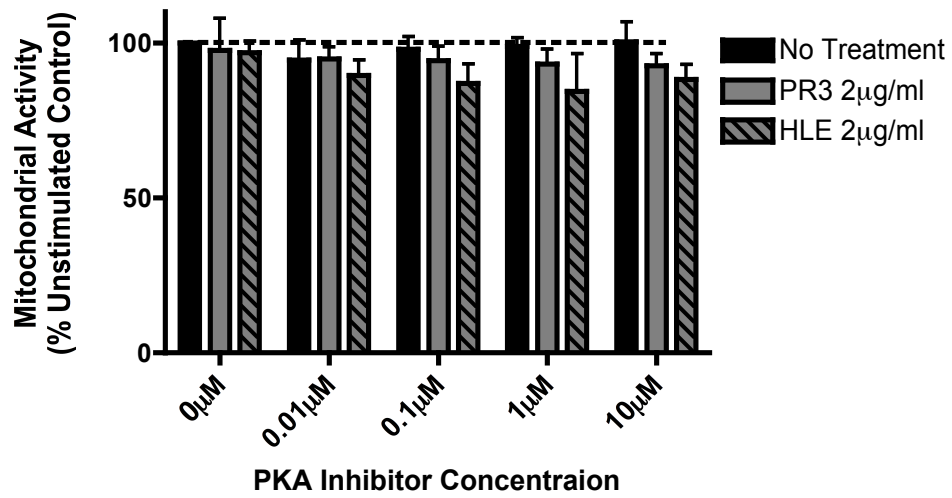
Glomerular endothelial cells were treated with PR3 with increasing doses of PKA inhibitor, myristoylated PKI (14-22) amide, for 2 hours. vWf was measured in cell culture supernatants by capture ELISA. The data shown here are the mean and standard error from 4 separate experiments. Statistical significance was assessed by 1-way ANOVA with Bonferroni post-test ($p=0.3276$).

Figure 67- HLE Mediated vWf Release following Inhibition of PKA



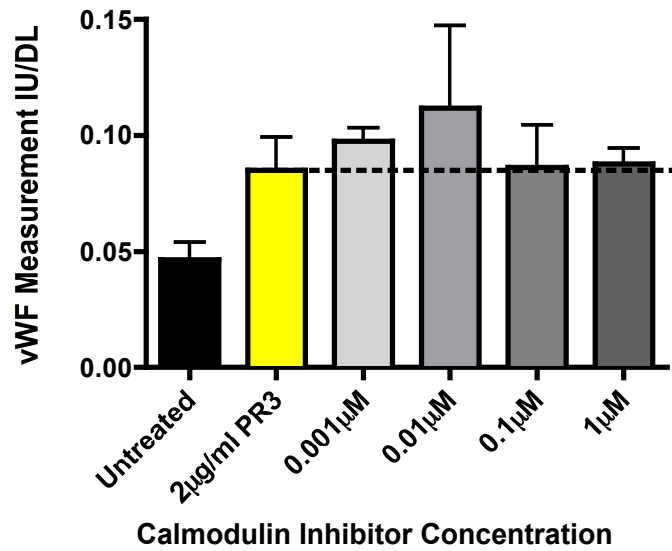
Glomerular endothelial cells were treated with HLE with increasing doses of PKA inhibitor, myristoylated PKI (14-22) amide, for 2 hours. vWf was measured in cell culture supernatants by capture ELISA. The data shown here are the mean and standard error from 4 separate experiments. Statistical significance was assessed by 1-way ANOVA with Bonferroni post-test ($p=0.3674$).

Figure 68 - Effect of PKA Inhibitor on Mitochondrial Activity



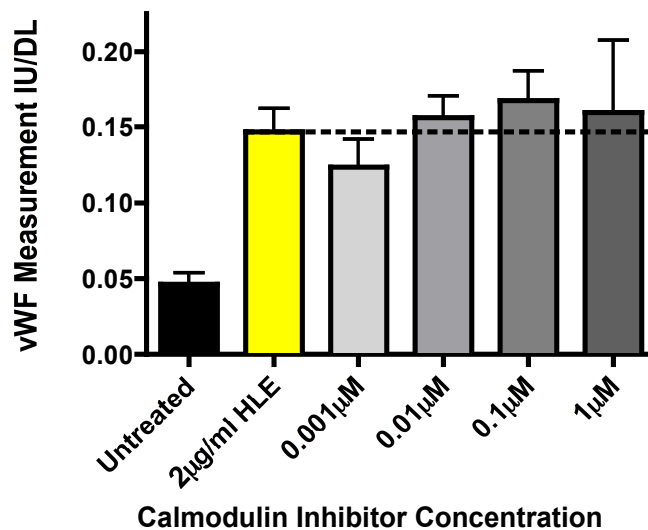
Glomerular endothelial cells were treated with 2µg/ml PR3 or HLE with increasing doses of PKA inhibitor, myristoylated PKI (14-22) amide, for 2 hours, fixed in 2% PFA and mitochondrial activity measured by MTT assay. The data shown here are the mean and standard error from 3 separate experiments. Statistical significance was assessed by 2-way ANOVA with Bonferroni post-test (inhibitor concentration $p=0.3766$).

Figure 69 - PR3 Mediated vWf Release following Inhibition of Calmodulin



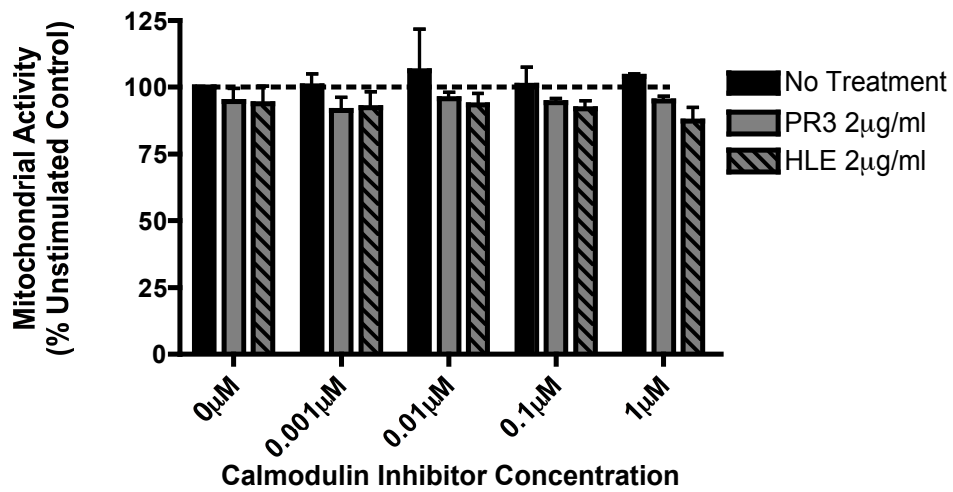
Glomerular endothelial cells were treated with PR3 with increasing doses of Calmodulin inhibitor, calmadizolium, for 2 hours. vWf was measured in cell culture supernatants by capture ELISA. The data shown here are the mean and standard error from 3 separate experiments. Statistical significance was assessed by 1-way ANOVA with Bonferroni post-test ($p=0.6589$).

Figure 70 - HLE Mediated vWf Release following Inhibition of Calmodulin



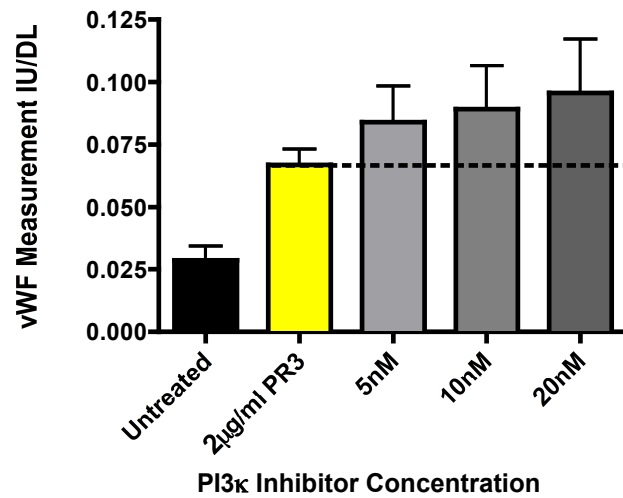
Glomerular endothelial cells were treated with HLE with increasing doses of Calmodulin inhibitor, calmadizolium, for 2 hours. vWf was measured in cell culture supernatants by capture ELISA. The data shown here are the mean and standard error from 3 separate experiments. Statistical significance was assessed by 1-way ANOVA with Bonferroni post-test ($p=0.5615$).

Figure 71 - Effect of Calmodulin Inhibitor on Mitochondrial Activity



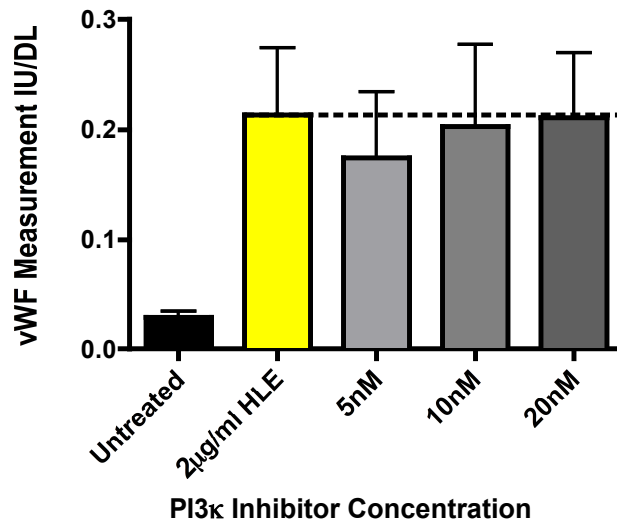
Glomerular endothelial cells were treated with 2µg/ml PR3 or HLE with increasing doses of Calmodulin inhibitor, calmadizolium, for 2 hours, fixed in 2% PFA and mitochondrial activity measured by MTT assay. The data shown here are the mean and standard error from 3 separate experiments. Statistical significance was assessed by 2-way ANOVA with Bonferroni post-test (inhibitor concentration p=0.5507).

Figure 72 - PR3 Mediated vWf Release following Inhibition of PI3k



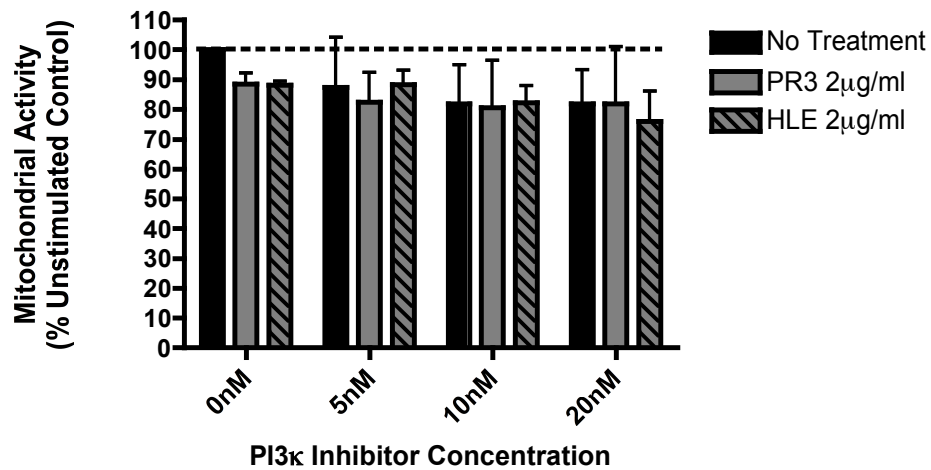
Glomerular endothelial cells were treated with PR3 with increasing doses of PI3-kinase inhibitor, wortmannin, for 2 hours. vWf was measured in cell culture supernatants by capture ELISA. The data shown here are the mean and standard error from 4 separate experiments. Statistical significance was assessed by 1-way ANOVA with Bonferroni post-test ($p=0.0734$).

Figure 73 - HLE Mediated vWf Release following Inhibition of PI3k



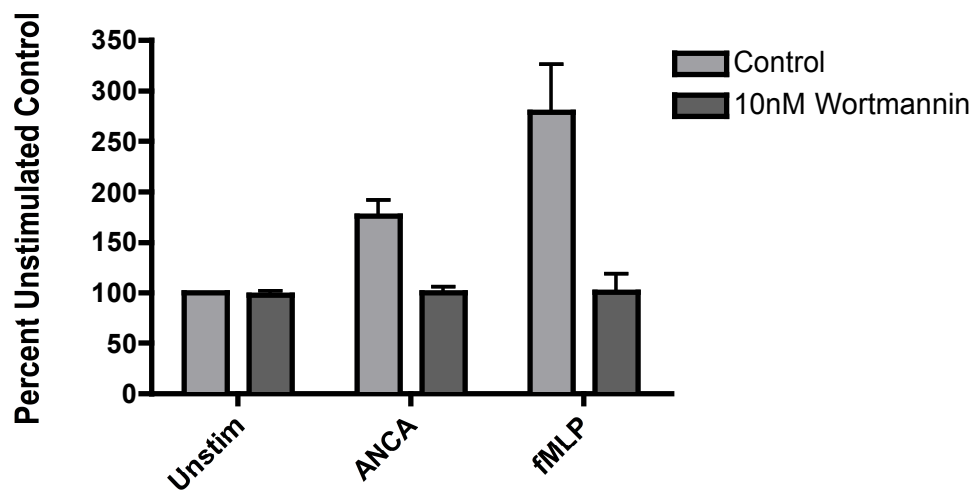
Glomerular endothelial cells were treated with HLE with increasing doses of PI3-kinase inhibitor, wortmannin, for 2 hours. vWf was measured in cell culture supernatants by capture ELISA. The data shown here are the mean and standard error from 4 separate experiments. Statistical significance was assessed by 1-way ANOVA with Bonferroni post-test ($p=0.1796$).

Figure 74 - Effect of PI3k Inhibitor on Mitochondrial Activity



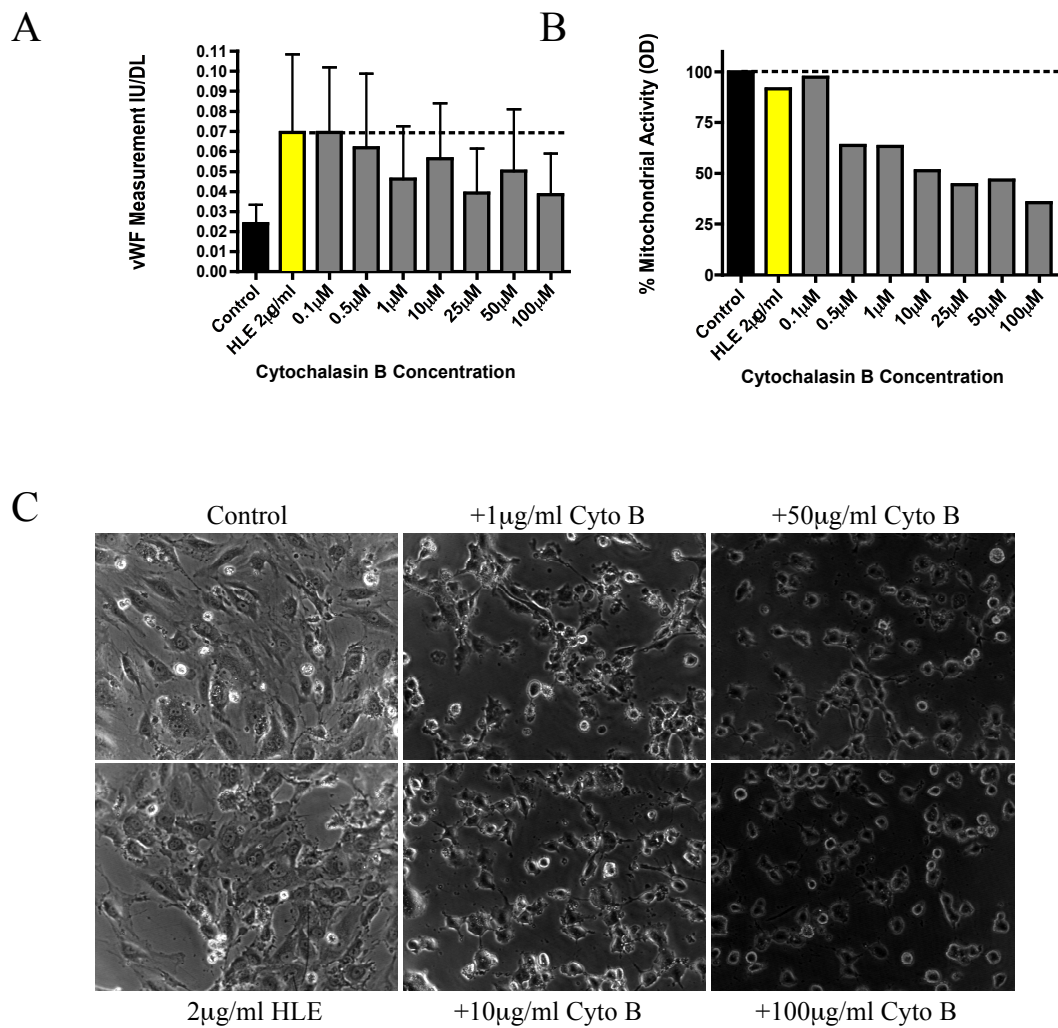
Glomerular endothelial cells were treated with 2µg/ml PR3 or HLE with increasing doses of PI3-kinase inhibitor, wortmannin, for 2 hours, fixed in 2% PFA and mitochondrial activity measured by MTT assay. The data shown here are the mean and standard error from 3 separate experiments. Statistical significance was assessed by 2-way ANOVA with Bonferroni post-test (inhibitor concentration $p=0.4897$).

Figure 75 - Confirmation of the PI3k Inhibitor by measuring Neutrophil Degranulation



The activity of wortmannin was assessed by its ability to inhibit ANCA IgG (200µg/ml) stimulated neutrophil degranulation (measured by MPO release). The data shown here is the mean and standard error from 10 experiments. Data produced by N Holden.

Figure 76 - Inhibition of Actin Polymerisation by Cytochalasin B



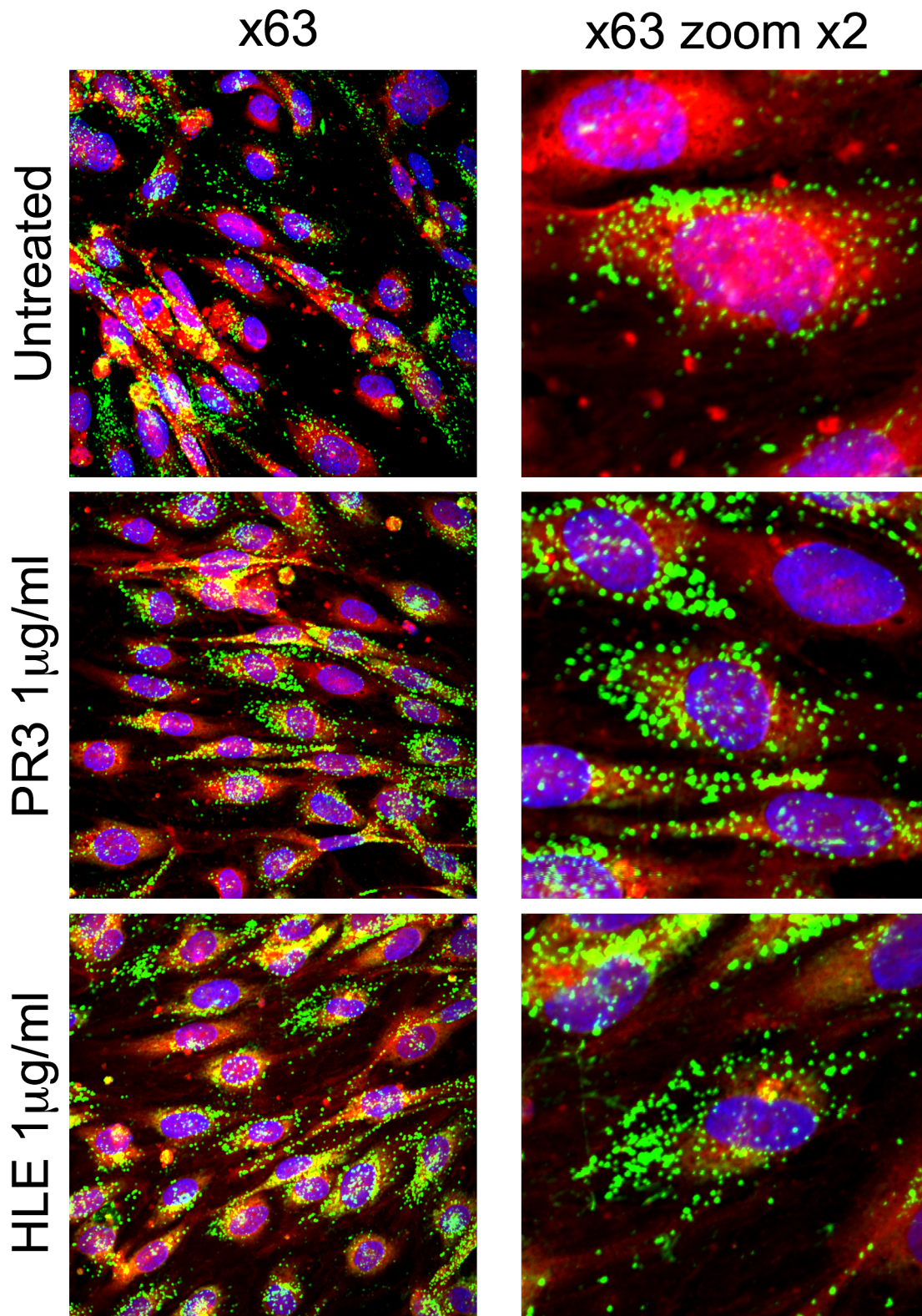
(A) vWf was measured in cell culture supernatants from HLE treated HUVEC with increasing doses of cytochalasin B. Cytochalasin B was pre-incubated for 5 minutes, before the addition of HLE for a further 2 hours. The data shown here are the mean and standard error from 2-3 separate experiments. Statistical significance was assessed by 1 way ANOVA with Bonferroni post test ($p=0.2456$). (B) Treated HUVEC were assessed for mitochondrial activity by MTT assay. The data shown here is from 1 experiment, displayed as a percentage of the unstimulated control. (C) Treated HUVEC were visualised by phase microscopy.

3.18 Inhibition of vWf Release by Inhibition of Actin Polymerisation

Cytochalasin B, a fungal metabolite that inhibits F-actin polymerisation, was used to investigate a role for the actin cytoskeleton in vWf release from serine protease treated endothelial cells. It was observed that treatment with increasing concentrations of cytochalasin B reduced the level of vWf release into cell culture supernatants, albeit not significantly (figure 76A). This reduction in the level of detectable vWf from HUVEC treated with 2 μ g/ml HLE occurred at the expense of endothelial cell viability. The disruption of the actin cytoskeleton by cytochalasin B, resulted in the endothelial cells becoming rounded and detached from the culture plates as well as displaying a decreased level of mitochondrial activity (figures 76B and C).

Furthermore, confocal staining for vWf and F-actin stain, Phalloidin, demonstrated that there was no evident interactions between the Weibel-Palade bodies and the actin cytoskeleton following treatment of GEnC with 1 μ g/ml of PR3 or HLE (figure 77), as previously demonstrated by CD63 staining. Interestingly, these confocal images further support a role for PR3 and HLE in increasing the level of detectable internal vWf, compared to levels observed in untreated endothelial cells.

Figure 77 - Confocal Staining for vWf and F-Actin



Glomerular endothelial cells treated for 2 hours with 1 μ g/ml PR3 or HLE were dual stained for vWf (FITC ■) and phalloidin toxin (RPE ■), which binds to F-Actin, and visualised by confocal microscopy. Nuclei were stained with DAPI (UV ■).

3.19 Inhibition of vWf Release by Inhibition of Phosphatase Activity

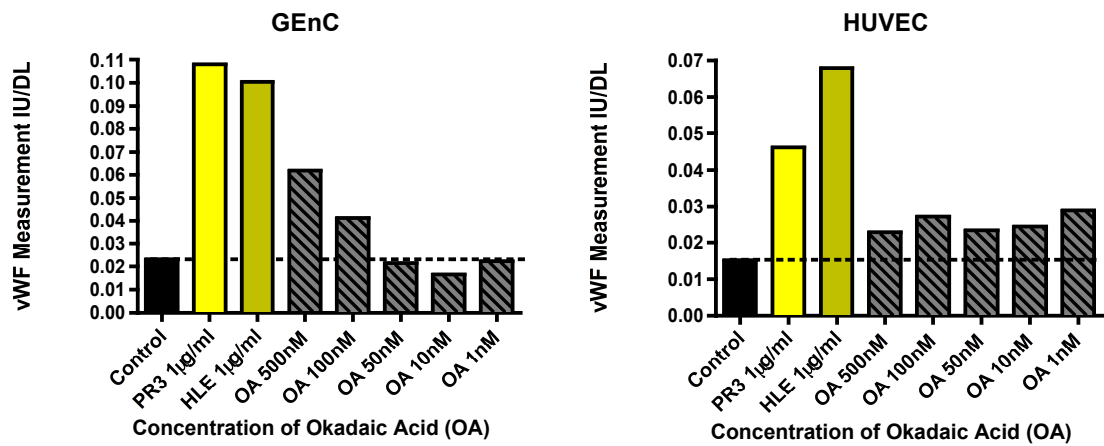
Okadaic acid, a phosphatase 2B inhibitor, was used to investigate a role for signalling molecule dephosphorylation in PR3 and HLE induction of Weibel-Palade body exocytosis. Preliminary experiments were performed to further assess the proposed role for okadaic acid to induce vWf in its own right. Here the level of vWf release from GEnC and HUVEC treated with increasing concentrations of okadaic acid was compared to the level of release observed following serine protease treatment. Figure 78 demonstrates that whilst higher concentrations of okadaic acid had the ability to induce vWf release from GEnC, the phosphatase 2B inhibitor had no effect on inducing vWf from HUVEC at any concentration. Furthermore, treatment with 500nM of okadaic acid appeared to induce endothelial detachment in HUVEC (figure 79). For future experiments into the effects of okadaic acid on vWf release we used a concentrations of 100nM, as this did not appear to induce endothelial detachment, whilst still displayed an increased level of vWf release from GEnC.

GEnC and HUVEC were treated with 100nM okadaic acid in the presence or absence of 1µg/ml PR3 or HLE to investigate a possible additive effect for okadaic acid on vWf release from endothelial cells. These endothelial cells were also treated with PR3, HLE and 100nM okadaic acid alone. Interestingly, okadaic acid treatment had different effects on the two types of endothelial cell. Again, okadaic acid treatment alone resulted in an increased level of vWf release into cell culture supernatants of GEnC (not significant), however it had no additive effect with PR3 or HLE treatment. Interestingly, okadaic acid not only had no effect on vWf release from HUVEC, but also appeared to abrogate the effects of PR3 and HLE on inducing vWf release (figure 80). It appears that whilst okadaic acid does not increase PR3 and HLE induced vWf release from GEnC, inhibition of the activity of phosphatase 2B also has no effect on reducing serine protease induced Weibel-Palade body exocytosis.

Alternatively, HUVEC inhibited for phosphatase 2B displayed complete abrogation of vWf release following PR3 or HLE treatment, suggesting a role for phosphatase 2B activity in PR3 and HLE induced vWf release in HUVEC.

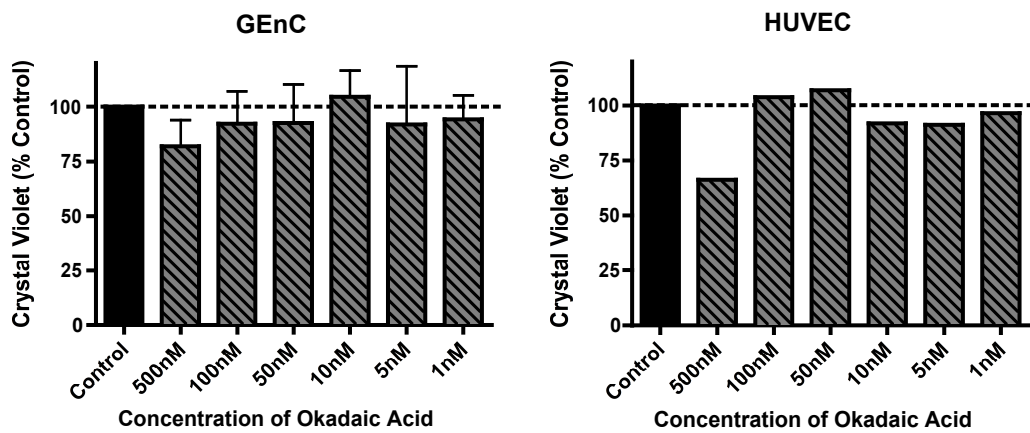
The assessment of mitochondrial activity following okadaic acid treatment demonstrated a significant decrease compared to the unstimulated control. Additionally, endothelial cells treated with PR3 or HLE with 100nM okadaic acid displayed a decreased mitochondrial activity to endothelial cells treated with serine protease alone (figure 81).

Figure 78 - vWf Release by Okadaic Acid



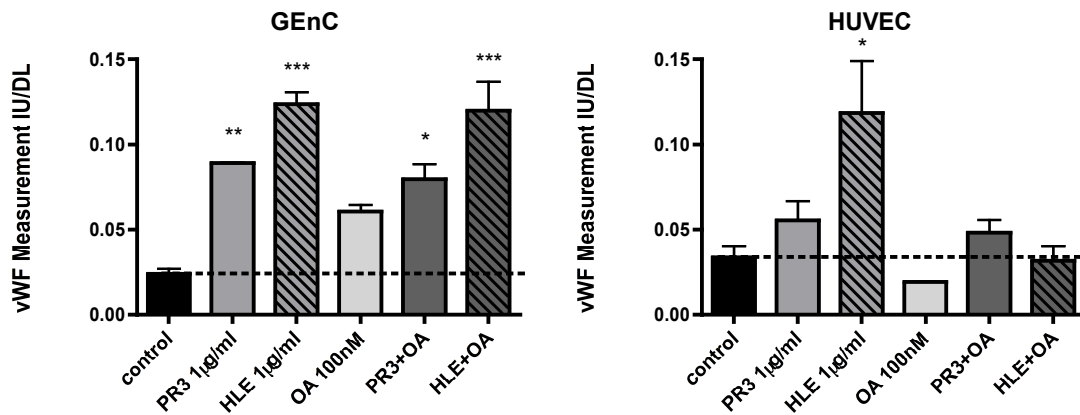
Preliminary experiments were performed to find an optimal concentration of okadaic acid for vWf release. Supernatants from treated endothelial cells were assessed for vWf by capture ELISA. The data shown here is the mean of 2 replicates from 1 experiment.

Figure 79 - Crystal Violet of Okadaic Acid Dose Curve



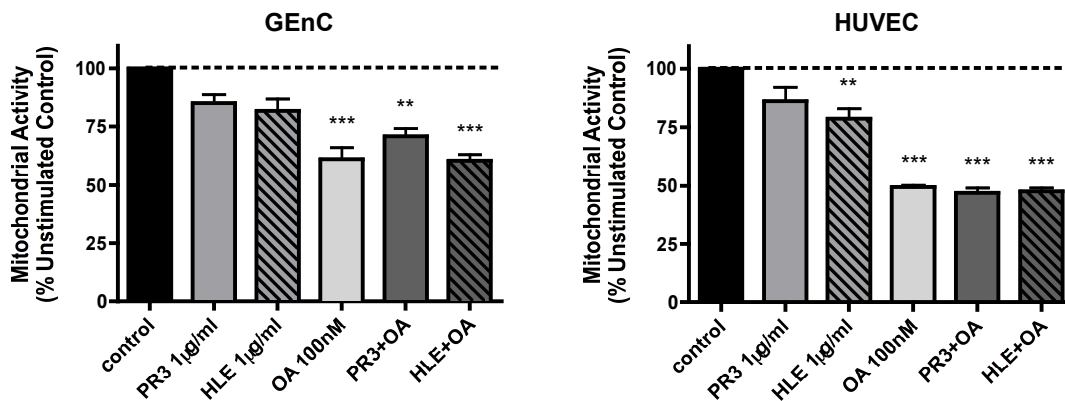
Endothelial cells treated with increasing concentrations of okadaic acid were stained with crystal violet to quantify the effects of the treatment of endothelial detachment. The GEnC data shown here are the mean and standard error from 2 experiments, displayed as a percentage of the untreated control. The HUVEC data is the mean from 1 experiment.

Figure 80 - Effects of Okadaic Acid on PR3 and HLE Mediated vWf Release



Endothelial cells were treated with 1µg/ml PR3 or HLE, 100nm okadaic acid, or a mixture of PR3/HLE and okadaic acid for 2 hours. vWf was measured in cell culture supernatants by capture ELISA. The data shown here are the mean and standard error from 3 separate experiments. Statistical significance was calculated using a 1-way ANOVA with Bonferroni post test (GEC $p=0.0001$, HUVEC $p=0.0092$). * $p<0.05$, ** $p<0.01$, *** $p<0.001$

Figure 81 - Mitochondrial Activity after Okadaic Acid Treatment



Mitochondrial activity was analysed in endothelial cells after 2 hour treatment with 1µg/ml PR3, 1µg/ml HLE, 100nm okadaic acid or a mixture of okadaic acid with PR3 or HLE, using a MTT assay. The data shown here are the mean and standard error from 3 separate experiments, displayed as a percentage of the unstimulated control. The data here is paired to the vWf release data in figure 80. Statistical significance was calculated using a 1-way ANOVA with Bonferroni post test (GEnC $p=0.0002$, HUVEC $p<0.0001$). ** $p<0.01$, *** $p<0.001$

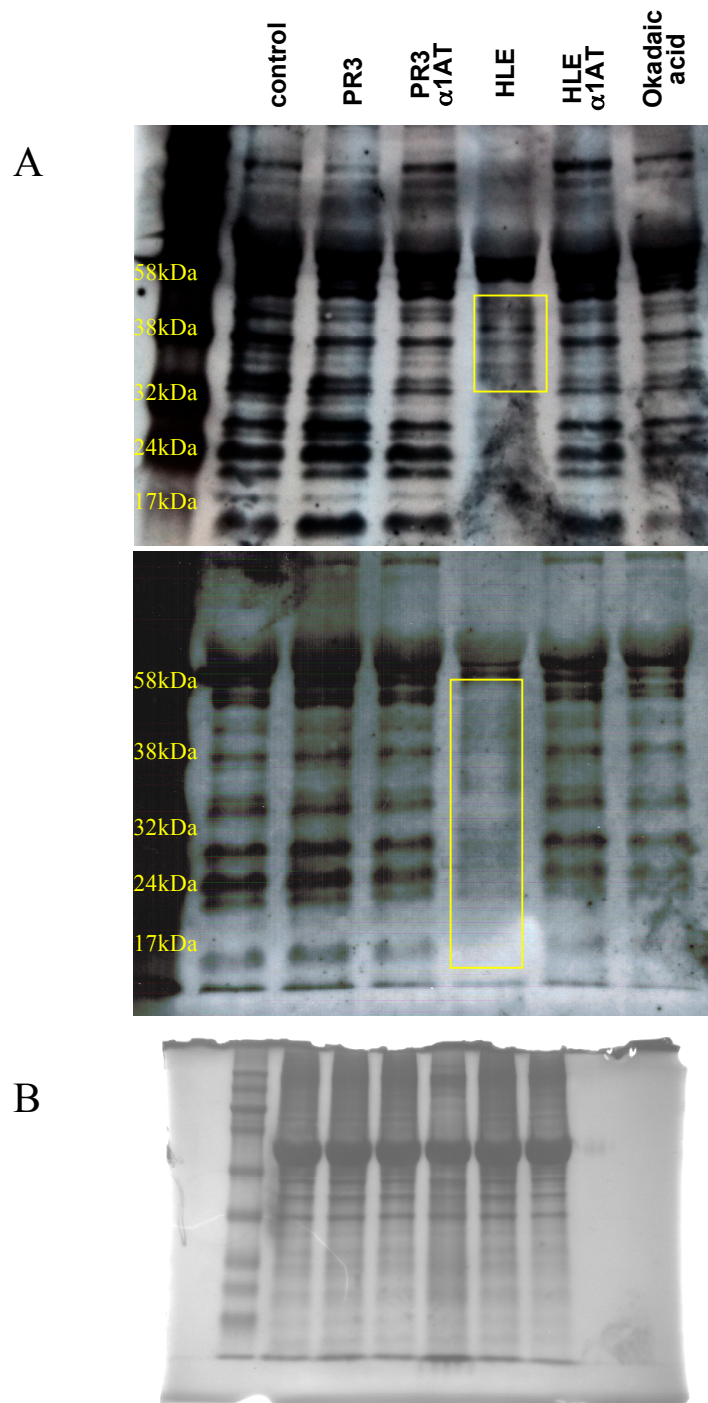
3.20 Changes in Phosphopeptides following Serine Protease Treatment

In the absence of any involvement of PKC, PKA, calmodulin or PI3k activity, we wanted to investigate whether the serine proteases were acting via an intracellular signalling pathway or whether they were inducing WPB exocytosis by cleavage mechanisms once internalised. To investigate a global role of PR3 and HLE in endothelial signalling we assessed changes in tyrosine and serine/threonine phosphorylation by western blotting (figures 82 and 83). Importantly, endothelial lysates were treated with a protease and phosphatase inhibitor cocktails to prevent any further changes in phosphopeptide expression. Interestingly, treatment of GEnC with HLE resulted in the loss of multiple phosphorylated tyrosine peptides compared to untreated endothelial cells. Furthermore, the identification of newly phosphorylated tyrosine peptides could be observed between the molecular weights of 52 and 31kDa. Again, the treatment with α 1AT inhibited the effects of HLE on protein phosphorylation/dephosphorylation. Endothelial treatment with PR3 did not display any changes in the pattern of phosphopeptides. Although, this may be due to changes in the phosphorylation of minor peptides that are masked by more dominant peptides on the western blot. Western blotting for serine/threonine phosphorylation was less successful. However, there does appear to be minor changes in the pattern of phosphopeptides between the molecular weights of 38 and 24kDa following HLE treatment. Interestingly, PR3 treated GEnC demonstrated the loss of a phosphorylated peptides with a molecule weight of around 225kDa.

These preliminary results can now be further explored by identifying the changes in peptide phosphorylation using a novel mass spectrometry method developed at the University of Birmingham by Dr Ashley Martin. To achieve this endothelial cells treated with PR3 and HLE will be lysed and the phosphopeptides extracted for mass spectrometry. This method

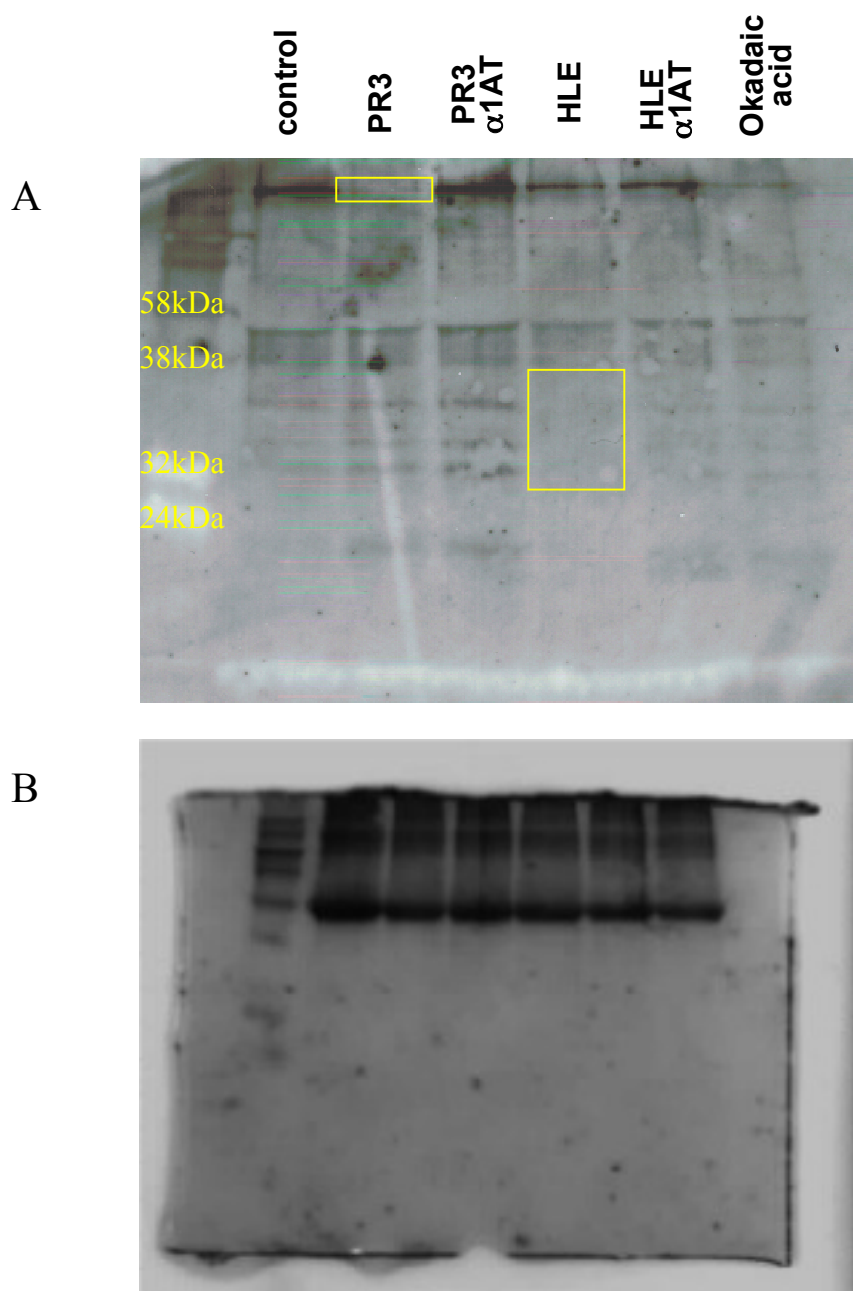
will allow us to assess changes in phosphorylated peptides that are less abundant within the endothelial cell and may be masked by more abundant peptides in our western blots.

Figure 82 - Western Blot for Tyrosine Phosphorylation



Lysates from serine protease treated glomerular endothelial cells were assessed for tyrosine phosphorylation by western blotting. Lysates were nano-dropped prior to loading and 250 μ g of protein was added to each lane. (A) 2 representative western blots of tyrosine phosphorylation from 1 μ g/ml PR3 or 1 μ g/ml HLE treated endothelial cells in the presence or absence of α 1AT (with one blot showing more clearly the presence of additional bands (top) and the other, missing phosphorylated proteins (bottom)). The blot was developed using ECL+ with a 15minute development exposure. This blot is an example from 5 separate experiments. Yellow boxes highlight changes in pattern of phosphorylated proteins. (B) The gel was simultaneously stained for protein by coomassie staining to demonstrate equal protein loading.

Figure 83 - Western Blot for Serine/Threonine Phosphorylation

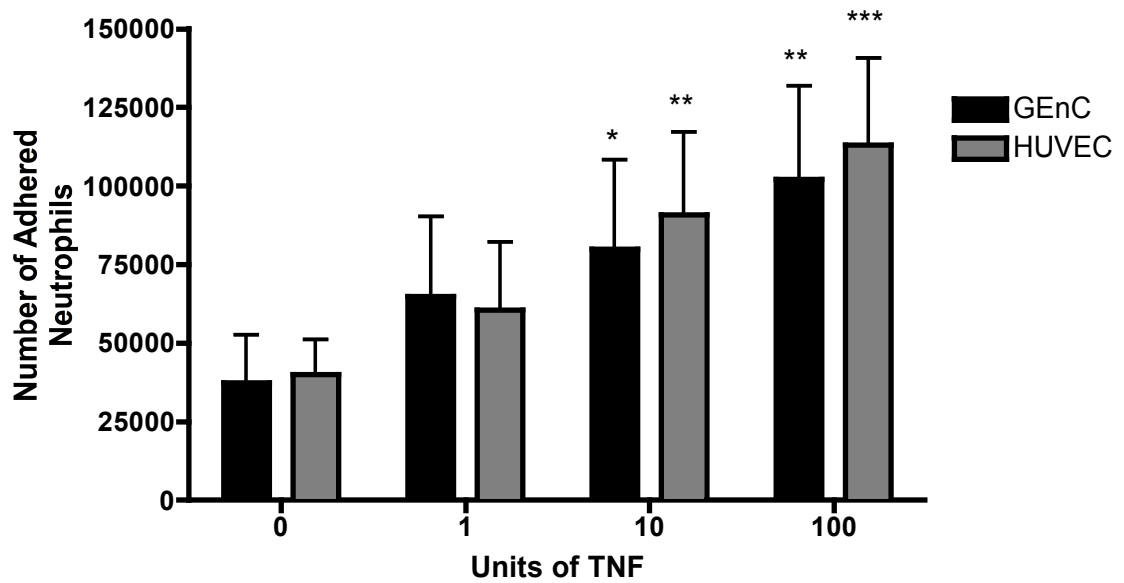


Lysates from serine protease treated glomerular endothelial cells were assessed for serine/threonine phosphorylation by western blotting. Lysates were nano-dropped prior to loading and 250 μ g of protein was added to each lane. (A) Western blot of serine/threonine phosphorylation from 1 μ g/ml PR3 or 1 μ g/ml HLE treated endothelial cells in the presence or absence of α 1AT. The blot was developed using ECL+ with a 15minute development exposure. This blot is an example from 3 separate experiments. Yellow boxes highlight changes in pattern of phosphorylated proteins. (B) The gel was simultaneously stained for protein by coomassie staining to demonstrate equal protein loading.

3.21 Neutrophil Adhesion to TNF α Treated Endothelial Cells

Neutrophil adhesion to TNF α treated endothelial cells was measured using a static model of adhesion, in which 2.5×10^5 unprimed neutrophils were co-cultured with endothelial cells treated with increasing concentrations of TNF α for 4 hours. The level of neutrophil adhesion to both GEnC and HUVEC increased in a dose-dependant fashion with increasing concentration of TNF α (figure 84). At the higher TNF α concentrations there is a statistically significant difference between the level of neutrophil adhesion when compared to the unstimulated control, which received 0 units of TNF α . This statistical difference became more apparent at the highest concentrations of TNF α i.e. 100 units. The dose-dependant increase in neutrophil adhesion was not statistically different between the two cell types, as determined by 2 way ANOVA, thereby implying that the conditionally immortalised glomerular cell line respond to activation by TNF α in the same manner as primary cells. This observation reinforces the idea that priming of endothelial cells with TNF α can result in endothelial activation and consequently increased adhesion of neutrophils, thereby supporting Gamble *et al.*, 1985, who proposed that neutrophil adhesion to TNF α treated HUVEC was maximal following 4 hours incubation, whilst also describing a dose-dependant appearance to the increased adhesion [208].

Figure 84 - Neutrophil Adhesion to TNF α Treated Endothelial Cells



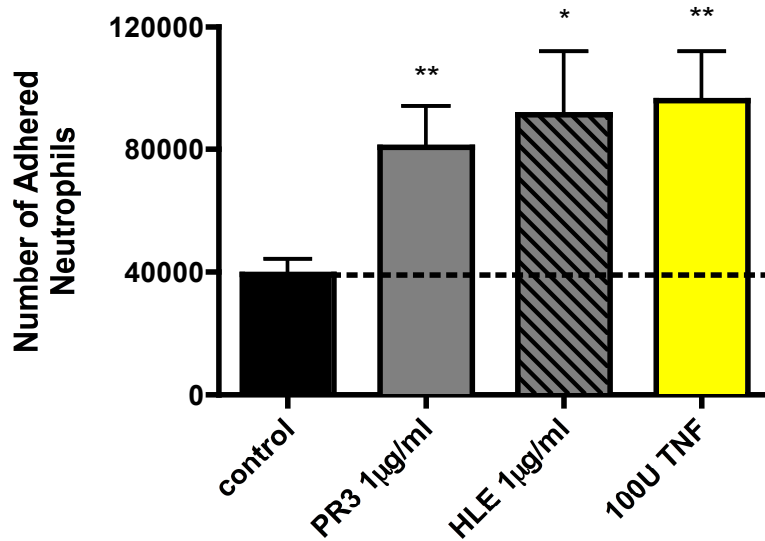
Neutrophil adhesion to endothelial cells was measured in a static model of adhesion. Endothelial cells were treated with increasing concentrations of TNF α for 4 hours, followed by 250,000 neutrophils for 1 hour. The level of adherence was measurement by conversion of OPD substrate by neutrophil myeloperoxidase. Cell numbers were calculated from a standard curve. The data shown here are the mean and standard error from 6 separate experiments. Statistical significance was assessed using a 1-way ANOVA with Bonferroni post test (GEnC p=0.0039, HUVEC p=0.0005). *p<0.05, **p<0.01, ***p<0.001

3.22 Neutrophil Adhesion to PR3 and HLE treated Endothelial Cells

To investigate an effect of the neutrophil serine proteases in neutrophil adhesion, endothelial cells were treated with increasing concentrations of PR3 and HLE for 2 hours, and then further incubated for 1 hour with 250,000 unprimed neutrophils in a static model of adhesion. The incubation time for serine protease treatment was previously determined by Samantha Tull (unpublished data), who demonstrated that neutrophil adhesion was optimal in these conditions. The level of neutrophil adhesion induced by PR3 or HLE treatment was compared to a 4 hour TNF α positive control. Figure 85 demonstrates a significantly increased level of neutrophils adhered to HUVEC treated with 1 μ g/ml PR3 or HLE. The level of neutrophil adhesion achieved was not statistically different from that achieved with TNF α treatment (PR3 p=0.3121, HLE p=0.8446). GEnC treated with PR3 and HLE also displayed significantly increased neutrophil adhesion, although this was lower than that observed on HUVEC (figure 86).

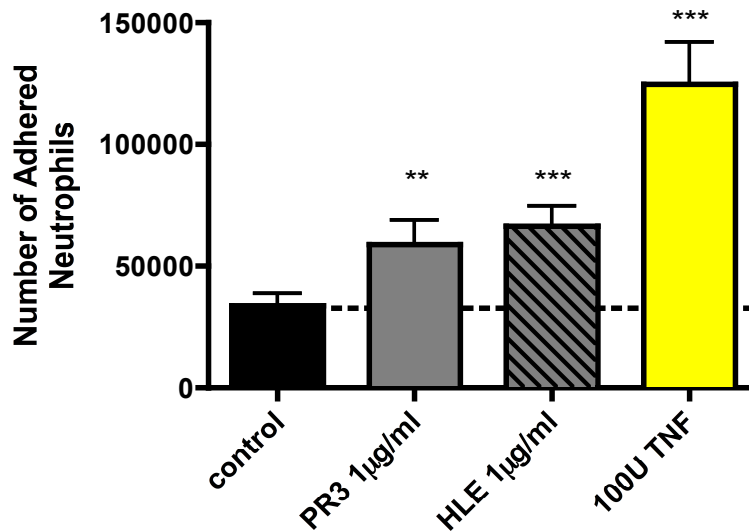
The addition of α 1-antitrypsin into this model of serine protease induced adhesion, significantly inhibited the number of neutrophils adhered to PR3 and HLE treated endothelial cells. This observation can be seen in both GEnC and HUVEC, following 2 hour treatment with 1 μ g/ml PR3 and HLE in the presence of α 1AT in molar excess (figures 87 and 88). Although, it is of note that the addition of α 1AT did not completely abolish neutrophil adhesion. Although significantly decreased compared to protease treatment alone, the inhibition of neutrophil adhesion to GEnC by α 1AT remained significantly increased above untreated levels (PR3 p=0.0282, HLE p=0.0236). HUVEC α 1AT treatment however, was not significantly different from neutrophil adhesion to untreated endothelial cells when analysed by paired T-Test (PR3 p=0.1665, HLE p=0.1623).

Figure 85 - Neutrophil Adhesion to PR3/HLE Treated HUVEC



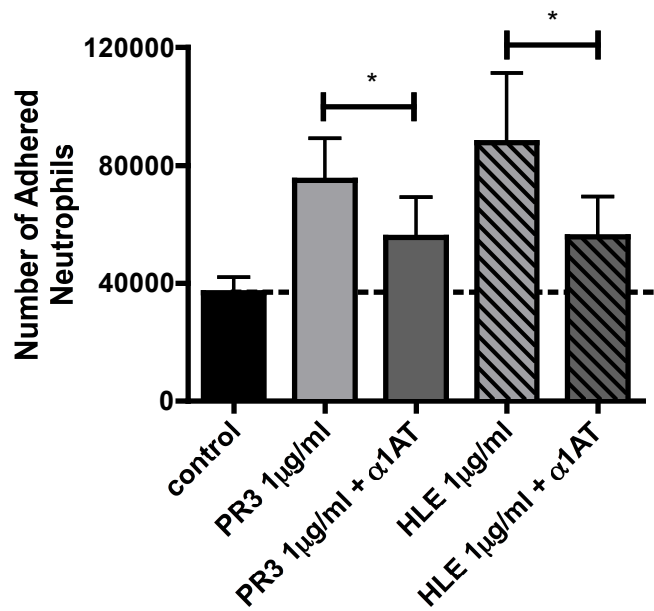
HUVEC treated for 2 hours with 1µg/ml PR3 or HLE, or 4 hours with 100 units TNFα as a positive control (yellow), were assessed for increased neutrophil adhesion using a static model of adhesion. The level of adherence was measurement by conversion of OPD substrate by neutrophil myeloperoxidase. The data shown here are the mean and standard error from 8 separate experiments. Statistical significance was calculated using a paired T-Test. *p<0.05, **p<0.01
* compared to the untreated control

Figure 86 - Neutrophil Adhesion to PR3/HLE Treated GENC



GENC treated for 2 hours with 1µg/ml PR3 or HLE, or 4 hours with 100 units TNFα as a positive control (yellow), were assessed for increased neutrophil adhesion using a static model of adhesion. The level of adherence was measurement by conversion of OPD substrate by neutrophil myeloperoxidase. The data shown here are the mean and standard error from 9 separate experiments. Statistical significance was calculated using a paired T-Test. **p<0.01, ***p<0.001
* compared to the untreated control

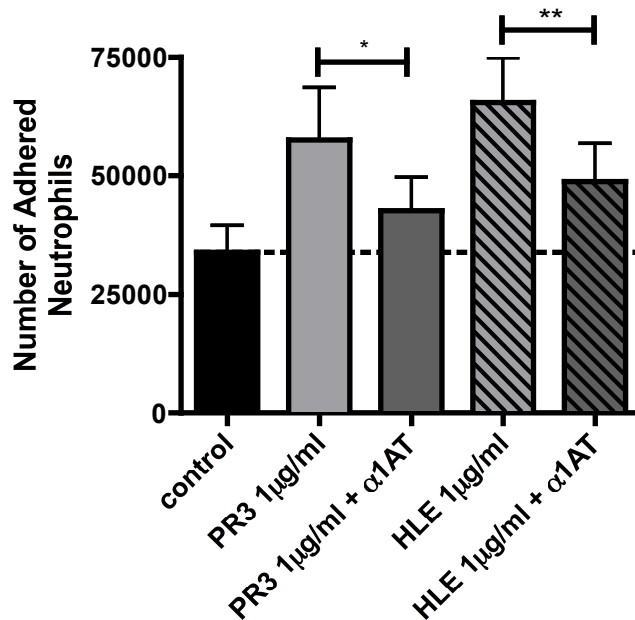
Figure 87 - Inhibition of Neutrophil Adhesion to HUVEC by α 1AT



HUVEC treated for 2 hours with 1µg/ml PR3 or HLE in the presence or absence of α 1-antitrypsin, were assessed for increased neutrophil adhesion using a static model of adhesion. The data shown here are the mean and standard error from 7 separate experiments. Statistical significance was calculated using a paired T-Test. *p<0.05

* compared to serine protease treatment alone

Figure 88 - Inhibition of Neutrophil Adhesion of GENC by α 1AT



GENC treated for 2 hours with 1µg/ml PR3 or HLE in the presence or absence of α 1-antitrypsin, were assessed for increased neutrophil adhesion using a static model of adhesion. The data shown here are the mean and standard error from 8 separate experiments. Statistical significance was calculated using a paired T-Test. *p<0.05, **p<0.01

* compared to serine protease treatment alone

3.23 Membrane Expression of E-Selectin Following Serine Protease Expression

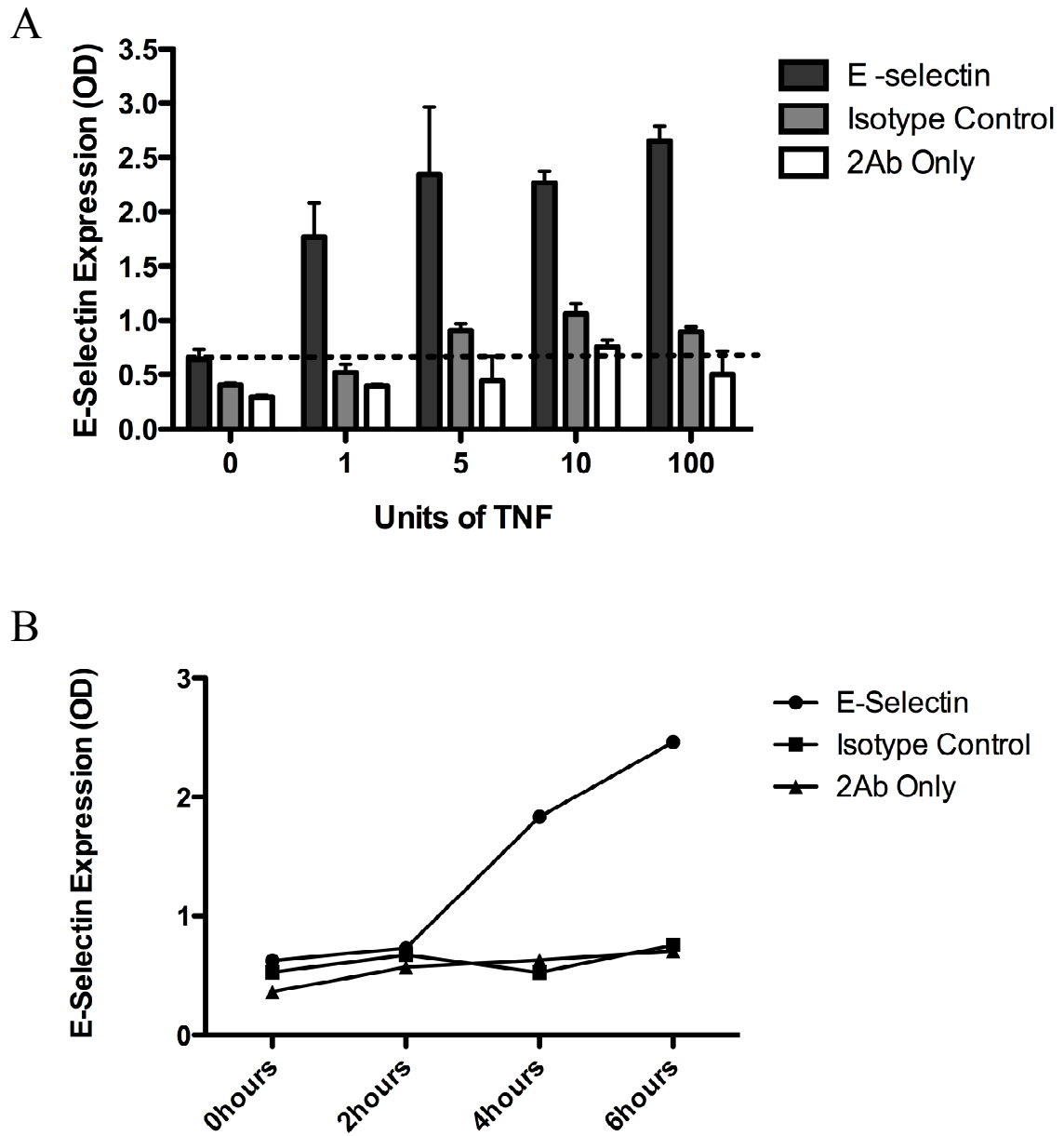
We next wanted to investigate a mechanism by which serine proteases treated endothelial cells could increase neutrophil adhesion. We began by assessing the changes in endothelial membrane expression of classical adhesion molecules, E-Selectin, ICAM-1 and VCAM-1, following 2 hour treatments with PR3 and HLE. Interestingly, we had already observed increased expression of endothelial P-Selectin. Optimal concentrations of the E-Selectin primary and secondary antibodies were determined by titration on HUVEC treated with 100 units TNF α for 4 hours (data not shown).

Next, HUVEC were treated with increasing concentrations of TNF α for 4 hours to assess the optimal concentration for increased E-Selectin expression (figure 89A). The membrane expression of E-Selectin on HUVEC increases in a dose-dependant manner with optimal surface expression observed with 100 units TNF α , although, even at lower concentrations, E-Selectin expression is increased above the untreated control. This concentration was further evaluated in a timecourse of TNF α treatment to assess at what time point increased E-Selectin expression could be observed (figure 89B). The earliest time point by which increased E-Selectin expression could be distinguished from the isotype control was at 4 hours, with expression increasing further at 6 hours following 100 units TNF α treatment. From this preliminary data, all future E-Selectin expression experiments were compared to a 4 hour 100 unit TNF α positive control.

Figures 90 and 91 demonstrate the level of membrane expression on PR3 and HLE treated HUVEC and GEnC, respectively. There was no apparent increase in the surface expression of E-Selectin on either cell type following 2 hour treatment with increasing concentrations of

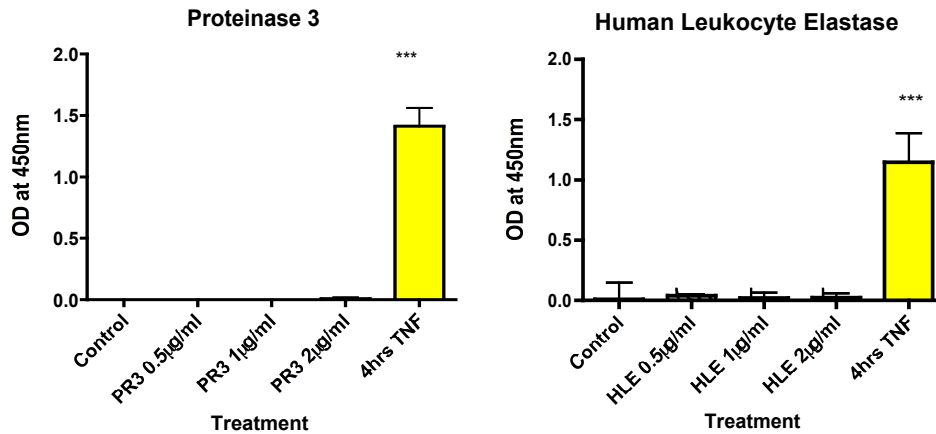
PR3 or HLE. E-Selectin expression was neither observed on untreated endothelial cells, with expression equal to that of the isotype control.

Figure 89 - Optimisation of E-Selectin ELISA



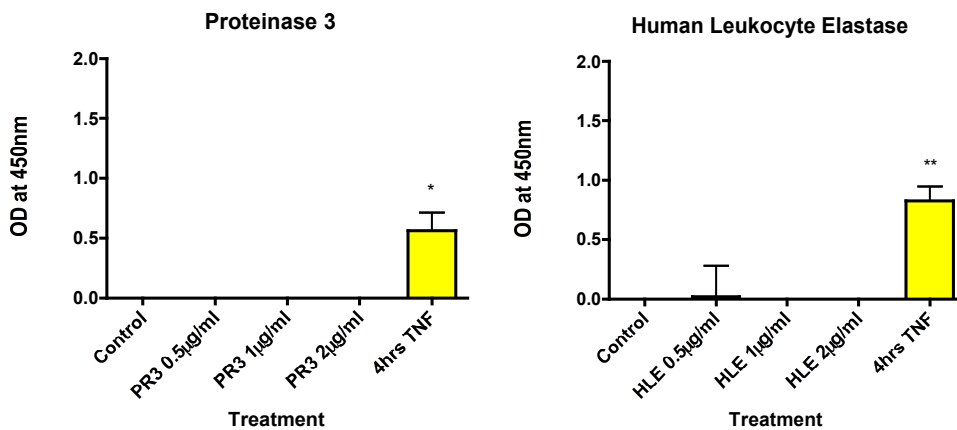
HUVEC were treated with increasing concentrations of TNF α for 4 hours (A), with 100 Units of TNF α over a timecourse of 0-6hours (B). Treated HUVEC were fixed in 2% PFA and assessed for membrane E-Selectin expression by ELISA. The data shown here is from 1 experiment.

Figure 90 - E-Selectin Expression on HUVEC following Serine Protease Treatment



HUVEC treated for 2 hours with increasing concentrations of PR3 and HLE, or 4 hours 100U TNF α as a positive control (yellow), were assessed for surface expression of E-Selectin by ELISA. The data shown here are the mean and standard error from 3 separate experiments minus the isotype control. Statistical significance was assessed by 1-way ANOVA with Bonferroni post-test (PR3 $p < 0.0001$, HLE $p = 0.0004$). *** $p < 0.001$

Figure 91 - E-Selectin Expression on GEnC following Serine Protease Treatment



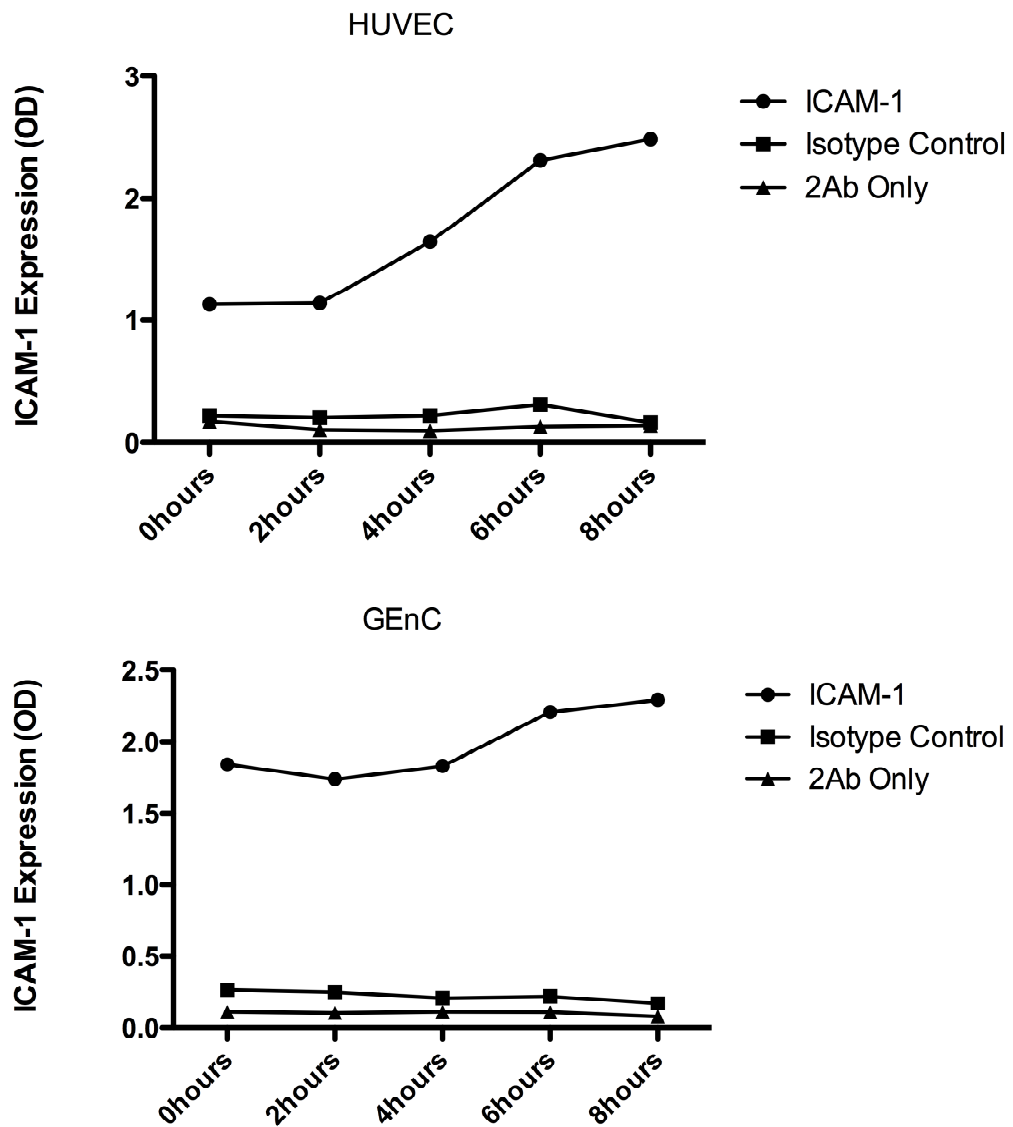
GEnC treated for 2 hours with increasing concentrations of PR3 and HLE, or 4 hours 100U TNF α as a positive control (yellow), were assessed for surface expression of E-Selectin by ELISA. The data shown here are the mean and standard error from 3 separate experiments minus the isotype control. Statistical significance was assessed by 1-way ANOVA with Bonferroni post test (PR3 $p = 0.0116$, HLE $p = 0.0057$). * $p < 0.05$, ** $p < 0.01$

3.24 Expression of Surface ICAM-1 following Serine Protease Treatment

Preliminary experiments were carried out to investigate the optimal time by which TNF α increased ICAM-1 expression on the surface of GEnC and HUVEC (figure 92). ICAM-1 is constitutively expressed on the surface of endothelial cells, and this is confirmed in these experiments. However, the expression of ICAM-1 on HUVEC was greatly increased over the untreated control in a time dependant manner with 100 units TNF α . Increased expression can first be observed at 4 hours, although this continues with maximal expression observed following 8 hours treatment. TNF α treated GEnC also displayed an increased expression of ICAM-1, although to a much lesser extent than seen on HUVEC. GEnC also appear to express a higher constitutive level of ICAM-1 than HUVEC. For future ICAM-1 expression experiments, an 8 hour treatment with 100 units TNF α was used as a positive control.

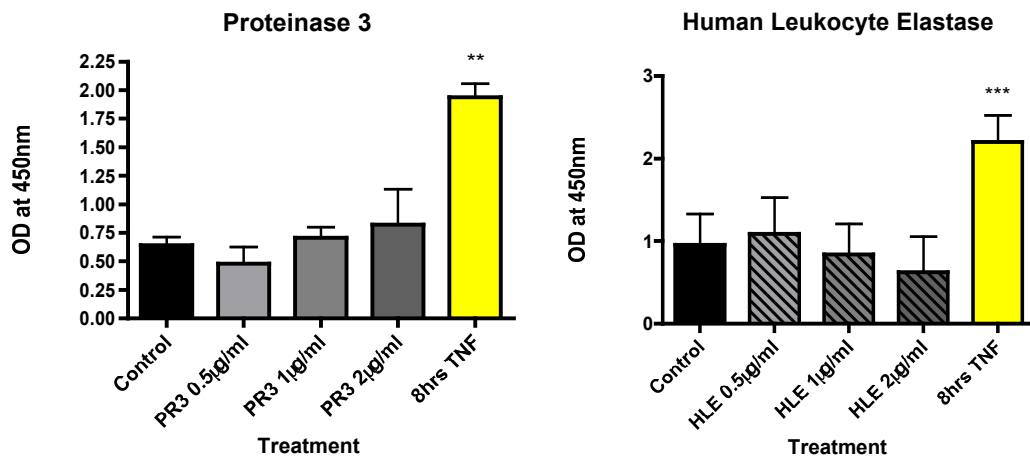
Next, HUVEC and GEnC were treated for 2 hours with increasing concentrations of PR3 and HLE (0.5 μ g/ml - 2 μ g/ml). Figures 93 and 94 show that following serine protease treatment, ICAM-1 expression was not significantly increased above constitutive expression on either HUVEC or GEnC, respectively. Again, endothelial cells treated with 100 units TNF α for 8 hours displayed significantly increased ICAM-1 expression.

Figure 92 - Optimisation of ICAM-1 ELISA



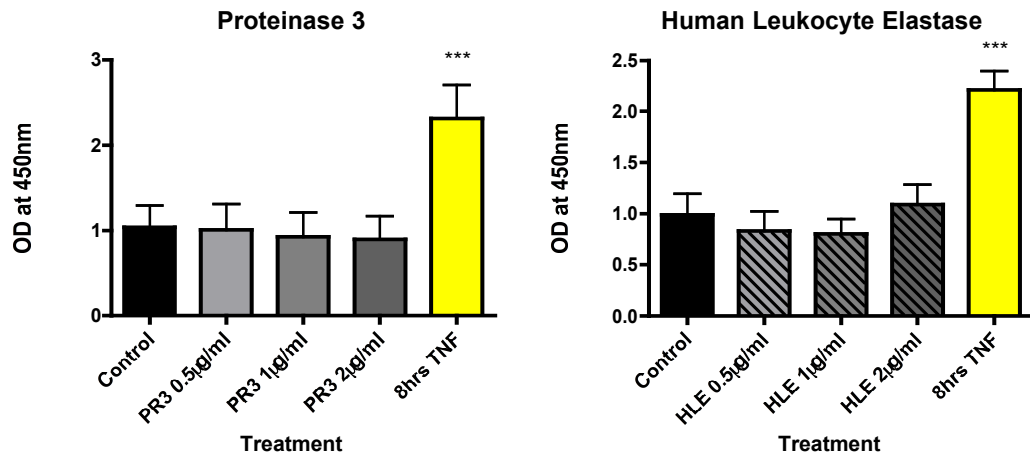
Confluent endothelial monolayers were treated for a timecourse with 100 units $\text{TNF}\alpha$. Treated endothelial cells were fixed in 2% PFA and assessed for ICAM-1 expression by ELISA. The data shown here is from 1 experiment.

Figure 93 - ICAM-1 Expression on HUVEC following Serine Protease Treatment



HUVEC treated for 2 hours with increasing concentrations of PR3 and HLE, or 8 hours 100U TNF α as a positive control (yellow), were assessed for surface expression of ICAM-1 by ELISA. The data shown here are the mean and standard error from 3 separate experiments minus the isotype control. Statistical significance was assessed by 1-way ANOVA with Bonferroni post test (PR3 $p=0.0011$, HLE $p<0.0001$). ** $p<0.01$, *** $p<0.001$

Figure 94 - ICAM-1 Expression on GEnC following Serine Protease Treatment



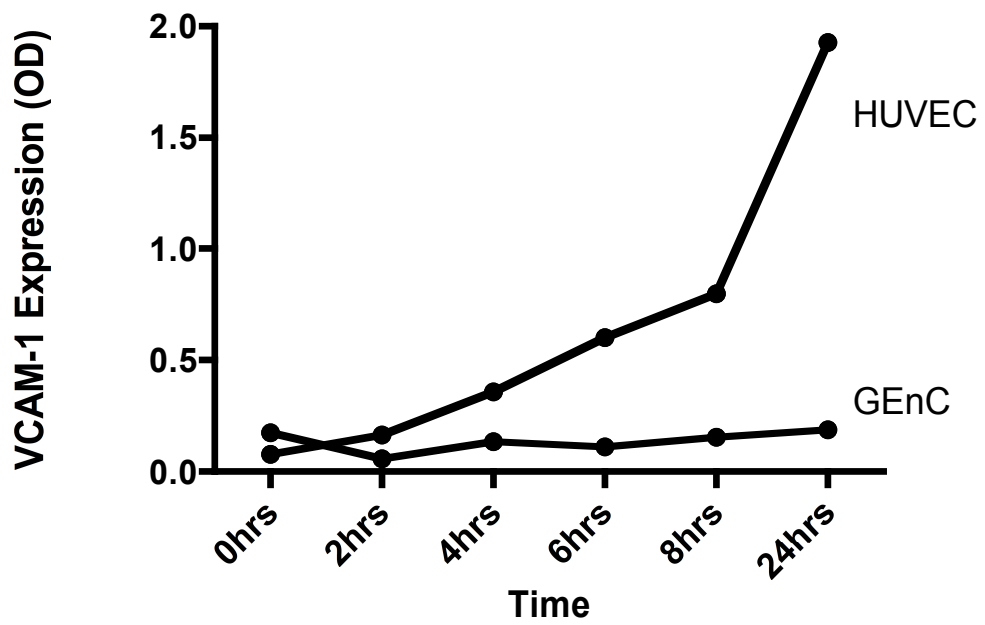
GEnC treated for 2 hours with increasing concentrations of PR3 and HLE, or 8 hours 100U TNF α as a positive control (yellow), were assessed for surface expression of ICAM-1 by ELISA. The data shown here are the mean and standard error from 3 separate experiments minus the isotype control. Statistical significance was assessed by 1-way ANOVA with Bonferroni post test (PR3 $p<0.0001$, HLE $p<0.0001$). *** $p<0.001$

3.25 Expression of VCAM-1 on Serine Protease treated Endothelial Cells

As with previous adhesion molecule ELISAs, preliminary experiments were performed to determine the optimal time point for increased VCAM-1 expression on 100 units TNF α treated endothelial cells. The expression of VCAM-1 on TNF α treated HUVEC increases steadily in a time dependant manner and was optimal following a 24 hour incubation. Interestingly, the expression of VCAM-1 on GEnC could not be stimulated with TNF α treatment, and remained at basal levels even after 24 hours treatment (figure 95). This observation has previously been reported in our laboratory by Tanya Pankhurst, who confirmed the absence of VCAM-1 in our GEnC line and also in primary GEnC (unpublished data).

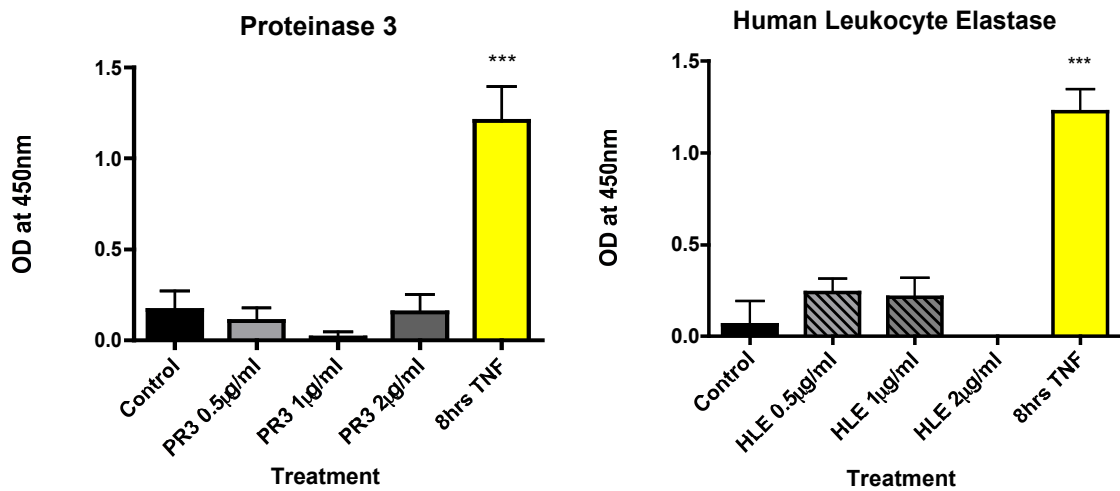
As expected, treatment with increasing concentrations of PR3 and HLE also had no effect on increasing VCAM-1 expression on GEnC (figure 97). The treatment of HUVEC, however, with 100 unit TNF α for 8 hours significantly increased the expression of surface VCAM-1, although no significantly increased expression could be observed following treatment with 0.5 μ g/ml - 2 μ g/ml of PR3 or HLE (figure 96).

Figure 95 - Optimisation of VCAM-1 ELISA



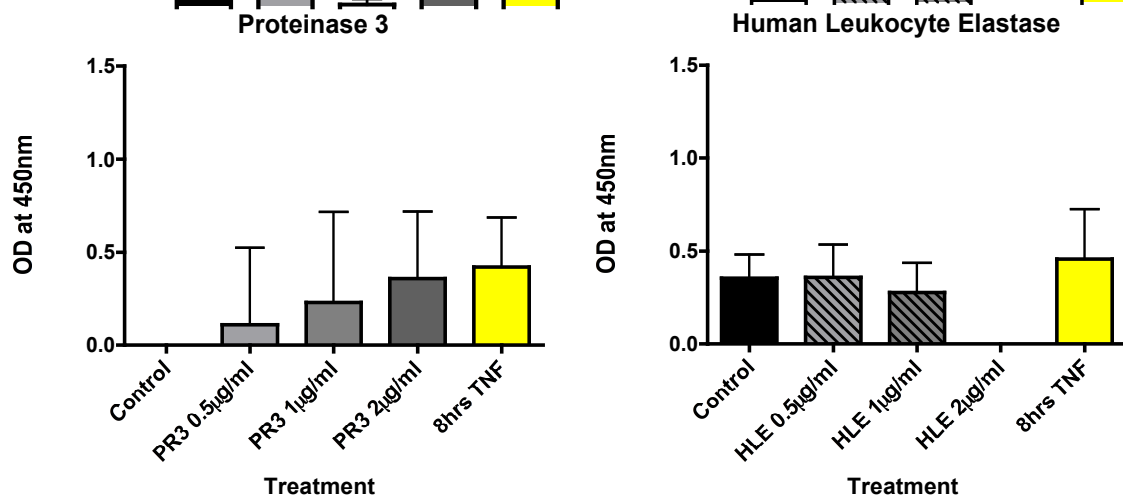
Endothelial cells were treated at 2 hour intervals in a timecourse with 100 units $TNF\alpha$ to determine optimal time points for VCAM-1 expression. A later time point of 24 hours was included due to absence of VCAM-1 expression on GEnC. Treated endothelial cells were fixed in 2% PFA and assessed for membrane VCAM-1 expression by ELISA. The data shown here is from 1 experiment.

Figure 96 - VCAM-1 Expression on HUVEC following Serine Protease Treatment



HUVEC treated for 2 hours with increasing concentrations of PR3 and HLE, or 8 hours 100U TNF α as a positive control (yellow), were assessed for surface expression of VCAM-1 by ELISA. The data shown here are the mean and standard error from 3 separate experiments minus the isotype control. Statistical significance was assessed by 1-way ANOVA with Bonferroni post test (PR3 $p < 0.0001$, HLE $p = 0.0002$). *** $p < 0.001$

Figure 97 - VCAM-1 Expression on GEnC following Serine Protease Treatment

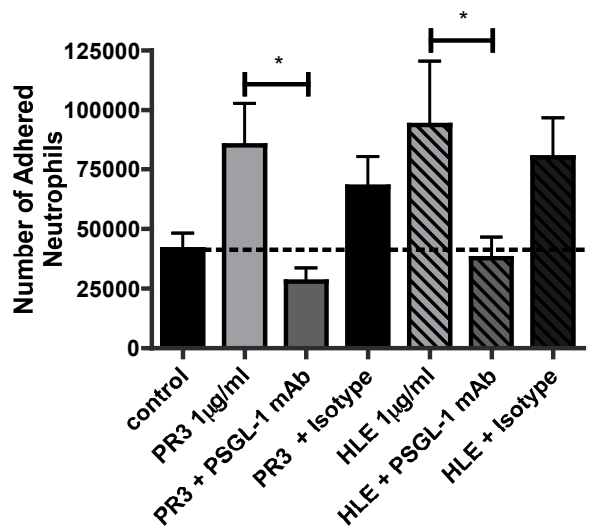


GEnC treated for 2 hours with increasing concentrations of PR3 and HLE, or 8 hours 100U TNF α (yellow), were assessed for surface expression of VCAM-1 by ELISA. The data shown here are the mean and standard error from 3 separate experiments minus the isotype control. Statistical significance was assessed by 1-way ANOVA with Bonferroni post test (PR3 $p = 0.6013$, HLE $p = 0.2480$).

3.26 Blocking PSGL-1 on Neutrophils Inhibits Adhesion

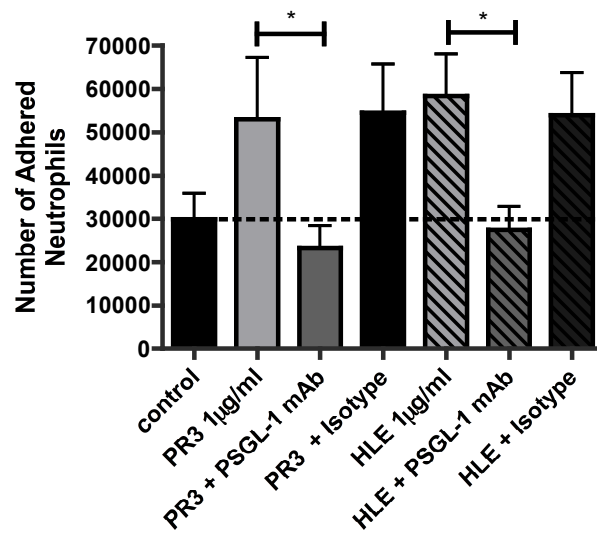
Previous data demonstrating an increased level of adhesion following serine protease treatment and an increased expression of adhesion molecule P-Selectin, posed the hypothesis that by blocking the P-Selectin ligand, PSGL-1, on the neutrophil we could potentially inhibit neutrophil adhesion to PR3 and HLE treated endothelial cells. Endothelial cells were routinely treated with 1 μ g/ml PR3 and HLE for 2 hours, and then further incubated with 250,000 neutrophils for a further hour. The neutrophils that were incubated with the serine protease treated endothelial cells were either untreated or else were incubated for 15 minutes with blocking antibodies directed at PSGL-1 or a relevant isotype control. Untreated endothelial cells were incubated with untreated neutrophils to indicate the basal level of neutrophil adhesion. Figures 98 and 99 demonstrate that the incubation of neutrophils with blocking antibodies directed at PSGL-1, we can significantly inhibit neutrophil adhesion to 1 μ g/ml PR3 and HLE treated HUVEC and GENC. The level of neutrophil adhesion following blocking PSGL-1 could be completely abolished to basal levels of adhesion achieved on unstimulated endothelial cells. Incubation of neutrophils with a non-specific isotype control was unable to inhibit neutrophil adhesion.

Figure 98 - Blocking PSGL-1 on Neutrophils Inhibits Adhesion to HUVEC



HUVEC were treated with either 1µg/ml PR3 or HLE for 2 hours, and then further incubated with 250,000 neutrophils in a static adhesion assay. Neutrophils were either untreated or incubated with blocking antibodies directed at PSGL-1, or the relevant isotype control for 15 minutes. The data shown here are the mean and standard error from 6 separate experiments. Samples were statistically tested for normality by D'Agostino & Pearson omnibus normality test with Wilcoxon signed rank test ($p=0.0312$). * $p<0.05$

Figure 99 - Blocking PSGL-1 on Neutrophils Inhibits Adhesion to GENC

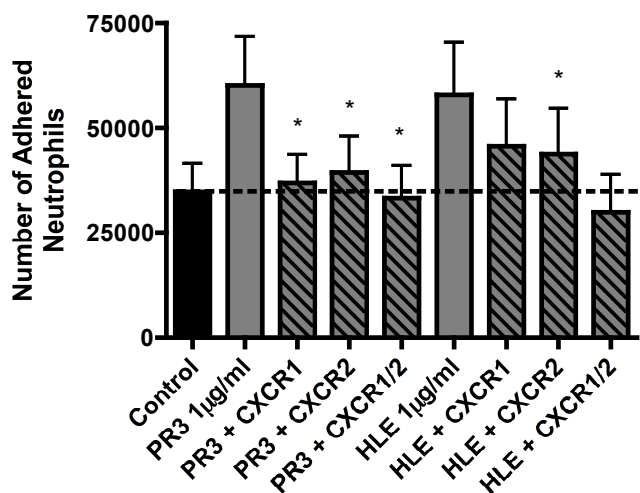


GENC were treated with either 1µg/ml PR3 or HLE for 2 hours, and then further incubated with 250,000 neutrophils in a static adhesion assay. Neutrophils were either untreated or incubated with blocking antibodies directed at PSGL-1, or the relevant isotype control for 15 minutes. The data shown here are the mean and standard error from 6 separate experiments. Samples were statistically tested for normality by D'Agostino & Pearson omnibus normality test with Wilcoxon signed rank test ($p=0.0312$). * $p<0.05$

3.27 Inhibition of CXCR1 and CXCR2 on Neutrophils Inhibits Adhesion

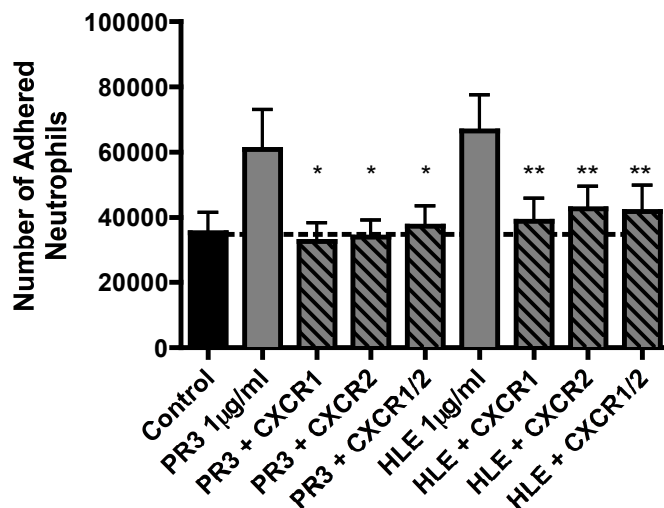
Previous data has suggested that blocking the CXCL8 receptors on neutrophils has the ability to inhibit ANCA induced neutrophil transmigration in a flow model of neutrophil adhesion [168]. We wanted to further investigate a role for interleukin-8 in our model of neutrophil adhesion. Previous experiments have demonstrated that the neutrophil serine proteases have the ability to cleave interleukin-8, potentially amplifying its inflammatory actions. Interestingly, blocking the CXCL8 receptors, CXCR1 and CXCR2, on neutrophils in a static model of adhesion significantly inhibits neutrophil adhesion to PR3 and HLE treated endothelial cells. Significant inhibition of neutrophil adhesion to both PR3 and HLE treated GEnC was achieved by both the CXCR1 and CXCR2 blocking antibodies (figure 101). There appeared to be no preferential action of one receptor over the other, with both abolishing adhesion to levels observed to untreated GEnC. Blocking CXCR1 and CXCR2 also significantly inhibited neutrophil adhesion to PR3 treated HUVEC, but had less of an effect on HLE treated cells. Moreover, only treatment of neutrophils with anti-CXCR2 had a significant effect on adhesion (figure 100). Interestingly, neutrophils incubated with blocking antibodies against both CXCR1 and CXCR2 did not have a significant effect on inhibiting adhesion to HLE treated HUVEC ($p=0.1200$).

Figure 100 - Blocking CXCR1 and CXCR2 on Neutrophils Inhibits Adhesion to HUVEC



HUVEC were treated with either 1µg/ml PR3 or HLE for 2 hours, and then further incubated with 250,000 neutrophils in a static adhesion assay. Neutrophils were either untreated or incubated with blocking antibodies directed at CXCR1 or CXCR2 for 15 minutes. The data shown here are the mean and standard error from 5 separate experiments. Samples were statistically tested for significance by paired T-Test. *p<0.05
* compared to serine protease treatment

Figure 101 - Blocking CXCR1 and CXCR2 on Neutrophils Inhibits Adhesion to GENC



GENC were treated with either 1µg/ml PR3 or HLE for 2 hours, and then further incubated with 250,000 neutrophils in a static adhesion assay. Neutrophils were either untreated or incubated with blocking antibodies directed at CXCR1 or CXCR2 for 15 minutes. The data shown here are the mean and standard error from 7 separate experiments. Samples were statistically tested for significance by paired T-Test. *p<0.05, **p<0.01
* compared to serine protease treatment

4. Discussion

4.1 Neutrophil Serine Proteases do not induce Endothelial Cell Injury following Short Incubations

It has previously been suggested that the neutrophil serine proteases may be responsible for the endothelial cell injury observed during ANCA-associated vasculitis, rather than the previously identified release of toxic oxygen radicals [309]. In this study, the level of endothelial injury following the release of serine proteases from ANCA activated neutrophils was demonstrated through the release of von Willebrand factor [309]. Indeed, HLE has been repeatedly linked to endothelial cell injury [376-378]. Furthermore, deposits of HLE have been identified in the glomerular endothelium in renal biopsies from patients with crescentic glomerulonephritis [379]. To further investigate this mechanism of endothelial injury, we incubated GEnC with two of these neutrophil serine proteases, PR3 and HLE, and monitored changes in endothelial injury. Here we have demonstrated that there is no significant difference in the level endothelial cell detachment or mitochondrial activity, following short durations of treatment of GEnC with physiological concentrations of PR3 and HLE. This observation was also noted when incubating the endothelial cells on a time course with 1µg/ml. Interestingly, the 2 hour treatment with a higher concentration (5µg/ml) of HLE did result in significant detachment from the endothelial monolayer *in vitro*, thereby confirming the ability of this neutrophil serine protease to cause vascular injury. The treatment of endothelial cells with HLE and more importantly, PR3, has been well documented to induce DNA fragmentation and apoptosis. It has been demonstrated that this PR3 induced apoptosis can occur following treatment with concentrations as low as 1µg/ml [106]. Using changes in the intracellular ATP and ADP ratios as markers of cellular apoptosis, we could observe no

significant changes in the ability of PR3 or HLE to induce apoptosis following short 2 hour treatments of glomerular endothelial cells with concentrations of up to 2 μ g/ml. Furthermore, recent data produced by Samantha Tull supports this observation, as the treatment of endothelial cells for 2 hours with 1 μ g/ml PR3 or HLE was not able to induce the expression of the active form of caspase 3 in western blots, whilst the enzymatic cleavage of P21^{waf1} at this time suggests that PR3 and HLE can prevent continuation of the cell cycle, and hence endothelial proliferation (unpublished data). The ability of PR3 to cleave P21^{waf1} has previously been identified, resulting in the loss of functional P21^{waf1} from the cytoplasm [138]. Interestingly, purified PR3 can cleave purified procaspase 3 following a 30 minute incubation in a cell-free model. Further to this, caspase 3 activity is increased in a PR3 transfected RBL mast cell line, whilst HLE transfection had no effect on caspase 3 expression [380]. The absence of caspase 3 in our PR3 treated endothelial cells may be due to the time taken for internalisation and translocation to the nuclei. It was therefore important to assess the injurious effects of PR3 at a later time point.

Investigation of a role for PR3 and HLE in endothelial cell injury at later time-points suggested that the neutrophil serine proteases are likely to have a later injurious effect. Using a 24 hour incubation, we demonstrated that PR3 and HLE induce a significant decrease in the level of intracellular ATP. This observation was more evident with HLE treatment, whilst only treatment with 2 μ g/ml PR3 demonstrated a significant change. Moreover, GEnC treated for 24 hours with PR3 and HLE displayed significantly decreased levels of intracellular ATP compared to cells treated for 2 hours. As a cell prepares to undergo apoptosis, it converts internal stores of ATP into ADP. The hugely increased rate of this conversion would be suggestive of a necrotic pathway of cell death, as seen following treatment of endothelial cells with 1x Triton X100 or water. Endothelial treatment with PR3 and HLE for 24 hours, resulted in increased ADP:ATP ratios, which together with a reduced

ATP concentration, suggests that at later time points PR3 and HLE have the ability to induce apoptosis. It is of note that the increased ADP was not comparable to the decrease in ATP, which suggests that there may be technical issues within this assay in which, not all intracellular ADP was converted to ATP for quantification. The technical limitations of this assay mean that the increased ADP:ATP ratio has to be taken with caution and supported by other evidence confirming apoptosis.

The 24 hour treated glomerular endothelial cells appear rounded and detached from the culture plates, with no confluent monolayer remaining. These observations may account for the increased number of circulating endothelial cells in the peripheral blood of ASV patients [381]. Furthermore, research in our laboratory has demonstrated the presence of active caspase 3 in endothelial cells treated for 24 hours with PR3 and HLE, although the absence of serum for a 24 hour duration also caused the upregulation of caspase 3 in untreated endothelial cells (Sahithi Panchagnula, unpublished data).

4.2 Release of vWf occurs due to Activation not Injury

Historically, vWf has been described as a marker for endothelial cell dysfunction, however this has many limitations. Whilst vWf release has been demonstrated to occur as a result of direct injury to the endothelial cell monolayer, itself playing key functions in coagulation and thrombus formation, vWf release has also been shown to occur following endothelial activation. In this situation, vWf is released from neighboring endothelial cells in response to activating stimuli, such as thrombin and histamine. Therefore, vWf cannot be used as a

marker of endothelial cell dysfunction in the absence of complimentary experiments that confirm the presence of cellular injury and death.

Previously Lu *et al.*, demonstrated the ability of ANCA-activated neutrophils to induce vWf release from endothelial cells in culture, and that this vWf release could be abolished by the addition of serine protease inhibitors [309]. This proposes a role for the neutrophil serine proteases in the induction of vWf release from endothelial cells. Our data supports this idea by demonstrating that endothelial incubation with PR3 and HLE for 2 hours results in significantly increased vWf in cell culture supernatants. However, the absence of any other markers of injury at this time implies that this release is occurring due to an activatory role of the serine proteases on the vascular endothelium. The treatment of GEnC with increasing concentrations of PR3 and HLE resulted in a dose-dependant increase in vWf release, with 2 μ g/ml of PR3 and HLE inducing significantly increased levels. Interestingly, HUVEC treatment with increasing concentrations did not display such a dose-dependant increase in vWf, rather an all or nothing response, with 0.5 μ g/ml causing a similar level of vWf release as treatment with 2 μ g/ml protease. In both cell types, HLE appeared to be the more potent stimuli, inducing increased levels of vWf release compared to PR3 treatment. The inhibition of the enzymatic activity of PR3 and HLE by the addition of the irreversible inhibitor α 1-antitrypsin, significantly abolished the release of vWf. α 1AT could also inhibit vWf release from endothelial cells treated with a higher concentration of PR3 and HLE (5 μ g/ml) and prevent endothelial detachment at this serine protease concentration.

Longer incubations (24 hours) of serine proteases with GEnC also caused increased release of vWf into cell culture supernatants, although vWf release from HUVEC treated with PR3 and HLE was not significantly increased compared to untreated control levels. As expected,

the level of detectable vWf after 24 hours was hugely increased compared to the levels present after 2 hours treatment. However, there appeared to be less of a distinction between endothelial cells that had received treatment with PR3 or HLE, and those cells that remained untreated. Moreover, vWf release appeared to decline with increasing concentrations of HLE. Given that we have previously demonstrated that at this 24 hour time point HLE and the higher concentrations of PR3 have the ability to induce endothelial apoptosis, it is likely that, as these cells undergo programmed cell death they stop producing and releasing vWf, hence the decreased levels in supernatants. It is therefore likely that these endothelial cells are undergoing apoptosis at an earlier time point, and at 24 hours they have been dead for some time.

It previously been described that patients with active Wegeners' granulomatosis or microscopic polyangiitis have an increased level of circulatory vWf [307, 308, 382]. The data discussed here suggests that this may be due to the early activation and consequent vWf release from serine protease stimulated endothelial cells. Although with longer exposures of endothelial cells to serine proteases vWf is further increased, here HLE also induces endothelial detachment and apoptosis, which limits the release of further vWf into cell culture supernatants, thereby displaying a decreasing level of vWf in supernatants of endothelial cells treated with increasing concentrations of HLE.

Apart from its haemostatic roles, vWf release has been implicated in the development of inflammation. vWf deficient mice display a decreased level of neutrophil recruitment in response to cytokine-induced meningitis, most likely because of a decreased ability to increase endothelial P-Selectin expression [383]. Furthermore, mice deficient for vWf and low-density lipoprotein receptor (LDLR) display a decreased level of monocytes recruitment to aortic fatty streaks than LDLR^{-/-}vWf^{+/+} mice [384]. This ability of vWf to increase

neutrophil and monocytes recruitment may be in part due its ability to bind selectin ligands (PSGL-1) [385] and integrins (VLA-4) [386]. Indeed, further investigation is required to outline the functional effects of this early vWf release.

4.3 Confocal Staining of vWf and the Endothelial Membrane produces Inconclusive Results

Confocal staining for vWf and a membrane marker confirmed that, with these early 2-hour serine protease treatments, there is indeed some co-localisation of vWf with the plasma membrane. Given that this method of microscopy captures vWf co-localisation at one window in time, it is impossible to decipher whether this is membrane bound vWf or else WPB budding with the plasma membrane. To get a more accurate account of vWf release from endothelial cells following PR3 and HLE treatment, one would need to capture the movement of WPBs over time. Furthermore, the staining of non-permeabilised cells would allow quantification of membrane bound vWf which could be subtracted from the amount of vWf in contact with the plasma membrane of permeabilised endothelial cells. A further complication of this method was the staining of intracellular compartment membranes with the wheat germ agglutinin stain. As mentioned previously, alternative stains for the plasma membrane should be investigated to overcome this undesired staining.

Furthermore, analysis of different depths of microscopy through the endothelial cell using the Z-stack feature, revealed the deposition of released vWf beneath the endothelial monolayer. The release of vWf through the endothelial basolateral membrane is a well-documented phenomenon. It has previously been demonstrated that unstimulated endothelial

cells constitutively release vWf through their basolateral membrane, whilst release through the apical membrane is increased following endothelial stimulation [375]. It is therefore likely that this build up of vWf release beneath the basolateral membrane of PR3 and HLE treated endothelial cells has accumulated during the culturing and growing of the cells prior to any treatment. The release of any vWf through the apical membrane cannot be detected through these methods, as it will have dispersed into cell culture supernatants.

4.4 PR3 and HLE cause exocytosis of Weibel-Palade Body Constituents

Whilst vWf comprises the main Weibel-Palade body constituent, these endothelial organelles are also known to contain P-Selectin, CXCL8, angiopoietin-2 and CD63. Following our observation that PR3 and HLE have the ability to cause release of vWf, it was important to investigate the effects of the neutrophil serine proteases on the release of other endothelial WPB constituents.

A role for CXCL8 in ANCA systemic vasculitis has previously been identified. Increased CXCL8 expression has been demonstrated in the crescentic glomeruli of ASV patients, whilst incubation of patient ANCA-IgG with healthy donor neutrophils increases CXCL8 release, and consequently, enhances neutrophil recruitment [387, 388]. Furthermore, chimeric IgG1 and IgG3 PR3-ANCA can increase CXCL8 release from healthy neutrophils, as well as inducing neutrophil degranulation and serine protease release [389]. During the investigation into the effects of PR3 and HLE on the release of CXCL8 from endothelial cells, early experiments indicated that these serine proteases could actively cleave CXCL8 thereby rendering it undetectable in our assays. Moreover, the decreased level of detectable

CXCL8 in cell culture supernatants occurred in a dose-dependant fashion with increasing concentrations of serine protease. This potential ability for PR3 and HLE to cleave CXCL8 has previously been demonstrated [113], in which it was proposed that this cleavage can act to amplify the functions of CXCL8, such as its chemotactic role in the recruitment of neutrophils to inflammatory sites. As with vWf release, HLE appeared to have a greater effect on the cleavage of CXCL8 than PR3, whilst the addition of α 1AT could significantly prevent this HLE mediated cleavage. To overcome this interference in the detection of CXCL8 caused by its cleavage by PR3 and HLE, we investigated the ability of serine protease treated endothelial cells to maintain the release of CXCL8 following the removal of PR3 and HLE from the system. Through this mechanism, we could demonstrate that GEnC treated with 2 μ g/ml PR3 and HLE, and further incubated with blank medium displayed increased CXCL8 in cell culture supernatants compared to cells that received no previous serine protease treatment. This allows us to conclude a role for PR3 and HLE in the induction of CXCL8 release from the endothelial monolayer. ANCA has been demonstrated to induce CXCL8 release from neutrophils, which is suggested to be increased in glomerular crescentic lesions [387]. Here we identify a second source of increased CXCL8 release that may contribute to intraglomerular expression. It is possible that ANCA induced neutrophil serine protease release can actively induce CXCL8 release from the glomerular endothelium, as well as the previously reported neutrophil release, which the serine proteases can then cleave to amplify the immune response and, potentially, disease propagation through the continued recruitment of neutrophils.

This same phenomenon of enzymatic cleavage was observed in angiopoietin-2 release from PR3 and HLE treated endothelial cells. Endothelial cells treated for 2 hours with physiological concentrations of PR3 or HLE displayed significantly decreased levels of angiopoietin-2 in cell culture supernatants compared to untreated endothelial cells.

Interestingly, PR3 had the greatest effect on cleavage of Ang-2. Again, the addition of α 1AT could significantly prevent the cleavage of Ang-2 by PR3 and HLE. It is of note that untreated glomerular endothelial cells constitutively release a much higher level of Ang-2 than HUVEC (1700pg/ml and 300pg/ml respectively), with PR3 and HLE having a greater role in cleavage of glomerular released Ang-2. This may be due to the required maintenance of the glomerular capillary structure. Ang-2 is expressed at sites of vascular remodelling, where it can act with VEGF to induce new vessel formation. The injection of VEGF into rats with glomerulonephritis has been demonstrated to have a beneficial role based on its angiogenic properties [390]. Alternatively, endothelial cells from the human umbilical vein require much less vascular remodelling, and hence Ang-2 release is lower.

Unlike CXCL8 release, the removal of PR3 and HLE from the system did not increase the detection of Ang-2 release from serine protease treated glomerular endothelial cells. It appears that the neutrophil serine proteases may not be inducing the release of Ang-2 from endothelial cells, and are further cleaving the angiopoietin-2 constitutively released. Alternatively, it is also possible that the removal of the enzyme and along with it the Ang-2 releasing stimulus, may mean that these cells cannot continue to release Ang-2 in the absence of PR3 and HLE, and not that these serine proteases have no effect on release. It is well-known that angiopoietin-2 is a natural antagonist for its sister ligand angiopoietin-1, thereby acting to promote vessel leakage, along with VEGF, by destabilization of the endothelial cell-cell junctions [286, 321]. Interestingly, 10 μ g/ml concentrations of HLE can partially degrade VEGF to produce a large VEGF fragment (VEGFf), which can potentiate the activity of VEGF through ERK1/2 signalling whilst itself able to signal through Akt activation in endothelial cells and monocytes [391]. Taken with the observation of increased circulating Ang-2 in ASV patients [324], I would suggest that the neutrophil serine proteases are unlikely to be inactivating Ang-2 but rather enhancing its actions on endothelial leakage

and cell detachment and hence, disease propagation. Indeed further research is required to investigate the effects of the neutrophil serine proteases on the activity and release of Ang-2, and its involvement in ANCA vasculitis.

It is proposed that there are different subclasses of Weibel-Palade bodies within endothelial cells, and in particular, Ang-2 and P-Selectin are never co-expressed in the same ones [286]. The absence of release of Ang-2 from endothelial cells in the presence of vWf and CXCL8 suggests that it may be a P-Selectin containing WPB that the serine proteases are selectively releasing. Indeed, the treatment of both GEnC and HUVEC resulted in a dose-dependant increase in membrane P-Selectin expression, thereby confirming the release of this subset of WPB. Again, the addition of α 1AT into this system significantly inhibited the effects of PR3 and HLE on P-Selectin expression.

4.5 vWf is Cleaved and Released

As previously discussed, the treatment of endothelial cells with PR3 and HLE resulted in an increased level of vWf into cell culture supernatants. We further demonstrated that treatment with 2 μ g/ml resulted in the release of between 40-50% of the total cell vWf. Interestingly, analysis of endothelial surface expression of vWf by ELISA identified a role for the neutrophil serine proteases in reducing the membrane bound vWf. The treatment of GEnC and HUVEC with increasing concentrations of PR3 and HLE resulted in a dose-dependant decrease in surface vWf expression. As with vWf release, HLE treatment had the greatest effect on surface expression causing around a 30% decrease in membrane bound vWf. As with all previous experiments the presence of α 1AT could significantly inhibit the effects of

PR3 and HLE. The ability of the serine proteases to cleave membrane bound vWf has recently been demonstrated by another group. Here they suggested that PR3 and HLE cleave multimeric membrane vWf between the V¹⁶⁰⁷-T¹⁶⁰⁸ peptide bond. Interestingly, cathepsin G, another neutrophil serine protease, has a separate point of cleavage from PR3 and HLE Y¹⁶⁰⁵-M¹⁶⁰⁶ [392].

To confirm that this loss of surface vWf expression was caused by enzymatic cleavage rather than re-internalisation of the protein, endothelial cells were permeabilised to allow detection of both internal and external vWf, and total levels compared to levels of membrane vWf only, following 2 hour treatment with 1µg/ml PR3 and HLE (figure 39). Glomerular endothelial cells treated with PR3 and HLE displayed a significantly decreased level of membrane bound and total (membrane and internal) vWf. More importantly, the reduction of total vWf following serine protease treatment was greater than the loss from the endothelial membrane. This observation confirms the previously proposed hypothesis that, along with cleavage of surface bound vWf, the neutrophil serine proteases can induce the release of further vWf from internal stores. The active cleavage of membrane bound vWf will also contribute to the increased circulating vWf in ASV patients [307, 308].

This data was not reproduced in HUVEC due to problems in their availability, however, given that HUVEC show the greatest increase in vWF release into supernatants and decrease in surface expression, we hypothesis that HUVEC data would have been similar to that observed in GEnC but more marked.

4.6 vWf protein and mRNA is Increased by Serine Proteases

Further to the effects of the neutrophil serine proteases on vWf release and cleavage, analysis of endothelial lysates after a 2 hour treatment with PR3 and HLE identified a possible role for the serine proteases in increasing early *de novo* synthesis of vWf. Lysates from GEnC and HUVEC displayed increased levels of internal vWf occurring in a dose-dependant fashion with increasing concentrations of PR3 and HLE, although this increase was only significant following treatment with 2 μ g/ml of enzyme. Furthermore, both endothelial cell types displayed an increased total level of vWf (the sum of the released and lysate concentration) compared to untreated cells. Following assessment of mRNA levels in glomerular endothelial lysates, it became apparent that PR3 and HLE could increase the relative expression of vWf mRNA. Endothelial cells have previously been shown to internalise PR3, which is rapidly distributed through the endothelial cytoplasm [136]. This ability to internalise PR3, and therefore potentially HLE, may account for the inability of α 1AT to inhibit the increased production of vWf mRNA, as once internalised, α 1AT is unable to inhibit their enzymatic activity. Endothelial cells have also been demonstrated to internalise MPO, which is suggested to increase the production of oxygen radicals associated with tissue injury [136, 393].

Knowing the ability of the serine proteases to cleave a host of cytokines and proteins, it was important to assess whether PR3 or HLE were having any effect on the detectable level of vWf. The incubation of 2 μ g/ml HLE with recombinant vWf in a cell-free system increased the level of detection by around 30%. As new vWf could not have been generated in such a system, it became apparent that HLE is having an effect on the structure of the vWf protein, potentially unfolding it to expose further antibody binding sites. This HLE modification of antibody binding, however, does not account for the entirety of the increased intracellular

vWf, as this increased by much more than 30%. Additionally, PR3 did not cause an increase in antibody binding, and detection remained the same as with untreated recombinant vWf. The inability of PR3 to cause protein modifications that increase antibody binding, and the unaccounted protein following HLE treatment, begs the questions of increased *de novo* synthesis of the vWf protein. It is of note that the ability of HLE and inability of PR3 to increase antibody binding, suggests that there may be less of a difference between the capability of these enzymes to induce vWf release as previously suggested from the ELISA measurements on supernatant levels of vWf (see figure 17).

The production of the multimeric form of vWf released from endothelial cells is very closely related to the formation of mature Weibel-Palade bodies. Moreover, the absence of WPB biogenesis can be restored by the expression of vWf [282]. Early PrePro-vWf, derived from the trans-golgi network, undergoes modification by the formation of disulfide bonds during its translocation to the endoplasmic reticulum. From here the protein undergoes further modifications and disulfide bond formation in the golgi-apparatus, after which, the resulting vWf multimers can 'bud off' the golgi in what we know as the Weibel-Palade bodies [279, 280]. Due to our early incubation point, it is likely that, should we be observing increased protein synthesis, we are detecting an early PrePro- or Pro-vWf rather than the complete multimeric vWf protein. It is likely that the complete lysis of our endothelial cells is releasing this early vWf protein from the trans-golgi network and thereby increasing our level of intracellular vWf detection. Comparatively, with E-Selectin *de novo* synthesis, an incubation of 4 hours is required to see significantly unregulated membrane expression, whilst increased mRNA can be first seen after a 1 hour stimulation [394].

4.7 vWf Expression in Renal Biopsies

After highlighting an activatory role for the neutrophil serine proteases in increasing circulating levels of vWf. We wanted to investigate changes in the distribution of renal vWf associated with ANCA systemic vasculitis. Using biopsies taken from patients with active ASV, changes in the staining pattern for vWf was compared to non-transplanted 'healthy' kidney. Acute tubular necrosis and anti-glomerular membrane disease were used as disease controls. The renal distribution of vWf in ASV appeared normal in unaffected glomeruli, with evenly dispersed vWf staining throughout the glomerular capillary structure, however, upon development of crescentic glomerulonephritis, vWf became localised to the areas surrounding the crescent formation. The glomerular crescents develop as huge infiltrates of immune cells and mediators enter the bowman's space and surround glomeruli. This causes compression of the glomeruli due to the limited space available. These early reversible cellular crescents are later replaced by fibrin and collagen deposits, during the development of irreversible glomerular fibrosis and scarring [395]. It is suggested that infiltrating macrophages are primarily responsible for the induction of glomerular fibrosis [213]. Interestingly, activation of the coagulation cascade appears to be important in the development of fibrous crescents, with macrophages themselves involved in the increased fibrin deposition [395].

The vWf staining within these crescentic glomeruli supports a role for the coagulation cascade as increased vWf was observed within the surrounding crescents. Intraglomerular vWf staining within crescentic glomeruli appears reduced, perhaps due to the glomerular compression caused by substantial cellular infiltration. A further explanation for the decreased intraglomerular vWf expression may be due to a loss of endothelial cells. It is also possible that there could be endothelial cells within the crescents as a result of angiogenesis

to maintain the required recruitment of inflammatory cells, although such an occurrence has not been reported. Furthermore, the vWf staining in the peritubular capillaries appears unchanged in ASV. Comparatively, anti-GBM disease biopsies, a type I rapidly progressive glomerulonephritis (RPGN), did not display this crescentic formation in the biopsies used in this study, rather, the affected glomeruli appeared collapsed and were not positive for vWf. This observation may be due to the severity of disease at the point that the biopsies were collected, as the literature suggests that crescent formation is prominent in anti-GBM disease [395]. Furthermore, glomerular vWf staining in acute tubular necrosis appeared normal. To further assess the cell specific expression of vWf in renal biopsies, one could utilise a fluorescence staining method to dual stain sections for vWf and endothelial cell markers such as CD31.

The severity of the crescentic development in ANCA-associated glomerulonephritis is proposed to be a good indicator of the renal outcome for the patient; in particular the percentage of fibrous crescents decreases the long-term renal outcome [396]. Until recently there has been no classification system for defining the severity of disease based on renal biopsies. Berden *et al.*, has proposed a four-point classification system for the severity of vasculitic disease in renal biopsies, namely focal, crescentic, mixed and sclerotic, based on the level of glomerular cellular infiltrate and fibrosis [396].

4.8 PR3 and HLE Signal through a Unique Pathway to induce vWf Release

We hypothesized a role for the protease-activated receptors in mediating the effects of the

serine proteases in endothelial cells, in particular the exocytosis of Weibel-Palade bodies. Endothelial surface expression of P-Selectin can be induced by stimulation with PAR-1 agonist peptide, TRAP-6 (SFLLRN) [397]. Similarly, Lindner *et al.*, showed that mice deficient for endothelial PAR-2 displayed a delayed onset of leukocyte recruitment, possibly due to a delayed upregulation of P-Selectin [366]. It has also been demonstrated that the knockdown of PAR-1 and PAR-2 results in a reduced rate of neutrophil transmigration [398]. Furthermore, PAR-2 agonists have been used to induce release of vWf [287]. Taken with the observation of an interaction between PAR-2 and PR3 [367], we investigated a role for the PAR-1 and PAR-2 receptors in PR3 and HLE mediated endothelial vWf release. As previously described by Cleator *et al.*, agonist peptides directed at PAR-1 and PAR-2 could induce the release of vWf from HUVEC, and to less of an extent, GEnC [287]. However, in endothelial cells treated with siRNA targeting PAR-1, PAR-2 or both, the serine protease induced release of vWf could not be inhibited. The observation that PR3 and HLE do not require signalling through the protease activated receptors for Weibel-Palade body exocytosis invited further investigation into the signalling pathways that may be involved.

Investigation into the mechanism of communication and initiation of endothelial signalling pathways has highlighted other groups of receptors of particular interest. Firstly, a role for the toll-like receptors in vWf release has been outlined, as mice deficient for TLR-2 and TLR-4 are unable to release vWf in response to uric acid [281]. More recently, the formation of PR3-kinin, by incubation of PR3 with high molecular weight kininogen, has been shown to interact with the B₂ receptors on endothelial cells [370]. Further to this, the endothelial expression of the B₁ receptors has been shown to be upregulated in glomeruli and renal interstitium of ANCA-vasculitis patients, whilst blocking these receptors reduces renal

macrophage recruitment and chemokine production [399]. Although, there is currently little evidence to support a role for the receptors discussed here in ASV, further investigation of these pathways may highlight potential therapeutic targets.

A recent review article by Goligorsky *et al.* highlighted the known signalling pathways for ligand induced vWf release (see figure 5 [281]). Moreover, thrombin and PAR-1 are suggested to signal through increased intracellular calcium and calmodulin activation, whilst VEGF utilizes PKA and PKC signalling [371, 372, 400]. Using these proposed signalling pathways we investigated whether inhibition of key signalling components would decrease PR3 and HLE mediated vWf release. In particular, the use of pharmacological inhibitors directed at PKC, PKA, calmodulin or PI3K had no effect on inhibiting vWf release from serine protease treated glomerular cells. Furthermore, these inhibitors could not reduce HLE mediated vWf release from HUVEC.

The use of pharmacological inhibitors within experiments is often viewed with caution, as we have previously discovered when PAR antagonists were unable to inhibit PAR agonist induced vWf release. A more accurate method for investigating cell signalling pathways would be to use siRNA to knockdown the key signalling molecules, either individually or combined, to more accurately investigate their roles in PR3 and HLE mediated vWf release.

The release of vWf from thrombin and histamine stimulated endothelial cells requires the reorganization of the actin cytoskeleton structure and the formation of stress fibers. Moreover, the preincubation of HUVEC with cytochalasin B and cytochalasin E, an inhibitor of actin polymerization, potentiated the release of vWf in response to thrombin [401]. The disruption of the actin cytoskeleton by cytochalasin D is also reported to increase vWf

release in response to PAR-1 and PAR-2 [361]. Here we further investigated a role for the actin cytoskeleton in the release of vWf from PR3 and HLE treated endothelial cell. Preliminary experiments aimed to investigate the potential ability of cytochalasin B to further release vWf from HLE treated endothelial cells. Interestingly, treatment of HUVEC with increasing concentrations cytochalasin B (0.1 - 100 μ M) resulted in a reduction of vWf release, with 100 μ M reducing vWf release by almost 50%. Moreover, cytochalasin B treated endothelial cells displayed a hugely decreased mitochondrial activity, became rounded and detached and no longer displayed a confluent monolayer. Clearly, maintenance of the actin cytoskeleton is essential for endothelial viability, whilst it is likely that the decreased release of vWf is not due to the requirement of actin disruption for WPB exocytosis, but more to endothelial apoptosis. To overcome this toxic effect of cytochalasin B on endothelial monolayers, we treated endothelial cells with PR3 and HLE and stained for F-actin using a RPE labeled phalloidin toxin. Interestingly, PR3 and HLE did not appear to change the actin cytoskeleton, nor did they appear to localize to the cytoskeleton to facilitate WPB exocytosis.

Phosphatase 2B (PP2B) is a serine/threonine phosphatase linked to the calcium dependant intracellular signalling. Incubation of endothelial cells with the phosphatase 2B inhibitor, okadaic acid, is reported to induce vWf release [402, 403]. Furthermore, treatment with other PP2B inhibitors cyclosporine A and FK506 also increased vWf release from HUVEC [402]. In preliminary experiments, we investigated the ability of okadaic acid to induce vWf release from HUVEC and GEnC without a second stimulus. Interestingly, whilst treatment with concentrations of 100nm and 500nm of okadaic acid increased vWf from GEnC, okadaic acid appeared to have an inhibitory effect on release from HUVEC. Moreover, whilst okadaic

acid had no additive effects on PR3 and HLE mediated vWf release from GEnC, treatment appeared to completely inhibit vWf release from HUVEC in response to PR3 and HLE treatment. The differing effects of okadaic acid on GEnC and HUVEC was an interesting observation. Whilst phosphatase 2B appears to have no role in PR3 and HLE signalling in GEnC, inhibition in HUVEC completely abrogates serine protease stimulated vWf release, potentially highlighting a role for PP2B in PR3 and HLE signalling. Further investigation demonstrated that okadaic acid caused decreased mitochondrial activity following treated with concentrations of 100nM. This effect appeared more potent on HUVEC, with mitochondrial activity reduced to only 50%. However, treatment with 100nM okadaic acid did not appear to cause endothelial detachment. Moreover, recent reports have confirmed the ability of okadaic acid induce cellular apoptosis [404, 405].

To further investigate a role for PR3 and HLE in endothelial cell signalling, serine protease treated endothelial cells were assessed for changes in their pattern of peptide phosphorylation. Interestingly, HLE treatment appeared to have a potent effect on endothelial cell phosphorylation. HLE treated GEnC displayed the loss of phosphorylated tyrosine and serine/threonine peptides, as well as the presence of newly phosphorylated tyrosine peptides with molecular masses of between 31 and 52kDa. PR3 treatment did not produce the same pattern of phosphorylation and remained much unchanged from unstimulated endothelial cells, although a missing serine/threonine phosphopeptide with a molecule weight of around 225kDa can be seen. It is possible, however, that PR3 may be inducing minor changes in protein phosphorylation, which is being masked by more abundant unaffected peptides. A role for PR3 and HLE in altering endothelial cell signal transduction has been outlined in the induction of apoptosis. Preston *et al.*, identified that PR3 and HLE

altered endothelial expression of members of the JNK and ERK signalling pathways. In particular, PR3 appeared to increase the expression of phosphorylated JNK-2, whilst HLE treatment decreased phospho-JNK-1 expression. Moreover, both serine proteases actively downregulate ERK-1 and -2 phosphorylation [137]. More recently, another neutrophil serine protease, cathepsin G, has been demonstrated to increase ERK-1/-2, p38 mitogen activated protein kinase (MAP-kinase) and Akt phosphorylation [406]. We are actively investigating the precise signalling targets of PR3 and HLE by mass spectrometry of phosphorylated peptides, following which it will be interesting to further assess the changes in phosphorylation of JNK and ERK, as well as other members of MAP-kinase pathway. It is of interest that PR3 and HLE do not appear to require signalling through PKC, PKA, calmodulin or PI3k, to mediate the exocytosis of vWf. We hope that identification of a novel signalling components targeted by the neutrophil serine proteases may highlight potential therapeutic targets.

Using a novel mass spectrometry method to assess changes in peptide phosphorylation will allow us to globally assess signalling pathways that are utilised by PR3 and HLE. Mass spectrometry will allow identification of proteins with known molecular masses. It will allow us to assess changes in phosphorylation that may be occurring in less abundant proteins that are currently masked by more abundant proteins when assessed by western blotting. The identification of these signalling pathways will not be specific to WPB, in particular vWf, release, however, we can take these observations and use inhibitors or siRNA *in vitro* to assess their actions in WPB exocytosis.

4.9 The Serine Proteases Increase Neutrophil Adhesion through Interactions between P-Selectin and PSGL-1

Two independent animal models of MPO-vasculitis have reported an increased level of leukocyte transmigration *in vivo* [165, 166]. Here we investigated the hypothesis by which this increased neutrophil adhesion may be the result of serine protease release from ANCA-activated neutrophils. The incubation of endothelial cells with 1 μ g/ml PR3 or HLE resulted in significantly increased neutrophil adhesion in a static *in vitro* model. The level of adhesion to serine protease treated HUVEC was not significantly different from those levels observed following treatment with 100 units TNF α (PR3 p=0.3121, HLE p=0.8446), a well-known stimulus for neutrophil activation. Furthermore, this increased neutrophil adhesion to serine protease treated endothelial cells appeared to be occurring in the absence of the upregulation of the classical endothelial adhesion molecules; namely, E-Selectin, ICAM-1 and VCAM-1.

The expression of E-Selectin on PR3 and HLE treated endothelial cells could not be increased at 2 hours with concentrations of protease up to 2 μ g/ml, whilst a 4 hour incubation with TNF α significantly increased surface expression. Similarly, ICAM-1 could not be upregulated with PR3 or HLE treatment, and was again significantly increased following 8 hour TNF α treatment on both cell types. Interestingly, whilst PR3 and HLE could not increase VCAM-1 expression of either cell type, treatment with TNF α for up to 24 hours also resulted in no expression on GEnC. Furthermore, Tanya Pankhurst demonstrated no VCAM-1 expression on primary endothelial cells (unpublished data). This absence of glomerular VCAM-1 may act as a safety mechanism to prevent inappropriate recruitment of T-cells and monocytes into the glomeruli. VCAM-1 expression is increased on renal tubules

and glomeruli in biopsies from patients with ANCA associated glomerulonephritis, whilst histological staining also demonstrates the presence of T-cells and macrophages in and around the glomeruli [184, 407]. The expression of VCAM-1 and ICAM-1 within the cellular crescents is also increased, whilst epithelial cells within fibrous crescents can maintain VCAM-1 expression [408]. Furthermore, treatment of nephrotoxic nephritic rats with blocking antibodies directed at VCAM-1 ligand VLA-4 significantly improved renal function [409]. The inability of TNF α or the neutrophil serine proteases to upregulate glomerular VCAM-1 expression suggests that VCAM-1 expression in ASV patients is the result of an unidentified stimulation. Alternatively, the glomerular epithelial cells may account for the increased expression of VCAM-1 in ASV, rather than the endothelial cells.

The increased surface expression of these 'classical' endothelial adhesion molecules that occurs during inflammation first requires *de novo* synthesis of these proteins before translocation to the membrane can occur. As previously mentioned, E-Selectin expression is not increased until 4 hours post stimulation, with increased protein synthesis becoming apparent after 1 hour [394]. It is therefore, not surprising that we observe no upregulation of these adhesion molecules following a short 2 hour incubation.

Unlike E-Selectin, P-Selectin, one of the key adhesion molecules involved in neutrophil rolling, is stored as a preformed molecule in endothelial Weibel-Palade bodies and can therefore be rapidly upregulated to the endothelial membrane upon stimulation. Treatment of GEnC or HUVEC with 1 unit of thrombin for 15 minutes significantly increased P-Selectin membrane expression, thereby reemphasizing the rapid ability of endothelial cells to increase expression upon stimulation. It was also observed that 2 hour treatment of endothelial cells

with increasing concentrations of PR3 and HLE could significantly increase surface P-Selectin expression in a dose-dependant manner, when measured by ELISA. We initially wanted to confirm this expression by flow cytometry, however, the removal of the enzyme following by 10 minutes of washing and spinning before fixation was sufficient for re-internalisation of the adhesion molecule (data not shown). It has previously been demonstrated that the half-time for the re-internalisation of membrane expressed P-Selectin and translocation to the trans-golgi network is only 20-25 minutes [330]. This data suggests that PR3 and HLE do not have prolonged effects on P-Selectin expression, as the removal of the serine proteases following endothelial treatment is sufficient to induce re-internalisation. Interestingly, this may suggest that the prolonged release of CXCL8 caused by PR3 and HLE, even after their removal, is not due to the release of Weibel-Palade bodies. Although this does not rule out their release completely, as it has been demonstrated that there is differential methods of release for the different sub-classes of WPB [287]. Furthermore, the localization of CXCL8 within the endothelial cells is a highly controversial topic, although there is evidence for a co-localisation with vWf [283, 284]. CXCL8 is suggested to be increased in the endothelial WPBs following the initiation of inflammation [283], and release may therefore be occurring from other sources within the endothelial cell.

One of the key ligands for P-Selectin during neutrophil rolling is PSGL-1. PSGL-1 is expressed on the surface of leukocytes and has been demonstrated to bind the endothelial selectins via its sialyl lewis^x domain. Although the primary ligand for P-Selectin, PSGL-1 is suggested to also weakly interact with E-Selectin and L-Selectin [175]. In the absence of E-Selectin expression on our serine protease treated endothelial cells, we aimed to further investigate the role of P-Selectin in increased neutrophil adhesion by blocking the PSGL-1

ligand on neutrophils, since antibodies that reliably block P-Selectin adhesion functions are lacking. The use of monoclonal blocking antibodies directed at PSGL-1 significantly inhibited the level of neutrophil adhesion to PR3 and HLE treated endothelial cells. Furthermore, this reduced level of neutrophil adhesion was similar to the number of neutrophils adhered to untreated endothelial cells. It is apparent, therefore, that the serine protease mediated upregulation of P-Selectin may be interacting with neutrophil PSGL-1 to increase adhesion. In the complex system of leukocyte transmigration, P-Selectin is involved in the initial sequestration of flowing neutrophils by forming weak bonds between the endothelium and PSGL-1. The repeated formation of these weak bonds, termed 'rolling', is not sufficient to support the required firm adhesion for transmigration. Alternatively, in our static model of neutrophil adhesion this increased expression of P-Selectin and its interactions with PSGL-1 may be able to support adhesion due to the constitutive expression of ICAM-1. Although ICAM-1 is not increased on serine protease treated endothelial cells, it is possible that the activation of constitutively expressed ICAM-1 may be sufficient for firm adhesion. Indeed, neutrophil derived HLE can cleave endothelial ICAM-1 after a 2 hour incubation [410, 411], whilst a role for HLE and cathepsin G in VCAM-1 cleavage has also been described [412]. Moreover, HLE^{-/-} neutrophils demonstrate decreased ability to transmigrate compared to wild-type neutrophils [410]. Interestingly, vWf may be involved in this increased PSGL-1 mediated neutrophil adhesion, firstly due to the requirement of vWf for increasing P-Selectin membrane expression [383] and secondly as a ligand for PSGL-1 in its own right [385]. Furthermore, vWf can induce firm neutrophil adhesion via interactions with the β_2 integrins [385], and therefore could support neutrophil adhesion in the absence of increased ICAM-1 expression.

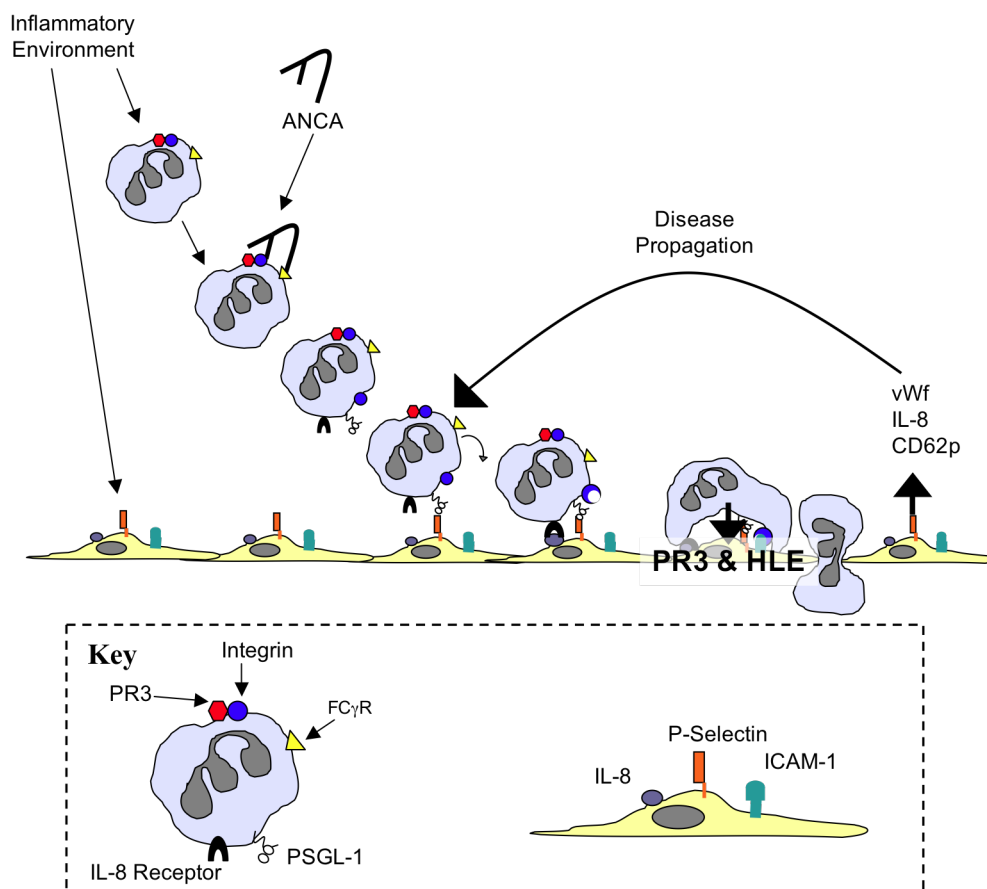
4.10 A Role for CXCL8 in Neutrophil Adhesion

CXCL8 is also proposed to be involved in neutrophil adhesion during inflammation. CXCL8 is a potent neutrophil chemotactic agent that has been demonstrated to increase the binding activity of β_2 integrins Mac-1 and LFA-1 to induce integrin mediated firm adhesion of neutrophils [191]. Furthermore, perfusion of CXCL8 over neutrophils rolling on P-Selectin can induce arrest and firm adhesion through ICAM-1/ β_2 integrin interactions [190]. Here we have demonstrated that the neutrophil serine proteases can increase release of CXCL8 from endothelial cells, after which CXCL8 is cleaved by PR3 and HLE in supernatants. The amplification of CXCL8 activity induced by this serine protease cleavage previously proposed by Padrines *et al.* [113] may account for the induction of firm adhesion of P-Selectin bound neutrophils through interactions between constitutively expressed endothelial ICAM-1 and its integrin ligands on neutrophils. Furthermore, CXCL8 could exert its effector functions before it is cleaved by PR3 and HLE.

To further evaluate this possibility, blocking antibodies directed at the CXCL8 receptors, CXCR1 and CXCR2, on neutrophils were used in our static model of adhesion. Neutrophils incubated with anti-CXCR1, anti-CXCR2 or both displayed a significantly reduced level of neutrophil adhesion to PR3 or HLE treated endothelial cells. The inhibition of this CXCL8 mediated firm adhesion decreased the number of adherent neutrophils to serine protease GEnC to levels observed in untreated endothelial cells. This observation confirms a role for CXCL8 in inducing a conformational change within the neutrophil to increase its binding activity, possibly through Mac-1 or LFA-1 interactions with endothelial ICAM-1. P-Selectin mediated weak interactions are insufficient to maintain increased neutrophil adhesion after

washing in the absence of firm neutrophil adhesion induced through CXCL8 activity. Furthermore, the inhibition of adhesion by blocking PSGL-1 demonstrates that CXCL8 alone cannot induce adhesion without an early capture phase by P-Selectin binding. Figure 102 highlights how signalling through the PSGL-1 and CXCR1/2 receptors may support disease propagation in ANCA-associated vasculitis.

Figure 102 - Serine Proteases cause Disease Propagation by Supporting Inflammatory Processes



An enhanced inflammatory environment causes the upregulation of PR3 on the surface of neutrophils, and the increased expression of endothelial adhesion molecules. ANCA can bind to its antigen on the surface of the neutrophil, inducing neutrophil activation and adhesion to the vascular endothelium. From here the ANCA activated neutrophil can degranulate and release the neutrophil serine proteases directly onto the endothelial surface. PR3 and HLE cause endothelial activation and release of the Weibel-Palade body constituents: vWf, CXCL8 and P-Selectin. The further amplification of CXCL8 by PR3 and HLE increase neutrophil recruitment to the site, which can interact with increased endothelial P-Selectin via their PSGL-1 ligand. CXCL8 further causes a conformational change in the neutrophil β_2 integrins to induce firm adhesion to endothelium via ICAM-1 or vWf interactions. Hence, the neutrophil serine proteases support the induction of inflammation by increased neutrophil recruitment.

A role for the serine proteases in the recruitment of inflammatory cells has previously been described in an dipeptidyl peptase I (DPPI) knock-out mouse, which lacks the ability to produce active serine proteases. Adkison *et al.*, 2002 demonstrated that these mice display reduced recruitment of inflammatory cells into synovial tissues in a model of murine

arthritis. Furthermore, the injection of CXCL8 restored neutrophil recruitment, suggesting that the serine proteases contribute to the cytokine production required for normal neutrophil recruitment, in particular, the release and processing of CXCL8 [413].

4.11 α 1-Antitrypsin – A Potential Therapy in ANCA Vasculitis?

Throughout this project, a therapeutic preparation of α 1-antitrypsin, Prolastin® (a preparation of α 1AT prepared from human plasma), has routinely been used to inhibit the actions of the neutrophil serine proteases. We have demonstrated that α 1AT can inhibit the release of vWf from Weibel-Palade bodies, inhibit membrane cleavage of vWf, as well as the cleavage of CXCL8 and Ang-2, can inhibit the effects of PR3 and HLE on increasing neutrophil adhesion, and the expression of membrane P-Selectin. It is proposed that it is the neutrophil serine proteases that are most important in the induction of endothelial activation, injury and therefore the propagation of inflammation, whilst inhibition of their effects would be beneficial. It is therefore worth exploring whether that Prolastin® would make a good addition to the current treatment regime.

Prolastin® is already being used as a therapeutic drug in restoring α 1AT in patients with alpha1-antitrypsin deficiency. Although currently, α 1AT has not been investigated in the treatment of ASV or any other immune mediated diseases. In vasculitis, there is no reason why Prolastin® could not be used alongside the current regime, but is there any need for it? At present there is no scientific grounds by which Prolastin® would make a beneficial

therapy, as α 1AT is naturally increased in the circulation during inflammation [152, 153]. α 1AT is a key inflammatory mediator released from hepatocytes, monocytes and macrophages during the acute phase response. This is a protective response induced by trauma, injury or infection, in which humoral mediators are released to prevent tissue damage and initiate repair mechanisms [154]. It is due to this increased presence of α 1AT during inflammation that there is unlikely to be a requirement for Prolastin® as a therapeutic treatment in immune mediated diseases. Furthermore, its presence in ASV may already be having an effect on dampening the injurious activities of the serine proteases. However, the effect of an over-saturation of α 1AT in these patients has not been investigated and so we cannot conclude that Prolastin® would have no beneficial effects.

Recently, a defective α 1AT allele (piZ) has been identified to occur at an increased frequency in patients with ANCA-associated vasculitis. Patients homozygous for this piZ allele display a significantly reduced level of functional α 1AT. It has been suggested that a deficiency in α 1AT may account for the high ANCA titres observed in some patients [160], furthermore, a cohort of 8 ASV patients with α 1AT deficiency typically manifested multiple organ involvement [414]. There have been multiple studies that suggest that patients with a heterozygous piZ phenotype more commonly present with PR3-ANCA associated vasculitis [162, 415, 416], moreover, in a study of 88 patients with microscopic vasculitis, 23% of the 66 Wegener's granulomatosis patients displayed the piZ phenotype [417]. This study further hypothesized that the piZ allele may predispose patients to WG. Interestingly, these piZ patients may not present a decrease in serum concentrations of α 1AT [415]. Alternatively, Audrain *et al.* demonstrated an increased incidence of ANCA directed at HLE or α GR in a cohort of 191 piZZ patients. These patients did not develop

systemic disease, and so α 1AT deficiency may not be sufficient for the development of ANCA-systemic vasculitis [161]. It would be of benefit to monitor serum levels and phenotypes of α 1AT in ASV patients, as Prolastin® may prove an effective supplement to these patients treatment regime.

4.12 Differential Roles for PR3 and HLE?

Both PR3 and HLE are stored in the primary granules of the neutrophils and released upon degranulation. Although both chymotrypsin-like serine proteases, they have been described to have both similarities and differences in their effector functions (see table 3). During this project we have used HLE as a comparative enzyme for the functional studies on PR3 as a target and mediator of disease in ASV. Interestingly, we have demonstrated that treatment with HLE appears to have a greater role than PR3 in the induction of endothelial cell injury. We have demonstrated that a 24 hours treatment with HLE has a greater effect on endothelial apoptosis compared to treatment with equivalent concentrations of PR3. In particular HLE treatment resulted in the most significant decrease in intracellular ATP, although treatment with 2 μ g/ml PR3 also resulted in a reduction. Although both serine proteases have previously been demonstrated to induce cellular apoptosis, there has been more interest into the mechanisms by which PR3 can enter endothelial cells and initiate apoptosis. Here we suggest that, if released in equal concentrations, HLE may be having a more detrimental effect of the endothelial cells than PR3. Furthermore, treatment with 5 μ g/ml HLE resulted in significant endothelial detachment. This phenomenon has also been reported by other members of our group, who demonstrated that HLE is more potent than PR3 at inducing

endothelial detachment and decreasing mitochondrial activity (Sahithi Panchagnula, unpublished data).

In regards to Weibel-Palade body exocytosis, HLE had a much greater effect on the release of vWf from both GEnC and HUVEC than PR3 treatment, whilst PR3 treated endothelial cells displayed a higher membrane expression of P-Selectin than those treated with HLE. Furthermore, endothelial cells treated with HLE demonstrated a decreased level of membrane bound vWf than PR3 treated endothelial cells. Interestingly, there was little difference between the ability of either serine protease to induce CXCL8 release, following removal of the enzyme and incubation for 2 hours in blank medium. Both serine proteases have previously been demonstrated to process a host of cytokines, however the result of this processing appears to differ. Specifically, whilst cleavage of TNF α by HLE results in its inactivation, PR3 appears to further activate the functions of TNF α . This difference in effector functions has also been suggested for CXCL8 cleavage, with HLE resulting in inactivation and PR3 in amplification. Interestingly, however, both serine proteases inactivate IL-6 and IL-2 (see table 3). In this research we have demonstrated that HLE has a greater affinity for the cleavage of CXCL8 than PR3, although the resulting functions of this cleavage were not investigated. HLE was also demonstrated to process recombinant vWf to enable increased antibody binding activity, whilst PR3 had no effect on the level of antibody binding. Alternatively, PR3 demonstrated an increased affinity for the cleavage of recombinant and released angiopoietin-2 than was demonstrated by HLE. These differences in protein cleavage by HLE and PR3 may be due to their different abilities to cleave certain peptide bonds. Interestingly, neither serine protease demonstrated a difference in their ability to induce neutrophil adhesion to either GEnC or HUVEC. Again, neither serine protease could increase the expression of ICAM-1, VCAM-1 or E-Selectin.

This work demonstrates that, whilst both serine proteases have similar effects on the endothelium in the induction of injury and Weibel-Palade body exocytosis, HLE in the main, has a more dominant effect than PR3 when used at the same concentration. There are few exceptions in which PR3 appeared the most potent stimulus, in particular, the expression of P-Selectin and cleavage of Ang-2. One factor that we were unable to account for when performing this research was to match the serine proteases not by concentration but by their enzymatic activity. Due to an absence in the market of a PR3 specific substrate we could not accurately account for any differences in the activity of the two enzymes, and this may account for some of the differences observed in their potency to perform effector functions.

4.13 Can a GEnC line Accurately Represent a Primary Glomerular Endothelial Cell?

Throughout this research we have used an immortalised microvascular glomerular endothelial cell line, in part, to overcome the difficulties and costs associated with using primary glomerular endothelial cells. To confirm that experimental results were due to their endothelial lineage, data was routinely collected on a primary macrovascular umbilical endothelial cell. HUVEC were used due their low cost and accessibility, but do not represent the microvascular endothelial cell targeted in ASV. The GEnC line appeared to be more hardy than the primary HUVEC, with less markers of endothelial injury observed following serine protease treatment, an observation also noted by Sahithi Panchagnula (unpublished data). HUVEC also displayed a greater response to serine protease treatment in vWf release and cleavage as well as neutrophil adhesion and expression of adhesion molecules. Although

both GEnC and HUVEC responded in the same manner, serine protease treatment of HUVEC consistently demonstrated a greater effect.

It is of note that, whilst in the main, these cells behaved in a similar manner, albeit to different capacities, we did note some distinct differences in the responses of the two cell types throughout this research. Firstly, GEnC do not express VCAM-1, unlike HUVEC, which is likely a characteristic of their glomerular microenvironment. Another difference between these micro- and macrovascular endothelial cells attributable to their specific environments is the level of constitutive release of Ang-2. Given the ability of endothelial cell to adapt to the requirements of their microenvironment, we believe that the high constitutive release of Ang-2 by glomerular cells is due to the required maintenance of the glomerular capillary structure, a function not required by HUVEC.

Whilst HUVEC confirmed the responses of the GEnC line to neutrophil serine proteases to be due to an endothelial lineage, with observed responses just more marked with HUVEC than GEnC, the use of a combination of these cells can not truly represent the responses of a primary glomerular endothelial cell. We can therefore not discount a possibility that this data may be skewed due to the use of an endothelial cell line.

5. Concluding Remarks

The data presented in this thesis supports the hypothesis that the neutrophil serine proteases have an early activatory role on the vascular endothelial that supports the development of an inflammatory response. At this early time point, PR3 and HLE do not appear to have effects on reducing endothelial viability, whilst we also support the idea of a later more injurious effect of the serine proteases in inducing endothelial detachment and apoptosis. This later injurious effect may account for the increased circulating and necrotic endothelial cells described in ASV patients [381].

We further describe an activated endothelial phenotype, induced by a 2 hour serine protease stimulation, that demonstrates increased WPB exocytosis and increased neutrophil adhesion, in the support of the development of an inflammatory response. We have demonstrated that PR3 and HLE can increase circulating vWf by the cleavage of membrane bound endothelial vWf as well as release from internal stores. This increased release of vWf may support a pro-coagulant state and the thrombus formation seen in the glomeruli of ASV patients. Furthermore, PR3 and HLE can increase the expression of vWf mRNA and increase intracellular protein concentrations, most probably by early *de novo* synthesis following the internalisation of the serine protease by endothelial cells.

The release of intracellular vWf occurs with an increased membrane expression of P-Selectin and release of CXCL8. Furthermore, we support the proposal that PR3 and HLE can actively cleave CXCL8, which is suggested to result in an amplified form of CXCL8 with enhanced functions. We propose that the formation of weak bonds between the upregulated endothelial P-Selectin and its PSGL-1 ligand on neutrophils results in increased neutrophil adhesion. This adhesion is further supported by an interplay between CXCL8 and its neutrophil

receptors CXCR1 and CXCR2. The stimulation of neutrophils by CXCL8 is reported to result in a conformational change of its β_2 integrins to enhance their binding activity. We believe that cleavage of the constitutively expressed ICAM-1 by the serine proteases could support the firm adhesion of weakly bound neutrophils via interactions with the activated β_2 integrins. Furthermore, vWf may also be involved in the increased neutrophil adhesion to serine protease stimulated endothelial cells, either by assisting in increasing P-Selectin expression during WPB exocytosis, or acting as a adhesion molecule for PSGL-1 and the β_2 integrins in its own right. Moreover, as a potent neutrophil chemoattractant, the enhanced CXCL8 activity induced by serine protease cleavage would increase neutrophil recruitment and hence, inflammation and disease propagation.

This project originally sought to investigate the transmigration of neutrophils across the glomerular capillary endothelium using a 2-compartmental co-culture system using glomerular endothelial and epithelial cells. Due to time restraints, only neutrophil adhesion to serine protease endothelial cells was investigated. The role of glomerular cross-talk and neutrophil migration using this co-culture system is currently being investigated by Sahithi Panchagnula.

We have demonstrated the ability of the serine proteases to cleave angiopoietin-2, although the functional consequences of this cleavage are unknown. We hypothesize that this cleavage would result in the amplification of Ang-2 activity to, along with VEGF, increase vascular leakiness and cause destabilisation of the cell-cell junctions to facilitate leukocyte recruitment. The high constitutive release of glomerular angiopoietin-2 is probably required for the maintenance of the complex capillary structure.

We have attempted to shed light on a mechanism by which the neutrophil serine proteases can induce endothelial cell activation. We have demonstrated that PR3 and HLE do not require signalling through the protease activated receptors, or through PKC, PKA, calmodulin or PI3k for vWf release, nor do they appear to co-localise with the actin cytoskeleton. Investigation into a role for PP2B has identified a possible link between the serine proteases and vWf release from HUVEC, but the decreased endothelial cell viability prevents us from drawing any conclusions from this work. We have, however, demonstrated a role for HLE, and to a lesser extent, PR3, in altering the pattern of tyrosine and serine/threonine phosphorylation. We are currently awaiting results as to identify a host of peptides with altered phosphorylation phenotypes, which will require further investigation to identify the signalling components associated with WPB exocytosis.

Investigation into the mechanisms underlying disease pathogenesis in ASV allows for the identification of novel targets for the development of therapies with an improved profile of adverse effects, rather than the current regime of wide-spread immunosuppression. Whilst the presence of Prolastin® proved beneficial in preventing the serine protease induced inflammatory responses, there appears to be no reason why it would be a beneficial addition to the current treatment regime. An exception to this would be the use of Prolastin® in patients with a piZ α 1AT phenotype.

6. Future Work

Research generated for this thesis has identified some interesting results that require further investigation. Firstly, we have demonstrated the ability of HLE to process the vWf protein and increase antibody binding by approximately 30%. We hypothesise that this is due to structural changes within the protein to unveil further antibody binding sites. It would be of interest to further evaluate the effects of HLE on the structure of endothelial vWf by using methods such as x-ray crystallography and 2-dimensional gel electrophoresis to determine atomic structure and protein unfolding respectively. Given that HLE cleavage can alter the functions of a number of cytokines, it would be of benefit to assess whether this cleavage of vWf results in any changes in its pro-coagulant or inflammatory functions. Furthermore, we have described a role for PR3 and HLE in the cleavage of angiopoietin-2. Again, identification of functional changes that result from this enzymatic cleavage could highlight a further role for Ang-2 in the pathogenesis of ASV, potentially acting in an amplified form to increase vascular leakage and facilitate the immune response. Indeed, circulating Ang-2 appears increased in serum of ASV patients [324].

We have identified a role for the serine proteases in increased neutrophil adhesion to the vascular endothelium via an interplay between P-Selectin/PSGL-1 and CXCL8/CXCR1/CXCR2. Not surprisingly, the expression of E-Selectin and ICAM-1 are not increased following a 2 hour incubation. It has been demonstrated that PR3 can be rapidly internalised by endothelial cells [136], and so may have a later role in inducing adhesion molecule expression. Given the time, it would have been interesting to see if PR3 and HLE can induce increased surface expression of E-Selectin and ICAM-1 following a 4 or 6 hour incubation, and whether, at 2 hours, relative mRNA expression for these adhesion molecules is increased. Furthermore, HLE has been demonstrated to cleave membrane bound ICAM-1.

Further investigation into the functional implications of this cleavage may provide evidence as to a mechanism by which the serine proteases can activate constitutively expressed ICAM-1 to facilitate firm adhesion at early time points. It would also be interesting to assess what role, if any, vWf is playing in the induction of neutrophil adhesion.

Recently, there has been much interest into an animal model of ANCA-vasculitis. The use of an animal model would be of benefit to this research to confirm the observation of neutrophil adhesion through PSGL-1 and CXCR signalling. Currently there are few successful animal models of PR3-ANCA vasculitis. The immunisation of mice and rats with human or murine PR3 has resulted in the generation of PR3-ANCA but these animals did not develop pathological disease [418, 419]. Only one PR3-vasculitis animal model has been successful in generating clinical disease. In this model the transfer of splenocytes from PR3 immunised non-obese diabetic (NOD) mice into NOD-severe combined immunodeficiency (SCID) mice resulted in crescent formation in 19% of glomeruli [419]. Further research involving this PR3 model of vasculitis is eagerly awaited.

Two successful mouse models of experimental MPO-ANCA vasculitis have been defined. Firstly, the transfer of splenocytes from MPO^{-/-} mice immunised with MPO, into Rag2^{-/-} mice, which lack B-cell function, induced production of MPO-ANCA, and severe crescentic glomerulonephritis in approximately 84% of glomeruli and pulmonary haemorrhage. This was also reproduced in Rag2^{-/-} mice that received MPO-ANCA alone with about 10% of glomeruli developing crescents [420]. A second model induced experimental MPO-vasculitis by the intraperitoneal injection of C57BL6 mice with anti-MPO IgG, which resulted in approximately 15% crescentic glomeruli. Interestingly, these mice displayed increased expression of CXCR2 within renal tissue during the development of disease; however blocking CXCR2 had no effect on renal disease [421]. The intraperitoneal injection of

C57BL6J mice with anti-MPO IgG has also been used to demonstrate the accumulation of neutrophils and macrophages within the glomerulus [422], and so this model could potentially be utilised to further investigate our *in vitro* observations. To achieve this we could treat experimental MPO-vasculitic mice with blocking antibodies for PSGL-1, or CXCR1 and CXCR2 together to see if neutrophil recruitment could be attenuated. We could also use these mice models to investigate a role for α 1AT in reducing clinical disease. A further rat model of experimental autoimmune vasculitis as also been described, with a mean of 10.5% crescentic glomeruli [423].

We have identified a role for the serine proteases in increasing vWf mRNA and intracellular protein levels. Due to the early time point by which we note this observation we believe this is a pro- form of the vWf protein. It would be of interest to further investigate a role for the serine proteases on *de novo* synthesis at later time points, and whether inhibition of protein synthesis, would prevent the increased intracellular vWf protein levels associated with serine protease treatment. It would be of interest to assess whether other Weibel-Palade body constituents are also increased.

Following the identification of phosphopeptides targeted by PR3 and HLE by mass spectrometry, further investigation will be required to identify which signalling components are involved in the endothelial activation, in particular during the exocytosis of WPBs.

7. Appendices

1. PCR Mastermixes

Table 20 – TaqMan® Reverse Transcription Mastermix

Reagent	1x Mastermix Volume
10x RT Buffer	5µl
MgCl ₂ Solution	11µl
dNTP Mixture	10µl
Random Hexamers	2.5µl
RNase Inhibitor	1µl
MultiScribe™ Reverse Transcriptase	3.1µl
RNA	16.9µl (1.5µg)

Table 21 - PCR Mastermix

Reagent	1x Mastermix Volume
10x DreamTaq™ Buffer	5µl
dNTP Mixture	5µl (0.2mM)
Forward Primer	1µl
Reverse Primer	1µl
DreamTaq™ DNA polymerase	0.25µl
Water	36.75µl
cDNA	1µl (1µg)

2. Real-Time PCR Mix

Table 22 - Real-Time PCR Mastermix

	PAR-1	PAR-2	Source
QuantiTech™ Probe Mastermix	12.5µl	12.5µl	Qiagen
QuantiTech™ RT Mastermix	0.25µl	0.25µl	Qiagen
β-Actin-VIC labelled Primer	1µl	1µl	Applied Biosystems
PAR-1/PAR-2-FAM labelled Primer	1µl	1µl	Applied Biosystems
RNase Free Water	8.25µl	8.25µl	Qiagen
RNA (5ng/µl)	2µl	2µl	N/A

3. Western Blot Recipes

Table 23 - Gel Recipes

10% Resolving Gel	Volume	Source
Protogel (National Diagnostics)	3.3ml	Geneflow
Tris 1.5M pH8.8 (181.71g in 1L)	2.5ml	Sigma-Aldrich
Distilled Water	4.07ml	N/A
10% SDS (0.1g in 1ml)	100µl	Sigma-Aldrich
10% APS (0.1g in 1ml)	100µl	Sigma-Aldrich
TEMED	10µl	Sigma-Aldrich

4% Stacking Gel	Volume	Source
Protogel (National Diagnostics)	1.3ml	Geneflow
Tris 0.5M pH6.8 (60.57g in 1L)	2.5ml	Sigma-Aldrich
Distilled Water	6.1ml	N/A
10% SDS	100µl	Sigma-Aldrich
10% APS	100µl	Sigma-Aldrich
TEMED	10µl	Sigma-Aldrich

Table 24 - Constituents of Western Blot Running Buffer

Medium and Additives	Volume	Source
Tris Base	12.11g	Sigma
Glycine	57.65g	Calbiochem
SDS	2g	Sigma
Distilled Water	2L	N/A

Table 25 - Constituents of Western Blot TBS-T

Medium and Additives	Volume	Source
Tris Base	2.42g	Sigma
Sodium Chloride	8g	Sigma
Distilled Water	1L	N/A
Tween 20	1ml	Sigma

Table 26 - Constituents of Western Blot Transfer Buffer

Medium and Additives	Volume	Source
Tris Base	5.81g	Sigma
Glycine	2.93g	Calbiochem
SDS	0.375g	Sigma
Methanol	200ml	BDH
Distilled Water	800ml	N/A

Table 27 - Constituents of SDS-PAGE Loading Buffer

Medium and Additives	Stock	Volume	Source
Tris Base	1M (121.14g in 1L)	1.2ml	Sigma-Aldrich
Glycerol	75%	4.8ml	Fisher Scientific
SDS	N/A	1.28g	Sigma-Aldrich
β -Mercaptoethanol	100%	0.5ml	Sigma-Aldrich
Distilled Water	N/A	1.2ml	N/A
Bromophenol Blue	100%	<i>To Colour</i>	Sigma-Aldrich

Table 28 - Constituents of Coomassie Stain/Destain

Medium and Additives	Volume	Source
Methanol	400ml	BDH
Distilled Water	500ml	N/A
Acetic Acid	100ml	Fisher Scientific
Brilliant Blue Dye	1g	Sigma-Aldrich

NB Destain does not contain Brilliant Blue Dye

4. ApoGlow® Assay Guideline Criteria

Apoptosis. Test gives lower levels of ATP compared to controls but shows an increase in ADP = Increase in ADP:ATP ratios over control ratios. These ratios vary according to the degree of apoptosis in the cell population.

Necrosis. Test gives considerably lower ATP levels than control but greatly increased ADP = Markedly increased ADP:ATP ratios over control ratios.

Arrested Proliferation. Test gives lower ATP values than control, with little or no change in ADP:ATP ratio; the treatment arrests proliferation but does not kill the cells.

Proliferation. Test gives markedly elevated ATP values compared to control wells with no significant increase in ADP levels. Stimulation with growth/mitogenic factors will induce proliferation and thus lead to an increase in ATP readings.

No effect. Test gives similar or slightly higher levels of ATP and with little or no change in ADP compared to control.

8. References

1. Jennette JC. Nomenclature of systemic vasculitides. *Arthritis Rheum* 1994; **37**:187-92.
2. Scott DGI, Watts RA. Classification and epidemiology of systemic vasculitis. *Rheumatology* 1994; **33**:897-9.
3. Savage COS, Bacon PA. Overview of vasculitis: classification and pathogenesis. *Curr Diagn Pathol* 1995; **2**:256-65.
4. Kamesh L, Harper L, Savage COS. ANCA-positive vasculitis. *J Am Soc Nephrol* 2002; **13**:1953-60.
5. Donnelly R, London N. *ABC of Arterial and Venous Disease*. 2nd Edn: BMJ Books, 2009.
6. Watts RA, Scott DGI. Epidemiology of the vasculitides. *Semin Respir Crit Care Medi* 2004; **25**:455-64.
7. Watts RA, Al-Taiar A, Scott DGI, MacGregor AJ. Prevalence and Incidence of Wegener's Granulomatosis in the UK General Practice Research Database. *Arthritis Rheum* 2009; **61**:1412-6.
8. Watts RA, Scott DG, Jayne DR, Ito-Ihara T, Muso E, Fujimoto S, Harabuchi Y, Kobayashi S, Suzuki K, Hashimoto H. Renal vasculitis in Japan and the UK--are there differences in epidemiology and clinical phenotype? *Nephrol Dial Transplant* 2008; **23**:3928-31.
9. Erwig LP, Savage CO. ANCA-associated vasculitides: advances in pathophysiology and treatment. *Neth J Med* 2010; **68**:62-7.
10. Schlieben DJ, Korbet SM, Kimura RE, Schwartz MM, Lewis EJ. Pulmonary-renal syndrome in a newborn with placental transmission of ANCA. *Am J Kidney Dis* 2005; **45**:758-61.
11. Blank MT, Y. Stein, M. Kopolovic, J. Wiik, A. Meroni, PL. Conforti, G. Shoenfeld, Y. Immunization with anti-neutrophil cytoplasmic antibody (ANCA) induces the production of mouse ANCA and perivascular lymphocyte infiltration. *Clin Exp Immunol* 1995; **102**:120-30.
12. Weidebach W, Viana VST, Leon EP, Bueno C, Leme AS, Arantes-Costa FM, Martins MA, Saldiva PHN, Bonfa E. C-ANCA-positive IgG fraction from patients with Wegener's granulomatosis induces lung vasculitis in rats. *Clin Exp Immunol* 2002; **129**:54-60.
13. Puechal X. Antineutrophil cytoplasmic antibody-associated vasculitides. *Joint Bone Spine* 2007; **74**:427-35.
14. Gomez-Puerta JA, Bosch X. Anti-Neutrophil Cytoplasmic Antibody Pathogenesis in Small-Vessel Vasculitis An Update. *Am J Pathol* 2009; **175**:1790-8.
15. Davies DJ, Moran JE, Niall JF, Ryan GB. Segmental Necrotizing Glomerulonephritis with Anti-Neutrophil Antibody - Possible Arbovirus Etiology. *BMJ* 1982; **285**:606-.
16. Falk RJ, Terrell RS, Charles LA, Jennette JC. Anti-Neutrophil Cytoplasmic Autoantibodies Induce Neutrophils to Degranulate and Produce Oxygen Radicals in vitro. *Proc Natl Acad Sci U S A* 1990; **87**:4115-9.
17. Kobold ACM, Kallenberg GGM, Tervaert JWC. Monocyte activation in patients with Wegener's granulomatosis. *Ann Rheum Dis* 1999; **58**:237-45.
18. Tervaert JWC, Vanderwoude FJ, Fauci AS, Ambrus JL, Velosa J, Keane WF, Meijer S, Vandergiesen M, The TH, Vanderhem GK, Kallenberg CGM. Association between Active Wegeners Granulomatosis and Anticytoplasmic Antibodies. *Arch Intern Med* 1989; **149**:2461-5.
19. Egnér W, Chapel HM. Titration of Antibodies against Neutrophil Cytoplasmic Antigens Is Useful in Monitoring Disease-Activity in Systemic Vasculitides. *Clin Exp Immunol* 1990; **82**:244-9.

20. Falk RJ, Jennette JC. Anti-neutrophil cytoplasmic autoantibodies with specificity for myeloperoxidase in patients with systemic vasculitis and idiopathic necrotizing and crescentic glomerulonephritis. *N Engl J Med* 1988; **318**:1651-7.
21. Kain R, Matsui K, Exner M, Binder S, Schaffner G, Sommer EM, Kerjaschki D. A novel class of autoantigens of anti-neutrophil cytoplasmic antibodies in necrotizing and crescentic glomerulonephritis: the lysosomal membrane glycoprotein h-lamp-2 in neutrophil granulocytes and a related membrane protein in glomerular endothelial cells. *J Exp Med* 1995; **181**:585-97.
22. Kain R, Exner M, Brandes R, Ziehermayr R, Cunningham D, Alderson CA, Davidovits A, Raab I, Jahn R, Ashour O, Spitzauer S, Sunder-Plassmann G, Fukuda M, Klemm P, Rees AJ, Kerjaschki D. Molecular mimicry in pauci-immune focal necrotizing glomerulonephritis. *Nat Med* 2008; **14**:1088-96.
23. Gough NR, Fambrough DM. Different steady state subcellular distributions of the three splice variants of lysosome-associated membrane protein LAMP-2 are determined largely by the COOH-terminal amino acid residue. *J Cell Biol* 1997; **137**:1161-9.
24. Sawada R, Tsuboi S, Fukuda M. Differential E-selectin-dependent adhesion efficiency in sublines of a human colon cancer exhibiting distinct metastatic potentials. *J Biol Chem* 1994; **269**:1425-31.
25. Jennette JC, Hoidal JR, Falk RJ. Specificity of anti-neutrophil cytoplasmic autoantibodies for proteinase 3 [letter; comment]. *Blood* 1990; **75**:2263-4.
26. Niles JL, McCluskey RT, Ahmad MF, Arnaout MA. Wegener's granulomatosis autoantigen is a novel neutrophil serine proteinase [see comments]. *Blood* 1989; **74**:1888-93.
27. Skogh T, Dahlgren C, Holmgren K, Peen E, Stendahl O. Antigranulocyte Antibodies (C-Anca, P-Anca, Gs-Ana) Studied by Confocal Scanning Laser Fluorescence Microscopy, Elisa, and Chemiluminescence Techniques. *Scand J Immunol* 1991; **34**:137-45.
28. Rollino C, Roccatello D, Coppo R, Menegatti E, Basolo B, Giraud G, Martina G, Piccoli G. Classic and Perinuclear Antineutrophil Cytoplasm Antibodies and Antimyeloperoxidase Antibodies in Rapidly Progressive Glomerulonephritis. *Am J Nephrol* 1991; **11**:318-24.
29. Tervaert JWC, Limburg PC, Elema JD, Huitema MG, The TH, Kallenberg CGM, Horst G. Detection of Autoantibodies against Myeloid Lysosomal-Enzymes - a Useful Adjunct to Classification of Patients with Biopsy-Proven Necrotizing Arteritis. *Am J Med* 1991; **91**:59-66.
30. Csernok E, Ernst M, Schmitt W, Bainton DF, Gross WL. Activated Neutrophils Express Proteinase-3 on Their Plasma-Membrane in-Vitro and in-Vivo. *Clin Exp Immunol* 1994; **95**:244-50.
31. Charles LA, Caldas ML, Falk RJ, Terrell RS, Jennette JC. Antibodies against granule proteins activate neutrophils in vitro. *J Leukoc Biol* 1991; **50**:539-46.
32. David A, Kacher Y, Specks U, Aviram I. Interaction of proteinase 3 with CD11b/CD18 (beta(2)integrin) on the cell membrane of human neutrophils. *J Leukoc Biol* 2003; **74**:551-7.
33. Reumaux D, Kuijpers TW, Hordijk PL, Duthilleul P, Roos D. Involvement of Fcgamma receptors and beta2 integrins in neutrophil activation by anti-proteinase-3 or anti-myeloperoxidase antibodies. *Clin Exp Immunol* 2003; **134**:344-50.
34. van Rossum AP, van der geld YM, Limburg PC, Kallenberg CGM. Human anti-neutrophil cytoplasm autoantibodies to proteinase 3 (PR3-ANCA) bind to neutrophils. *Kidney Int* 2005; **68**:537-41.

35. Hewins P, Williams JM, Wakelam MJO, Savage COS. Activation of Syk in neutrophils by antineutrophil cytoplasm antibodies occurs via Fc gamma receptors and CD18. *J Am Soc Nephrol* 2004; **15**:796-808.
36. Williams JM, Ben-Smith A, Hewins P, Dove SK, Hughes P, McEwan R, Wakelam MJO, Savage COS. Activation of the G(i) heterotrimeric G protein by ANCA IgG F(ab')(2) fragments is necessary but not sufficient to stimulate the recruitment of those downstream mediators used by intact ANCA IgG. *J Am Soc Nephrol* 2003; **14**:661-9.
37. Hussain A, Pankhurst T, Goodall M, Colman R, Jefferis R, Savage CO, Williams JM. Chimeric IgG4 PR3-ANCA induces selective inflammatory responses from neutrophils through engagement of Fc gamma receptors. *Immunology* 2009; **128**:236-44.
38. Ewert BH, Jennette JC, Falk RJ. Antimyeloperoxidase Antibodies Stimulate Neutrophils to Damage Human Endothelial-Cells. *Kidney Int* 1992; **41**:375-83.
39. Savage COS, Pottinger BE, Gaskin G, Pusey CD, Pearson JD. Autoantibodies Developing to Myeloperoxidase and Proteinase-3 in Systemic Vasculitis Stimulate Neutrophil Cytotoxicity toward Cultured Endothelial-Cells. *Am J Pathol* 1992; **141**:335-42.
40. Savage COS. Vascular biology and vasculitis. *APMIS* 2009; **117**:37-40.
41. Franssen CFM, Huitema MG, Kobold ACM, Oost-Kort WW, Limburg PC, Tiebosch A, Stegeman CA, Kallenberg CGM, Tervaert JWC. In vitro neutrophil activation by antibodies to proteinase 3 and myeloperoxidase from patients with crescentic glomerulonephritis. *J Am Soc Nephrol* 1999; **10**:1506-15.
42. Kettritz R, Jennette JC, Falk RJ. Crosslinking of ANCA-antigens stimulates superoxide release by human neutrophils. *J Am Soc Nephrol* 1997; **8**:386-94.
43. Kobold ACM, van der Geld YM, Limburg PC, Tervaert JWC, Kallenberg GGM. Pathophysiology of ANCA-associated glomerulonephritis. *Nephrol Dial Transplant* 1999; **14**:1366-75.
44. Halbwachsmecarelli L, Bessou G, Lesavre P, Lopez S, Witkosarsat V. Bimodal Distribution of Proteinase-3 (Pr3) Surface Expression Reflects a Constitutive Heterogeneity in the Polymorphonuclear Neutrophil Pool. *FEBS Lett* 1995; **374**:29-33.
45. Schreiber A, Busjahn A, Luft FC, Kettritz R. Membrane expression of proteinase 3 is genetically determined. *J Am Soc Nephrol* 2003; **14**:68-75.
46. Preston G, Ciavatta D, Yang JJ, Hewins P, Badhwar A, Jennette C, Falk R. Normal gene silencing mechanisms in mature neutrophils are disrupted in ANCA vasculitis. *APMIS* 2009; **117**:122-3.
47. Yang JJ, Pendergraft WF, Alcorta DA, Nachman PH, Hogan SL, Thomas RP, Sullivan P, Jennette JC, Falk RJ, Preston GA. Circumvention of normal constraints on granule protein gene expression in peripheral blood neutrophils and monocytes of patients with antineutrophil cytoplasmic autoantibody-associated glomerulonephritis. *J Am Soc Nephrol* 2004; **15**:2103-14.
48. Xiao H, Schreiber A, Heeringa P, Falk RJ, Jennette JC. Alternative complement pathway in the pathogenesis of disease mediated by anti-neutrophil cytoplasmic autoantibodies. *Am J Pathol* 2007; **170**:52-64.
49. Mellbye OJ, Mollnes TE, Steen LS. IgG subclass distribution and complement activation ability of autoantibodies to neutrophil cytoplasmic antigens (ANCA). *Clin Immunol Immunopathol* 1994; **70**:32-9.
50. Huugen D, van Esch A, Xiao H, Peutz-Kootstra CJ, Buurman WA, Tervaert JWC, Jennette JC, Heeringa P. Inhibition of complement factor C5 protects against anti-myeloperoxidase antibody-mediated glomerulonephritis in mice. *Kidney Int* 2007; **71**:646-54.

51. Alexopoulos E, Gionanlis L, Papayianni E, Kokolina E, Leontsini M, Memmos D. Predictors of outcome in idiopathic rapidly progressive glomerulonephritis (IRPGN). *BMC Nephrol* 2006; **7**:16.
52. Pendergraft WF, Preston GA, Shah RR, Tropsha A, Carter CW, Jennette JC, Falk RJ. Autoimmunity is triggered by cPR-3(105-201), a protein complementary to human autoantigen proteinase-3. *Nat Med* 2004; **10**:72-9.
53. Brinkmann V, Reichard U, Goosmann C, Fauler B, Uhlemann Y, Weiss DS, Weinrauch Y, Zychlinsky A. Neutrophil extracellular traps kill bacteria. *Science* 2004; **303**:1532-5.
54. Kessenbrock K, Krumbholz M, Schonermarck U, Back W, Gross WL, Werb Z, Grone HJ, Brinkmann V, Jenne DE. Netting neutrophils in autoimmune small-vessel vasculitis. *Nat Med* 2009; **15**:623-5.
55. Fuchs TA, Abed U, Goosmann C, Hurwitz R, Schulze I, Wahn V, Weinrauch Y, Brinkmann V, Zychlinsky A. Novel cell death program leads to neutrophil extracellular traps. *J Cell Biol* 2007; **176**:231-41.
56. Leadbetter EA, Rifkin IR, Hohlbaum AM, Beaudette BC, Shlomchik MJ, Marshak-Rothstein A. Chromatin-IgG complexes activate B cells by dual engagement of IgM and Toll-like receptors. *Nature* 2002; **416**:603-7.
57. Stegeman CA, Tervaert JW, Sluiter WJ, Manson WL, de Jong PE, Kallenberg CG. Association of chronic nasal carriage of *Staphylococcus aureus* and higher relapse rates in Wegener granulomatosis. *Ann Intern Med* 1994; **120**:12-7.
58. Popa ER, Stegeman CA, Kallenberg CG, Tervaert JW. *Staphylococcus aureus* and Wegener's granulomatosis. *Arthritis Res* 2002; **4**:77-9.
59. Stegeman CA, Tervaert JW, de Jong PE, Kallenberg CG. Trimethoprim-sulfamethoxazole (co-trimoxazole) for the prevention of relapses of Wegener's granulomatosis. Dutch Co-Trimoxazole Wegener Study Group. *N Engl J Med* 1996; **335**:16-20.
60. Stankus SJ, Johnson NT. Propylthiouracil-induced hypersensitivity vasculitis presenting as respiratory failure. *Chest* 1992; **102**:1595-6.
61. Gunton JE, Stiel J, Clifton-Bligh P, Wilmshurst E, McElduff A. Prevalence of positive anti-neutrophil cytoplasmic antibody (ANCA) in patients receiving anti-thyroid medication. *Eur J Endocrinol* 2000; **142**:587.
62. Choi HK, Merkel PA, Tervaert JW, Black RM, McCluskey RT, Niles JL. Alternating antineutrophil cytoplasmic antibody specificity: drug-induced vasculitis in a patient with Wegener's granulomatosis. *Arthritis Rheum* 1999; **42**:384-8.
63. Ohtsuka M, Yamashita Y, Doi M, Hasegawa S. Propylthiouracil-induced alveolar haemorrhage associated with antineutrophil cytoplasmic antibody. *Eur Respir J* 1997; **10**:1405-7.
64. Nakamori Y, Tominaga T, Inoue Y, Shinohara K. Propylthiouracil (PTU)-induced vasculitis associated with antineutrophil antibody against myeloperoxidase (MPO-ANCA). *Intern Med* 2003; **42**:529-33.
65. Lee E, Hirouchi M, Hosokawa M, Sayo H, Kohno M, Kariya K. Inactivation of peroxidases of rat bone marrow by repeated administration of propylthiouracil is accompanied by a change in the heme structure. *Biochem Pharmacol* 1988; **37**:2151-3.
66. Hogan SL, Satterly KK, Dooley MA, Nachman PH, Jennette JC, Falk RJ. Silica exposure in anti-neutrophil cytoplasmic autoantibody-associated glomerulonephritis and lupus nephritis. *J Am Soc Nephrol* 2001; **12**:134-42.
67. Gregorini G, Ferioli A, Donato F, Tira P, Morassi L, Tardanico R, Lancini L, Maiorca R. Association between silica exposure and necrotizing crescentic glomerulonephritis with p-ANCA and anti-MPO antibodies: a hospital-based case-control study. *Adv Exp Med Biol* 1993; **336**:435-40.

68. Stratta P, Messuerotti A, Canavese C, Coen M, Luccoli L, Bussolati B, Giorda L, Malavenda P, Cacciabue M, Bugiani M, Bo M, Ventura M, Camussi G, Fubini B. The role of metals in autoimmune vasculitis: epidemiological and pathogenic study. *Sci Total Environ* 2001; **270**:179-90.
69. Rihova Z, Maixnerova D, Jancova E, Pelclova D, Bartunkova J, Fenclova Z, Vankova Z, Reiterova J, Merta M, Rysava R, Tesar V. Silica and asbestos exposure in ANCA-associated vasculitis with pulmonary involvement. *Ren Fail* 2005; **27**:605-8.
70. Knight A, Sandin S, Askling J. Risks and relative risks of Wegener's granulomatosis among close relatives of patients with the disease. *Arthritis Rheum* 2008; **58**:302-7.
71. Willcocks LC, Lyons PA, Rees AJ, Smith KG. The contribution of genetic variation and infection to the pathogenesis of ANCA-associated systemic vasculitis. *Arthritis Res Ther* 2010; **12**:202.
72. Witko-Sarsat V, Lesavre P, Lopez S, Bessou G, Hieblot C, Prum B, Noel LH, Guillevin L, Ravaud P, Sermet-Gaudelus I, Timsit J, Grunfeld JP, Halbwachs-Mecarelli L. A large subset of neutrophils expressing membrane proteinase 3 is a risk factor for vasculitis and rheumatoid arthritis. *J Am Soc Nephrol* 1999; **10**:1224-33.
73. Rarok AA, Stegeman CA, Limburg PC, Kallenberg CGM. Neutrophil membrane expression of proteinase 3 (PR3) is related to relapse in PR3-ANCA-associated vasculitis. *J Am Soc Nephrol* 2002; **13**:-
74. Borregaard N, Cowland JB. Granules of the Human Neutrophilic Polymorphonuclear Leukocyte. *Blood* 1997; **89**:3503-21.
75. Bainton DF, Ulliyot JL, Farquhar MG. The development of neutrophilic polymorphonuclear leukocytes in human bone marrow: Origin and content of azurophilic and specific granules. *J Exp Med* 1971; **134**:907-34.
76. Gallin JI. Neutrophil specific granules: a fuse that ignites the inflammatory response. *Clin Res* 1984; **32**:320-8.
77. Spitznagel JK, Chi HY. Cationic Proteins and Antibacterial Properties of Infected Tissues and Leukocytes. *Am J Pathol* 1963; **43**:697.
78. Welsh IRH, Spitznagel JK. Distribution of Lysosomal Enzymes, Cationic Proteins, and Bactericidal Substances in Subcellular Fractions of Human Polymorphonuclear Leukocytes. *Infect Immun* 1971; **4**:97-102.
79. Bainton DF, Farquhar MG. Origin of granules in polymorphonuclear leukocytes: Two Types Derived from Opposite Faces of the Golgi Complex in Developing Granulocytes. *J Cell Biol* 1966; **28**:277-301.
80. Kjeldsen L, Bainton DF, Sengelov H, Borregaard N. Structural and functional heterogeneity among peroxidase-negative granules in human neutrophils: identification of a distinct gelatinase- containing granule subset by combined immunocytochemistry and subcellular fractionation. *Blood* 1993; **82**:3183-91.
81. Rice WG, Ganz T, Kinkade JM, Jr., Selsted ME, Lehrer RI, Parmley RT. Defensin-rich dense granules of human neutrophils. *Blood* 1987; **70**:757-65.
82. Oren A. The subcellular localization of defensins and myeloperoxidase in human neutrophils: immunocytochemical evidence for azurophil granule heterogeneity. *J Lab Clin Med* 1995; **125**:340-7.
83. Wright DG, Bralove DA, Gallin JI. The differential mobilization of human neutrophil granules. Effects of phorbol myristate acetate and ionophore A23187. *Am J Pathol* 1977; **87**:237-84.
84. Matsumoto T. Spontaneous Induction of Superoxide Release and Degranulation of Neutrophils in Isotonic Potassium Medium: The Role of Intracellular Calcium. *J Biol Chem* 1986; **99**:1591-6.

85. Miller LJ, Bainton DF, Borregaard N, Springer TA. Stimulated Mobilization of Monocyte Mac-1 and P150,95 Adhesion Proteins from an Intracellular Vesicular Compartment to the Cell-Surface. *J Clin Invest* 1987; **80**:535-44.
86. Kuijpers TW, Tool AT, van der Schoot CE, Ginsel LA, Onderwater JJ, Roos D, Verhoeven AJ. Membrane surface antigen expression on neutrophils: a reappraisal of the use of surface markers for neutrophil activation. *Blood* 1991; **78**:1105-11.
87. Borregaard N, Heiple JM, Simons ER, Clark RA. Subcellular localization of the b-cytochrome component of the human neutrophil microbicidal oxidase: translocation during activation. *J Cell Biol* 1983; **97**:52-61.
88. Waddell TK, Fialkow L, Chan CK, Kishimoto TK, Downey GP. Potentiation of the Oxidative Burst of Human Neutrophils - a Signaling Role for L-Selection. *J Biol Chem* 1994; **269**:18485-91.
89. Crockett-Torabi E, Sulenbarger B, Smith CW, Fantone JC. Activation of human neutrophils through L-selectin and Mac-1 molecules. *J Immunol* 1995; **154**:2291-302.
90. Jeannin P, Delneste Y, Gosset P, Molet S, Lassalle P, Hamid Q, Tsicopoulos A, Tonnel AB. Histamine induces interleukin-8 secretion by endothelial cells. *Blood* 1994; **84**:2229-33.
91. Patel KD, Modur V, Zimmerman GA, Prescott SM, McIntyre TM. The Necrotic Venom of the Brown Recluse Spider Induces Dysregulated Endothelial Cell-Dependent Neutrophil Activation - Differential Induction of Gm-Csf, Il-8, and E-Selectin Expression. *J Clin Invest* 1994; **94**:631-42.
92. Weiss SJ, Klein R, Slivka A, Wei M. Chlorination of Taurine by Human-Neutrophils - Evidence for Hypochlorous Acid Generation. *J Clin Invest* 1982; **70**:598-607.
93. Jesaitis AJ. Structure of human phagocyte cytochrome b and its relationship to microbicidal superoxide production. *J Immunol* 1995; **155**:3286-8.
94. Weiss SJ. Oxidative autoactivation of latent collagenase by human neutrophils. *Science* 1985; **227**:747-9.
95. Peppin GJ, Weiss SJ. Activation of the Endogenous Metalloproteinase, Gelatinase, by Triggered Human-Neutrophils. *Proc Natl Acad Sci U S A* 1986; **83**:4322-6.
96. Delclaux C, Delacourt, C., D'Ortho, MP., Boyer, V., Lafuma, C., Harf, A. Role of gelatinase B and elastase in human polymorphonuclear neutrophil migration across basement membrane. *Am J Respir Cell Mol Biol* 1996; **14**:288-95.
97. Branden C, Tooze J. Introduction to Protein Structure. 2nd Edn: Garland Publishing Inc., 1999.
98. Baggiolini M, Bretz U, Dewald B, Feigenson ME. Polymorphonuclear Leukocyte. Agents and Actions 1978; **8**:3-10.
99. Goldschmeding R, Vanderschoot CE, Huinink DT, Hack CE, Vandenende ME, Kallenberg CGM, Vondemborne AEGK. Wegener Granulomatosis Autoantibodies Identify a Novel Diisopropylfluorophosphate Binding-Protein in the Lysosomes of Normal Human-Neutrophils. *J Clin Invest* 1989; **84**:1577-87.
100. Kao RC, Wehner NG, Skubitz KM, Gray BH, Hoidal JR. Proteinase-3 - a Distinct Human Polymorphonuclear Leukocyte Proteinase That Produces Emphysema in Hamsters. *J Clin Invest* 1988; **82**:1963-73.
101. Ludemann J, Utecht B, Gross WL. Anti-neutrophil cytoplasm antibodies in Wegener's granulomatosis recognize an elastinolytic enzyme. *J Exp Med* 1990; **171**:357-62.
102. Campanelli D, Melchior M, Fu Y, Nakata M, Shuman H, Nathan C, Gabay JE. Cloning of cDNA for proteinase 3: a serine protease, antibiotic, and autoantigen from human neutrophils. *J Exp Med* 1990; **172**:1709-15.

103. Rao NV, Wehner NG, Marshall BC, Gray WR, Gray BH, Hoidal JR. Characterization of Proteinase-3 (Pr-3), a Neutrophil Serine Proteinase - Structural and Functional-Properties. *J Biol Chem* 1991; **266**:9540-8.
104. Tervaert JW, Mulder L, Stegeman C, Elema J, Huitema M, The H, Kallenberg C. Occurrence of autoantibodies to human leucocyte elastase in Wegener's granulomatosis and other inflammatory disorders. *Ann Rheum Dis* 1993; **52**:115-20.
105. Patry YC, Trewick DC, Gregoire M, Audrain MAP, Moreau AMN, Muller J-Y, Meflah K, Esnault VLM. Rats Injected with Syngenic Rat Apoptotic Neutrophils Develop Antineutrophil Cytoplasmic Antibodies. *J Am Soc Nephrol* 2001; **12**:1764-8.
106. Yang JJ, Kettritz R, Falk RJ, Jennette JC, Gaido ML. Apoptosis of endothelial cells induced by the neutrophil serine proteases proteinase 3 and elastase. *Am J Pathol* 1996; **149**:1617-26.
107. Berger SP, Seelen MAJ, Hiemstra PS, Gerritsma JSJ, Heemskerk E, vanderWoude FJ, Daha MR. Proteinase 3, the major autoantigen of Wegener's granulomatosis, enhances IL-8 production by endothelial cells in vitro. *J Am Soc Nephrol* 1996; **7**:694-701.
108. Taekema-Roelvink MEJ, Kooten CV, Kooij SVD, Heemskerk E, Daha MR. Proteinase 3 Enhances Endothelial Monocyte Chemoattractant Protein-1 Production and Induces Increased Adhesion of Neutrophils to Endothelial Cells by Upregulating Intercellular Cell Adhesion Molecule-1. *J Am Soc Nephrol* 2001; **12**:932-40.
109. Day CJ, Hewins P, Savage COS. New developments in the pathogenesis of ANCA-associated vasculitis. *Clin Exp Rheumatol* 2003; **21**:S35-S48.
110. Mayet WJ, Schwarting A, Orth T, Duchmann R, Meyer zum Buschenfelde KH. Antibodies to proteinase 3 mediate expression of vascular cell adhesion molecule-1 (VCAM-1). *Clin Exp Immunol* 1996; **103**:259-67.
111. Witko-Sarsat V, Cramer EM, Hieblot C, Guichard J, Nusbaum P, Lopez S, Lesavre P, Halbwachs-Mecarelli L. Presence of proteinase 3 in secretory vesicles: evidence of a novel, highly mobilizable intracellular pool distinct from azurophil granules. *Blood* 1999; **94**:2487-96.
112. Rao NV, Wehner NG, Marshall BC, Sturrock AB, Huecksteadt TP, Rao GV, Gray BH, Hoidal JR. Proteinase-3 (Pr-3) - a Polymorphonuclear Leukocyte Serine Proteinase. *Ann N Y Acad Sci* 1991; **624**:60-8.
113. Padrines M, Wolf M, Walz A, Baggiolini M. Interleukin-8 Processing by Neutrophil Elastase, Cathepsin-G and Proteinase-3. *FEBS Lett* 1994; **352**:231-5.
114. Ruef C, Jefferson DM, Schlegel-Haueter SE, Suter S. Regulation of cytokine secretion by cystic fibrosis airway epithelial cells. *Eur Respir J* 1993; **6**:1429-36.
115. Bank U, Kupper B, Reinhold D, Hoffmann T, Ansorge S. Evidence for a crucial role of neutrophil-derived serine proteases in the inactivation of interleukin-6 at sites of inflammation. *FEBS Lett* 1999; **461**:235-40.
116. Bopst M, Haas C, Car B, Eugster HP. The combined inactivation of tumor necrosis factor and interleukin-6 prevents induction of the major acute phase proteins by endotoxin. *Eur J Immunol* 1998; **28**:4130-7.
117. Ariel A, Yavin EJ, Hershkoviz R, Avron A, Franitza S, Hardan I, Cahalon L, Fridkin M, Lider O. IL-2 induces T cell adherence to extracellular matrix: inhibition of adherence and migration by IL-2 peptides generated by leukocyte elastase. *J Immunol* 1998; **161**:2465-72.
118. Scuderi P, Nez PA, Duerr ML, Wong BJ, Valdez CM. Cathepsin-G and leukocyte elastase inactivate human tumor necrosis factor and lymphotoxin. *Cell Immunol* 1991; **135**:299-313.

119. van Kessel KP, van Strijp JA, Verhoef J. Inactivation of recombinant human tumor necrosis factor-alpha by proteolytic enzymes released from stimulated human neutrophils. *J Immunol* 1991; **147**:3862-8.
120. Nortier J, Vandenabeele P, Noel E, Bosseloir Y, Goldman M, Deschodt-Lanckman M. Enzymatic degradation of tumor necrosis factor by activated human neutrophils: role of elastase. *Life Sci* 1991; **49**:1879-86.
121. Leavell KJ, Peterson MW, Gross TJ. Human neutrophil elastase abolishes interleukin-8 chemotactic activity. *J Leukoc Biol* 1997; **61**:361-6.
122. Robache-Gallea S, Morand V, Bruneau JM, Schoot B, Tagat E, Realo E, Chouaib S, Roman-Roman S. In vitro processing of human tumor necrosis factor-alpha. *J Biol Chem* 1995; **270**:23688-92.
123. Coeshott C, Ohnemus C, Pilyavskaya A, Ross S, Wieczorek M, Kroona H, Leimer AH, Cheronis J. Converting enzyme-independent release of tumor necrosis factor alpha and IL-1beta from a stimulated human monocytic cell line in the presence of activated neutrophils or purified proteinase 3. *Proc Natl Acad Sci U S A* 1999; **96**:6261-6.
124. Thorne KJ, Oliver RC, Barrett AJ. Lysis and killing of bacteria by lysosomal proteinases. *Infect Immun* 1976; **14**:555-63.
125. Odeberg H, Olsson I. Microbicidal mechanisms of human granulocytes: synergistic effects of granulocyte elastase and myeloperoxidase or chymotrypsin-like cationic protein. *Infect Immun* 1976; **14**:1276-83.
126. Lehrer RI, Ganz T. Antimicrobial polypeptides of human neutrophils. *Blood* 1990; **76**:2169-81.
127. Campanelli D, Detmers PA, Nathan CF, Gabay JE. Azurocidin and a homologous serine protease from neutrophils. Differential antimicrobial and proteolytic properties. *J Clin Invest* 1990; **85**:904-15.
128. Takahashi H, Nukiwa T, Yoshimura K, Quick CD, States DJ, Holmes MD, Whang-Peng J, Knutsen T, Crystal RG. Structure of the human neutrophil elastase gene. *J Biol Chem* 1988; **263**:14739-47.
129. Campbell EJ, Campbell MA, Owen CA. Bioactive proteinase 3 on the cell surface of human neutrophils: quantification, catalytic activity, and susceptibility to inhibition. *J Immunol* 2000; **165**:3366-74.
130. Rainger GE, Rowley AF, Nash GB. Adhesion-dependent release of elastase from human neutrophils in a novel, flow-based model: specificity of different chemotactic agents. *Blood* 1998; **92**:4819-27.
131. Damiano VV, Kucich U, Murer E, Laudenslager N, Weinbaum G. Ultrastructural Quantitation of Peroxidase- and Elastase-Containing Granules in Human-Neutrophils. *Am J Pathol* 1988; **131**:235-45.
132. Campbell EJ, Silverman EK, Campbell MA. Elastase and cathepsin G of human monocytes. Quantification of cellular content, release in response to stimuli, and heterogeneity in elastase-mediated proteolytic activity. *J Immunol* 1989; **143**:2961-8.
133. Kafienah W, Buttle DJ, Burnett D, Hollander AP. Cleavage of native type I collagen by human neutrophil elastase. *Biochem J* 1998; **330 (Pt 2)**:897-902.
134. Gabay JE, Scott RW, Campanelli D, Griffith J, Wilde C, Marra MN, Seeger M, Nathan CF. Antibiotic proteins of human polymorphonuclear leukocytes. *Proc Natl Acad Sci U S A* 1989; **86**:5610-4.
135. Ballieux BE, Hiemstra PS, Klar-Mohamad N, Hagen EC, van Es LA, van der Woude FJ, Daha MR. Detachment and cytolysis of human endothelial cells by proteinase 3. *Eur J Immunol* 1994; **24**:3211-5.
136. Yang JJ, Preston GA, Pendergraft WF, Segelmark M, Heeringa P, Hogan SL, Jennette JC, Falk RJ. Internalization of proteinase 3 is concomitant with endothelial

- cell apoptosis and internalization of myeloperoxidase with generation of intracellular oxidants. *Am J Pathol* 2001; **158**:581-92.
137. Preston GA, Zarella CS, Pendergraft WF, Rudolph EH, Yang JJ, Sekura SB, Jennette JC, Falk RJ. Novel effects of neutrophil-derived proteinase 3 and elastase on the vascular endothelium involve in vivo cleavage of NF-kappa B and proapoptotic changes in JNK, ERK, and p38 MAPK signaling pathways. *J Am Soc Nephrol* 2002; **13**:2840-9.
 138. Pendergraft WF, Rudolph EH, Falk RJ, John JE, Grimmmer M, Hengst L, Jennette JC, Preston GA. Proteinase 3 sidesteps caspases and cleaves(p21Waf1/Cip1/Sdil) to induce endothelial cell apoptosis (vol 65, pg 75, 2004). *Kidney Int* 2004; **65**:1130-1.
 139. Bank U, Ansorge S. More than destructive: neutrophil-derived serine proteases in cytokine bioactivity control. *J Leukoc Biol* 2001; **69**:197-206.
 140. Sugawara S, Uehara A, Nochi T, Yamaguchi T, Ueda H, Sugiyama A, Hanzawa K, Kumagai K, Okamura H, Takada H. Neutrophil proteinase 3-mediated induction of bioactive IL-18 secretion by human oral epithelial cells. *J Immunol* 2001; **167**:6568-75.
 141. Bank U, Reinhold D, Schneemilch C, Kunz D, Synowitz HJ, Ansorge S. Selective proteolytic cleavage of IL-2 receptor and IL-6 receptor ligand binding chains by neutrophil-derived serine proteases at foci of inflammation. *J Interferon Cytokine Res* 1999; **19**:1277-87.
 142. Mueller SG, Paterson AJ, Kudlow JE. Transforming growth factor alpha in arterioles: cell surface processing of its precursor by elastases. *Mol Cell Biol* 1990; **10**:4596-602.
 143. Javelaud D, Besancon F. Inactivation of p21WAF1 sensitizes cells to apoptosis via an increase of both p14ARF and p53 levels and an alteration of the Bax/Bcl-2 ratio. *J Biol Chem* 2002; **277**:37949-54.
 144. Witko-Sarsat V, Canteloup S, Durant S, Desdouets C, Chabernaud R, Lemarchand P, Descamps-Latscha B. Cleavage of p21waf1 by proteinase-3, a myeloid-specific serine protease, potentiates cell proliferation. *J Biol Chem* 2002; **277**:47338-47.
 145. Potempa J, Korzus E, Travis J. The serpin superfamily of proteinase inhibitors: structure, function, and regulation. *J Biol Chem* 1994; **269**:15957-60.
 146. Hood JM, Koep LJ, Peters RL, Schroter GP, Weil R, 3rd, Redeker AG, Starzl TE. Liver transplantation for advanced liver disease with alpha-1-antitrypsin deficiency. *N Engl J Med* 1980; **302**:272-5.
 147. Perlmutter DH, Cole FS, Kilbridge P, Rossing TH, Colten HR. Expression of the alpha 1-proteinase inhibitor gene in human monocytes and macrophages. *Proc Natl Acad Sci U S A* 1985; **82**:795-9.
 148. Olsen GN, Harris JO, Castle JR, Waldman RH, Karmgard HJ. Alpha-1-antitrypsin content in the serum, alveolar macrophages, and alveolar lavage fluid of smoking and nonsmoking normal subjects. *J Clin Invest* 1975; **55**:427-30.
 149. Kalsheker N, Morley S, Morgan K. Gene regulation of the serine proteinase inhibitors alpha1-antitrypsin and alpha1-antichymotrypsin. *Biochem Soc Trans* 2002; **30**:93-8.
 150. Boutten A, Venembre P, Seta N, Hamelin J, Aubier M, Durand G, Dehoux MS. Oncostatin M is a potent stimulator of alpha1-antitrypsin secretion in lung epithelial cells: modulation by transforming growth factor-beta and interferon-gamma. *Am J Respir Cell Mol Biol* 1998; **18**:511-20.
 151. Rogers J, Kalsheker N, Wallis S, Speer A, Coutelle CH, Woods D, Humphries SE. The isolation of a clone for human alpha 1-antitrypsin and the detection of alpha 1-antitrypsin in mRNA from liver and leukocytes. *Biochem Biophys Res Commun* 1983; **116**:375-82.

152. Travis J, Shieh B-H, Potempa J. The Functional Role of Acute Phase Plasma Proteinase Inhibitors. *Tokai J Exp Clin Med* 1988; **13**:313-20.
153. Aronsen KF, Ekelund G, Kindmark CO, Laurell CB. Sequential changes of plasma proteins after surgical trauma. *Scand J Clin Lab Invest Suppl* 1972; **124**:127-36.
154. Baumann H, Gauldie J. The acute phase response. *Immunol Today* 1994; **15**:74-80.
155. Knoell DL, Ralston DR, Coulter KR, Wewers MD. Alpha 1-antitrypsin and protease complexation is induced by lipopolysaccharide, interleukin-1beta, and tumor necrosis factor-alpha in monocytes. *Am J Respir Crit Care Med* 1998; **157**:246-55.
156. Barbey-Morel C, Pierce JA, Campbell EJ, Perlmutter DH. Lipopolysaccharide modulates the expression of alpha 1 proteinase inhibitor and other serine proteinase inhibitors in human monocytes and macrophages. *J Exp Med* 1987; **166**:1041-54.
157. Crystal RG. Alpha 1-antitrypsin deficiency, emphysema, and liver disease. Genetic basis and strategies for therapy. *J Clin Invest* 1990; **85**:1343-52.
158. Gadek JE, Fells GA, Zimmerman RL, Rennard SI, Crystal RG. Antielastases of the human alveolar structures. Implications for the protease-antiprotease theory of emphysema. *J Clin Invest* 1981; **68**:889-98.
159. Banda MJ, Rice AG, Griffin GL, Senior RM. The inhibitory complex of human alpha 1-proteinase inhibitor and human leukocyte elastase is a neutrophil chemoattractant. *J Exp Med* 1988; **167**:1608-15.
160. Meier P, Dayer E, Lemoine R, Blanc E. Henoch-Schonlein purpura with IgG PR3-ANCA in a PiZZ alpha 1-antitrypsin deficient patient. *Nephrol Dial Transplant* 2001; **16**:1932-5.
161. Audrain MA, Sesboue R, Baranger TA, Elliott J, Testa A, Martin JP, Lockwood CM, Esnault VL. Analysis of anti-neutrophil cytoplasmic antibodies (ANCA): frequency and specificity in a sample of 191 homozygous (PiZZ) alpha1-antitrypsin-deficient subjects. *Nephrol Dial Transplant* 2001; **16**:39-44.
162. Esnault VL, Testa A, Audrain M, Roge C, Hamidou M, Barrier JH, Sesboue R, Martin JP, Lesavre P. Alpha 1-antitrypsin genetic polymorphism in ANCA-positive systemic vasculitis. *Kidney Int* 1993; **43**:1329-32.
163. Callea F, Gregorini G, Sinico A, Gonzales G, Bossolasco M, Salvidio G, Radice A, Tira P, Candiano G, Rossi G, Petti A, Ravera G, Ghiggeri G, Gusmano R. alpha 1-Antitrypsin (AAT) deficiency and ANCA-positive systemic vasculitis: genetic and clinical implications. *Eur J Clin Invest* 1997; **27**:696-702.
164. Henson PM, Johnston RB. Tissue-Injury in Inflammation - Oxidants, Proteinases, and Cationic Proteins. *J Clin Invest* 1987; **79**:669-74.
165. Nolan SL, Kalia N, Nash GB, Kamel D, Heeringa P, Savage COS. Mechanisms of ANCA-Mediated Leukocyte-Endothelial Cell Interactions In Vivo. *J Am Soc Nephrol* 2008; **19**:973-84.
166. Little MA, Smyth CL, Yadav R, Ambrose L, Cook HT, Nourshargh S, Pusey CD. Antineutrophil cytoplasm antibodies directed against myeloperoxidase augment leukocyte-microvascular interactions in vivo. *Blood* 2005; **106**:2050-8.
167. Radford DJ, Luu NT, Hewins P, Nash GB, Savage COS. Antineutrophil cytoplasmic antibodies stabilize adhesion and promote migration of flowing neutrophils on endothelial cells. *Arthritis Rheum* 2001; **44**:2851-61.
168. Calderwood JW, Williams JM, Morgan MD, Nash GB, Savage COS. ANCA induces β_2 integrin and CXC chemokine-dependent neutrophil-endothelial cell interactions that mimic those of highly cytokine-activated endothelium. *J Leukoc Biol* 2005; **77**:33-43.
169. Ley K, Gaehtgens P, Fennie C, Singer MS, Lasky LA, Rosen SD. Lectin-Like Cell-Adhesion Molecule-1 Mediates Leukocyte Rolling in Mesenteric Venules In vivo. *Blood* 1991; **77**:2553-5.

170. Vonandrian UH, Chambers JD, Mcevoy LM, Bargatze RF, Arfors KE, Butcher EC. 2-Step Model of Leukocyte Endothelial-Cell Interaction in Inflammation - Distinct Roles for Lecam-1 and the Leukocyte Beta-2 Integrins In Vivo. *Proc Natl Acad Sci U S A* 1991; **88**:7538-42.
171. Dore M, Korthuis RJ, Granger DN, Entman ML, Smith CW. P-Selectin Mediates Spontaneous Leukocyte Rolling in-Vivo. *Blood* 1993; **82**:1308-16.
172. Nolte D, Schmid P, Jager U, Botzlar A, Roesken F, Hecht R, Uhl E, Messmer K, Vestweber D. Leukocyte rolling in venules of striated muscle and skin is mediated by P-selectin, not by L-selectin. *Am J Physiol Heart Circ Physiol* 1994; **267**:H1637-42.
173. Ley K. Molecular mechanisms of leukocyte recruitment in the inflammatory process. *Cardiovasc Res* 1996; **32**:733-42.
174. Foxall C, Watson SR, Dowbenko D, Fennie C, Lasky LA, Kiso M, Hasegawa A, Asa D, Brandley BK. The three members of the selectin receptor family recognize a common carbohydrate epitope, the sialyl Lewis(x) oligosaccharide. *J Cell Biol* 1992; **117**:895-902.
175. Cummings RD. Structure and function of the selectin ligand PSGL-1. *Braz J Med Biol Res* 1999; **32**:519-28.
176. Li F, Wilkins PP, Crawley S, Weinstein J, Cummings RD, McEver RP. Post-translational modifications of recombinant P-selectin glycoprotein ligand-1 required for binding to P- and E-selectin. *J Biol Chem* 1996; **271**:3255-64.
177. Takagi J, Petre BM, Walz T, Springer TA. Global Conformational Rearrangements in Integrin Extracellular Domains in Outside-In and Inside-Out Signaling. *Cell* 2002; **110**:599-611.
178. Tse WY, Nash GB, Hewins P, Savage COS, Adu D. ANCA-induced neutrophil F-actin polymerization: Implications for microvascular inflammation. *Kidney Int* 2005; **67**:130-9.
179. Anderson DC, Springer TA. Leukocyte Adhesion Deficiency - an Inherited Defect in the Mac-1, Lfa-1, and P150,95 Glycoproteins. *Annu Rev Med* 1987; **38**:175-94.
180. Dustin ML, Springer TA. Lymphocyte function-associated antigen-1 (LFA-1) interaction with intercellular adhesion molecule-1 (ICAM-1) is one of at least three mechanisms for lymphocyte adhesion to cultured endothelial cells. *J Cell Biol* 1988; **107**:321-31.
181. Diamond MS, Staunton DE, Defougerolles AR, Stacker SA, Garciaaguilar J, Hibbs ML, Springer TA. Icam-1 (Cd54) - a Counter-Receptor for Mac-1 (Cd11b Cd18). *J Cell Biol* 1990; **111**:3129-39.
182. Staunton DE, Dustin ML, Springer TA. Functional Cloning of Icam-2, a Cell-Adhesion Ligand for Lfa-1 Homologous to Icam-1. *Nature* 1989; **339**:61-4.
183. Krieglstein CF, Granger DN. Adhesion molecules and their role in vascular disease. *Am J Hypertens* 2001; **14**:44S-54S.
184. Rastaldi MP. Intraglomerular and interstitial leukocyte infiltration, adhesion molecules, and interleukin-1 α expression in 15 cases of antineutrophil cytoplasmic autoantibody—associated renal vasculitis. *Am J Kidney Dis* 1996; **27**:48-57.
185. Pall AA, Howie AJ, Adu D, Richards GM, Inward CD, Milford DV, Richards NT, Michael J, Taylor CM. Glomerular vascular cell adhesion molecule-1 expression in renal vasculitis. *J Clin Pathol* 1996; **49**:238-42.
186. Kuijpers TW, Hakkert BC, Hart MH, Roos D. Neutrophil migration across monolayers of cytokine-prestimulated endothelial cells: a role for platelet-activating factor and IL-8. *J Cell Biol* 1992; **117**:565-72.
187. Smith WB, Gamble JR, Clark-Lewis I, Vadas MA. Interleukin-8 induces neutrophil transendothelial migration. *Immunology* 1991; **72**:65-72.
188. Baggiolini M, Clarklewis I. Interleukin-8, a Chemotactic and Inflammatory Cytokine. *FEBS Lett* 1992; **307**:97-101.

189. Detmers PA, Lo SK, Olsen-Egbert E, Walz A, Baggiolini M, Cohn ZA. Neutrophil-activating protein 1/interleukin 8 stimulates the binding activity of the leukocyte adhesion receptor CD11b/CD18 on human neutrophils. *J Exp Med* 1990; **171**:1155-62.
190. DiVietro JA, Smith MJ, Smith BR, Petruzzelli L, Larson RS, Lawrence MB. Immobilized IL-8 triggers progressive activation of neutrophils rolling in vitro on P-selectin and intercellular adhesion molecule-1. *J Immunol* 2001; **167**:4017-25.
191. Seo SM, McIntire LV, Smith CW. Effects of IL-8, Gro-alpha, and LTB(4) on the adhesive kinetics of LFA-1 and Mac-1 on human neutrophils. *Am J Physiol Cell Physiol* 2001; **281**:C1568-78.
192. Chuntharapai A, Kim KJ. Regulation of the Expression of Il-8 Receptor a/B by Il-8 - Possible Functions of Each Receptor. *J Immunol* 1995; **155**:2587-94.
193. Addison CL, Daniel TO, Burdick MD, Liu H, Ehlert JE, Xue YY, Buechi L, Walz A, Richmond A, Strieter RM. The CXC chemokine receptor 2, CXCR2, is the putative receptor for ELR+ CXC chemokine-induced angiogenic activity. *J Immunol* 2000; **165**:5269-77.
194. Smith WB, Gamble JR, Clarklewis I, Vadas MA. Chemotactic Desensitization of Neutrophils Demonstrates Interleukin-8 (Il-8)-Dependent and Il-8-Independent Mechanisms of Transmigration through Cytokine-Activated Endothelium. *Immunology* 1993; **78**:491-7.
195. Arndt H, Bolanowski MA, Granger DN. Role of interleukin 8 on leucocyte-endothelial cell adhesion in intestinal inflammation. *Gut* 1996; **38**:911-5.
196. Itoh S, Susuki C, Takeshita K, Nagata K, Tsuji T. Redistribution of P-selectin glycoprotein ligand-1 (PSGL-1) in chemokine-treated neutrophils: a role of lipid microdomains. *J Leukoc Biol* 2007; **81**:1414-21.
197. Westlin WF, Kiely JM, Gimbrone MA, Jr. Interleukin-8 induces changes in human neutrophil actin conformation and distribution: relationship to inhibition of adhesion to cytokine-activated endothelium. *J Leukoc Biol* 1992; **52**:43-51.
198. Noronha IL, Kruger C, Andrassy K, Ritz E, Waldherr R. In situ Production of Tnf-Alpha, Il-1-Beta and Il-2r in Anca-Positive Glomerulonephritis. *Kidney Int* 1993; **43**:682-92.
199. Tomer Y, Barak V, Gilburd B, Shoenfeld Y. Cytokines in experimental autoimmune vasculitis: Evidence for a Th2 type response. *Clin Exp Rheumatol* 1999; **17**:521-6.
200. Ludviksson BR, Sneller MC, Chua KS, Talar-Williams C, Langford CA, Ehrhardt RO, Fauci AS, Strober W. Active Wegener's Granulomatosis Is Associated with HLA-DR+ CD4+ T Cells Exhibiting an Unbalanced Th1-Type T Cell Cytokine Pattern: Reversal with IL-10. *J Immunol* 1998; **160**:3602-9.
201. Porges AJ, Redecha PB, Kimberly WT, Csernok E, Gross WL, Kimberly RP. Antineutrophil Cytoplasmic Antibodies Engage and Activate Human Neutrophils Via Fc-Gamma-Riia. *J Immunol* 1994; **153**:1271-80.
202. Mulder AHL, Heeringa P, Brouwer E, Limburg PC, Kallenberg CGM. Activation of Granulocytes by Antineutrophil Cytoplasmic Antibodies (Anca) - a Fc-Gamma-Rii-Dependent Process. *Clin Exp Immunol* 1994; **98**:270-8.
203. Reumaux D, Vosseveld PJ, Roos D, Verhoeven AJ. Effect of tumor necrosis factor-induced integrin activation on Fc gamma receptor II-mediated signal transduction: relevance for activation of neutrophils by anti-proteinase 3 or anti-myeloperoxidase antibodies. *Blood* 1995; **86**:3189-95.
204. Matsumoto T, Kaneko T, Seto M, Wada H, Kobayashi T, Nakatani K, Tonomura H, Tono Y, Ohyabu M, Nobori T, Shiku H, Sudo A, Uchida A, Stearns Kurosawa DJ, Kurosawa S. The Membrane Proteinase 3 Expression on Neutrophils Was Downregulated After Treatment With Infliximab in Patients With Rheumatoid Arthritis. *Clin Appl Thromb Hemost* 2008; **14**:186-92.

205. Brachemi S, Mambole A, Fakhouri F, Mouthon L, Guillevin L, Lesavre P, Halbwegs-Mecarelli L. Increased membrane expression of proteinase 3 during neutrophil adhesion in the presence of anti proteinase 3 antibodies. *J Am Soc Nephrol* 2007; **18**:2330-9.
206. Kettritz R, Scheumann J, Xu Y, Luft FC, Haller H. TNF-[agr]-accelerated apoptosis abrogates ANCA-mediated neutrophil respiratory burst by a caspase-dependent mechanism. *Kidney Int* 2002; **61**:502-15.
207. Harper L, Ren Y, Savill J, Adu D, Savage COS. Antineutrophil Cytoplasmic Antibodies Induce Reactive Oxygen-Dependent Dysregulation of Primed Neutrophil Apoptosis and Clearance by Macrophages. *Am J Pathol* 2000; **157**:211-20.
208. Gamble JR, Harlan JM, Klebanoff SJ, Vadas MA. Stimulation of the Adherence of Neutrophils to Umbilical Vein Endothelium by Human Recombinant Tumor Necrosis Factor. *Proc Natl Acad Sci U S A* 1985; **82**:8667-71.
209. Briscoe DM, Cotran RS, Pober JS. Effects of tumor necrosis factor, lipopolysaccharide, and IL-4 on the expression of vascular cell adhesion molecule-1 in vivo. Correlation with CD3+ T cell infiltration. *J Immunol* 1992; **149**:2954-60.
210. Weller A, Isenmann S, Vestweber D. Cloning of the mouse endothelial selectins. Expression of both E- and P-selectin is inducible by tumor necrosis factor alpha. *J Biol Chem* 1992; **267**:15176-83.
211. Burke-Gaffney A, Hellewell PG. Tumour necrosis factor-alpha-induced ICAM-1 expression in human vascular endothelial and lung epithelial cells: modulation by tyrosine kinase inhibitors. *Br J Pharmacol* 1996; **119**:1149-58.
212. Erwig LP, Kluth DC, Rees AJ. Macrophage heterogeneity in renal inflammation. *Nephrol Dial Transplant* 2003; **18**:1962-5.
213. Ricardo SD, van Goor H, Eddy AA. Macrophage diversity in renal injury and repair. *J Clin Invest* 2008; **118**:3522-30.
214. Mantovani A, Sica A, Locati M. New vistas on macrophage differentiation and activation. *Eur J Immunol* 2007; **37**:14-6.
215. Wang Y, Wang YP, Zheng G, Lee VW, Ouyang L, Chang DH, Mahajan D, Coombs J, Wang YM, Alexander SI, Harris DC. Ex vivo programmed macrophages ameliorate experimental chronic inflammatory renal disease. *Kidney Int* 2007; **72**:290-9.
216. Kurts C, Heymann F, Lukacs-Kornek V, Boor P, Floege J. Role of T cells and dendritic cells in glomerular immunopathology. *Semin Immunopathol* 2007; **29**:317-35.
217. Kalluri R, Danoff TM, Okada H, Neilson EG. Susceptibility to anti-glomerular basement membrane disease and Goodpasture syndrome is linked to MHC class II genes and the emergence of T cell-mediated immunity in mice. *J Clin Invest* 1997; **100**:2263-75.
218. Chadban SJ, Atkins RC. Glomerulonephritis. *Lancet* 2005; **365**:1797-806.
219. Kluth DC, Ainslie CV, Pearce WP, Finlay S, Clarke D, Anegon I, Rees AJ. Macrophages transfected with adenovirus to express IL-4 reduce inflammation in experimental glomerulonephritis. *J Immunol* 2001; **166**:4728-36.
220. Cattell V. Macrophages in Acute Glomerular Inflammation. *Kidney Int* 1994; **45**:945-52.
221. Atkins RC, Glasgow EF, Holdsworth SR, Matthews FE. Macrophage in Human Rapidly Progressive Glomerulonephritis. *Lancet* 1976; **1**:830-2.
222. Weidner S, Carl M, Riess R, Rupperecht HD. Histologic analysis of renal leukocyte infiltration in antineutrophil cytoplasmic antibody-associated vasculitis: importance of monocyte and neutrophil infiltration in tissue damage. *Arthritis Rheum* 2004; **50**:3651-7.

223. Ferrario F, Rastaldi MP. Necrotizing-crescentic glomerulonephritis in ANCA-associated vasculitis: the role of monocytes. *Nephrol Dial Transplant* 1999; **14**:1627-31.
224. Marinaki S, Neumann I, Kalsch AI, Grimminger P, Breedijk A, Birck R, Schmitt W, Waldherr R, Yard BA, Van Der Woude FJ. Abnormalities of CD4(+) T cell subpopulations in ANCA-associated vasculitis. *Clin Exp Immunol* 2005; **140**:181-91.
225. Iking-Konert C, Vogl T, Prior B, Wagner C, Sander O, Bleck E, Ostendorf B, Schneider M, Andrassy K, Hansch GM. T lymphocytes in patients with primary vasculitis: expansion of CD8+ T cells with the propensity to activate polymorphonuclear neutrophils. *Rheumatology* 2008; **47**:609-16.
226. Christensson M, Pettersson E, Sundqvist KG, Christensson B. T cell activation in patients with ANCA-associated vasculitis: inefficient immune suppression by therapy. *Clin Nephrol* 2000; **54**:435-42.
227. Schlesier M, Kaspar T, Gutfleisch J, Wolffvorbeck G, Peter HH. Activated Cd4(+) and Cd8(+) T-Cell Subsets in Wegeners Granulomatosis. *Rheumatol Int* 1995; **14**:213-9.
228. Moosig F, Csernok E, Wang G, Gross WL. Costimulatory molecules in Wegener's granulomatosis (WG): lack of expression of CD28 and preferential up-regulation of its ligands B7-1 (CD80) and B7-2 (CD86) on T cells. *Clin Exp Immunol* 1998; **114**:113-8.
229. Giscombe R, Wang XB, Kakoulidou M, Lefvert AK. Characterization of the expanded T-cell populations in patients with Wegener's granulomatosis. *J Intern Med* 2006; **260**:224-30.
230. Steiner K, Moosig F, Csernok E, Selleng K, Gross WL, Fleischer B, Broker BM. Increased expression of CTLA-4 (CD152) by T and B lymphocytes in Wegener's granulomatosis. *Clin Exp Immunol* 2001; **126**:143-50.
231. Pandiyan P, Gartner D, Soezeri O, Radbruch A, Schulze-Osthoff K, Brunner-Weinzierl MC. CD152 (CTLA-4) determines the unequal resistance of Th1 and Th2 cells against activation-induced cell death by a mechanism requiring PI3 kinase function. *J Exp Med* 2004; **199**:831-42.
232. Slot MC, Sokolowska MG, Savelkoul KG, Janssen RGJH, Damoiseaux JGMC, Tervaert JWC. Immunoregulatory gene polymorphisms are associated with ANCA-related vasculitis. *Clin Immunol* 2008; **128**:39-45.
233. Abdulahad WH, Stegeman CA, Limburg PC, Kallenberg CGA. Skewed distribution of Th17 lymphocytes in patients with Wegener's granulomatosis in remission. *Arthritis Rheum* 2008; **58**:2196-205.
234. Jovanovic DV, Di Battista JA, Martel-Pelletier J, Jolicoeur FC, He Y, Zhang M, Mineau F, Pelletier JP. IL-17 stimulates the production and expression of proinflammatory cytokines, IL-beta and TNF-alpha, by human macrophages. *J Immunol* 1998; **160**:3513-21.
235. Abdulahad WH, Stegeman CA, van der Geld YM, Doornbos-van der Meer B, Limburg PC, Kallenberg CGM. Functional defect of circulating regulatory CD4+T cells in patients with Wegener's granulomatosis in remission. *Arthritis Rheum* 2007; **56**:2080-91.
236. Walsh M, Jayne D. Targeting the B cell in vasculitis. *Pediatr Nephrol* 2009; **24**:1267-75.
237. Janeway CA, Travers P, Walport M, Shlomchik MJ. *Immunobiology*. 5th Edn: Garland Science, 2001.
238. Mandler R, Chu CC, Paul WE, Max EE, Snapper CM. Interleukin 5 induces S mu-S gamma 1 DNA rearrangement in B cells activated with dextran-anti-IgD antibodies and interleukin 4: a three component model for Ig class switching. *J Exp Med* 1993; **178**:1577-86.

239. Stavnezer J. Immunoglobulin class switching. *Curr Opin Immunol* 1996; **8**:199-205.
240. Shlomchik MJ, Craft JE, Mamula MJ. From T to B and back again: positive feedback in systemic autoimmune disease. *Nat Rev Immunol* 2001; **1**:147-53.
241. Takemura S, Klimiuk PA, Braun A, Goronzy JJ, Weyand CM. T cell activation in rheumatoid synovium is B cell dependent. *J Immunol* 2001; **167**:4710-8.
242. Cohen CD, Calvaresi N, Armelloni S, Schmid H, Henger A, Ott U, Rastaldi MP, Kretzler M. CD20-positive infiltrates in human membranous glomerulonephritis. *J Nephrol* 2005; **18**:328-33.
243. Csernok E, Moosig F, Gross WL. Pathways to ANCA production: from differentiation of dendritic cells by proteinase 3 to B lymphocyte maturation in Wegener's granuloma. *Clin Rev Allergy Immunol* 2008; **34**:300-6.
244. Jones RB, Tervaert JW, Hauser T, Luqmani R, Morgan MD, Peh CA, Savage CO, Segelmark M, Tesar V, van Paassen P, Walsh D, Walsh M, Westman K, Jayne DR. Rituximab versus cyclophosphamide in ANCA-associated renal vasculitis. *N Engl J Med* 2010; **363**:211-20.
245. Stone JH, Merkel PA, Spiera R, Seo P, Langford CA, Hoffman GS, Kallenberg CG, St Clair EW, Turkiewicz A, Tchao NK, Webber L, Ding L, Sejismundo LP, Mieras K, Weitzenkamp D, Ikle D, Seyfert-Margolis V, Mueller M, Brunetta P, Allen NB, Fervenza FC, Geetha D, Keogh KA, Kissin EY, Monach PA, Peikert T, Stegeman C, Ytterberg SR, Specks U. Rituximab versus cyclophosphamide for ANCA-associated vasculitis. *N Engl J Med* 2010; **363**:221-32.
246. Arroyo AG, Iruela-Arispe ML. Extracellular matrix, inflammation, and the angiogenic response. *Cardiovasc Res* 2010; **86**:226-35.
247. Sessa WC. Molecular control of blood flow and angiogenesis: role of nitric oxide. *J Thromb Haemost* 2009; **7 Suppl 1**:35-7.
248. Parikh SM, Mammoto T, Schultz A, Yuan HT, Christiani D, Karumanchi SA, Sukhatme VP. Excess circulating angiopoietin-2 may contribute to pulmonary vascular leak in sepsis in humans. *PLoS Med* 2006; **3**:e46.
249. Dejana E, Orsenigo F, Lampugnani MG. The role of adherens junctions and VE-cadherin in the control of vascular permeability. *J Cell Sci* 2008; **121**:2115-22.
250. Komarova Y, Malik AB. Regulation of endothelial permeability via paracellular and transcellular transport pathways. *Annu Rev Physiol* 2010; **72**:463-93.
251. Thomas M, Augustin HG. The role of the Angiopoietins in vascular morphogenesis. *Angiogenesis* 2009; **12**:125-37.
252. Augustin HG, Koh GY, Thurston G, Alitalo K. Control of vascular morphogenesis and homeostasis through the angiopoietin-Tie system. *Nat Rev Mol Cell Biol* 2009; **10**:165-77.
253. Hirahashi J, Hishikawa K, Kaname S, Tsuboi N, Wang Y, Simon DI, Stavrakis G, Shimosawa T, Xiao L, Nagahama Y, Suzuki K, Fujita T, Mayadas TN. Mac-1 (CD11b/CD18) links inflammation and thrombosis after glomerular injury. *Circulation* 2009; **120**:1255-65.
254. Hirahashi J, Mekala D, Van Ziffle J, Xiao L, Saffaripour S, Wagner DD, Shapiro SD, Lowell C, Mayadas TN. Mac-1 signaling via Src-family and Syk kinases results in elastase-dependent thrombohemorrhagic vasculopathy. *Immunity* 2006; **25**:271-83.
255. Springer TA. Traffic signals on endothelium for lymphocyte recirculation and leukocyte emigration. *Annu Rev Physiol* 1995; **57**:827-72.
256. Sano H, Nakagawa N, Chiba R, Kurasawa K, Saito Y, Iwamoto I. Cross-linking of intercellular adhesion molecule-1 induces interleukin-8 and RANTES production through the activation of MAP kinases in human vascular endothelial cells. *Biochem Biophys Res Commun* 1998; **250**:694-8.

257. Wang Q, Doerschuk CM. The p38 mitogen-activated protein kinase mediates cytoskeletal remodeling in pulmonary microvascular endothelial cells upon intracellular adhesion molecule-1 ligation. *J Immunol* 2001; **166**:6877-84.
258. Lorenzon P, Vecile E, Nardon E, Ferrero E, Harlan JM, Tedesco F, Dobrina A. Endothelial cell E- and P-selectin and vascular cell adhesion molecule-1 function as signaling receptors. *J Cell Biol* 1998; **142**:1381-91.
259. Matheny HE, Deem TL, Cook-Mills JM. Lymphocyte migration through monolayers of endothelial cell lines involves VCAM-1 signaling via endothelial cell NADPH oxidase. *J Immunol* 2000; **164**:6550-9.
260. Deem TL, Cook-Mills JM. Vascular cell adhesion molecule 1 (VCAM-1) activation of endothelial cell matrix metalloproteinases: role of reactive oxygen species. *Blood* 2004; **104**:2385-93.
261. Herren B, Levkau B, Raines EW, Ross R. Cleavage of beta-catenin and plakoglobin and shedding of VE-cadherin during endothelial apoptosis: evidence for a role for caspases and metalloproteinases. *Mol Biol Cell* 1998; **9**:1589-601.
262. Mackman N. The role of tissue factor and factor VIIa in hemostasis. *Anesth Analg* 2009; **108**:1447-52.
263. Stan R-V, Kubitzka M, Palade GE. PV-1 is a component of the fenestral and stomatal diaphragms in fenestrated endothelia. *Proc Natl Acad Sci U S A* 1999; **96**:13203-7.
264. Lote C. Principles of Renal Physiology. 4th Edn: Kluwer Academic Publishers, 2000.
265. Chang RL, Deen WM, Robertson CR, Brenner BM. Permselectivity of the glomerular capillary wall: III. Restricted transport of polyanions. *Kidney Int* 1975; **8**:212-8.
266. Singh A, Satchell SC, Neal CR, McKenzie EA, Tooke JE, Mathieson PW. Glomerular endothelial glycocalyx constitutes a barrier to protein permeability. *J Am Soc Nephrol* 2007; **18**:2885-93.
267. Friden V, Oveland E, Tenstad O, Ebefors K, Nystrom J, Nilsson UA, Haraldsson B. The glomerular endothelial cell coat is essential for glomerular filtration. *Kidney Int* 2011; **79**:1322-30.
268. Jeansson M, Haraldsson B. Morphological and functional evidence for an important role of the endothelial cell glycocalyx in the glomerular barrier. *Am J Physiol Renal Physiol* 2006; **290**:F111-6.
269. Salmon AH, Neal CR, Sage LM, Glass CA, Harper SJ, Bates DO. Angiopoietin-1 alters microvascular permeability coefficients in vivo via modification of endothelial glycocalyx. *Cardiovasc Res* 2009; **83**:24-33.
270. Petri B, Phillipson M, Kubes P. The physiology of leukocyte recruitment: an in vivo perspective. *J Immunol* 2008; **180**:6439-46.
271. Chappell D, Dorfler N, Jacob M, Rehm M, Welsch U, Conzen P, Becker BF. Glycocalyx protection reduces leukocyte adhesion after ischemia/reperfusion. *Shock* 2010; **34**:133-9.
272. Henry CB, Duling BR. TNF-alpha increases entry of macromolecules into luminal endothelial cell glycocalyx. *Am J Physiol Heart Circ Physiol* 2000; **279**:H2815-23.
273. Devaraj S, Yun JM, Adamson G, Galvez J, Jialal I. C-reactive protein impairs the endothelial glycocalyx resulting in endothelial dysfunction. *Cardiovasc Res* 2009; **84**:479-84.
274. Striker GE, Soderland C, Bowen-Pope DF, Gown AM, Schmer G, Johnson A, Luchtel D, Ross R, Striker LJ. Isolation, characterization, and propagation in vitro of human glomerular endothelial cells. *J Exp Med* 1984; **160**:323-8.
275. Satchell SC, Tasman CH, Singh A, Ni L, Geelen J, von Ruhland CJ, O'Hare MJ, Saleem MA, van den Heuvel LP, Mathieson PW. Conditionally immortalized human glomerular endothelial cells expressing fenestrations in response to VEGF. *Kidney Int* 2006; **69**:1633-40.

276. Boneu B, Abbal M, Plante J, Bierme R. Factor-VIII complex and endothelial damage. *Lancet* 1975; **305**:1430.
277. Wagner DD, Olmsted JB, Marder VJ. Immunolocalization of von Willebrand protein in Weibel-Palade bodies of human endothelial cells. *J Cell Biol* 1982; **95**:355-60.
278. Mcever RP, Beckstead JH, Moore KL, Marshallcarlson L, Bainton DF. Gmp-140, a Platelet Alpha-Granule Membrane-Protein, Is Also Synthesized by Vascular Endothelial-Cells and Is Localized in Weibel-Palade Bodies. *J Clin Invest* 1989; **84**:92-9.
279. Sadler JE. von Willebrand factor assembly and secretion. *J Thromb Haemost* 2009; **7**:24-7.
280. Lui-Roberts WWY, Collinson LM, Hewlett LJ, Michaux G, Cutler DF. An AP-1/clathrin coat plays a novel and essential role in forming the Weibel-Palade bodies of endothelial cells. *J Cell Biol* 2005; **170**:627-36.
281. Goligorsky MS, Patschan D, Kuo MC. Weibel-Palade bodies-sentinels of acute stress. *Nat Rev Nephrol* 2009; **5**:423-6.
282. Haberichter SL, Merricks EP, Fahs SA, Christopherson PA, Nichols TC, Montgomery RR. Re-establishment of VWF-dependent Weibel-Palade bodies in VWD endothelial cells. *Blood* 2005; **105**:145-52.
283. Utgaard JO, Jahnsen FL, Bakka A, Brandtzaeg P, Haraldsen G. Rapid secretion of prestored interleukin 8 from Weibel-Palade bodies of microvascular endothelial cells. *J Exp Med* 1998; **188**:1751-6.
284. Wolff B, Burns AR, Middleton J, Rot A. Endothelial cell "memory" of inflammatory stimulation: Human venular endothelial cells store interleukin 8 in Weibel-Palade bodies. *J Exp Med* 1998; **188**:1757-62.
285. de Wit TR, de Leeuw HPJC, Rondaij MG, de Laaf RTM, Sellink E, Brinkman HJ, Voorberg J, van Mourik JA. Von Willebrand factor targets IL-8 to Weibel-Palade bodies in an endothelial cell line. *Exp Cell Res* 2003; **286**:67-74.
286. Fiedler U, Scharpfenecker M, Koidl S, Hegen A, Grunow V, Schmidt JM, Kriz W, Thurston G, Augustin HG. The Tie-2 ligand angiopoietin-2 is stored in and rapidly released upon stimulation from endothelial cell Weibel-Paladebodies. *Blood* 2004; **103**:4150-6.
287. Cleator JH, Zhu WQ, Vaughan DE, Hamm HE. Differential regulation of endothelial exocytosis of P-selectin and von Willebrand factor by protease-activated receptors and cAMP. *Blood* 2006; **107**:2736-44.
288. Tranquille N, Emeis JJ. On the Role of Calcium in the Acute Release of Tissue-Type Plasminogen-Activator and Vonwillebrand-Factor from the Rat Perfused Hindleg Region. *Thromb Haemost* 1991; **66**:479-83.
289. Metcalf DJ, Nightingale TD, Zenner HL, Lui-Roberts WW, Cutler DF. Formation and function of Weibel-Palade bodies. *J Cell Sci* 2008; **121**:19-27.
290. Knop M, Aareskjold E, Bode G, Gerke V. Rab3D and annexin A2 play a role in regulated secretion of vWF, but not tPA, from endothelial cells. *EMBO J* 2004; **23**:2982-92.
291. Rondaij MG, Sellink E, Gijzen KA, ten Klooster JP, Hordijk PL, van Mourik JA, Voorberg J. Small GTP-binding protein ral is involved in cAMP-mediated release of von Willebrand factor from endothelial cells. *Arterioscler Thromb Vasc Biol* 2004; **24**:1315-20.
292. de Leeuw HPJC, Wijers-Koster PM, van Mourik JA, Voorberg J. Small GTP-binding protein RalA associates with Weibel-Palade bodies in endothelial cells. *Thromb Haemost* 1999; **82**:1177-81.
293. Rondaij MG, Bierings R, Kragt A, van Mourik JA, Voorberg J. Dynamics and plasticity of Weibel-Palade bodies in endothelial cells. *Arterioscler Thromb Vasc Biol* 2006; **26**:1002-7.

294. Paulinska P, Spiel A, Jilma B. Role of von Willebrand factor in vascular disease. *Hamostaseologie* 2009; **29**:32-8.
295. Reininger AJ. VWF attributes - impact on thrombus formation. *Thromb Res* 2008; **122**:S9-S13.
296. Sadler JE. Biochemistry and genetics of von Willebrand factor. *Annu Rev Biochem* 1998; **67**:395-424.
297. Rand JH, Patel ND, Schwartz E, Zhou SL, Potter BJ. 150-Kd Vonwillebrand-Factor Binding-Protein Extracted from Human Vascular Subendothelium Is Type-Vi Collagen. *J Clin Invest* 1991; **88**:253-9.
298. Handa M, Titani K, Holland LZ, Roberts JR, Ruggeri ZM. The von Willebrand factor-binding domain of platelet membrane glycoprotein Ib. Characterization by monoclonal antibodies and partial amino acid sequence analysis of proteolytic fragments. *J Biol Chem* 1986; **261**:12579-85.
299. Savage B, Saldivar E, Ruggeri ZM. Initiation of platelet adhesion by arrest onto fibrinogen or translocation on von Willebrand factor. *Cell* 1996; **84**:289-97.
300. Andre P, Denis CV, Ware J, Saffaripour S, Hynes RO, Ruggeri ZM, Wagner DD. Platelets adhere to and translocate on von Willebrand factor presented by endothelium in simulated veins. *Blood* 2000; **96**:3322-8.
301. Plow EF, Ginsberg MH. Specific and saturable binding of plasma fibronectin to thrombin- stimulated human platelets. *J Biol Chem* 1981; **256**:9477-82.
302. Marguerie GA, Plow EF, Edgington TS. Human platelets possess an inducible and saturable receptor specific for fibrinogen. *J Biol Chem* 1979; **254**:5357-63.
303. Fredrickson BJ, Dong JF, McIntire LV, Lopez JA. Shear-dependent rolling on von Willebrand factor of mammalian cells expressing the platelet glycoprotein Ib-IX-V complex. *Blood* 1998; **92**:3684-93.
304. Mannucci PM. von Willebrand Factor : A Marker of Endothelial Damage? *Arterioscler Thromb Vasc Biol* 1998; **18**:1359-62.
305. de Wit TR, Rondaij MG, Hordijk PL, Voorberg J, van Mourik JA. Real-time imaging of the dynamics and secretory behavior of Weibel-Palade bodies. *Arterioscler Thromb Vasc Biol* 2003; **23**:755-61.
306. Jones TR, Kao KJ, Pizzo SV, Bigner DD. Endothelial Cell-Surface Expression and Binding of Factor-Viii-Vonwillebrand Factor. *Am J Pathol* 1981; **103**:304-8.
307. Savage COS, Pottinger BE, Gaskin G, Lockwood CM, Pusey CD, Pearson JD. Vascular Damage in Wegeners Granulomatosis and Microscopic Polyarteritis - Presence of Antiendothelial Cell Antibodies and Their Relation to Antineutrophil Cytoplasm Antibodies. *Clin Exp Immunol* 1991; **85**:14-9.
308. D'cruz D, Direskeneli H, Khamashta M, Hughes GRV. Lymphocyte activation markers and von Willebrand factor antigen in Wegener's granulomatosis: Potential markers for disease activity. *J Rheumatol* 1999; **26**:103-9.
309. Lu X, Garfield A, Rainger GE, Savage COS, Nash GB. Mediation of endothelial cell damage by serine proteases, but not superoxide, released from antineutrophil cytoplasmic antibody-stimulated neutrophils. *Arthritis Rheum* 2006; **54**:1619-28.
310. Holash J, Wiegand SJ, Yancopoulos GD. New model of tumor angiogenesis: dynamic balance between vessel regression and growth mediated by angiopoietins and VEGF. *Oncogene* 1999; **18**:5356-62.
311. Kim I, Kim HG, So JN, Kim JH, Kwak HJ, Koh GY. Angiopoietin-1 regulates endothelial cell survival through the phosphatidylinositol 3'-kinase/Akt signal transduction pathway. *Circ Res* 2000; **86**:24-9.
312. Papapetropoulos A, Fulton D, Mahboubi K, Kalb RG, O'Connor DS, Li FZ, Altieri DC, Sessa WC. Angiopoietin-1 inhibits endothelial cell apoptosis via the Akt/survivin pathway. *J Biol Chem* 2000; **275**:9102-5.

313. Thurston G, Rudge JS, Ioffe E, Zhou H, Ross L, Croll SD, Glazer N, Holash J, McDonald DM, Yancopoulos GD. Angiopoietin-1 protects the adult vasculature against plasma leakage. *Nat Med* 2000; **6**:460-3.
314. Fiedler U, Reiss Y, Scharpfenecker M, Grunow V, Koidl S, Thurston G, Gale NW, Witzenrath M, Rosseau S, Suttorp N, Sobke A, Herrmann M, Preissner KT, Vajkoczy P, Augustin HG. Angiopoietin-2 sensitizes endothelial cells to TNF-alpha and has a crucial role in the induction of inflammation. *Nat Med* 2006; **12**:235-9.
315. Scharpfenecker M, Fiedler U, Reiss Y, Augustin HG. The Tie-2 ligand Angiopoietin-2 destabilizes quiescent endothelium through an internal autocrine loop mechanism. *J Cell Sci* 2005; **118**:771-80.
316. Visconti RP, Richardson CD, Sato TN. Orchestration of angiogenesis and arteriovenous contribution by angiopoietins and vascular endothelial growth factor (VEGF). *Proc Natl Acad Sci U S A* 2002; **99**:8219-24.
317. Zachary I. VEGF signalling: integration and multi-tasking in endothelial cell biology. *Biochem Soc Trans* 2003; **31**:1171-7.
318. Kumar P, Shen Q, Pivetti CD, Lee ES, Wu MH, Yuan SY. Molecular mechanisms of endothelial hyperpermeability: implications in inflammation. *Expert Rev Mol Med* 2009; **11**:e19.
319. Wu MH, Guo M, Yuan SY, Granger HJ. Focal adhesion kinase mediates porcine venular hyperpermeability elicited by vascular endothelial growth factor. *J Physiol* 2003; **552**:691-9.
320. Sun H, Breslin JW, Zhu J, Yuan SY, Wu MH. Rho and ROCK signaling in VEGF-induced microvascular endothelial hyperpermeability. *Microcirculation* 2006; **13**:237-47.
321. Behzadian MA, Windsor LJ, Ghaly N, Liou G, Tsai NT, Caldwell RB. VEGF-induced paracellular permeability in cultured endothelial cells involves urokinase and its receptor. *FASEB J* 2003; **17**:752-4.
322. Fiedler U, Krissl T, Koidl S, Weiss C, Koblizek T, Deutsch U, Martiny-Baron G, Marme D, Augustin HG. Angiopoietin-1 and angiopoietin-2 share the same binding domains in the Tie-2 receptor involving the first Ig-like loop and the epidermal growth factor-like repeats. *J Biol Chem* 2003; **278**:1721-7.
323. Procopio WN, Pelavin PI, Lee WMF, Yeilding NM. Angiopoietin-1 and-2 coiled coil domains mediate distinct homo-oligomerization patterns, but fibrinogen-like domains mediate ligand activity. *J Biol Chem* 1999; **274**:30196-201.
324. Kumpers P, Hellpap J, David S, Horn R, Leitolf H, Haller H, Haubitz M. Circulating angiopoietin-2 is a marker and potential mediator of endothelial cell detachment in ANCA-associated vasculitis with renal involvement. *Nephrol Dial Transplant* 2009; **24**:1845-50.
325. Hattori R, Hamilton KK, Fugate RD, McEver RP, Sims PJ. Stimulated secretion of endothelial von Willebrand factor is accompanied by rapid redistribution to the cell surface of the intracellular granule membrane protein GMP-140. *J Biol Chem* 1989; **264**:7768-71.
326. Harper L, Radford D, Plant T, Drayson M, Adu D, Savage COS. IgG from myeloperoxidase-antineutrophil cytoplasmic antibody-positive patients stimulates greater activation of primed neutrophils than IgG from proteinase 3-antineutrophil cytoplasmic antibody-positive patients. *Arthritis Rheum* 2001; **44**:921-30.
327. Radford DJ, Savage CO, Nash GB. Treatment of rolling neutrophils with antineutrophil cytoplasmic antibodies causes conversion to firm integrin-mediated adhesion. *Arthritis Rheum* 2000; **43**:1337-45.
328. Hannah MJ, Williams R, Kaur J, Hewlett LJ, Cutler DF. Biogenesis of Weibel-Palade bodies. *Semin Cell Dev Biol* 2002; **13**:313-24.

329. Hattori R, Hamilton KK, Mcever RP, Sims PJ. Complement Proteins C5b-9 Induce Secretion of High Molecular-Weight Multimers of Endothelial Vonwillebrand-Factor and Translocation of Granule Membrane-Protein Gmp-140 to the Cell-Surface. *J Biol Chem* 1989; **264**:9053-60.
330. Straley KS, Green SA. Rapid Transport of Internalized P-Selectin to Late Endosomes and the TGN: Roles in Regulating Cell Surface Expression and Recycling to Secretory Granules. *J Cell Biol* 2000; **151**:107-16.
331. Arribas M, Cutler DF. Weibel-Palade body membrane proteins exhibit differential trafficking after exocytosis in endothelial cells. *Traffic* 2000; **1**:783-93.
332. Harrison-Lavoie KJ, Michaux G, Hewlett L, Kaur J, Hannah MJ, Lui-Roberts WWY, Norman KE, Cutler DF. P-selectin and CD63 use different mechanisms for delivery to Weibel-Palade bodies. *Traffic* 2006; **7**:647-62.
333. Pols MS, Lumperman J. Trafficking and function of the tetraspanin CD63. *Exp Cell Res* 2009; **315**:1584-92.
334. Schroder JM, Christophers E. Secretion of novel and homologous neutrophil-activating peptides by LPS- stimulated human endothelial cells. *J Immunol* 1989; **142**:244-51.
335. Moser B, Barella L, Mattei S, Schumacher C, Boulay F, Colombo MP, Baggiolini M. Expression of Transcripts for 2 Interleukin-8 Receptors in Human Phagocytes, Lymphocytes and Melanoma-Cells. *Biochem J* 1993; **294**:285-92.
336. Strieter RM, Kunkel SL, Showell HJ, Remick DG, Phan SH, Ward PA, Marks RM. Endothelial-Cell Gene-Expression of a Neutrophil Chemotactic Factor by Tnf-Alpha, Lps, and Il-1-Beta. *Science* 1989; **243**:1467-9.
337. Salcedo R, Resau JH, Halverson D, Hudson EA, Dambach M, Powell D, Wasserman K, Oppenheim JJ. Differential expression and responsiveness of chemokine receptors (CXCR1-3) by human microvascular endothelial cells and umbilical vein endothelial cells. *FASEB J* 2000; **14**:2055-64.
338. Schraufstatter IU, Chung J, Burger M. IL-8 activates endothelial cell CXCR1 and CXCR2 through Rho and Rac signaling pathways. *Am J Physiol Lung Cell Mol Physiol* 2001; **280**:L1094-L103.
339. Li AH, Dubey S, Varney ML, Dave BJ, Singh RK. IL-8 directly enhanced endothelial cell survival, proliferation, and matrix metalloproteinases production and regulated angiogenesis. *J Immunol* 2003; **170**:3369-76.
340. Peveri P, Walz A, Dewald B, Baggiolini M. A novel neutrophil-activating factor produced by human mononuclear phagocytes. *J Exp Med* 1988; **167**:1547-59.
341. Chaly YV, Selvan RS, Fegeding KV, Kolesnikova TS, Voitenok NN. Expression of IL-8 gene in human monocytes and lymphocytes: Differential regulation by TNF and IL-1. *Cytokine* 2000; **12**:636-43.
342. Strieter RM, Phan SH, Showell HJ, Remick DG, Lynch JP, Genord M, Raiford C, Eskandari M, Marks RM, Kunkel SL. Monokine-induced neutrophil chemotactic factor gene expression in human fibroblasts. *J Biol Chem* 1989; **264**:10621-6.
343. Eckmann L, Jung HC, Schurermaly C, Panja A, Morzyckawroblewska E, Kagnoff MF. Differential Cytokine Expression by Human Intestinal Epithelial-Cell Lines - Regulated Expression of Interleukin-8. *Gastroenterology* 1993; **105**:1689-97.
344. Lakshminarayanan V, Beno DWA, Costa RH, Roebuck KA. Differential regulation of interleukin-8 and intercellular adhesion molecule-1 by H₂O₂ and tumor necrosis factor-alpha in endothelial and epithelial cells. *J Biol Chem* 1997; **272**:32910-8.
345. Blease K, Chen Y, Hellewell PG, Burke-Gaffney A. Lipoteichoic acid inhibits lipopolysaccharide-induced adhesion molecule expression and IL-8 release in human lung microvascular endothelial cells. *J Immunol* 1999; **163**:6139-47.

346. Rot A, Hub E, Middleton J, Pons F, Rabeck C, Thierer K, Wintle J, Wolff B, Zsak M, Dukor P. Some aspects of IL-8 pathophysiology .3. Chemokine interaction with endothelial cells. *J Leukoc Biol* 1996; **59**:39-44.
347. Nyhlen K, Linden M, Andersson R, Uppugunduri S. Corticosteroids and interferons inhibit cytokine-induced production of IL-8 by human endothelial cells. *Cytokine* 2000; **12**:355-60.
348. Baggiolini M, Moser B, Clark-Lewis I. Interleukin-8 and Related Chemotactic Cytokines: The Giles Filley Lecture. *Chest* 1994; **105**:95S-8.
349. Baggiolini M, Walz A, Kunkel SL. Neutrophil-Activating Peptide-1 Interleukin-8, a Novel Cytokine That Activates Neutrophils. *J Clin Invest* 1989; **84**:1045-9.
350. Baggiolini M, Loetscher P, Moser B. Interleukin-8 and the Chemokine Family. *Int J Immunopharmac* 1995; **17**:103-8.
351. Gimbrone MA, Obin MS, Brock AF, Luis EA, Hass PE, Hebert CA, Yip YK, Leung DW, Lowe DG, Kohr WJ, Darbonne WC, Bechtol KB, Baker JB. Endothelial Interleukin-8 - a Novel Inhibitor of Leukocyte-Endothelial Interactions. *Science* 1989; **246**:1601-3.
352. Harper L, Cockwell P, Adu D, Savage COS. Neutrophil priming and apoptosis in anti-neutrophil cytoplasmic autoantibody-associated vasculitis. *Kidney Int* 2001; **59**:1729-38.
353. Asokanathan N, Graham PT, Fink J, Knight DA, Bakker AJ, McWilliam AS, Thompson PJ, Stewart GA. Activation of protease-activated receptor (PAR)-1, PAR-2, and PAR-4 stimulates IL-6, IL-8, and prostaglandin E-2 release from human respiratory epithelial cells. *J Immunol* 2002; **168**:3577-85.
354. Compton SJ, Cairns JA, Holgate ST, Walls AF. Human mast cell tryptase stimulates the release of an IL-8-dependent neutrophil chemotactic activity from human umbilical vein endothelial cells (HUVEC). *Clin Exp Immunol* 2000; **121**:31-6.
355. Fox MT, Harriott P, Walker B, Stone SR. Identification of potential activators of proteinase-activated receptor-2. *FEBS Lett* 1997; **417**:267-9.
356. Hollenberg MD. Protease-activated receptors: PAR4 and counting: how long is the course? *Trends Pharmacol Sci* 1999; **20**:271-3.
357. Hamilton JR, Frauman AG, Cocks TM. Increased expression of protease-activated receptor-2 (PAR2) and PAR4 in human coronary artery by inflammatory stimuli unveils endothelium-dependent relaxations to PAR2 and PAR4 agonists. *Circ Res* 2001; **89**:92-8.
358. Ossovskaya VS, Bunnett NW. Protease-activated receptors: Contribution to physiology and disease. *Physiol Rev* 2004; **84**:579-621.
359. Macfarlane SR, Seatter MJ, Kanke T, Hunter GD, Plevin R. Proteinase-activated receptors. *Pharmacol Rev* 2001; **53**:245-82.
360. Coughlin SR. Thrombin signalling and protease-activated receptors. *Nature* 2000; **407**:258-64.
361. Klarenbach SW, Chipiuk A, Nelson RC, Hollenberg MD, Murray AG. Differential actions of PAR(2) and PAR(1) in stimulating human endothelial cell exocytosis and permeability - The role of Rho-GTPases. *Circ Res* 2003; **92**:272-8.
362. Langer F, Morys-Wortmann C, Kusters B, Storck J. Endothelial protease-activated receptor-2 induces tissue factor expression and von Willebrand factor release. *Br J Haematol* 1999; **105**:542-50.
363. Storck J, Kusters B, Vahland M, MorysWortmann C, Zimmermann ER. Trypsin induced von willebrand factor release from human endothelial cells is mediated by PAR-2 activation. *Thromb Res* 1996; **84**:463-73.
364. Nystedt S, Emilsson K, Wahlestedt C, Sundelin J. Molecular Cloning of a Potential Proteinase Activated Receptor. *Proc Natl Acad Sci U S A* 1994; **91**:9208-12.

365. D'Andrea MR, Derian CK, Leturcq D, Baker SM, Brunmark A, Ling P, Darrow AL, Santulli RJ, Brass LF, Andrade-Gordon P. Characterization of Protease-activated Receptor-2 Immunoreactivity in Normal Human Tissues. *J Histochem Cytochem* 1998; **46**:157-64.
366. Lindner JR, Kahn ML, Coughlin SR, Sambrano GR, Schauble E, Bernstein D, Foy D, Hafezi-Moghadam A, Ley K. Delayed onset of inflammation in protease-activated receptor-2-deficient mice. *J Immunol* 2000; **165**:6504-10.
367. Uehara A, Sugawara S, Muramoto K, Takada H. Activation of Human Oral Epithelial Cells by Neutrophil Proteinase 3 Through Protease-Activated Receptor-2. *J Immunol* 2002; **169**:4594-603.
368. Uehara A, Sugawara Y, Sasano T, Takada H, Sugawara S. Proinflammatory Cytokines Induce Proteinase 3 as Membrane-Bound and Secretory Forms in Human Oral Epithelial Cells and Antibodies to Proteinase 3 Activate the Cells through Protease-Activated Receptor-2. *J Immunol* 2004; **173**:4179-89.
369. Csernok E, Ai M, Gross WL, Wicklein D, Petersen A, Lindner B, Lamprecht P, Holle JU, Hellmich B. Wegener autoantigen induces maturation of dendritic cells and licenses them for Th1 priming via the protease-activated receptor-2 pathway. *Blood* 2006; **107**:4440-8.
370. Kahn R, Hellmark T, Leeb-Lundberg LMF, Akbari N, Todiras M, Olofsson T, Wieslander J, Christensson A, Westman K, Bader M, Muller-Esterl W, Karpman D. Neutrophil-Derived Proteinase 3 Induces Kallikrein-Independent Release of a Novel Vasoactive Kinin. *J Immunol* 2009; **182**:7906-15.
371. Lorenzi O, Frieden M, Villemin P, Fournier M, Foti M, Vischer UM. Protein kinase C-delta mediates von Willebrand factor secretion from endothelial cells in response to vascular endothelial growth factor (VEGF) but not histamine. *J Thromb Haemost* 2008; **6**:1962-9.
372. Xiong Y, Huo YQ, Chen C, Zeng HY, Lu XF, Wei CL, Ruan CG, Zhang XY, Hu ZQ, Shibuya M, Luo JC. Vascular Endothelial Growth Factor (VEGF) Receptor-2 Tyrosine 1175 Signaling Controls VEGF-induced von Willebrand Factor Release from Endothelial Cells via Phospholipase C-gamma 1-and Protein Kinase A-dependent Pathways. *J Biol Chem* 2009; **284**:23217-24.
373. Rondaij MG, Bierings R, Kragt A, Gijzen KA, Sellink E, van Mourik JA, Fernandez-Borja M, Voorberg J. Dynein-dynactin complex mediates protein kinase A-dependent clustering of Weibel-Palade bodies in endothelial cells. *Arterioscler Thromb Vasc Biol* 2006; **26**:49-55.
374. Birch KA, Pober JS, Zavoico GB, Means AR, Ewenstein BM. Calcium Calmodulin Transduces Thrombin-Stimulated Secretion - Studies in Intact and Minimally Permeabilized Human Umbilical Vein Endothelial-Cells. *J Cell Biol* 1992; **118**:1501-10.
375. van Buul-Wortelboer MF, Brinkman HJ, Reinders JH, van Aken WG, van Mourik JA. Polar secretion of von Willebrand factor by endothelial cells. *Biochim Biophys Acta* 1989; **1011**:129-33.
376. Nakatani K, Takeshita S, Tsujimoto H, Kawamura Y, Sekine I. Inhibitory effect of serine protease inhibitors on neutrophil-mediated endothelial cell injury. *J Leukoc Biol* 2001; **69**:241-7.
377. Smedly LA, Tonnesen MG, Sandhaus RA, Haslett C, Guthrie L, Johnston RB, Henson PM, Worthen GS. Role of Elastase in Endotoxin-Enhanced, Neutrophil-Mediated, Injury to Endothelial-Cells. *Fed Proc* 1985; **44**:1544-.
378. Carden D, Xiao F, Moak C, Willis BH, Robinson-Jackson S, Alexander S. Neutrophil elastase promotes lung microvascular injury and proteolysis of endothelial cadherins. *Am J Physiol* 1998; **275**:H385-92.

379. Kuzniar J, Kuzniar TJ, Marchewka Z, Lembas-Bogaczyk J, Rabczynski J, Kopec W, Klinger M. Elastase deposits in the kidney and urinary elastase excretion in patients with glomerulonephritis--evidence for neutrophil involvement in renal injury. *Scand J Urol Nephrol* 2007; **41**:527-34.
380. Pederzoli M, Kantari C, Gausson V, Moriceau S, Witko-Sarsat V. Proteinase-3 induces procaspase-3 activation in the absence of apoptosis: potential role of this compartmentalized activation of membrane-associated procaspase-3 in neutrophils. *J Immunol* 2005; **174**:6381-90.
381. Woywodt A, Streiber F, de Groot K, Regelsberger H, Haller H, Haubitz M. Circulating endothelial cells as markers for ANCA-associated small-vessel vasculitis. *Lancet* 2003; **361**:206-10.
382. de Leeuw K, Bijzet J, van der Graaf AM, Stegeman CA, Smit AJ, Kallenberg CG, Bijl M. Patients with Wegener's granulomatosis: a long-term follow-up study. *Clin Exp Rheumatol* 2010; **28**:18-23.
383. Denis CV, Andre P, Saffaripour S, Wagner DD. Defect in regulated secretion of P-selectin affects leukocyte recruitment in von Willebrand factor-deficient mice. *Proc Natl Acad Sci U S A* 2001; **98**:4072-7.
384. Methia N, Andre P, Denis CV, Economopoulos M, Wagner DD. Localized reduction of atherosclerosis in von Willebrand factor-deficient mice. *Blood* 2001; **98**:1424-8.
385. Pendu R, Terraube V, Christophe OD, Gahmberg CG, de Groot PG, Lenting PJ, Denis CV. P-selectin glycoprotein ligand 1 and beta2-integrins cooperate in the adhesion of leukocytes to von Willebrand factor. *Blood* 2006; **108**:3746-52.
386. Isobe T, Hisaoka T, Shimizu A, Okuno M, Aimoto S, Takada Y, Saito Y, Takagi J. Propolypeptide of von Willebrand factor is a novel ligand for very late antigen-4 integrin. *J Biol Chem* 1997; **272**:8447-53.
387. Cockwell P, Brooks CJ, Adu D, Savage COS. Interleukin-8: A pathogenetic role in antineutrophil cytoplasmic autoantibody-associated glomerulonephritis. *Kidney Int* 1999; **55**:852-63.
388. Hsieh SC, Yu HS, Cheng SH, Li KJ, Lu MC, Wu CH, Tsai CY, Yu CL. Anti-myeloperoxidase antibodies enhance phagocytosis, IL-8 production, and glucose uptake of polymorphonuclear neutrophils rather than anti-proteinase 3 antibodies leading to activation-induced cell death of the neutrophils. *Clin Rheumatol* 2007; **26**:216-24.
389. Colman R, Hussain A, Goodall M, Young SP, Pankhurst T, Lu XM, Jefferis R, Savage COS, Williams JM. Chimeric antibodies to proteinase 3 of IgG1 and IgG3 subclasses induce different magnitudes of functional responses in neutrophils. *Ann Rheum Dis* 2007; **66**:676-82.
390. Masuda Y, Shimizu A, Mori T, Ishiwata T, Kitamura H, Ohashi R, Ishizaki M, Asano G, Sugisaki Y, Yamanaka N. Vascular endothelial growth factor enhances glomerular capillary repair and accelerates resolution of experimentally induced glomerulonephritis. *Am J Pathol* 2001; **159**:599-608.
391. Kurtagic E, Jedrychowski MP, Nugent MA. Neutrophil elastase cleaves VEGF to generate a VEGF fragment with altered activity. *Am J Physiol Lung Cell Mol Physiol* 2009; **296**:L534-46.
392. Raife TJ, Cao W, Atkinson BS, Bedell B, Montgomery RR, Lentz SR, Johnson GF, Zheng XL. Leukocyte proteases cleave von Willebrand factor at or near the ADAMTS13 cleavage site. *Blood* 2009; **114**:1666-74.
393. Tirupathi C, Naqvi T, Wu Y, Vogel SM, Minshall RD, Malik AB. Albumin mediates the transcytosis of myeloperoxidase by means of caveolae in endothelial cells. *Proc Natl Acad Sci U S A* 2004; **101**:7699-704.
394. Montgomery KF, Osborn L, Hession C, Tizard R, Goff D, Vassallo C, Tarr PI, Bomsztyk K, Lobb R, Harlan JM, et al. Activation of endothelial-leukocyte adhesion

- molecule 1 (ELAM-1) gene transcription. *Proc Natl Acad Sci U S A* 1991; **88**:6523-7.
395. Mathieson PW. The ins and outs of glomerular crescent formation. *Clin Exp Immunol* 1997; **110**:155-7.
396. Berden AE, Ferrario F, Hagen EC, Jayne DR, Jennette JC, Joh K, Neumann I, Noel LH, Pusey CD, Waldherr R, Bruijn JA, Bajema IM. Histopathologic classification of ANCA-associated glomerulonephritis. *J Am Soc Nephrol* 2010; **21**:1628-36.
397. Fu J, Naren AP, Gao X, Ahmmed GU, Malik AB. Protease-activated receptor-1 activation of endothelial cells induces protein kinase Calpha-dependent phosphorylation of syntaxin 4 and Munc18c: role in signaling p-selectin expression. *J Biol Chem* 2005; **280**:3178-84.
398. Chin AC, Lee WY, Nusrat A, Vergnolle N, Parkos CA. Neutrophil-mediated activation of epithelial protease-activated receptors-1 and -2 regulates barrier function and transepithelial migration. *J Immunol* 2008; **181**:5702-10.
399. Klein J, Gonzalez J, Decramer S, Bandin F, Neau E, Salant DJ, Heeringa P, Pesquero JB, Schanstra JP, Bascands JL. Blockade of the kinin B1 receptor ameliorates glomerulonephritis. *J Am Soc Nephrol* 2010; **21**:1157-64.
400. van den Eijnden-Schrauwen Y, Atsma DE, Lupu F, de Vries RE, Kooistra T, Emeis JJ. Involvement of calcium and G proteins in the acute release of tissue-type plasminogen activator and von Willebrand factor from cultured human endothelial cells. *Arterioscler Thromb Vasc Biol* 1997; **17**:2177-87.
401. Vischer UM, Barth H, Wollheim CB. Regulated von Willebrand factor secretion is associated with agonist-specific patterns of cytoskeletal remodeling in cultured endothelial cells. *Arterioscler Thromb Vasc Biol* 2000; **20**:883-91.
402. Nolasco LH, Gushiken FC, Turner NA, Khatlani TS, Pradhan S, Dong JF, Moake JL, Vijayan KV. Protein phosphatase 2B inhibition promotes the secretion of von Willebrand factor from endothelial cells. *J Thromb Haemost* 2009; **7**:1009-18.
403. Potapova IA, Cohen IS, Doronin SV. Apoptotic endothelial cells demonstrate increased adhesiveness for human mesenchymal stem cells. *J Cell Physiol* 2009; **219**:23-30.
404. Kitazumi I, Maseki Y, Nomura Y, Shimanuki A, Sugita Y, Tsukahara M. Okadaic acid induces DNA fragmentation via caspase-3-dependent and caspase-3-independent pathways in Chinese hamster ovary (CHO)-K1 cells. *FEBS J* 2010; **277**:404-12.
405. Dogliotti G, Galliera E, Dozio E, Vianello E, Villa RE, Licastro F, Barajon I, Corsi MM. Okadaic acid induces apoptosis in Down syndrome fibroblasts. *Toxicol In Vitro* 2010; **24**:815-21.
406. Rafiq K, Hanscom M, Valerie K, Steinberg SF, Sabri A. Novel mode for neutrophil protease cathepsin G-mediated signaling: membrane shedding of epidermal growth factor is required for cardiomyocyte anoikis. *Circ Res* 2008; **102**:32-41.
407. Arrizabalaga P, Sole M, Abellana R, Ascaso C. Renal expression of adhesion molecules in anca-associated disease. *J Clin Immunol* 2008; **28**:411-9.
408. Moon KC, Park SY, Kim HW, Hong HK, Lee HS. Expression of intercellular adhesion molecule-1 and vascular cell adhesion molecule-1 in human crescentic glomerulonephritis. *Histopathology* 2002; **41**:158-65.
409. Khan SB, Allen AR, Bhargal G, Smith J, Lobb RR, Cook HT, Pusey CD. Blocking VLA-4 prevents progression of experimental crescentic glomerulonephritis. *Nephron Exp Nephrol* 2003; **95**:e100-10.
410. Kaynar AM, Houghton AM, Lum EH, Pitt BR, Shapiro SD. Neutrophil elastase is needed for neutrophil emigration into lungs in ventilator-induced lung injury. *Am J Respir Cell Mol Biol* 2008; **39**:53-60.
411. Champagne B, Tremblay P, Cantin A, St Pierre Y. Proteolytic cleavage of ICAM-1 by human neutrophil elastase. *J Immunol* 1998; **161**:6398-405.

412. Levesque JP, Takamatsu Y, Nilsson SK, Haylock DN, Simmons PJ. Vascular cell adhesion molecule-1 (CD106) is cleaved by neutrophil proteases in the bone marrow following hematopoietic progenitor cell mobilization by granulocyte colony-stimulating factor. *Blood* 2001; **98**:1289-97.
413. Adkison AM, Raptis SZ, Kelley DG, Pham CT. Dipeptidyl peptidase I activates neutrophil-derived serine proteases and regulates the development of acute experimental arthritis. *J Clin Invest* 2002; **109**:363-71.
414. Mazodier P, Elzouki AN, Segelmark M, Eriksson S. Systemic necrotizing vasculitides in severe alpha1-antitrypsin deficiency. *QJM* 1996; **89**:599-611.
415. Savige JA, Chang L, Cook L, Burdon J, Daskalakis M, Doery J. Alpha 1-antitrypsin deficiency and anti-proteinase 3 antibodies in anti-neutrophil cytoplasmic antibody (ANCA)-associated systemic vasculitis. *Clin Exp Immunol* 1995; **100**:194-7.
416. Griffith ME, Lovegrove JU, Gaskin G, Whitehouse DB, Pusey CD. C-antineutrophil cytoplasmic antibody positivity in vasculitis patients is associated with the Z allele of alpha-1-antitrypsin, and P-antineutrophil cytoplasmic antibody positivity with the S allele. *Nephrol Dial Transplant* 1996; **11**:438-43.
417. Elzouki AN, Segelmark M, Wieslander J, Eriksson S. Strong link between the alpha 1-antitrypsin PiZ allele and Wegener's granulomatosis. *J Intern Med* 1994; **236**:543-8.
418. van der Geld YM, Hellmark T, Selga D, Heeringa P, Huitema MG, Limburg PC, Kallenberg CG. Rats and mice immunised with chimeric human/mouse proteinase 3 produce autoantibodies to mouse Pr3 and rat granulocytes. *Ann Rheum Dis* 2007; **66**:1679-82.
419. Primo VC, Marusic S, Franklin CC, Goldmann WH, Achaval CG, Smith RN, Arnaout MA, Nikolic B. Anti-PR3 immune responses induce segmental and necrotizing glomerulonephritis. *Clin Exp Immunol* 2010; **159**:327-37.
420. Xiao H, Heeringa P, Hu P, Liu Z, Zhao M, Aratani Y, Maeda N, Falk RJ, Jennette JC. Antineutrophil cytoplasmic autoantibodies specific for myeloperoxidase cause glomerulonephritis and vasculitis in mice. *J Clin Invest* 2002; **110**:955-63.
421. van der Veen BS, Petersen AH, Belperio JA, Satchell SC, Mathieson PW, Molema G, Heeringa P. Spatiotemporal expression of chemokines and chemokine receptors in experimental anti-myeloperoxidase antibody-mediated glomerulonephritis. *Clin Exp Immunol* 2009; **158**:143-53.
422. Xiao H, Heeringa P, Liu Z, Huugen D, Hu P, Maeda N, Falk RJ, Jennette JC. The role of neutrophils in the induction of glomerulonephritis by anti-myeloperoxidase antibodies. *Am J Pathol* 2005; **167**:39-45.
423. Little MA, Smyth L, Salama AD, Mukherjee S, Smith J, Haskard D, Nourshargh S, Cook HT, Pusey CD. Experimental autoimmune vasculitis: an animal model of anti-neutrophil cytoplasmic autoantibody-associated systemic vasculitis. *Am J Pathol* 2009; **174**:1212-20.